EGFR & HER2 Trafficking and Signaling Dynamics:
Experimental and Modeling Studies

By

Bart S. Hendriks

B.S., Biomedical Engineering
The Johns Hopkins University, 1998

SUBMITTED TO THE DEPARTMENT OF CHEMICAL ENGINEERING
IN PARTIAL FULFILLMENT OF THE REQUIREMENTS FOR THE DEGREE OF

Doctor of Philosophy in Chemical Engineering

at the

Massachusetts Institute of Technology

June, 2003

Signature of Author _____
Department of Chemical Engineering

Certified by _____
Douglas A. Lauffenburger
Professor of Chemical Engineering
Thesis Supervisor

Accepted by _____
Daniel Blankschtein
Professor of Chemical Engineering
Chairman, Committee for Graduate Students

EGFR & HER2 Trafficking and Signaling Dynamics:
Experimental and Modeling Studies

by

Bart S. Hendriks

Submitted to the Department of Chemical Engineering on June 26, 2003
in partial fulfillment of the requirements for the degree of
Doctor of Philosophy in Chemical Engineering

Abstract

EGFR and HER2 expression levels have distinguished themselves as important factors in contributing to various types of cancers including breast and ovarian cancers, but quantitative linkages between receptor expression levels and aberrant cell behaviors are not well understood. The ability to interpret and predict cell responses in a multi-parameter space will be vital in efforts to manipulate cell behavior for therapeutic purposes.

HER2 acts as a co-receptor of the EGFR family of receptor tyrosine kinases. HER2 does not bind any known ligand, but plays an active signaling role following heterodimerization with a ligand-bound EGFR family receptor. EGFR family receptors undergo a dynamic process termed trafficking in which receptors and ligands are internalized and then either recycled to the surface or targeted for degradation. Trafficking is intimately connected to cell signaling by controlling the quantity and location of ligand-receptor complexes and is sensitive to disruption via the overexpression of the receptors involved.

In this work, we quantitatively establish the role of HER2 and heterodimerization in EGFR trafficking and signaling. A hierarchy of mathematical models describing the trafficking behavior of EGFR and HER2 was developed at various levels of mechanistic detail. At the macroscopic level the trafficking of EGFR and HER2 fall into two regimes, one whose downregulation is sorting-limited (EGFR) and one whose downregulation is internalization-limited (HER2). Subordinate models yield mechanistic detail into the endocytic and endosomal sorting processes supporting the notions that heterodimers internalize as single entities and that HER2 is able to disrupt EGFR sorting through a competitive mechanism.

The development of a comprehensive model of EGFR and HER2 trafficking enables the predictions of the quantity and distribution of various receptor species, including homo- and heterodimers as a function of time. Point by point comparison with ERK signaling data for different HER2 expressing cell clones allows the calculation of the signal generated per activated HER2 and per activated EGFR. These results suggest that EGFR and HER2 do not differ significantly in their ERK signaling ability and that HER2-mediated differences in ERK signaling can entirely be explained by interactions at the level of receptor trafficking.

Thesis Supervisor: Douglas A. Lauffenburger, Professor of Chemical Engineering

Acknowledgements

There are many people that have touched my life throughout this journey. First and foremost I would like to thank my advisor, Douglas Lauffenburger, without whom this would have never been possible. He has been a phenomenal mentor, provided inspiration, kept me motivated and taught me in countless ways while allowing me personal and intellectual freedoms that are difficult to come by in academia. I am grateful to Kam Leong and Hai-Quan Mao from Johns Hopkins for introducing me to research, giving me confidence and playing an instrumental role in getting me to MIT. I am especially indebted to our collaborator Steve Wiley and members of his past group at the University of Utah, particularly Lee Opresko who constructed the cell lines on which this entire work is based. I would also like to thank William Deen, Dane Wittrup and Alan Wells for providing their insights at various points in this endeavor. I would like to thank the past and present members of the DALLAB and LGGLAB for providing a fun scientific and social working environment, I will miss it deeply. JoAnn Sorrento has been a pillar of administrative support every step of the way that has been greatly appreciated, including her cheerful disposition and candy dish that never goes empty. I would like to thank all of the scientists and researchers that have come before me and made my experience far less painful than those in the past – computers, the internet, modern plastics – have revolutionized the way we live and do research. I would like to thank Genentech for the generous donation of antibodies and the Whitaker Foundation for a graduate fellowship that made this work all the more enjoyable. I would like to thank my friends, both in and outside of MIT for their social and emotional support particularly, my roommates, ultimate Frisbee teammates and competitors and ski buddies. Finally, I extend my deepest thanks to my parents, Ferdinand and Marijke and my brother, Erik for providing love and support through the peaks and valleys of this process. Someday, we will go over all the vocabulary so that you can make sense of this and judge it for yourself.

Table of Contents

Chapter 1: Introduction

Increased complexity brings with it the need for increased control. Generally, the greater the degree of control required in order to maintain 'normal' operation, the greater and more catastrophic the consequences of a failed control operation. For a computer, failed control might be exemplified by the crashing of an application or operating system, for a chemical plant it could mean an explosion, and for the human body, failed control can be exemplified by unregulated cell growth as manifested in cancer. Cancer is possibly the best example of a loss of cellular control and is a pathology that, to a first approximation, has reasonable *in vitro* models allowing its study at the cellular level. In the inanimate realm, the majority of the focus is on creating and implementing control structures to constrain the behavior of complex machinery. Biology, by contrast, currently presents the complementary problem in which aberrant cell behavior, such as cancer, is used to deduce the topology of control structures and understand the engineering design principles guiding cellular behavior. Understanding the mechanisms by which cells maintain or lose control will yield insight into the development of therapeutics to combat aberrant cell behavior in various pathologies. Over the long term, these studies seek to better the ability to fight disease, directly affecting human health and the quality of life.

Regulation of the flow of information – in the form of chemical, electrical and physical stimuli – from the extracellular environment into the cell is at the core of

maintaining normal cell behavior. Receptor tyrosine kinases (RTKs) lie at the interface between the cell and extracellular environment and are one of principle mediators of chemical signals that dictate various aspects of cell behavior, including cell survival, growth, differentiation, and motility. The epidermal growth factor receptor (EGFR) family of RTKs is heavily implicated in a host of cancers, most notably, breast, ovarian, prostate and colon cancer, mostly through over expression (Yarden and Sliwkowski, 2001). It is arguably the best-studied receptor system, as documented in over 15,000 (Pubmed) different papers; yet despite intense investigation, there has been only one anti-cancer therapeutic to be approved by the FDA – Genentech's Herceptin® – that targets an EGFR family member.

The basic fundamentals of the EGFR family, their interaction, signal generation and downstream consequences are extremely well documented in over 1000 (Pubmed) different review articles. Some of those most appropriate to this body of work are listed here:

ErbB/EGF Mini-Review Issue. *Experimental Cell Research*, 284 (2003).

Yarden, Y. and Sliwkowski, M.X. Untangling the ErbB Signaling Network. *Nature Reviews: Molecular Cell Biology* 2: 127-137 (2001).

Yarden, Y. Biology of HER2 and Its Importance in Breast Cancer. *Oncology*, 61 (suppl. 2): 1-13.

Wiley, H.S. and Burke, P.M. Regulation of Receptor Tyrosine Kinase Signaling by Endocytic Trafficking. *Traffic* 2: 12-18 (2001).

Rather than restate the details that have been so comprehensively and deeply covered in these reviews, I will provide some basic EGFR family background followed by a discussion on how this body work is able to complement current methodologies.

1.1 EGFR Family Overview

The EGFR family of RTKs is comprised of four structurally related family members – EGFR/HER1/ErbB1, HER2/ErbB2/neu, HER3/ErbB3 and HER4/ErbB4 – each with a distinct personality. Structurally, each consists of an extracellular ligand-binding domain, a single membrane-spanning domain, and a cytoplasmic domain containing a tyrosine kinase doman and several tyrosine residues, which may become phosphorylated upon receptor activation (Figure 1.1). Each of these receptors binds a subset of the EGF-family ligands: epidermal growth factor (EGF), transforming growth factor-□ (TGF□), heparin-binding EGF-like factor (HB-EGF), amphiregulin (AR), epiregulin (EPR), betacellulin (BTC), the neuregulins (NRGs) (Riese and Stern, 1998) (Figure 1.2). To date, there is no known high-affinity ligand for HER2. Consequently, it relies on lateral-interaction with other family members for its complete activation. Ligand binding stimulates the dimerization of these receptors leading to a wide-array of possible

homo- and heterodimers. Dimerization induces the activation of kinase domains, which lead to the autophosphorylation of cytoplasmic tyrosine residues that serve as docking sites for molecules involved in intracellular signaling cascades. HER3, however, has an inactive kinase domain so that, like HER2, it requires a co-receptor in order to transduce signals. The sum total activity of these signaling cascades in response to receptor activation ultimately affect gene expression and whole cell biologic responses (Figure 1.2).

1.1.1 Structure/Dimerization

Recent crystallographic studies of the extracellular regions of EGFR and HER2 have yielded insight into the mechanisms of their interaction (Cho et al., 2003; Ferguson et al., 2003; Ogiso et al., 2002). The extracellular region of each receptor is made up of four domains, designated I, II, III and IV. The unligated EGFR resides in a conformation stabilized by interactions between domains II and IV which autoinhibit dimerization (Ferguson et al., 2003) (Figure 1.3). Domains I-III are arranged in a C-shape and allow for the docking of EGF between domains I and III, which relieves the autoinhibition. Dimerization of EGF-EGFR complexes occurs through direct receptor-receptor interactions in domain II (Figure 1.4). In contrast with EGFR, the structure of HER2 reveals a fixed conformation, lacking the domain II-IV interaction in non-activated EGFR or HER3 (Cho et al., 2003) (Figure 1.5). Close proximity between domains I and III is seen, resembling a ligand-activated state, as found in structures of EGFR complexed with

EGF or TGF□. This suggests that HER2 is primed for interaction with other receptors and may act solely as a co-receptor without a ligand binding role.

1.1.2 Significance

EGFR family receptors are expressed, either alone or in combination, in a variety of cell types, including those of epithelial, mesenchymal and neuronal origin. Under normal physiology, these receptors play important roles in development, differentiation and proliferation, including wound healing.

In development, null mutations of the individual EGFR family receptors are lethal. Loss of EGFR results in lethality with mice showing abnormalities in the brain, skin, lung and gastrointestinal tract. HER2 or HER4 knockout mice die due to trabeculae malformation in the heart. When HER3 is knocked out, mice display defective heart valve formation. In addition to role of HER2 and HER3 in cardiac development, they have also been shown to be involved in glial and neuronal cell development as well as mammary gland development (Olayioye et al., 2000).

In the adult organism, all EGFR family members play a role in normal function of the mammary gland. EGFR function promotes ductal growth during mammary gland development while HER2 and HER4 are involved in lobuloalveolar differentiation and lactation. The precise function of HER3 in the mammary gland has not been investigated. Further, EGFR family receptors are basolaterally located on the epithelium allowing them to mediate signaling between the mesenchyme and epithelium for cell growth (Stern, 2003).

Disruption of the normal behavior of EGFR family receptors, through over expression of receptors, ligands, or other means, can result in unregulated signaling that has been heavily implicated in the formation of a variety of cancers (Table 1.1). In particular, HER2 is over-expressed in approximately one-third of breast and ovarian cancers and has been negatively correlated with patient prognoses (Hamilton and Piccart, 2000; Menard et al., 2001; Slamon et al., 1987). In addition to its clinical presence as a prognostic factor, HER2 overexpression has been shown to contribute to cell transformation, anchorage-independent cell growth, increased proliferation and mitogenic sensitivity, as well as increase tumor cell migration and invasiveness (Brandt et al., 1999; Chazin et al., 1992; DiFiore et al., 1987; Ignatoski et al., 1999; Spencer et al., 2000; Wiechen et al., 1999; Wright et al., 1989; Yu and Hung, 2000).

1.3 EGFR Family Signaling

The EGFR family represents one possible input into an intricate signaling and regulatory network with complexity at several, highly intertwined levels, including ligand binding, receptor dimerization, receptor trafficking and signal recruitment. With four distinct interacting receptors and more than 10 EGFR family ligands there is a combinatorial explosion of possible dimers feeding into the ERK, PLCγ, P13K and other pathways (see Figure 1.2). The amplitude, duration and quality of signals generated by a given ligand are complex functions of receptor activation states, quantities and locations, as determined by their intracellular trafficking. Altering the expression level of a single

receptor, such as EGFR or HER2, is able to simultaneously perturb each of these processes.

Receptor phosphorylation following ligand binding and dimerization stimulates the recruitment of a repertoire signaling molecules by both EGFR and HER2. EGFR complex homodimers and EGF-EGFR/HER2 heterodimers associate with many of the same signaling molecules including Src, Shc, PLC□, Sos, Grb2, Grb7 and Crk (Alroy and Yarden, 1997; Yarden, 2001). However, controlled dimerization of these receptors and other studies has shown evidence for differential signaling between homodimers and heterodimers. For example, c-Cbl is able to associate with homodimers, but unable to associate with heterodimers (Muthuswamy et al., 1999; Olayioye et al., 1998). Heterodimers were also found to have an increased proliferative capacity and focus forming ability than homodimers (Muthuswamy et al., 1999; Pinkas-Kramarski et al., 1996).

Among the pathways common to both the EGFR and HER2, the ERK MAP kinase (MAPK) pathway is implicated in cell proliferation and tumor progression. The ERK cascade is a central element in transducing and processing signals from the cell surface to the nucleus. Molecular details of this cascade are diagrammed in Figure 1.2. Overexpression of HER2 has been shown to potentiate and prolong EGF induced ERK activation (Graus-Porta et al., 1995; Karunagaran et al., 1996).

Activated receptors recruit cascades of intracellular signaling molecules, including members of the Ras/MAPK and PLC-□pathways that control a diverse range of cell responses. The signals that are recruited depend heavily on receptor location. For

example, PLC-□, calpain, and Grb2, are primarily activated or recruited by surface EGFR, while Eps8 is associated with only intracellular receptors and the Ras pathway may be activated by both surface and intracellular EGFR (Burke et al., 2001; Glading et al., 2001; Haugh et al., 1999a; Haugh et al., 1999b).

Receptor overexpression could potentially influence cell behavior in multiple ways. The presence of excess receptors could recruit additional signaling molecules, resulting in an increase in signal amplitude. Alternatively, excess receptors could saturate and interfere with processes involved in receptor down-regulation and signal attenuation (French et al., 1994; Wiley, 1988). This second phenomenon is a receptor trafficking effect that may affect the duration of the signaling by interfering with receptor degradation and ligand dissociation. For example, in addition to the signal amplification role played by elevated HER2 expression, HER2 also affects the normal trafficking behavior of the EGFR, disrupting the processes that control receptor degradation (Worthylake et al., 1999).

1.4 EGFR Family Trafficking

Intracellular receptor trafficking is responsible for the short and long-term down-regulation of receptor number from the cell surface in response to ligand stimulation as well as determining the distribution of receptors and ligands between surface and internal compartments. It is principally composed of two steps: (i) internalization, wherein ligand binding stimulates clathrin coated pit endocytosis to early endosomal sorting compartment inside of the cell, and (ii) endosomal sorting, wherein receptors and ligands

are either targeted for lysosomal degradation or recycled to the surface for successive rounds of trafficking , diagrammed in Figure 1.6 (Burke et al., 2001; Carpenter, 2000). Both steps are subject to interference by over expression of EGFR or HER2 (Hendriks et al., 2003a (Chapter 2); Worthylake et al., 1999).

Studies have shown the trafficking defects in receptors can facilitate cell transformation (Wells et al., 1990), suggesting that signal duration may be more of a determining factor in mitogenic sensitivity than signal amplitude, particularly at physiological ligand concentrations. Overexpression or mutation of the EGFR has been shown to impair down-regulation, as a consequence of altered trafficking, indicating the importance of proper trafficking for the normal regulation of cell growth (Vieira et al., 1996; Wells et al., 1990). It appears likely that receptor expression levels are directly connected to their trafficking behavior, which, in turn, affects signaling.

1.4.1 EGFR Trafficking

The trafficking behavior of the EGFR, in the absence of other family members, has been well-characterized (Wiley and Burke, 2001). EGF binding initiates the rapid internalization of EGF-EGFR complexes via clathrin coated pit endocytosis to early endosomal compartments. This process can be saturated in cases where surface complex number exceeds the capacity of the adaptor proteins involved in receptor-mediated endocytosis (Lund et al., 1990; Wiley, 1988). Dimerization with other EGFR family members is also thought to slow this process as HER2, HER3 and HER4 all exhibit some

degree of endocytic impairment (Baulida et al., 1996; Hendriks et al., 2003b (Chapter 3); Sorkin et al., 1993; Wang et al., 1999).

The postendocytic trafficking of the EGFR is mediated through the selective retention of occupied receptors via a di-leucine motif in the juxtamembrane region (Kil and Carlin, 2000; Kil et al., 1999). The endosomal retention of occupied receptors has been demonstrated to be both specific and saturable, requiring cytoplasmic sequences for efficient retention and lysosomal targeting, but independent of intrinsic tyrosine kinase ability (French et al., 1994; Herbst et al., 1994; Opresko et al., 1995; Wiley et al., 1991). Two regions of the EGFR, residues 1022-1063 and, to a lesser extent, 1063-1123, are believed to contribute in targeting receptors to the degradative pathway (Kornilova et al., 1996). Additionally, EGFR residues 943-957 are known to interact with SNX1, a putative endosomal sorting protein believed to be involved in targeting EGFR to degradative fates (Kurten et al., 1996; Zhong et al., 2002). EGFR deactivation and degradation also vary with the sorting behavior of different ligands (EGF vs. TGF) (French et al., 1995).

Ligand stimulus also results in EGFR mediated phosphorylation of c-Cbl, a protein involved in the ubiquitination and degradation of EGFR. Overexpression of c-Cbl enhances ubiquitination and degradation of EGFR, while oncogenic viral Cbl interferes with the sorting function of c-Cbl, directing EGFR to recycling fates (Levkowitz et al., 1999; Levkowitz et al., 1998). Interestingly, c-Cbl does not interact with other EGFR family members, including HER2 (Levkowitz et al., 1996).

Elevated EGFR expression may interfere with efficient endosomal sorting towards degradation through the saturation of limited quantities of sorting machinery involved in these processes (French et al., 1994; Lund et al., 1990; Wiley, 1988).

1.4.2 HER2 Trafficking

The precise trafficking behavior of HER2 remains unclear. The internalization rate of HER2, HER3 and HER4 have been studied through the construction of chimeras consisting of the EGFR extracellular domain and different HER cytoplasmic domains. All EGFR/ErbB chimeras are internalized several fold more slowly than the EGFR (Baulida et al., 1996; Muthuswamy et al., 1999; Sorkin et al., 1993). EGF induced HER2 down-regulation has also been reported (Worthylake et al., 1999). However, other investigators have failed to observe any EGF-induced HER2 internalization or EGFR-HER2 internalization (Wang et al., 1999).

HER2 expression has been shown to shunt ligand-activated receptors to recycling fates suggesting that receptor heterodimer species may have superior signaling potency as a consequence of their altered intracellular routing (Lenferink et al., 1998; Waterman et al., 1998).

The intimate interaction between the EGFR and HER2 should result in reciprocal effects on the trafficking of both receptors when either is over-expressed. Overexpression of HER2 has been demonstrated to inhibit down-regulation of the EGFR and of itself, as well as increase the fraction of EGF recycled (Worthylake et al., 1999).

1.4.3 HER3/HER4 Trafficking

Little is known about the trafficking behavior of HER3 or HER4. Studies using EGFR/HER3 or EGFR/HER4 chimeras have lead to the conclusion that their internalization is impaired relative to that of the native EGFR (Baulida et al., 1996). In general, the lack of experimental reagents has impeded their study. In the context of EGF-induced signaling these receptors play a passive role and have very minimal involvement. They are, however, proving to be of tremendous importance in the study of HRG signaling as HER2/HER3 heterodimers are believed to have the strongest signaling ability of all possible EGFR family dimer species as gauged by a proliferative index (Pinkas-Kramarski et al., 1996).

1.5 Perspective

The clinical and biological prominence of the EGFR family underscores the importance of its study. The first studies of receptor systems began with the notion of linear signaling pathways implying that one ligand would bind one receptor, inducing one output. Over the past 10 years or so it has become apparent that multiple receptors feed into multiple, overlapping signaling pathways and cell responses represent the integration of various stimuli over various timescales. As our scope broadens to include several interacting receptors, their mutual trafficking and signaling crosstalk, it becomes increasingly difficult to predict and, perhaps more importantly, interpret cell behavior in a multi-parameter space. Clearly, when one considers a ‘systems’ view of the components

of a cell it will be desirable, and frequently necessary, to apply computational methodologies in order to understand various non-linear phenomena. A natural accompaniment to these methodologies, for both their development and validation, are rigorous and quantitative experimental techniques.

The EGFR family has complexity at many levels and time scales including, but not limited to, ligand binding, receptor dimerization, trafficking and signal recruitment. The EGFR has long been a model system for the development of mathematical trafficking models (Wiley et al., 2003) and has recently also been used for the modeling of signal transduction cascades (Kholodenko et al., 1999; Schoeberl et al., 2002). Until now, however, there has not been any such work examining the interaction of EGFR and HER2 in the context of these trafficking and signaling phenomena. This is in part due to a lack of mechanistic information and quantitative parameter values in these processes, both of which are addressed in this work. Specifically, we have utilized a combined experimental and modeling approach to dissect trafficking and signaling phenomena in order to quantitatively understand the role of HER2 in signal generation through the EGFR.

The structure of this body of work is shown in Figure 1.7. Chapter 2 details the development and validation of a general receptor trafficking model to describe the overall trafficking of EGFR and HER2 with a minimal amount of mechanistic detail. Chapter 3 explores the precise mechanisms that lead to observed characteristics in EGFR and HER2 internalization including the estimation of rate constants critical to these processes. Chapter 4 examines the biophysical basis for HER2 effects on EGFR endosomal sorting.

Finally, Chapter 5 synthesizes the models from Chapter 2 and Chapter 3 into a comprehensive trafficking model and applies it to the analysis of quantitative signaling data.

1.6 Tables

Table 1.1: Expression of EGFR Family Members and Their Ligands in Cancer*

Molecule	Nature of dysregulation	Type of cancer	Notes
Ligands			
TGF-□	Overexpression	Prostate	Expressed by stroma in early, adrogen-dependent prostate cancer and by tumors in advanced, androgen-independent cancer
	Overexpression	Pancreatic	Correlates with tumor size and decreased patient survival; may be due to overexpression of Ki-Ras, which also drives expression of HB-EGF and NRG1
	Overexpression	Lung, ovary, colon	Correlates with poor prognosis when co-expressed with EGFR
NRG1	Overexpression	Mammary adeno-carcinomas	Necessary, but not sufficient for tumorigenesis in animal models
Receptors			
EGFR	Overexpression	Head and neck, breast, bladder, prostate, kidney, non-small-cell lung cancer	Significant indicator for recurrence in operable breast tumors; associated with shorter diseases-free and overall survival in advanced breast cancer; may serve as a prognostic marker for bladder, prostate and non-small-cell lung cancer
	Overexpression	Glioma	Amplification occurs in 40% of gliomas; overexpression correlates with higher grade and reduced survival
	Mutation	Glioma, lung, ovary, breast	Deletion of part of the extracellular domain yields a constitutively active receptor
HER2	Overexpression	Breast, lung, pancreas, colon, esophagus, endometrium, cervix	Overexpressed owing to gene amplifcation in 15-30% of invasive ductatl breast cancers. Overexpression correlates with tumor size, spread of the tumor to lymph nodes, high grade, high percentage of S-phase cells, aneuploidy and lack of steroid hormone receptors
HER3	Expression	Breast, colon, gastric, prostate, other carcinomas	Co-expression of HER2 with EGFR or HER3 in breast cancer improves predicting power
	Overexpression	Oral squamous cell cancer	Overexpression correlates with lymph node involvement in patient survival
HER4	Reduced expression	Breast, prostate	Correlates with a differentiated phenotype
	Expression	Childhood medulloblastoma	Co-expression with HER2 has a prognostic value

*Taken directly from Yarden and Sliwkowski, 2001.

1.7 Figures

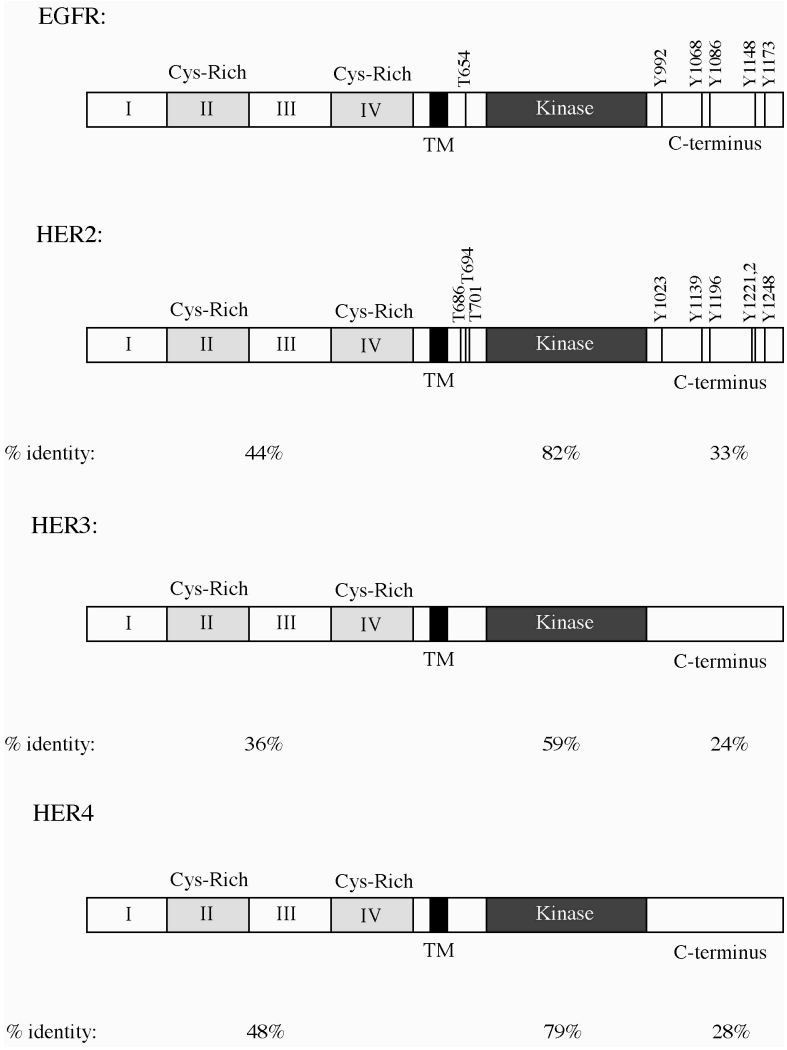

Figure 1.1 EGFR Family Receptors.

Structure of EGFR family receptors is diagrammed with extracellular domains including cysteine-rich domains, trans-memebrane domain, kinase domain and C-terminal domain indicated by boxes. Potential phosphorylation sites are indicated as vertical lines for EGFR and HER2. Figure adapted from adapted from Earp et al., 1995; Hynes and Stern, 1994; Wells, 1999.

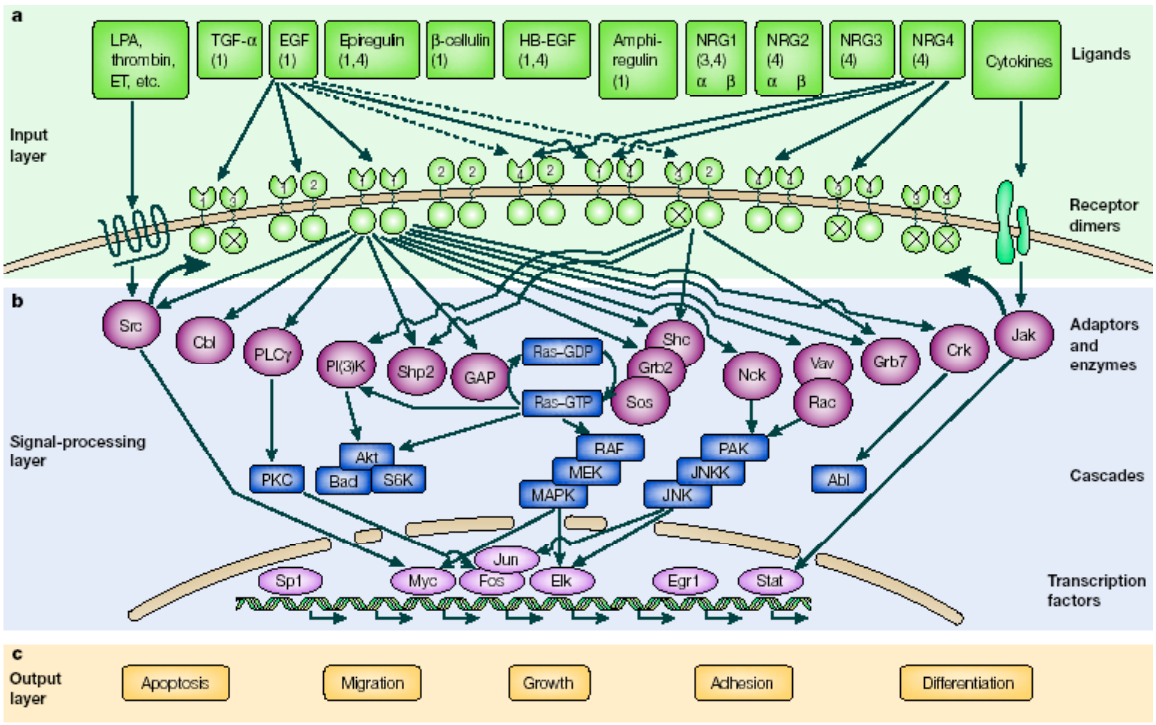

Figure 1.2 EGFR Family Signaling Network.

Input into the cell consists of ten dimeric receptor combinations with their associated ligands. Ligand specificities are shown for only EGF and NRG for simplicity. HER2 binds no known ligand with high affinity and HER3 homodimers are catalytically inactive. Signaling to the adaptor/enzyme layer is shown for two possible dimers. Only some of the signaling pathways and molecules are shown for simplicity. How transcription factors and pathways are translated into cellular outputs is poorly understood at present. Figure taken directly from Yarden and Sliwkowski, 2001.

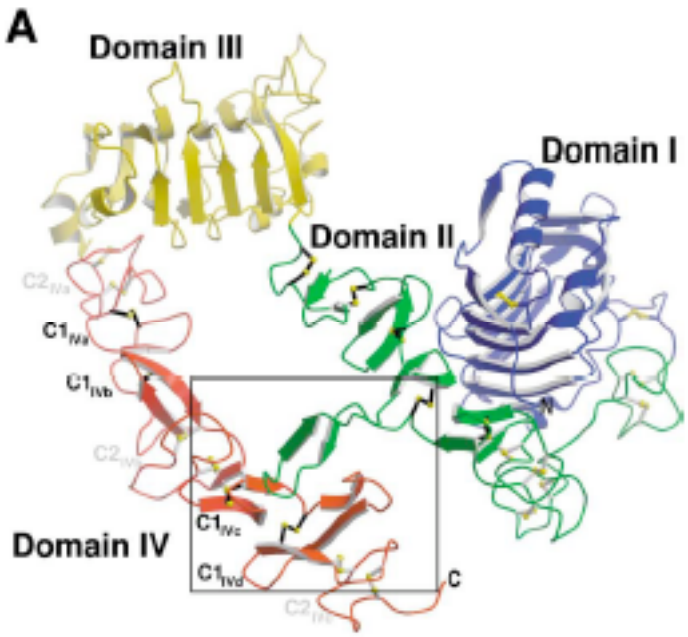

Figure 1.3 EGFR Structure.

Ribbon diagram of extracellular domain of EGFR. Domains I, II, III and IV are colored blue, green, yellow and red, respectively. Boxed region details autoinhibitory interactions between domains II and IV. Figure taken directly from Ferguson et al., 2003.

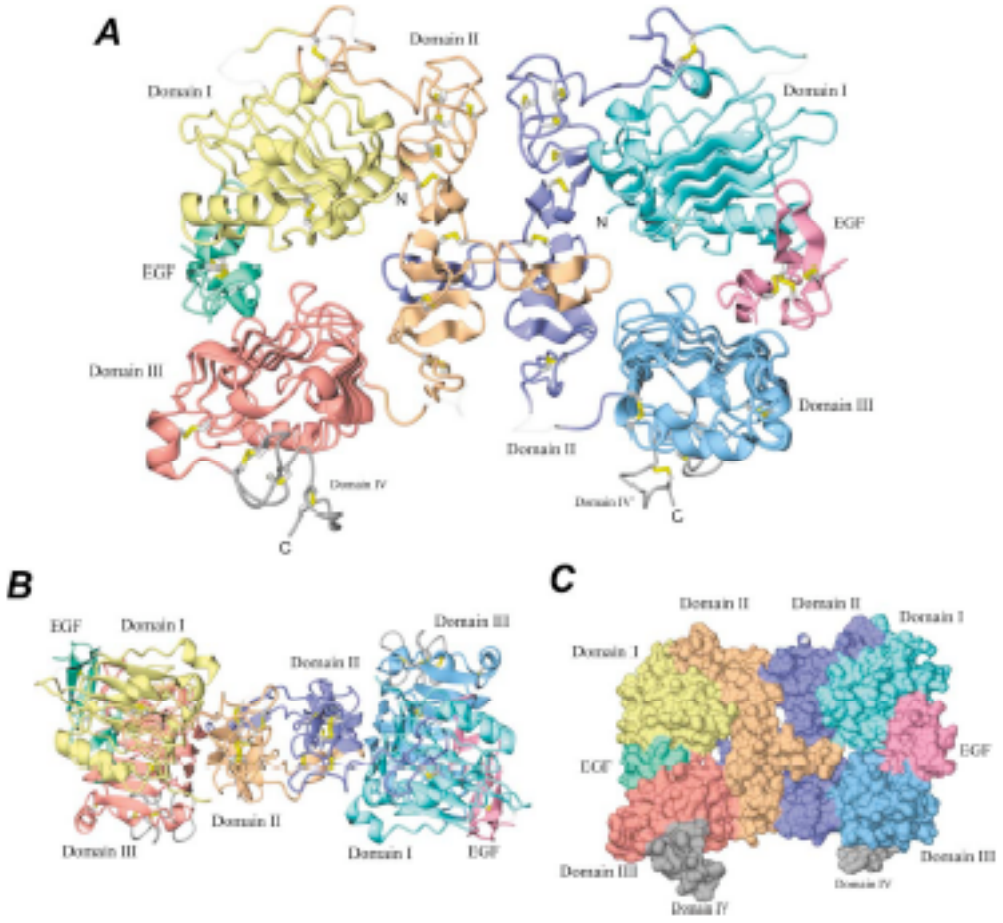

Figure 1.4 EGF-EGFR Complex Structure.

A, ribbon diagram of crystal structure of 2:2 EGF-EGFR complexes. One EGF chain in the 2:2 EGF-EGFR complex is pale green, and the other EGF chain is pink. Domains I, II, III and IV in one receptor are colored yellow, orange, red and gray, respectively and cyan, dark blue, pale blue and gray, respectively in the other receptor. *B*, top view of *A*. *C*, surface model corresponding to *A*. Figure taken directly from Ogiso et al., 2002.

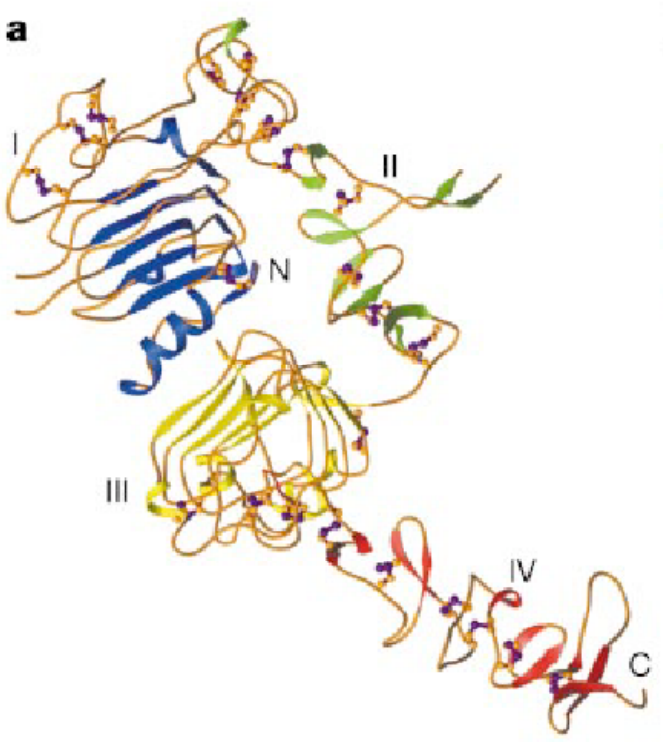

Figure 1.5 HER2 Structure.

Ribbon diagram of the structure of the extracellular domain of HER2. Domains I, II, III and IV are colored blue, green, yellow and red, respectively. Figure taken directly from Cho et al., 2003.

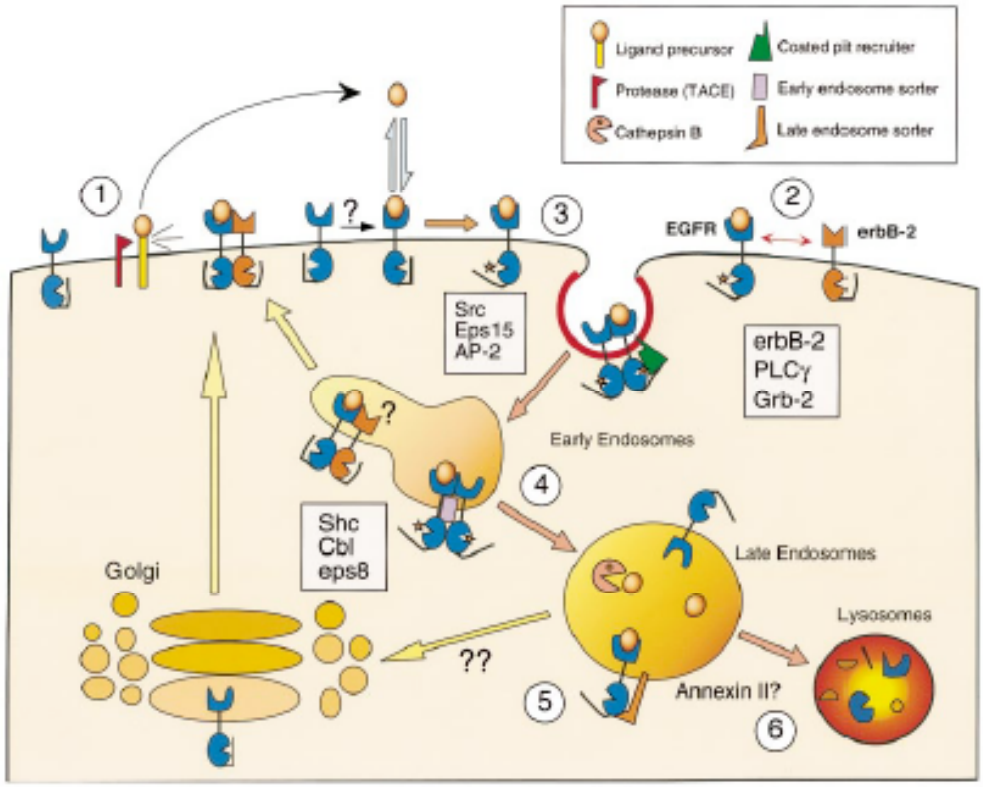

Figure 1.6 EGFR Family Intracellular Trafficking.

Intracellular trafficking of EGFR family receptors is tightly regulated. ① Ligands for the EGFR are produced by regulated proteolysis, usually by an autocrine mechanism. ② Ligand binding activates surface EGFRs resulting in heterodimerization with HER2 and activation of a specific set of surface-restricted signaling partners. ③ EGFR to bind to a coated pit complex that could include Eps15 and AP-2. ④ EGFR is rapidly sorted from early endosomes through binding of the di-leucine motif of the juxtamembrane domain to an unknown sorting protein. Heterodimerization with HER2 has been reported to interfere with sorting, leading to EGFR recycling. The internalized receptor is still active and carries along many signaling proteins, such as Shc. Other regulatory proteins, such as

Cbl, preferentially associate with the EGFR within endosomes. ⑤ Inside the late endosomes, the receptor can associate with a distinct sorting complex, which may involve sorting nexin (SNX) proteins. This interaction may be facilitated by ubiquinitation and perhaps by Annexin II. Otherwise, the receptor is recycled back to the cell surface. ⑥ Dissociated ligands are degraded within either endosomes or lysosomes. Although receptors are generally thought to be degraded within lysosomes, the proteosome may also play a role. Figure taken directly from Wiley and Burke, 2001.

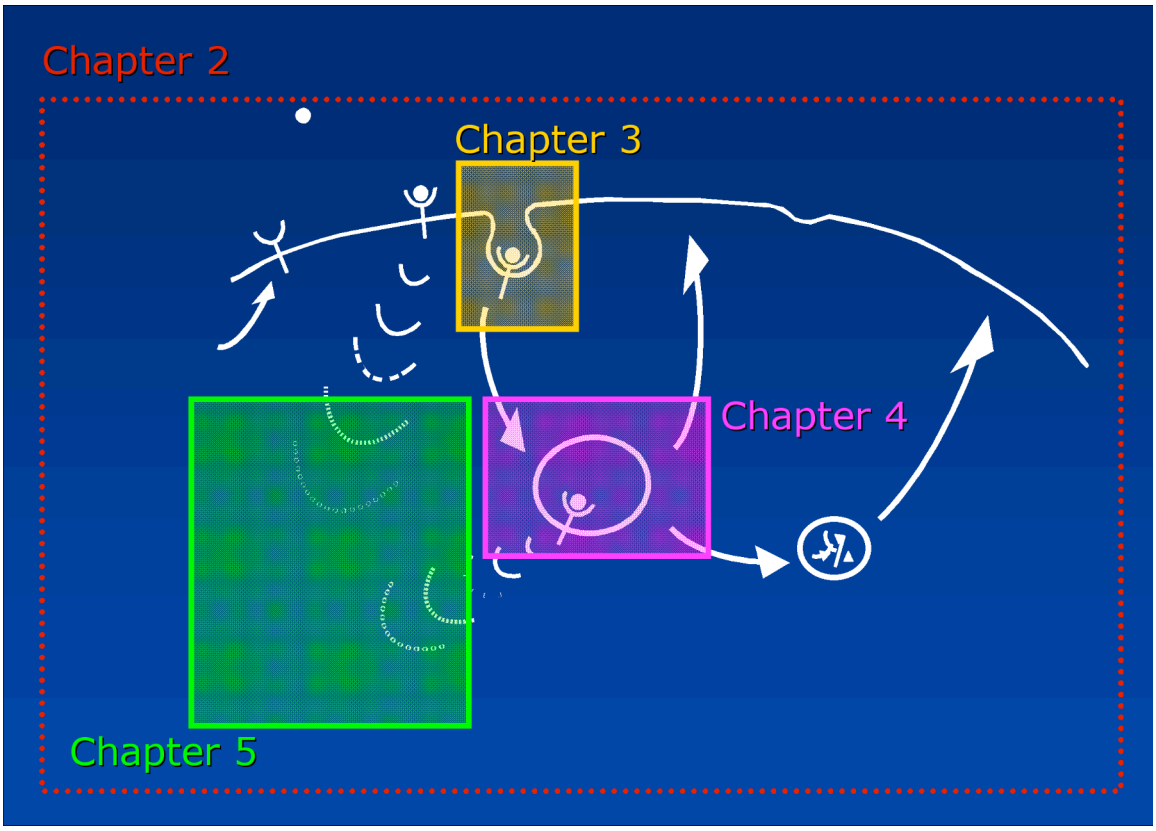

Figure 1.7 Thesis Chapter Overview.

Chapter 2 describes the overall trafficking behavior of EGFR and HER2. Chapters 3 and 4 focus on the detailed aspects of internalization and recycling, respectively. Chapter 5 considers the downstream signaling consequences of the combined effect of all trafficking phenomena.

1.8 References

Alroy, I. and Yarden, Y. (1997) The ErbB signaling network in embryogenesis and oncogenesis: signal diversification through combinatorial ligand-receptor interactions. *Federation of European Biological Sciences Letters*, **410**, 83-86.

Baulida, J., Kraus, M.H., Alimandi, M., DiFiore, P.P. and Carpenter, G. (1996) All ErbB Receptors Other Than the Epidermal Growth Factor Receptor Are Endocytosis Impaired. *The Journal of Biological Chemistry*, **271**, 5251-5257.

Brandt, B.H., Roetger, A., Dittmar, T., Nikolia, G., Seeling, M., Merschjann, A., Nofer, J.-R., Dehmer-Moller, G., Junker, R., Assmann, G. and Zaenker, K. (1999) c-erbB-2/EGFR as dominant heterodimerization partners determine a motogenic phenotype in human breast cancer cells. *The FASEB Journal*, **13**, 1939-1950.

Burke, P.M., Schooler, K. and Wiley, H.S. (2001) Regulation of Epidermal Growth Factor Receptor Signaling by Endocytosis and Intracellular Trafficking. *Molecular Biology of the Cell*, **12**, 1897-1910.

Carpenter, G. (2000) The EGF receptor: a nexus for trafficking and signaling. *BioEssays*, **22**, 697-707.

Chazin, V.R., Kaleko, M., Miller, A.D. and Slamon, D.J. (1992) Transformation mediated by the human HER-2 gene independent of the epidermal growth factor receptor. *Oncogene*, **7**, 1859-1866.

Cho, H.S., Mason, K., Ramyar, K.X., Stanley, A.M., Gabelli, S.B., Denney, D.W., Jr. and Leahy, D.J. (2003) Structure of the extracellular region of HER2 alone and in complex with the Herceptin Fab. *Nature*, **421**, 756-760.

DiFiore, P.P., Pierce, J.H., Kraus, M.H., Segatto, O., King, C.R. and Aaronson, S.A. (1987) erbB-2 Is a Potent Oncogene When Overexpressed in NIH/3T3 Cells. *Science*, **237**, 178-182.

Earp, H.S., Dawson, T.L., Li, X. and Yu, H. (1995) Heterodimerization and function interaction between EGF receptor family members: A new signaling paradigm with implications for breast cancer research. *Breast Cancer Research and Treatment*, **35**, 115-132.

Ferguson, K.M., Berger, M.B., Mendrola, J.M., Cho, H.S., Leahy, D.J. and Lemmon, M.A. (2003) EGF activates its receptor by removing interactions that autoinhibit ectodomain dimerization. *Mol Cell*, **11**, 507-517.

French, A.R., Sudlow, G.P., Wiley, H.S. and Lauffenburger, D.A. (1994) Postendocytic Trafficking of Epidermal Growth Factor-Receptor Complexes Is Mediated through Saturable and Specific Endosomal Interactions. *The Journal of Biological Chemistry*, **269**, 15749-15755.

French, A.R., Tadaki, D.K., Niyogi, S.K. and Lauffenburger, D.A. (1995) Intracellular Trafficking of Epidermal Growth Factor Family Ligands Is Directly Influenced by the pH Sensitivity of the Receptor/Ligand Interaction. *The Journal of Biological Chemistry*, **270**, 4334-4340.

Glading, A., Uberall, F., Keyse, S.M., Lauffenburger, D.A. and Wells, A. (2001) Membrane Proximal ERK Signaling Is Required for M-calpain Activation Downstream of Epidermal Growth Factor Receptor Signaling. *The Journal of Biological Chemistry*, **276**, 23341-23348.

Graus-Porta, D., Beerli, R.R. and Hynes, N.E. (1995) Single-Chain Antibody-Mediated Intracellular Retention of ErbB-2 Impairs Neu Differentiation Factor and Epidermal Growth Factor Signaling. *Molecular and Cellular Biology*, **15**, 1182-1191.

Hamilton, A. and Piccart, M. (2000) The contribution of molecular markers to the prediction of response in the treatment of breast cancer: A review of the literature on HER-2, p53 and BCL-2. *Annals of Oncology*, **11**, 647-663.

Haugh, J.M., Huang, A.C., Wiley, H.S., Wells, A. and Lauffenburger, D.A. (1999a) Internalized Epidermal Growth Factor Receptors Participate in the Activation of p21ras in Fibroblasts. *The Journal of Biological Chemistry*, **274**, 34350-34360.

Haugh, J.M., Schooler, K., Wells, A., Wiley, H.S. and Lauffenburger, D.A. (1999b) Effect of Epidermal Growth Factor Receptor Internalization on Regulation of the Phospholipase C-g1 Signaling Pathway. *The Journal of Biological Chemistry*, **274**, 8958-8965.

Hendriks, B.S., Opresko, L.K., Wiley, H.S. and Lauffenburger, D.A. (2003a) Co-Regulation of EGFR/HER2 Levels and Locations: Quantitative Analysis of HER2 Overexpression Effects. *Cancer Research*, **63**, 1130-1137.

Hendriks, B.S., Opresko, L.K., Wiley, H.S. and Lauffenburger, D.A. (2003b) Quantitative Analysis of HER2-mediated Effects on HER2 and EGFR Enodcytosis: Distribution of Homo- and Hetero-dimers Depends on Relative HER2 Levels. *The Journal of Biological Chemistry*, **278**, 23343-23351.

Herbst, J.J., Opresko, L.K., Walsh, B.J., Lauffenburger, D.A. and Wiley, H.S. (1994) Regulation of Postendocytic Trafficking of the Epidermal Growth Factor Receptor Through Endosomal Retention. *The Journal of Biological Chemistry*, **269**, 12865-12873.

Hynes, N.E. and Stern, D.F. (1994) The biology of erbB-2/neu/HER-2 and its role in cancer. *Biochimica et Biophysica Acta*, **1198**, 165-184.

Ignatoski, K.M.W., Lapointe, A.J., Radany, E.H. and Ethier, S.P. (1999) erbB-2 Overexpression in Human Mammary Epithelial Cells Confers Growth Factor Independence. *Endocrinology*, **140**, 3615-3622.

Karunagaran, D., Tzahar, E., Beerli, R.R., Chen, X., Graus-Porta, D., Ratzkin, B.J., Seger, R., Hynes, N.E. and Yarden, Y. (1996) ErbB-2 is a common auxiliary subunit of NDF and EGF receptors: implications for breast cancer. *The European Molecular Biology Organization Journal*, **15**, 254-264.

Kholodenko, B.N., Demin, O.V., Moehren, G. and Hoek, J.B. (1999) Quantification of Short Term Signaling by the Epidermal Growth Factor Receptor. *The Journal of Biological Chemistry*, **274**, 30169-30181.

Kil, S.J. and Carlin, C. (2000) EGF Receptor Residues Leu679, Leu680 Mediate Selective Sorting of Ligand-Receptor Complexes in Early Endosomal Compartments. *Journal of Cellular Physiology*, **185**, 47-60.

Kil, S.J., Hobert, M. and Carlin, C. (1999) A leucine-based determinant in the epidermal growth factor receptor juxtamembrane domain is required for the efficient transport of ligand-receptor complexes to lysosomes. *The Journal of Biological Chemistry*, **274**, 3141-3150.

Kornilova, E.S., Sorkina, T., Beguinot, L. and Sorkin, A. (1996) Lysosomal Targeting of Epidermal Growth Factor Receptors via a Kinase-dependent Pathway Is Mediated by the Receptor Carboxyl-terminal Residues 1022-1123. *The Journal of Biological Chemistry*, **271**, 30340-30346.

Kurten, R.C., Cadena, D.L. and Gill, G.N. (1996) Enhanced Degradation of EGF Receptors by a Sorting Nexin, SNX1. *Science*, **272**, 1008-1010.

Lenferink, A.E.G., Pinkas-Kramarski, R., Poll, M.L.M.v.d., Vugt, M.J.H.v., Klapper, L.N., Tzahar, E., Waterman, H., Sela, M., Zoelen, E.J.J.v. and Yarden, Y. (1998) Differential endocytic routing of homo- and hetero-dimeric ErbB tyrosine kinases confers signaling superiority to receptor heterodimers. *The European Molecular Biology Organization Journal*, **17**, 3385-3397.

Levkowitz, G., Klapper, L.N., Tzahar, E., Freywald, A., Sela, M. and Yarden, Y. (1996) Coupling of the c-Cbl protooncogene product to ErbB-1/EGF-receptor but not to other Erbb proteins. *Oncogene*, **12**, 1117-1125.

Levkowitz, G., Waterman, H., Ettenberg, S.A., Katz, M., Tsygankov, A.Y., Alroy, I., Lavi, S., Iwai, K., Reiss, Y., Ciechanover, A., Lipkowitz, S. and Yarden, Y. (1999) Ubiquitin Ligase Activity and Tyrosine Phosphorylation Underlie Suppression of Growth Factor Signaling by c-Cbl/Sli-1. *Molecular Cell*, **4**, 1029-1040.

Levkowitz, G., Waterman, H., Zamir, E., Kam, Z., Oved, S., Langdon, W.Y., Beguinot, L., Geiger, B. and Yarden, Y. (1998) c-Cbl/sli-1 regulates endocytic sorting and ubiquitination of the epidermal growth factor receptor. *Genes & Development*, **12**, 3663-3674.

Lund, K.A., Opresko, L.K., Starbuck, C., Walsh, B.J. and Wiley, H.S. (1990) Quantitative Analysis of the Endocytic System Involved in Hormone-induced Receptor Internalization. *The Journal of Biological Chemistry*, **265**, 15713-15723.

Menard, S., Casalini, P., Campiglio, M., Pupa, S., Agresti, R. and Tagliabue, E. (2001) HER2 overexpression in various tumor types, focussing on its relationship to the development of invasive breast cancer. *Annals of Oncology*, **12**, S15-S19.

Muthuswamy, S., Gilman, M. and Brugge, J.S. (1999) Controlled Dimerization of ErbB Receptors Provides Evidence for Differential Signaling by Homo- and Heterodimers. *Molecular and Cellular Biology*, **19**, 6845-6957.

Ogiso, H., Ishitani, R., Nureki, O., Fukai, S., Yamanaka, M., Kim, J.H., Saito, K., Sakamoto, A., Inoue, M., Shirouzu, M. and Yokoyama, S. (2002) Crystal structure of the complex of human epidermal growth factor and receptor extracellular domains. *Cell*, **110**, 775-787.

Olayioye, M.A., Graus-Porta, D., Beerli, R.R., Rohrer, J., Gay, B. and Hynes, N.E. (1998) ErbB-1 and ErbB-2 Acquire Distinct Signaling Properties Dependent upon Their Dimerization Partner. *Molecular and Cellular Biology*, **18**, 5042-5051.

Olayioye, M.A., Neve, R.M., Lane, H.A. and Hynes, N.E. (2000) The ErbB signaling network: receptor heterodimerization in development and cancer. *Embo J*, **19**, 3159-3167.

Opresko, L., Chang, C., Will, B., Burke, P.M., Gill, G.N. and Wiley, H.S. (1995) Endocytosis and lysosomal targeting of epidermal growth factor receptors are mediated by distinct sequences independent of tyrosine kinase domain. *The Journal of Biological Chemistry*, **270**, 4325-4333.

Pinkas-Kramarski, R., Soussan, L., Waterman, H., Levkowitz, G., Alroy, I., Klapper, L., Lavi, S., Seger, R., Ratzkin, B.J., Sela, M. and Yarden, Y. (1996) Diversification of Neu differentiation factor and epidermal growth factor signaling by combinatorial receptor interactions. *The European Molecular Biology Organization Journal*, **15**, 2452-2467.

Riese, D.J. and Stern, D.F. (1998) Specificity within the EGF family/ErbB receptor family signaling network. *BioEssays*, **20**, 41-48.

Schoeberl, B., Eichler-Jonsson, C., Gilles, E.D. and Muller, G. (2002) Computational modeling of the dynamics of the MAP kinase cascade activated by surface and internalized EGF receptors. *Nature Biotechnology*, **20**, 370-375.

Slamon, D.J., Clark, G.M., Wong, S.G., Levin, W.J., Ullrich, A. and McGuire, W.L. (1987) Human Breast Cancer: Correlation of Relapse and Survival with Amplification of the HER-2/neu Oncogene. *Science*, **235**, 177-182.

Sorkin, A., DiFiore, P.P. and Carpenter, G. (1993) The carboxyl terminus of epidermal growth factor receptor/erbB-2 chimerae is internalization impaired. *Oncogene*, **8**, 3021-3028.

Spencer, K.S.R., Graus-Porta, D., Leng, J., Hynes, N. and Klemke, R.L. (2000) ErbB2 Is Necesary for Induction of Carcinoma Cell Invasion by ErbB Family Receptor Tyrosine Kinases. *The Journal of Cell Biology*, **148**, 385-397.

Stern, D.F. (2003) ErbBs in mammary development. *Exp Cell Res*, **284**, 89-98.

Vieira, A.V., Lamaze, C. and Schmid, S.L. (1996) Control of EGF Receptor Signaling by Clathrin-Mediated Endocytosis. *Science*, **274**, 2086-2089.

Wang, Z., Zhang, L., Yeung, T.K. and Chen, X. (1999) Endocytosis Deficiency of Epidermal Growth Factor (EGF) Receptor-ErbB2 Heterodimers in Response to EGF Stimulation. *Molecular Biology of the Cell*, **10**, 1621-1636.

Waterman, H., Sabanai, I., Geiger, B. and Yarden, Y. (1998) Alternative Intracellular Routing of ErbB Receptors May Determine Signaling Potency. *The Journal of Biological Chemistry*, **273**, 13819-13827.

Wells, A. (1999) Molecules in focus: EGF receptor. *The International Journal of Biochemistry and Cell Biology*, **31**, 637-643.

Wells, A., Welsh, J.B., Lazar, C.S., Wiley, H.S., Gill, G.N. and Rosenfeld, M.G. (1990) Ligand-Induced Transformation by a Noninternalizing Epidermal Growth Factor Receptor. *Science*, **247**, 962-964.

Wiechen, K., Karaaslan, S. and Dietel, M. (1999) Involvement of the c-erbB-2 Oncogene Product in the EGF-Induced Cell Motility of SK-OV-3 Ovarian Cancer Cells. *International Journal of Cancer*, **83**, 409-411.

Wiley, H.S. (1988) Anomalous Binding of Epidermal Growth Factor to A431 Cells is Due to the Effect of High Receptor Densities and a Saturable Endocytic System. *The Journal of Cell Biology*, **107**, 801-810.

Wiley, H.S. and Burke, P.M. (2001) Regulation of Receptor Tyrosine Kinase Signaling by Endocytic Trafficking. *Traffic*, **2**, 12-18.

Wiley, H.S., Herbst, J.J., Walsh, B.J., Lauffenburger, D.A., Rosenfeld, M.G. and Gill, G.N. (1991) The Role of Tyrosine Kinase Activity in Endocytosis, Compartmentation, and Down-regulation of the Epidermal Growth Factor Receptor. *The Journal of Biological Chemistry*, **266**, 11083-11094.

Wiley, H.S., Shvartsman, S.Y. and Lauffenburger, D.A. (2003) Computational modeling of the EGF-receptor system: a paradigm for systems biology. *Trends in Cell Biology*, **13**, 43-50.

Worthylake, R., Opresko, L.K. and Wiley, H.S. (1999) ErbB-2 Amplification Inhibits Down-regulation and Induces Constitutive Activation of Both ErbB-2 and Epidermal Growth Factor Receptors. *The Journal of Biological Chemistry*, **274**, 8865-8874.

Wright, C., Angus, B., Nicholson, S., Sainsbury, J.R.C., Cairns, J., Gullick, W.J., Kelly, P., Harris, A.L. and Horne, C.H.W. (1989) Expression of c-erbB-2 Oncoprotein: A Prognostic Indicator in Human Breast Cancer. *Cancer Research*, **49**, 2087-2090.

Yarden, Y. (2001) The EGFR family and its ligands in human cancer: signalling mechanisms and therapeutic opportunities. *European Journal of Cancer*, **37**, S3-S8.

Yarden, Y. and Sliwkowski, M.X. (2001) Untangling the ErbB Signalling Network. *Nature Reviews: Molecular Cell Biology*, **2**, 127-137.

Yu, D. and Hung, M.-C. (2000) Role of erbB2 in breast cancer chemosensitivity. *BioEssays*, **22**, 673-680.

Zhong, Q., Lazar, C.S., Tronchere, H., Sato, T., Meerloo, T., Yeo, M., Songyang, Z., Emr, S.D. and Gill, G.N. (2002) Endosomal localization and function of sorting nexin 1. *Proceedings of the National Academy of Sciences - USA*, **99**, 6767-6772.

Chapter 2: EGFR & HER2 Overall Trafficking Dynamics

Elevated expression of HER2 is known to alter cell signaling and behavioral responses implicated in tumor progression. However, multiple diverse mechanisms may be involved in these overall effects, including signaling by HER2 itself, modulation of signaling by EGFR, and modification of trafficking dynamics for both EGFR and HER2. Because these processes are so tightly interrelated, the net effect of HER2 overexpression is difficult to reliably attribute to any single particular mechanism. To take an important first step towards dissecting the effects of HER2 overexpression on cell responses in terms of the various specific underlying mechanisms, we have developed and validated a quantitative model of the relevant trafficking processes. We then employ our model for successful prediction of EGFR and HER2 level and location changes due to HER2 overexpression in 184A1 human mammary epithelial cells expressing a series of HER2 levels by means of retroviral infection. Model predictions are based upon our independent experimental measurement of key trafficking parameters for both EGFR and HER2. In terms of trafficking processes, HER2 overexpression reduces the EGFR internalization rate constant and increases the fraction of EGFR recycled. In consequence, our model successfully predicts that HER2 increases the overall level of activated EGFR by both enhancing its recycling and reducing its internalization, but increases activated EGFR localization at the cell surface almost solely by its reduction of internalization. Further, the model also successfully predicts the effects of mAb 2C4,

which interferes with HER2/EGFR heterodimerization, on EGFR and HER2 levels and compartmental locations. We anticipate that this model should ultimately be useful in parsing the relative contributions of direct effects of HER2 via signaling *vis-a-vis* indirect effects of HER2 via modification of EGFR signaling.

2.1 Introduction

EGFR and HER2 expression levels have distinguished themselves as important factors in contributing to various types of cancers including breast and ovarian cancers (Menard et al., 2001), but quantitative linkages between receptor expression levels and aberrant cell behaviors are not well understood.

Mounting evidence suggests that receptor compartmental location plays a crucial role in determining cellular responses to external stimuli (Burke et al., 2001; Carraway and Sweeney, 2001; Ceresa and Schmid, 2000; Leof, 2000; Wiley and Burke, 2001). Clearly, changes in receptor trafficking can affect the duration and quality of signals generated. This, in turn, could ultimately be responsible for the pathological behaviors associated with receptor overexpression, such as heightened mitogenic sensitivity and increased cell motility.

In order to better understand the effects of HER2 overexpression on cell responses in terms of the specific underlying mechanisms, we have developed a computational model geared at capturing EGFR and HER2 trafficking dynamics with a minimal level of complexity. The model presented here is able to generate *a priori* predictions of EGFR and HER2 levels and compartmental locations based on the empirical measurement of

their relative trafficking behaviors. Most importantly, the model yields insight into which rate processes are the most influential in dictating the overall system behavior.

2.2 Experimental Methods

2.2.1 Reagents/Cell Culture

7C2 Fab fragments, 2C4 mAb, 13A9 mAb and 4D5 mAb were generous gifts from Genentech, Inc. Monoclonal antibody 225 was purified from hybridomas obtained from American Type Culture Collection (Gill et al., 1984). 7C2 Fab, 13A9, 225 and EGF were labeled with ^{125}I (NEN) using iodobeads (Pierce) as described elsewhere (Burke and Wiley, 1999). Human EGF was obtained from Peprotech. 184A1 human mammary epithelial cells were a kind gift from Martha Stampfer and maintained in DFCI-1 medium supplemented with 12.5 ng/ml EGF (Band and Sager, 1989).

2.2.2 Expression of HER2 by Retroviral Transduction

Different levels of HER2 expression were achieved in HMEC 184A1 cells by retroviral transduction. The retroviral vector was constructed by excising HER2 from the LTR-2 vector (DiFiore et al., 1987) with Xho1, adding Not1 linkers and inserting this into the MFG vector (Eming et al., 1995) that was modified to contain neomycin resistance as well as a Not1 site. The resulting HER2 vector was transfected into the □-CRIP packaging cell line as described (Danos and Mulligan, 1988). Clones of transfectants were screened for HER2 expression using mAb 4D5 and virus-containing supernatants were collected and screened for high titer. Cells were transfected with retrovirus stock

using 4 μg/ml polybrene for 2 h and grown for 2 days before plating at clonal density. Individual colonies were isolated using cloning rings and then screened by immunofluorescence and by flow cytometry. Surface HER2 levels were characterized by flow cytometry and equilibrium binding studies using ^{125}I-7C2 Fab.

2.2.3 Binding Studies

Prior to experiments, cells were grown to confluency and brought to quiescence in binding medium (DFCI-1, without sodium bicarbonate, EGF, bovine pituitary extract or fetal bovine serum) overnight and placed in an air incubator. Cell number per plate was determined with parallel plates using a Coulter Counter.

2.2.4 Strip Protocol

Surface bound ligand was determined by removal with an acid strip solution (Lund et al., 1990; Wiley and Cunningham, 1982). Cells were washed 5 times with ice-cold wash buffer (1 mg/ml polyvinylpyrrolidone, 130 mM NaCl, 5 mM KCl, 0.5 mM $MgCl_2$, 1 mM $CaCl_2$, 20 mM HEPES, pH 7.4) and incubated on ice with acid strip solution (50 mM glycine-HCl, 100 mM NaCl, 1 mg/ml polyvinylpyrrolidone, 2M urea, pH 3.0). Surface bound ligand was quantified by counting acid strip solutions in a gamma-counter. Internalized ligand was determined by solubilizing cells following the acid strip with 1N NaOH and counting on a gamma-counter.

2.2.5 Internalization Rate Constant Measurement

Internalization rate constants were determined as described previously (Lund et al., 1990). Unoccupied EGFR, bound EGFR and HER2 internalization measurements were done with ^{125}I-225, ^{125}I-EGF and ^{125}I 7C2 Fab, respectively (Wiley and Cunningham, 1982).

2.2.6 Endosomal Sorting Assay

Endosomal sorting trafficking parameters are determined as described previously (French et al., 1994; French et al., 1995). Cells were incubated at 37°C with binding medium containing varying levels of ^{125}I-EGF or 200 ng/ml ^{125}I-7C2-Fab for 2.5 hours to allow the sorting process to reach steady state. Cells were washed with PBS and surface bound ligand was removed with acid strip solution without urea for 2 min at 4°C. Cells were washed twice with PBS and returned to 37°C with binding medium containing excess ligand (160 nM unlabeled EGF or 1 μg/ml unlabeled 7C2-Fab). After 10 min, degraded and intact (recycled) ligand in the medium were separated via centrifugal ultrafiltration using 5000 MWCO filter units (Millipore).

2.2.7 Receptor Distribution (Inside/Surface) Measurement

Cells were incubated at 37°C with ^{125}I-EGF, ^{125}I-7C2 Fab, or ^{125}I-13A9 in binding medium and allowed to reach steady state (2.5-5 hours). Surface bound and internal ligand was quantified as detailed above.

2.2.8 Surface Receptor Down-Regulation

Cells were treated with or without 100 ng/ml EGF for 5 hours. Surface receptor number was then quantified by the addition of saturating quantities (600 ng/ml) of ^{125}I-13A9, for EGFR, or by equilibrium binding studies with ^{125}I-7C2 Fab, for HER2. At equilibrium, surface bound ligand was determined as described above in the Strip Protocol. Fractional down regulation is defined as surface receptors (EGFR or HER2) after EGF treatment divided by surface receptors prior to treatment.

2.3 Model Development

A mathematical model for HER2/EGFR trafficking dynamics can include different levels of detail. At a maximal extreme, it could explicitly include thermodynamic/kinetic interactions regulating each of the individual trafficking processes and combine them into a very large system with dozens of equations and parameters. At a minimal opposite, as we have chosen, it could account for these interactions implicitly through lumped rate constants describing the various processes, with quantitative experimental measurements providing empirical characterization of these rate constants. This results in a reduced number of equations with a minimized set of system parameters. Thus, we are following a "top down" approach in which each lumped rate constant for a given process could be expanded into a subordinate model for greater molecular-level detail.

2.3.1 EGFR Model

At the most macroscopic level, the trafficking of a given receptor can be divided into 4 steps: synthesis, internalization, recycling and degradation. Collectively, the behavior of these processes governs both the number of receptors present on a cell as well as their distribution between surface and internal compartments.

EGFR trafficking can be modeled with a simple set of differential equations describing the motion of empty and occupied receptors from one compartment to another (illustrated in Figure 2.1) (Lauffenburger and Linderman, 1993):

$$\frac{dRs}{dt} = -k_f L R_s + k_r Cs - k_{er} Rs + k_{xr}(f_{xr}) Ri + S_R$$

$$\frac{dCs}{dt} = +k_f LRs - k_r Cs - k_{ec} Cs + k_{xc}(f_{xc}) Ci$$

$$\frac{dRi}{dt} = +k_{er} Rs - k_{xr}(f_{xr}) Ri - k_{xr}(1 - f_{xr}) Ri$$

$$\frac{dCi}{dt} = +k_{ec} Cs - k_{xc}(f_{xc}) Ci - k_{xc}(1 - f_{xc}) Ci$$

Free EGFR (Rs) are synthesized at rate S_R, internalized at the constitutive rate (k_{er}) and exit endosomes at rate k_{xr} with fraction f_{xr} recycling to the surface and fraction ($1-f_{xr}$) being degraded. EGF (L) reversibly binds free EGFR with on and off-rate k_f and k_r, respectively. EGF-EGFR complexes (in all forms, including homodimers and

heterodimers with HER2) internalize at rate k_{ec} and are sorted in endosomes with exit rate k_{xc}, recycling fraction f_{xc}, and degradation fraction ($1-f_{xc}$). EGFR-HER2 interactions following ligand addition are implicitly incorporated by allowing k_{ec} and f_{xc} to depend on HER2 expression level. These dependencies have been empirically determined for this study (see Figures 2.3, 2.4 and Table 2.2). We assume that all EGF remains bound once internalized.

2.3.2 HER2 Model

For HER2, the model is completely analogous to that of EGFR in the absence of ligand (illustrated in Figure 2.1):

$$\frac{dHs}{dt} = -k_{eh}Hs + k_{xh}f_{xh}Hi + S_H$$

$$\frac{dHi}{dt} = +k_{eh}Hs - k_{xh}(f_{xh})Hi - k_{xh}(1-f_{xh})Hi$$

HER2 synthesis, internalization, endosomal exit and sorting fraction are given by S_H, k_{eh}, k_{xh} and f_{xh}, respectively. HER2-EGFR interaction and the effect of ligand addition is implicitly contained in the k_{eh} term, where k_{eh} is a complex function of both HER2 level and EGF stimulation (see Figure 2.3b and Table 2.2). Hs and Hi include both free HER2 and HER2 that is homo or heterodimerized.

2.4 Results

The primary focus of our effort here is to understand how expression of HER2 affects the distribution and levels of activated EGFR utilizing a quantitative, systems modeling approach. In general, the distribution of receptors depends on their rate of entry into cells (internalization) and rate of exit (recycling and degradation). To describe internalization, we use the concept of the "endocytotic rate constant" which has been well characterized in a variety of cell types (Burke and Wiley, 1999; Reddy et al., 1994; Starbuck et al., 1990; Wiley and Cunningham, 1982; Worthylake et al., 1999). This lumped constant encapsulated information of a variety of endocytic parameters, such as number of coated pits, receptor activation state and binding to proteins within coated pits (Starbuck et al., 1990; Wiley and Cunningham, 1982). To describe the loss of receptors from cells, we use two parameters: an endosomal exit constant (k_x) and a recycling fraction (f_x). Mechanistically, k_x describes the first order rate of receptor transit through the endosomal compartment per unit time whereas f_x is simply the fraction of receptors that recycle intact back to the cell surface. These lumped parameters allow us to consolidate several molecular-level events into experimentally accessible parameters and thus permit identification of where the system is altered.

For our approach to be useful, expression of HER2 must cause predictable and reproducible alterations in our model parameters. In addition, these alterations must be reasonable from a mechanistic viewpoint. For this, we used a series of cloned 184A1 human mammary epithelial cell lines expressing varying levels of HER2, constructed by retroviral-mediated gene transfer. The uniformity of HER2 expression in each clonal

population is shown in Figure 2.2. Approximate surface EGFR and HER2 expression levels in these cells are listed in Table 2.1.

2.4.1 Effect of HER2 Expression on EGFR and HER2 Trafficking

2.4.1.1 Internalization

To examine the relationship between HER2 levels and EGFR internalization, we measured EGF internalization in the different clonal cell lines using the method of Wiley (Lund et al., 1990; Wiley and Cunningham, 1982). As shown in Figure 2.3a, increasing HER2 expression elicited up to a 60% decrease in the EGF endocytotic rate constant from 0.25 min^{-1}, for the parental line, to 0.10 min^{-1}, for HER2 clones 24H and 1. To probe the role of heterodimerization in this effect we repeated these measurements following pretreatment with 2C4, an anti-HER2 monoclonal antibody found to block both heterodimerization and transactivation of the EGFR (Baselga, 2002; Fendly et al., 1990; Lewis et al., 1996). Pretreatment with 2C4 mAb abrogated the HER2 dependent effect on EGF internalization (Figure 2.3a), suggesting that heterodimerization between HER2 and EGFR leads to a reduction in EGFR internalization rates.

To determine whether activation of the EGFR had a reciprocal effect on HER2 internalization, we used 7C2 Fab as an artificial HER2 ligand. 7C2 mAb binds to an extracellular epitope on HER2, but does not interfere with heterodimerization (Fendly et al., 1990). HER2 internalization was measured in the presence and absence of 10 ng/ml EGF in our set of HER2 clones (Figure 2.3b). We found that HER2 is internalized very slowly in the absence of EGF, at a rate consistent with constitutive membrane turnover

(~0.01 min^{-1}) (Lund et al., 1990; Wiley et al., 1991). Activation of the cellular complement of EGFR elicits an increase in HER2 internalization that decreases from three to two-fold with increasing HER2 expression.

HER2 expression had no observable effect on the constitutive internalization rate constant of unoccupied EGFR (data not shown), as measured with ^{125}I-225, an antagonistic monoclonal antibody that binds to the EGFR (Opresko et al., 1995). The EGF association (k_f) and dissociation (k_r) rate constants, were also measured and found to be 9.7 □10^7 $M^{-1}min^{-1}$ and 0.24 min^{-1}, respectively.

2.4.1.2 Receptor Recycling

The values of the endosomal exit constant (k_{xc}) and a recycling fraction (f_{xc}) were determined using a steady state sorting assay that follows the fate of ^{125}I-EGF. At steady state, the rate at which EGF is lost from the cells (both degraded and intact) is equal to the rate at which it exits from the endosomes. Because the fraction of EGF recycled is somewhat dependent on the size of the internal pool of ligand, we incubated cells with different concentrations of ^{125}I-EGF. By 2.5 hours, the intracellular sorting process reaches quasi-steady state as evidenced by an approximately constant amount of internal EGF. Surface-bound EGF was removed with a mild acid strip and the cells were returned to medium with excess unlabeled EGF to prevent rebinding. After 10 minutes, intact and degraded ^{125}I-EGF in the medium were separated by centrifugal ultrafiltration. The fraction of EGF recycled (f_{xc}) was calculated from the ratio of intact ^{125}I-EGF to the total

^{125}I-EGF (intact and degraded) in the medium (French et al., 1994). The value of k_{xc} was determined from the rate at which total ^{125}I-EGF appeared in the medium.

Consistent with our previously published studies (Worthylake et al., 1999), increasing levels of HER2 expression resulted in an increased fraction of EGF recycling back to the cell surface (Figure 2.4), from 0.5 up to 0.7. The extent to which HER2 expression affected recycling was dependent on the size of the intracellular pool of ligand, with the effect being more pronounced at higher levels of internalized EGFR.

Blocking heterodimerization with 2C4 pretreatment was sufficient to reverse the effect of elevated HER2 expression on the EGF sorting fraction (Figure 2.4) and had no effect on sorting in the parental cell line (data not shown). The observation that HER2 expression affected only the fraction of recycled ligand, but not the transit of ligand through the endosomes suggests that HER2 interferes with lysosomal targeting of the EGFR. The enhanced effect observed at high levels of internalized EGF is consistent with this idea. The endosomal exit constant of EGF (k_{xc}) was essentially constant across all HER2 clones at 0.036 min^{-1}.

The sorting of HER2 was measured by following the fate of attached 7C2 Fab, in a manner analogous to that of EGF. We found that for all of the HER2-expressing lines, the fraction of recycled 7C2 Fab was very high (0.94). The endosomal exit constant of 7C2 Fab was also very similar in all of the cell lines at 0.07 min^{-1}. This value is about twice that observed for EGF, indicating that the occupied EGFR transits the endosomal apparatus slower than HER2. The addition of EGF had no measurable effect on either the fraction of recycled 7C2 or its endosomal exit constant. Recycling was the predominant

fate of 7C2 Fab and was always much faster than internalization. We conclude that HER2 is primarily localized to the cell surface due to a slow internalization rate and relatively fast recycling rate.

The complete set of trafficking parameters is shown in Table 2.2.

2.4.2 Model Predictions

2.4.2.1 Effect of HER2 Expression on Receptor Location

We next determined whether our model could accurately describe the distribution of EGFR and HER2. *A priori* predictions of EGFR distribution can be made based on experimental data for the individual trafficking steps and tested against an independent set of experimental results. We used the inside/surface receptor ratio as an endpoint, rather than absolute amounts, to remove the dependence on receptor synthesis (S_R). Thus, we have a model which is completely defined in an experimental sense with relative EGFR and HER2 expression as the relevant parameters. At steady state the processes of synthesis and degradation are balanced so that the inside/surface distribution simply is the ratio of the internalization (ke) and the rate at which receptors transit the endosome (kx). This shown by the solution to our model equations at steady state:

$$Inside{:}Surface_{\mathrm{EGF}} = \frac{Ci}{Cs} = \frac{k_{\mathrm{ec}}}{k_{\mathrm{xc}}}$$

For the case of HER2, the same relationship would hold in that the Inside/Surface ratio would be equal to k_{eh}/k_{xh}. We determined whether cells displaying a given value of k_{ec} or k_{eh} would display an inside/surface ratio predicted from the previously determined values of k_{xc} and k_{xh}, which were roughly constant across all HER2 expression levels.

Following EGF treatment, the inside/surface distribution of EGF reached a steady state within 2 hours (data not shown). The inside/surface EGF ratio was measured and plotted as a function of k_{ec} for the parental and HER2-expressing lines, shown in Figure 2.5a. We also determined the inside/surface distribution of HER2 before and after EGF treatment using steady state ^{125}I-7C2 Fab binding. This was plotted as a function of the measured value of k_{eh}, also shown in Figure 2.5a. A diagonal line corresponding to a theoretical endosomal exit constant of 0.1 min^{-1} has been provided for comparison. The inside/surface data for both HER2 and EGF from all of the cell lines shows good accordance with *a priori* model predictions and falls parallel to the line describing a constant endosomal exit constant (Figure 2.5a). The fact that our model has the same slope as the experimental data suggests that our experimental measurement of the endosomal exit rate constant is correct. The offset from the data arises from our simplification of the sorting process – in particular we have only one sorting compartment. A fast recycling compartment could conceivably shift the curves to match the data, however, this necessitates the incorporation of additional parameters that are not directly measurable.

These results suggest that HER2 expression does not change the rate at which either the EGFR or HER2 transits the endosomal apparatus, but simply alters the sorting

pattern within endosomes. This explicit assumption of our model appears to be entirely consistent with the data. The addition of EGF appears to cause a shift of HER2 towards a faster endosomal transit. The approximately 50% faster endosomal transit appears independent of HER2 expression level and may reflect the enhanced membrane turnover stimulated by EGF (Wiley and Kaplan, 1984). Note that the EGF data is shifted considerably from the diagonal line describing the HER2 data, indicating that the EGFR transits the endosomal apparatus much slower than HER2. This is consistent with previous work suggesting that endosomal retention is a major mechanism by which intracellular EGFR is regulated (Herbst et al., 1994).

2.4.2.2 Effect of HER2 Expression on Surface Receptor Loss

A second set of predictions that can be made relates to the loss of receptor at the cell surface as a result of both internalization and accelerated degradation (down regulation). Fractional surface receptor loss is determined by solving the model at steady state in the presence of 100 ng/ml EGF. The number of receptors remaining on the surface following EGF stimulus is divided by the original number present on the surface to yield the fractional surface loss:

$$D_{\mathrm{EGFR}} = \frac{k_{\mathrm{er}}(1 - f_{\mathrm{xr}})}{k_{\mathrm{f}}L + k_{\mathrm{er}}(1 - f_{\mathrm{xr}})} + \left[\frac{k_{\mathrm{r}}}{k_{\mathrm{f}}L + k_{\mathrm{er}}(1 - f_{\mathrm{xr}})} + 1\right] \frac{k_{\mathrm{f}}L[k_{\mathrm{er}}(1 - f_{\mathrm{xr}})]}{[k_{\mathrm{er}}(1 - f_{\mathrm{xr}})[k_{\mathrm{ec}}(1 - f_{\mathrm{xc}}) - k_{\mathrm{r}}] + k_{\mathrm{ec}}(1 - f_{\mathrm{xc}})k_{\mathrm{f}}L]}$$

The effect of EGFR activation on HER2 loss (D_H) is much simpler and of the form:

$$D_{HER2} = \frac{Hs^+}{Hs^-} = \frac{k_{eh}^-}{k_{eh}^+} \frac{(1-f_{xh})^-}{(1-f_{xh})^+}$$

where superscript + or – indicates the parameter values associated with the with or without EGF treatment, respectively.

Levels of EGFR and HER2 at the cell surface were measured by comparing steady state binding of ^{125}I-13A9 and ^{125}I-7C2 Fab before and after 5-hour incubation with 100 ng/ml EGF in the different cell lines. The data, shown in Figure 2.6a, are plotted as a function of k_{ec} and k_{eh}. We found that increasing HER2 expression inhibited the fractional loss of both itself and EGFR. Because EGFR loss is also a function of the recycling fraction (f_{xc}), and because HER2 expression causes an increase in this parameter, we have plotted model predictions using values from both high HER2 expressing cells and the parental cells (Figure 2.6a).

For the EGFR data, the rate of internalization is fast relative to the endosomal exit rate, so that the down-regulation is limited by the ability of the sorting machinery to target receptors for degradation. From this we expect the down-regulation to vary more with changes in recycling fraction than internalization rate. The effect of changing

recycling fraction is less dramatic than the HER2 case because we a farther away from the singularity that occurs when the recycling fraction is unity.

The HER2 experimental data is steep relative to the EGFR data because the endosomal exit rate is fast relative to the internalization rate, particularly for high HER2 expression. HER2 down-regulation is limited by the ability to get receptors internalized, especially since EGF had little to no effect on the fraction recycled. Intuitively, the amount of receptors remaining is going to be inversely related to the fraction of receptors that get degraded. The model is very sensitive to changes in recycling fraction because the recycling fraction is very close to 1, such that the fraction degraded is very nearly 0 (at which point a singularity exists). In our experimental measurements, EGF had no discernible effect on HER2 recycling, but changes within experimental error may have large effects on the model output. As such, we consider two cases in Figure 2.6a: (i) EGF elicits no change in HER2 sorting fraction (fxh+ = 0.94) and (ii) a scenario where EGF treatment elicits a small degree of sorting saturation resulting in a 4% increase in HER2 sorting fraction (fxh+ = 0.98). An increased recycling fraction would also be compatible with the likely increase in endosomal transit rates of HER2 suggested by the results presented in Figure 2.5a.

For both inside/surface ratio and down-regulation EGFR and HER2 fall into two distinct regimes: one where internalization is slower than endosomal exit (HER2) and one where internalization is faster than recycling (EGFR). These differences are best illustrated by their inside/surface ratios which directly reflect these processes (ke/kx).

2.4.2.3 Effects of 2C4 Monoclonal Antibody

Finally, *a priori* predictions from the model can be tested for the effects of the 2C4 mAb, which interferes with HER2/EGFR heterodimerization. We evaluated predictions of EGFR loss from the cell surface and steady state inside/surface ratios. The EGFR model was evaluated using parameter values measured following pre-incubation with 2C4 (Table 2.2) and compared with experimental measurements of inside/surface ratios and surface receptor levels, also following 2C4 treatment (Figures 2.5b and 2.6b). For both the model and experiments, 2C4 treatment returned the EGF inside/surface ratio and fractional surface EGFR down regulation for clone 24H to levels similar to the parental cell line. 2C4 had no effect on the parental cell line (data not shown). The model successfully predicts the direction of change resulting from the addition of 2C4 mAb, however there are some minor discrepancies in the prediction of magnitudes. It is unclear whether these are due to cell-cell variations or errors in parameter estimations.

2.5 Discussion

Changes in HER2 expression levels have significant effects on EGF family ligand-induced signaling that contribute to alterations in cell behavior, such as found in breast cancer (Brandt et al., 1999; Ignatoski et al., 1999; Ignatoski et al., 2000; Karunagaran et al., 1996). Because signaling can be simultaneously regulated by receptor type (*e.g.*, EGFR versus HER2), receptor location (*e.g.*, cell surface versus intracellular compartment), and receptor levels, a reliable integrative model for EGFR/HER2 co-

regulation should be very helpful toward deconvoluting the effects of HER2 overexpression on cell responses.

We have employed a quantitative 'top-down' approach in the development, validation, and application of a dynamic systems model capable of *a priori* prediction of HER2 and EGFR levels and compartmental locations. We have predicted the overall effects of HER2 expression on the quantity and distribution of EGFR and HER2 with reasonable accuracy and without fitting any parameters.

The empirical measurement of individual trafficking parameters and their dependence on HER2 expression adds to a growing body of EGFR and HER2 trafficking data. With regard to internalization, we have confirmed that: [a] HER2 is indeed internalized, albeit slowly; [b] demonstrated that EGF addition accelerates HER2 internalization, although not to the same degree as reported in some other cell types or chimeric constructs (Baulida et al., 1996; Sorkin et al., 1993); and [c] found that hetero-dimerization, as a consequence of increased HER2 expression, reduces but does not block EGF internalization. Our experimental results provide some interesting new insights into HER2 dynamics in mammary epithelial cells. We report here the first measurements of the recycling rate constant and sorting fraction of HER2, and demonstrate that these are essentially independent of HER2 expression and minimally dependent on EGF stimulation. Second, our EGF sorting results demonstrate an increase in fraction recycled with increased HER2 expression, consistent with that observed in HB2 cells with varying levels of HER2 expression (Worthylake et al., 1999). The EGFR trafficking model and experiments following 2C4 intervention provide quantitative support for the notion that

blocking heterodimerization can significantly affect EGFR signaling due to effects on receptor trafficking. Some of the therapeutic effect of Herceptin® could be due to such a mechanism.

Our modeling allows us to easily scan a multi-parameter space and critically discern which regulatory processes are the most sensitive or insensitive to disruption. From these calculations, it is evident that EGFR compartmental location is primarily controlled at the level of internalization. The down regulation of EGFR, however, is controlled by a balance of both internalization and endosomal sorting (see Figure 2.6a).

HER2 overexpression appears to disrupt EGFR trafficking at both internalization and endosomal sorting. The mechanism(s) by which HER2 overexpression is able to alter each step is unclear, but heterodimerization appears to be required. This may imply that homodimerization of the EGFR is necessary for efficient trafficking, or that the conformation of the heterodimerized EGFR is not optimally recognized by the endocytic machinery.

The majority of the model error lies in predictions of down regulation. This suggests that most of the error arises from the sorting fraction parameter, in part from experimental uncertainty but mainly from the tremendous simplification of sorting behavior. The current model does not propose the existence of more than a single recycling compartment and does not account for differential sorting of ligands and receptors within endosomes. Clearly, more detail at the level of endosomal sorting is needed to precisely capture the behavior, but this will come at the expense of having an experimentally measurable parameter set (French and Lauffenburger, 1996).

This model is specific for HER2 expression effects in the face of EGF stimulus. Because parameter dependencies were empirically determined, they implicitly include interaction with all other EGFR family receptors and not just EGFR. In principle, we could write such a model for HER3 and HER4 and use this approach for the effects of any receptor overexpression in the presence of any combination of stimuli – it simply requires the empirical determination of parameters spanning the desired space.

From both the model and data, it is clear that the net trafficking effect of elevated HER2 expression, following EGF stimulus, is to increase receptor lifetime and to shift the receptor distribution towards to the surface. This should increase the half-life of a given ligand stimulus, resulting in prolonged signaling. The decrease in inside/surface ratio may also impact the quality of the signals generated, preferentially activating signaling pathways that are restricted to the cell surface. Increased surface signaling relative to total signaling may alter cell motility via increased PLC-γ, calpain and gelsolin activation (Chen et al., 1996; Glading et al., 2000; Glading et al., 2001; Haugh et al., 1999).

2.6 Tables

Table 2.1 Approximate Surface Receptors per Cell.

cell clone	*EGFR*	*HER2*
184A1 HMEC (Parental)	$2\square10^5$	$3\square10^4$
A1-1 HER2 clone 29L	$2\square10^5$	$1\square10^5$
A1-1 HER2 clone 12	$2\square10^5$	$2\square10^5$
A1-1 HER2 clone 24H	$2\square10^5$	$6\square10^5$
A1-1 HER2 clone 1	$2\square10^5$	$6\square10^5$

Table 2.2 Trafficking Parameters[a].

EGFR Model Parameter	*Description*	*Value*
S_R	EGFR synthesis rate	NR[b]
k_f	EGF association rate constant ($M^{-1}min^{-1}$)	$9.7 \square 10^7$
k_r	EGF dissociation rate constant (min^{-1})	0.24
k_{er}	unoccupied EGFR internalization rate constant (min^{-1})	0.07±0.02
k_{ec}	EGF internalization rate constant (min^{-1})	0.10 – 0.25
k_{ec}, + 2C4	EGF internalization rate, + 2C4 (min^{-1})	0.28±0.02
f_{xr}	unoccupied EGFR recycling fraction	0.8[c]
f_{xc}	EGF recycling fraction	0.5 – 0.7
f_{xc}, + 2C4	EGF recycling fraction, + 2C4	0.47±0.06
k_{xc}	EGF endosomal exit rate constant (min^{-1})	0.036±0.003
k_{xc}, + 2C4	EGF endosomal exit rate constant, + 2C4 (min^{-1})	0.034±0.002
HER2 Model Parameter	***Description***	***Value***
S_H	HER2 synthesis	NR[b]
k_{eh}	HER2 internalization rate constant, No EGF (min^{-1})	0.012±0.004
k_{eh}	HER2 internalization rate constant, + EGF (min^{-1})	0.027 – 0.059
f_{xh}^-	HER2 recycling fraction, No EGF	0.94±0.03
f_{xh}^+	HER2 recycling fraction, + EGF	0.94±0.05
k_{xh}	HER2 endosomal exit rate constant (min^{-1})	0.07±0.01

[a] values are reported as: mean ± SD or as a range of values, as appropriate.
[b] value not required
[c] literature estimate from Lauffenburger and Linderman, 1993.

2.7 Figures

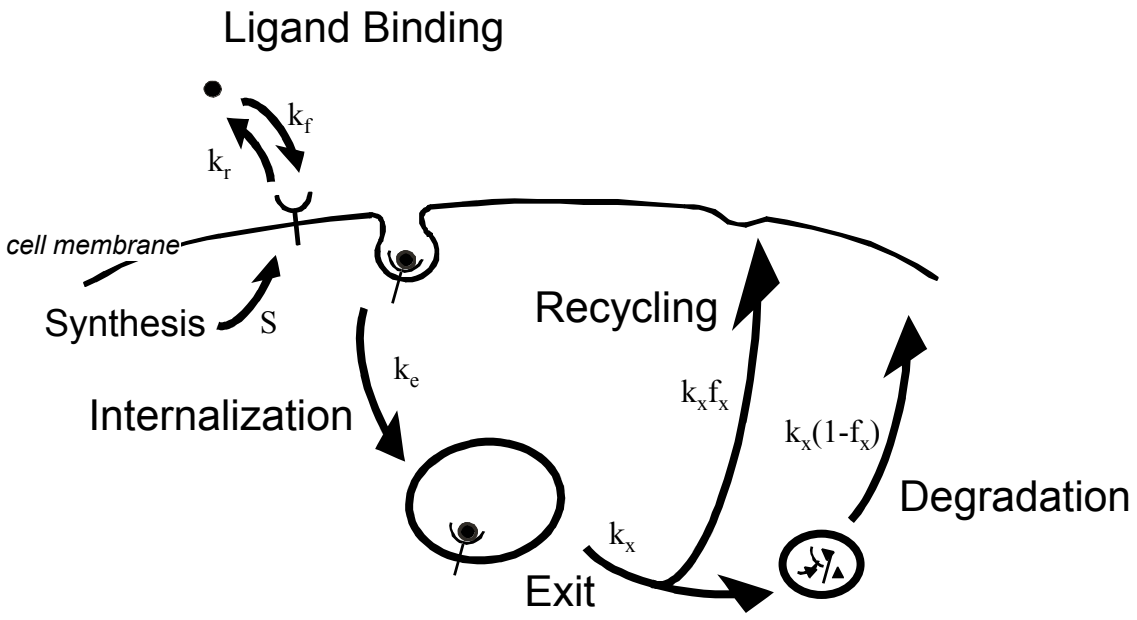

Figure 2.1 Generalized Receptor Trafficking Model.

EGFR Model. EGFR are synthesized and inserted into the cell membrane at a rate S_R. Empty EGFR are constitutively internalized into early (sorting) endosomes at rate k_{er}. EGF reversibly binds empty EGFR on the surface with association and dissociation rate k_f and kr, respectively. EGF-EGFR complexes are internalized at rate k_{ec}. Within the endosomes, empty EGFR exit at rate k_{xr}, with fraction f_{xr} recycling to the surface and fraction $(1-f_{xr})$ being targeted to lysosomal degradation. Complexes exit endosomes at rate k_{xc}, with fractions f_{xc} and $(1-f_{xc})$ targeted for recycling and degradation, respectively.

Parameters k_{ec} and f_{xc} vary with HER2 expression level. All rates, with the exception of receptor synthesis, are assumed to be first order.

HER2 Model. HER2 are synthesized and inserted into the cell membrane at rate S_H. Surface HER2 are internalized into early (sorting) endosomes at rate k_{eh}, which is a complex function of HER2 expression level and ligand stimulus. Within the endosomes, HER2 exit at rate k_{xh}, with fraction f_{xh} recycling to the surface and fraction $(1-f_{xh})$ being targeted to lysosomal degradation. All rates, with the exception of receptor synthesis, are assumed to be first order.

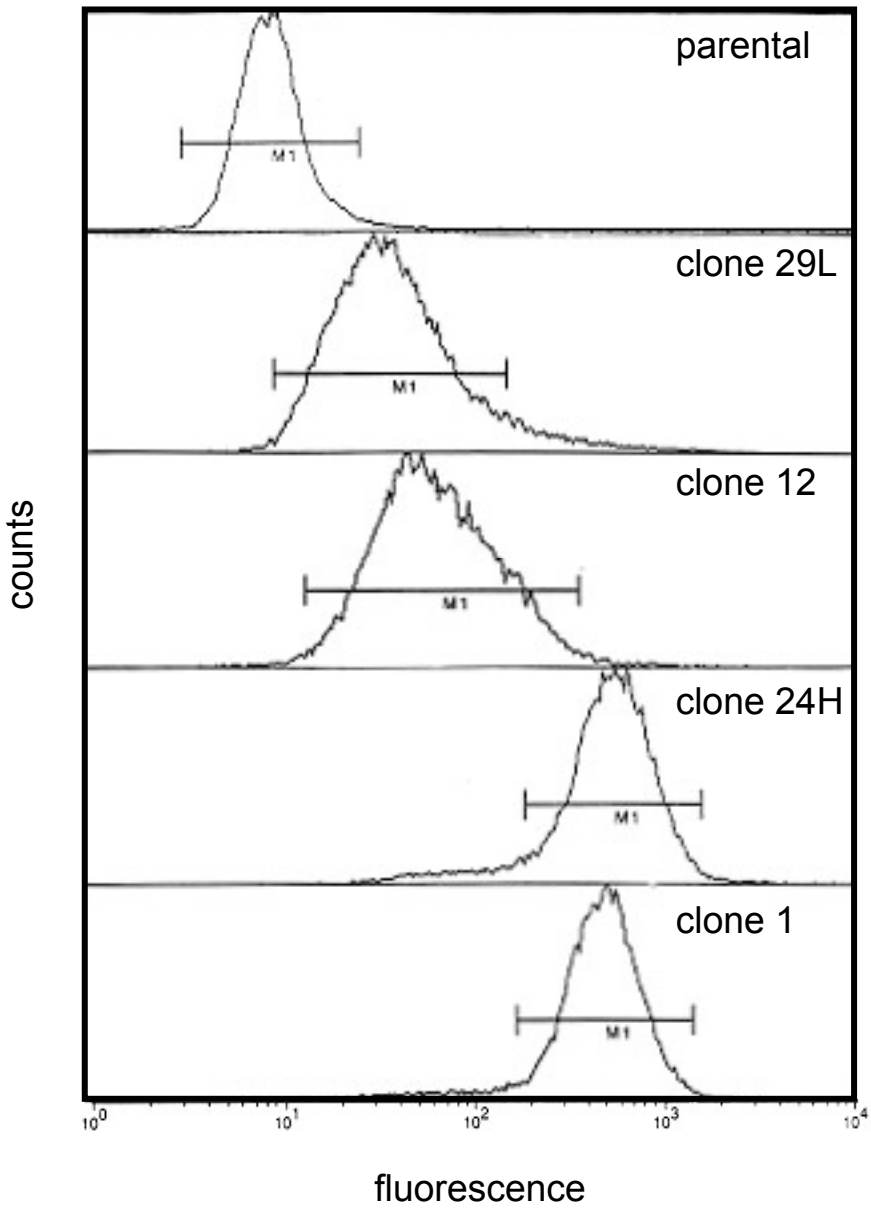

Figure 2.2 Receptor Populations.

Immunofluorescence and flow cytometry were used to generate histograms of HER2 expression for various clonal populations to demonstrate the uniformity of HER2 expression in each population.

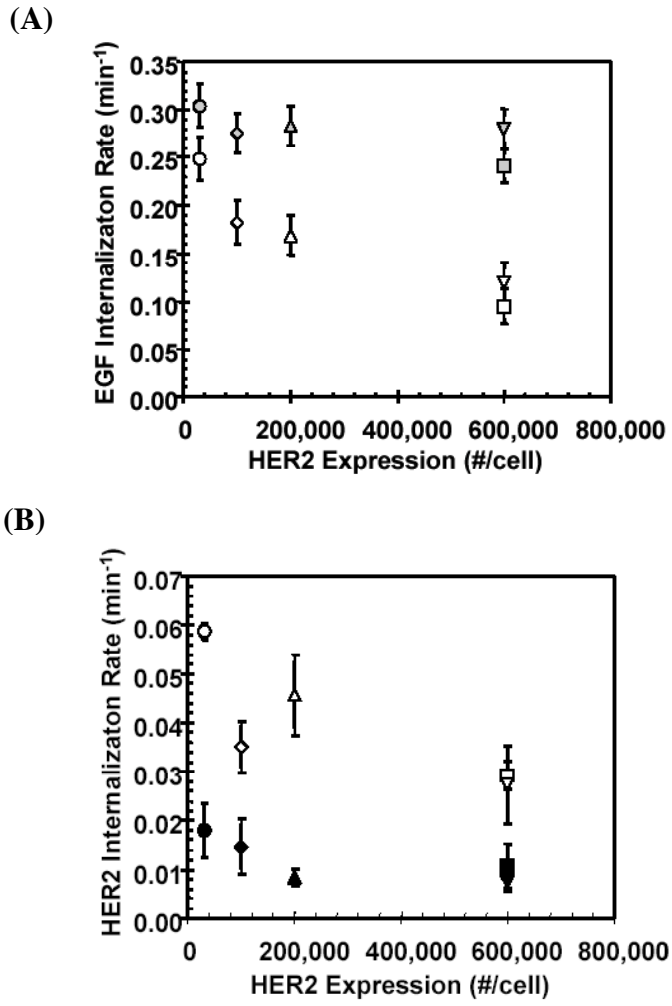

Figure 2.3 Internalization Rate Constants.

Internalization rate constants are measured as described in *Materials and Methods* for each cell clone (parental–circles; clone 29L–diamonds; clone 12–right side up triangles; clone 24H–squares; clone 1–upside down triangles) and plotted as a function of HER2 expression, as determined from equilibrium binding studies. *A*, EGF internalization rate constant. *B*, HER2 internalization rate constant in the presence (open symbols) and absence (filled symbols) of 10 ng/ml EGF stimulation. Data is plotted as mean ± SD.

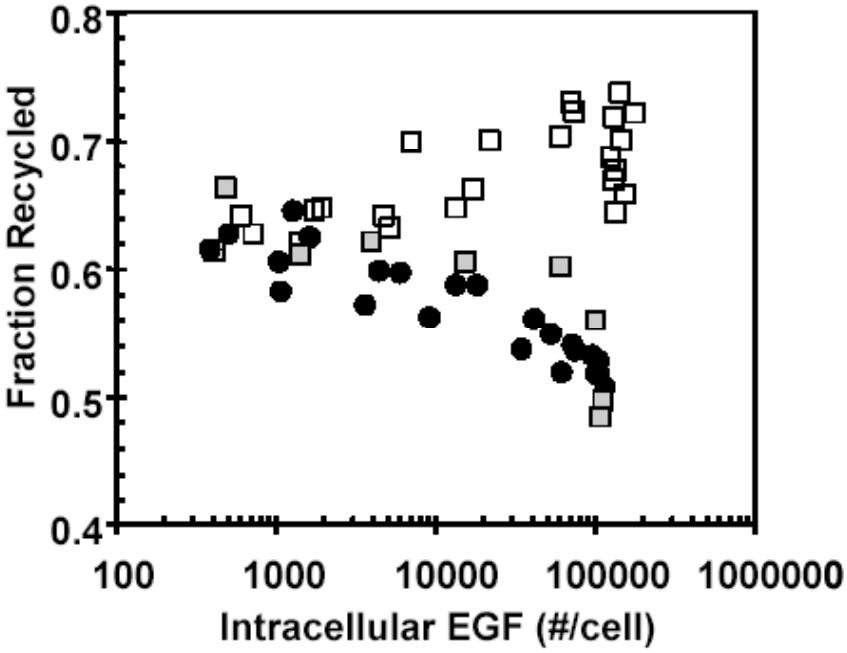

Figure 2.4 Fraction EGF Recycled.

Fraction of EGF recycled for parental (filled circles) and clone 24H (open squares) and clone 24H with 2C4 mAb pretreatment (shaded squares) is measured as described in *Materials and Methods*. Addition of heterodimerization blocking antibodies (2C4 mAb) abrogates the HER2-mediated effect on EGF recycling.

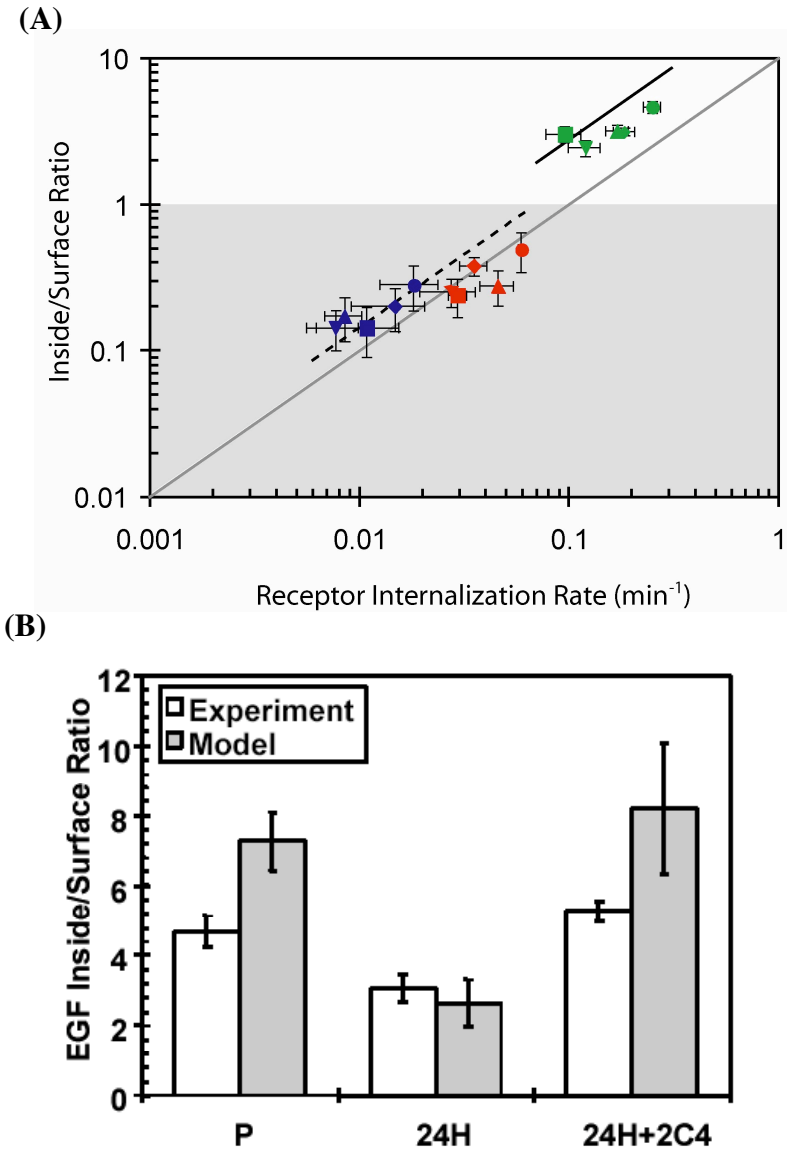

Figure 2.5 Inside/Surface Distribution.

A, experimental data for each cell clone (parental–circles; clone 29L–diamonds; clone 12–right side up triangles; clone 24H–squares; clone 1–upside down triangles) and model results for steady state inside/surface distribution of EGF and HER2. EGF inside/surface ratio (green symbols) is determined by incubating cells with ^{125}I-EGF to steady state. HER2 inside/surface ratio with and without 10 ng/ml EGF (red symbols and blue

symbols, respectively) is determined by incubating cells with ^{125}I-7C2 Fab to steady state. Surface bound and internal ^{125}I-EGF or ^{125}I-7C2 Fab is determined by acid stripping and solubilization with NaOH, as described in *Materials and Methods*. EGFR (solid line) and HER2 (dashed line) model predictions, based on experimental measurements of recycling parameters, are plotted as functions of receptor internalization rates. The dotted line shows a model prediction of corresponding to $k_x = 0.1$, for comparison. *B*, experimental data and model results for steady state EGF inside/surface distribution with and without 2C4 mAb pretreatment for parental and clone 24H cell lines. Error bars for experimental data represent one SD from the mean. Error bars for the model represent the propagation of error from the error associated with individual parameter measurements.

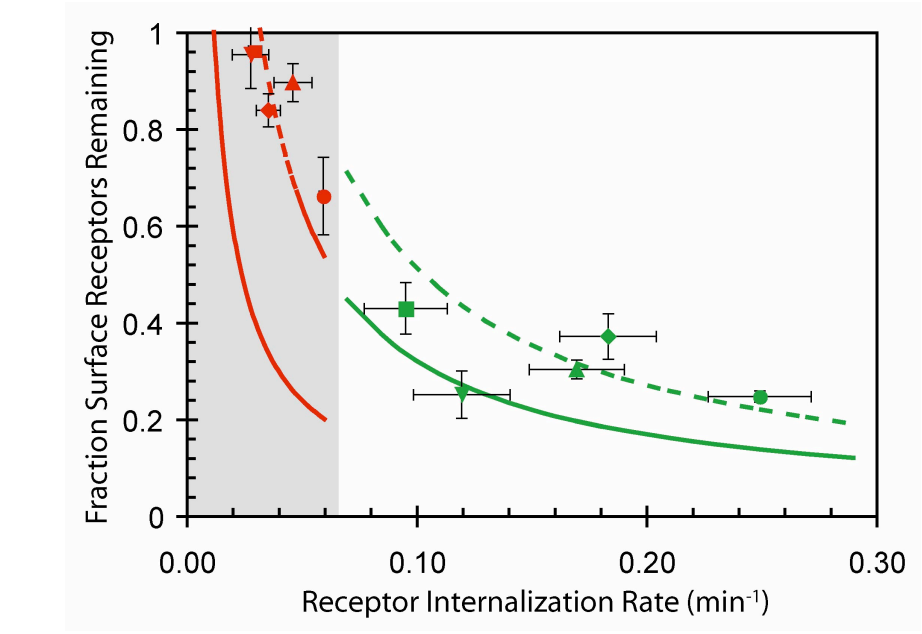

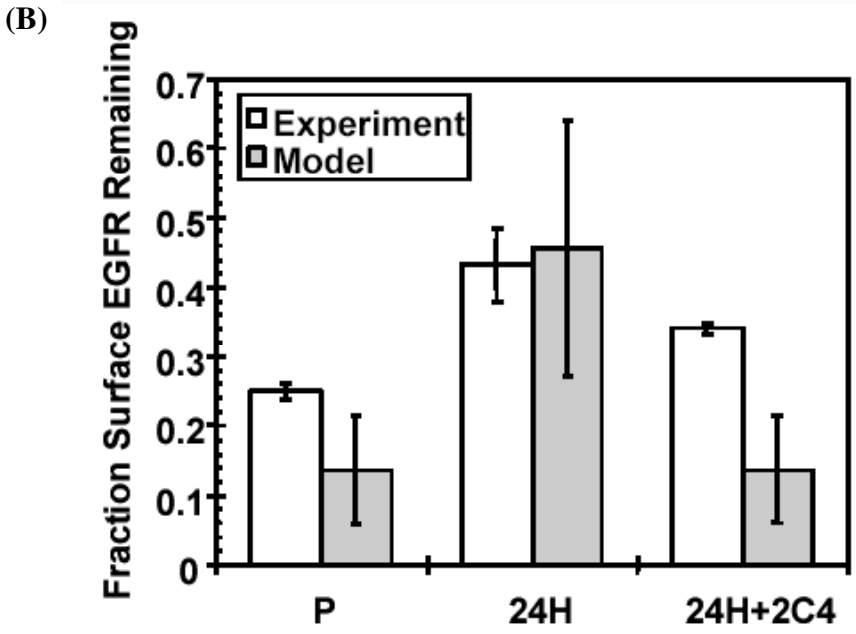

Figure 2.6 Receptor Down-regulation.

A, experimental data for each cell clone (parental–circles; clone 29L–diamonds; clone 12–right side up triangles; clone 24H–squares; clone 1–upside down triangles) and model results for steady state EGFR and HER2 down regulation. Fractional surface EGFR down

regulation (green symbols) was quantified by equilibrium binding of saturating amounts (600 ng/ml) of ^{125}I-13A9 before and after 5 hour treatment with 100 ng/ml EGF. Fractional surface HER2 down regulation (red symbols) is determined by Scatchard analysis with ^{125}I-7C2 Fab before and after 5 hour treatment with 100 ng/ml EGF. Surface amounts of ^{125}I-13A9 or ^{125}I-7C2 Fab are quantified by acid stripping and counting on a gamma counter, as described in *Materials and Methods*. The EGFR model (green solid and green dashed lines) is plotted as a function of EGFR internalization rate for EGF sorting fractions from 0.5 and 0.7, respectively. The HER2 model (red solid line, fxh+ = 0.94) is plotted as a function of HER2 internalization rate (with EGF). The case where EGF addition causes an increase in HER2 sorting fraction is also shown (red dashed line, fxh+ = 0.98). *B*, experimental data and model results for steady state EGFR down regulation with and without 2C4 mAb pretreatment for parental and clone 24H cell lines. Error bars for the experimental data represent one SD from the mean. Error bars for the model represent the propagation of error from the error associated with individual parameter measurements.

2.8 References

Band, V. and Sager, R. (1989) Distinctive traits of normal and tumor-derived human mammary epithelial cells expressed in a medium that supports long-term growth of both cell types. *Proceedings of the National Academy of Sciences - USA*, **86**, 1249-1253.

Baselga, J. (2002) A new anti-ErbB2 strategy in the treatment of cancer: Prevention of ligand-dependent ErbB2 receptor heterodimerization. *Cancer Cell*, **2**, 93-94.

Baulida, J., Kraus, M.H., Alimandi, M., DiFiore, P.P. and Carpenter, G. (1996) All ErbB Receptors Other Than the Epidermal Growth Factor Receptor Are Endocytosis Impaired. *The Journal of Biological Chemistry*, **271**, 5251-5257.

Brandt, B.H., Roetger, A., Dittmar, T., Nikolia, G., Seeling, M., Merschjann, A., Nofer, J.-R., Dehmer-Moller, G., Junker, R., Assmann, G. and Zaenker, K. (1999) c-erbB-2/EGFR as dominant heterodimerization partners determine a motogenic phenotype in human breast cancer cells. *The FASEB Journal*, **13**, 1939-1950.

Burke, P.M., Schooler, K. and Wiley, H.S. (2001) Regulation of Epidermal Growth Factor Receptor Signaling by Endocytosis and Intracellular Trafficking. *Molecular Biology of the Cell*, **12**, 1897-1910.

Burke, P.M. and Wiley, H.S. (1999) Human Mammary Epithelial Cells Rapidly Exchange Empty EGFR Between Surface and Intracellular Pools. *Journal of Cellular Physiology*, **180**, 448-460.

Carraway, K.L. and Sweeney, C. (2001) Localization and modulation of ErbB receptor tyrosine kinase. *Current Opinion in Cell Biology*, **13**, 125-130.

Ceresa, B.P. and Schmid, S.L. (2000) Regulation of signal transduction by endocytosis. *Current Opinion in Cell Biology*, **12**, 204-210.

Chen, P., Murphy-Ullrich, J. and Wells, A. (1996) A role for gelsolin in actuating epidermal growth factor receptor-mediated cell motility. *The Journal of Cell Biology*, **134**, 689-698.

Danos, O. and Mulligan, R. (1988) Safe and efficient generation of recombinant retroviruses with amphotropic and ecotropic host ranges. *Proceedings of the National Academy of Sciences - USA*, **85**, 6460-6464.

DiFiore, P.P., Pierce, J.H., Kraus, M.H., Segatto, O., King, C.R. and Aaronson, S.A. (1987) erbB-2 Is a Potent Oncogene When Overexpressed in NIH/3T3 Cells. *Science*, **237**, 178-182.

Eming, S., Lee, J., Snow, R., Tompkins, R., Yarmush, M. and Morgan, J. (1995) Genetically modified human epidermis overexpressing PDGF-A directs the development of a cellular and vascular connective tissue stroma when transplanted to athymic mice--implications for the use of genetically modified keratinocytes to modulate dermal regeneration. *J Invest Dermatol*.

Fendly, B.M., Winget, M., Hudziak, R.M., Lipari, M.T., Napier, M.A. and Ullrich, A. (1990) Characterization of Murine Monoclonal Antibodies Reactive to Either the Human Epidermal Growth Factor Receptor or HER2/neu Gene Product. *Cancer Research*, **50**, 1550-1558.

French, A.R. and Lauffenburger, D.A. (1996) Intracellular Receptor/Ligand Sorting Based on Endosomal Retention Components. *Biotechnology and Bioengineering*, **51**, 281-297.

French, A.R., Sudlow, G.P., Wiley, H.S. and Lauffenburger, D.A. (1994) Postendocytic Trafficking of Epidermal Growth Factor-Receptor Complexes Is Mediated through Saturable and Specific Endosomal Interactions. *The Journal of Biological Chemistry*, **269**, 15749-15755.

French, A.R., Tadaki, D.K., Niyogi, S.K. and Lauffenburger, D.A. (1995) Intracellular Trafficking of Epidermal Growth Factor Family Ligands Is Directly Influenced by the pH Sensitivity of the Receptor/Ligand Interaction. *The Journal of Biological Chemistry*, **270**, 4334-4340.

Gill, G.N., Kawamoto, T., Cochet, C., Le, A., Sato, J.D., Masui, H., McLeod, C. and Mendelsohn, J. (1984) Monoclonal Anti-epidermal Growth Factor Receptor Antibodies Which Are Inhibitors of Epidermal Growth Factor Binding and Antagonists of Epidermal Growth Factor-stimulated Tyrosine Protein Kinase Activity. *The Journal of Biological Chemistry*, **259**, 7755-7760.

Glading, A., Chang, P., Lauffenburger, D.A. and Wells, A. (2000) Epidermal Growth Factor Receptor Acitivation of Calpain Is Required for Fibroblast Motility and Occurs via an ERK/MAP Kinase Signaling Pathway. *The Journal of Biological Chemistry*, **275**, 2390-2398.

Glading, A., Uberall, F., Keyse, S.M., Lauffenburger, D.A. and Wells, A. (2001) Membrane Proximal ERK Signaling Is Required for M-calpain Activation

Downstream of Epidermal Growth Factor Receptor Signaling. *The Journal of Biological Chemistry*, **276**, 23341-23348.

Haugh, J.M., Schooler, K., Wells, A., Wiley, H.S. and Lauffenburger, D.A. (1999) Effect of Epidermal Growth Factor Receptor Internalization on Regulation of the Phospholipase C-□1 Signaling Pathway. *The Journal of Biological Chemistry*, **274**, 8958-8965.

Herbst, J.J., Opresko, L.K., Walsh, B.J., Lauffenburger, D.A. and Wiley, H.S. (1994) Regulation of Postendocytic Trafficking of the Epidermal Growth Factor Receptor Through Endosomal Retention. *The Journal of Biological Chemistry*, **269**, 12865-12873.

Ignatoski, K.M.W., Lapointe, A.J., Radany, E.H. and Ethier, S.P. (1999) erbB-2 Overexpression in Human Mammary Epithelial Cells Confers Growth Factor Independence. *Endocrinology*, **140**, 3615-3622.

Ignatoski, K.W., Maehama, T., Markwart, S., Dixon, J., Livant, D. and Ethier, S. (2000) ErbB-2 overexpression confers PI3' kinase-dependent invasion capacity on human mammary epithelial cells. *British Journal of Cancer*, **82**, 666-674.

Karunagaran, D., Tzahar, E., Beerli, R.R., Chen, X., Graus-Porta, D., Ratzkin, B.J., Seger, R., Hynes, N.E. and Yarden, Y. (1996) ErbB-2 is a common auxiliary subunit of NDF and EGF receptors: implications for breast cancer. *The European Molecular Biology Organization Journal*, **15**, 254-264.

Lauffenburger, D.A. and Linderman, J.J. (1993) *Receptors*. Oxford University Press, Inc., New York.

Leof, E.B. (2000) Growth factor receptor signalling: location, location, location. *Trends in Cell Biology*, **10**, 343-348.

Lewis, G.D., Lofgren, J.A., McMurtrey, A.E., Nuijens, A., Fendly, B.M., Bauer, K.D. and Sliwkowski, M.X. (1996) Growth Regulation of Human Breast and Ovarin Tumor Cells by Heregulin: Evidence of the Requirement of ErbB2 as a Critical Component in Mediating Heregulin Responsiveness. *Cancer Research*, **56**, 1457-1465.

Lund, K.A., Opresko, L.K., Starbuck, C., Walsh, B.J. and Wiley, H.S. (1990) Quantitative Analysis of the Endocytic System Involved in Hormone-induced Receptor Internalization. *The Journal of Biological Chemistry*, **265**, 15713-15723.

Menard, S., Casalini, P., Campiglio, M., Pupa, S., Agresti, R. and Tagliabue, E. (2001) HER2 overexpression in various tumor types, focussing on its relationship to the development of invasive breast cancer. *Annals of Oncology*, **12**, S15-S19.

Opresko, L., Chang, C., Will, B., Burke, P.M., Gill, G.N. and Wiley, H.S. (1995) Endocytosis and lysosomal targeting of epidermal growth factor receptors are mediated by distinct sequences independent of tyrosine kinase domain. *The Journal of Biological Chemistry*, **270**, 4325-4333.

Reddy, C.C., Wells, A. and Lauffenburger, D.A. (1994) Proliferative Response of Fibroblasts Expresing Internalization-Deficient Epidermal Growth Factor (EGF) Receptors Is Altered via Differential EGF Depletion Effect. *Biotechnology Progress*, **10**, 377-384.

Sorkin, A., DiFiore, P.P. and Carpenter, G. (1993) The carboxyl terminus of epidermal growth factor receptor/erbB-2 chimerae is internalization impaired. *Oncogene*, **8**, 3021-3028.

Starbuck, C., Wiley, H.S. and Lauffenburger, D.A. (1990) Epidermal Growth Factor Binding and Trafficking Dynamics in Fibroblasts: Relationship to Cell Proliferation. *Chemical Engineering Science*, **45**, 2367-2373.

Wiley, H.S. and Burke, P.M. (2001) Regulation of Receptor Tyrosine Kinase Signaling by Endocytic Trafficking. *Traffic*, **2**, 12-18.

Wiley, H.S. and Cunningham, D.D. (1982) The Endocytotic Rate Constant. *The Journal of Biological Chemistry*, **257**, 4222-4229.

Wiley, H.S., Herbst, J.J., Walsh, B.J., Lauffenburger, D.A., Rosenfeld, M.G. and Gill, G.N. (1991) The Role of Tyrosine Kinase Activity in Endocytosis, Compartmentation, and Down-regulation of the Epidermal Growth Factor Receptor. *The Journal of Biological Chemistry*, **266**, 11083-11094.

Wiley, H.S. and Kaplan, J. (1984) Epidermal growth factor rapidly induces a redistribution of transferrin receptor pools in human fibroblasts. *Proceedings of the National Academy of Sciences - USA*, **81**, 7456-7460.

Worthylake, R., Opresko, L.K. and Wiley, H.S. (1999) ErbB-2 Amplification Inhibits Down-regulation and Induces Constitutive Activation of Both ErbB-2 and Epidermal Growth Factor Receptors. *The Journal of Biological Chemistry*, **274**, 8865-8874.

Chapter 3: HER2-Mediated Effects on EGFR and HER2 Endocytosis

Endocytic trafficking plays an important role in the regulation of the EGFR family. Many cell types express multiple EGFR family members (including EGFR, HER2, HER3 and/or HER4) that interact to form an array of homo- and heterodimers. Differential trafficking of these receptors should strongly affect signaling through this system by changing substrate access and heterodimerization efficiency. Because of the complexity of these dynamic processes we used a quantitative, computational model to understand their integrated operation. Parameters characterizing EGFR and HER2 interactions were determined using experimental data obtained from mammary epithelial cells constructed to express different levels of HER2, enabling us to estimate receptor-specific internalization rate constants and dimer uncoupling rate constants. Significant novel results obtained from this work are: first, that EGFR homodimerization and EGFR/HER2 heterodimerization occur with comparable affinities; and, second, that EGFR/HER2 heterodimers traffic as single entities. Further, model predictions of the relationship of HER2 expression levels to consequent distribution of EGFR homodimers and EGFR/HER2 heterodimers suggest that the levels of HER2 found on normal cells are barely at the threshold necessary to drive efficient heterodimerization. Thus, altering HER2 concentrations, either overall or local, could provide an effective mechanism for

regulating EGFR/HER2 heterodimerization and may explain why HER2 overexpression found in some cancers has such a profound effect on cell physiology.

3.1 Introduction

In the EGFR family, endocytic trafficking processes can strongly influence cell responses to EGF family ligands. Many cell types express multiple EGFR family members that can interact to form an array of homo- and heterodimers (Alroy and Yarden, 1997). HER2 is commonly postulated to be the 'preferred dimerization partner' of all EGFR family receptors (Graus-Porta et al., 1997; Qian et al., 1994; Tzahar et al., 1996), however, this has not been rigorously examined in terms of expression levels and mass-action kinetics.

Regulation of the distribution of EGFR family receptors among cell compartments can significantly modulate the overall signaling through this system by changing access to heterodimerization partners. Because of the potential complexity of EGFR family interactions associated with concomitant receptor trafficking and signaling, application of quantitative experimental and computational modeling techniques to its analysis should be very useful.

In this work, we examine the endocytic portion of the trafficking pathway in detail with the aim of quantitatively understanding how EGFR and HER2 interact in the process of internalization. We found that: (i) EGFR/HER2 heterodimers are internalized as single entities, with other models of internalization being inconsistent with literature data (Hendriks et al., 2003 (Chapter 2)), (ii) EGFR/HER2 have a comparable

dimerization affinity as EGFR/EGFR homodimers, thus the notion of HER2 as a 'preferred dimerization partner' should be re-assessed, and (iii) there appears to be a threshold level of HER2 above which heterodimerization is maximal, but increased HER2 expression is still able to alter signaling through longer term effects.

3.2 Experimental Procedures

3.2.1 Reagents/Cell Culture

Antibodies 13A9 against the EGFR (Winkler et al., 1989), monoclonal antibodies 7C2 and 2C4 against HER2 (Fendly et al., 1990; Sliwkowski et al., 1994) and the fAb fragment of monoclonal 7C2 were gifts from Genentech. The human mammary epithelial cell lines MTSV1-7 and ce2 have been described previously (D'Souza et al., 1993) and were provided as a generous gift from Dr. Joyce Taylor-Papadimitriou. These cells were grown in Dulbecco's modified Eagle's medium (Flow laboratories) containing 10% calf serum (HyClone) supplemented with 1μM insulin and 5μM dexamethasone. ErbB-2 expression in ce2 cells was maintained by the addition of 500ug/ml G418 (Sigma Chemical Company). Antibodies and EGF were iodinated with iodobeads (Pierce) according to the manufacturer's directions to specific activities of 2.7 x 10^6 cpm/pmol (mab), 8 x 10^5 cpm/pmol for the fAb fragment of 7C2 and 1.6 x 10^6 cpm/pmol for EGF.

3.2.2 Binding Analysis

Numbers of EGFR and HER2 molecules on the cell surface were determined by steady state analysis (Wiley and Cunningham, 1981). Cells were incubated with

concentrations from 6.7 x 10^{-11} to 2 x 10^{-8} M for 3.5 hr at 37°C. The relative amount of antibody associated with the cell surface was determined by acid stripping and the data was analyzed as previously described (Worthylake et al., 1999). Specific internalization rates (k_e) for the EGFR were determined as described (Lund et al., 1990) using 17 nM ligand and a 5 min incubation period. Specific internalization rates for the labeled mAbs were determined using a concentration of 1.3 nM antibody and 2 min intervals for a total of 10 min. Values were calculated as regression slope of the integral surface-associated ligand against the amount internalized (Lund et al., 1990).

3.3 Model Development

3.3.1 Constitutive Case

Our model was designed to output results that can be compared to the internalization experiments used to generate the data (Hendriks et al., 2003 (Chapter 2); Lund et al., 1990; Wiley and Cunningham, 1982). The constitutive internalization of EGFR and HER2 is modeled with a set of coupled mass action kinetic equations. Consistent with published reports, we assume that a constitutive level of EGFR and HER2 homo- and hetero-dimerization takes place (Mendrola et al., 2002; Penuel et al., 2002; Yu et al., 2002). As diagrammed in Figure 3.1, (in the absence of any stimulation) EGFRs are allowed three states: free EGFR (R1), homodimerized with another EGFR (R1R1), or heterodimerized with HER2 (R1R2). HER2 is allowed similar freedom: free HER2 (R2), homodimerized with another HER2 (R2R2), or heterodimerized with EGFR (R1R2). The behavior of each species with regard to internalization is characterized by an

internalization rate constant. Each dimerization and uncoupling act is characterized by its own, but not necessarily unique, kinetic rate constant.

3.3.2 Ligand-Stimulated Case

Using the constitutive internalization model as a basis, ligand-induced interactions were added (diagrammed in Figure 3.1). We have included the complete set of binary interactions between the EGFR and HER2 with and without EGF. Higher-order oligomerization of receptors is neglected, as this is a first approximation of possible EGF/EGFR/HER2 interactions. Additionally, HER3 and HER4 are left out of our analysis because we are examining the effects of EGF stimulation and they are typically expressed at lower levels.

In addition to the constitutive receptor species (R1, R1R1, R1R2, R2, R2R2) and their interactions, EGFRs now bind ligand (L) to form complexes (R1L). Complexes may homodimerize with another complex to form doubly bound EGFR homodimers (LR1R1L) or heterodimerize with HER2 to form EGF-EGFR/HER2 heterodimers (R1R2L). Additionally, the existence of singly bound EGFR homodimers (R1R1L) is permitted and each species may be formed in any order. For example, singly bound EGFR homodimers can be formed by ligand dissociation from doubly bound EGFR homodimers or by ligand binding to unbound EGFR homodimers or by dimerization of an empty EGFR with an EGF-EGFR complex. As before, each receptor species may have a unique internalization rate constant and every interaction is reversible with its own set of kinetic rate constants.

Superimposed on the surface level receptor interactions are two additional processes: (i) the binding of radiolabeled antibodies to HER2, corresponding to the actual experiment and (ii) the internalization of each receptor species. Under resting conditions, each receptor species is assumed to be at steady state, wherein rates of receptor internalization are perfectly balanced by rates of receptor synthesis and degradation. Thus, internalization and recycling of unlabeled receptor species can be left out of the model. Receptor species that have been bound by EGF, an antibody or antibody Fab fragment, however, are internalized at a rate specific to each species to an inside compartment. Recycling of each species is assumed to be negligible over the 7.5 min timescale of the model/experiment (Wiley and Cunningham, 1981).

Inside and surface data are generated with the model and manipulated in the same manner as the experimental data to calculate the observed internalization rate constants for specific EGFR and HER2 expression levels. The model parameters are list in Table 3.1. The overall observed internalization rate for EGF or Fab-bound species is essentially a weighted sum of the individual internalization rate of each EGF- or Fab-bound receptor species. Model equations corresponding to the interactions diagrammed in Figure 3.1 with Fab binding superimposed are listed in the Appendix.

3.3.3 Parameter Estimation & Determination

The model parameters can be divided into three categories: (i) binding parameters, which govern EGF and antibody binding and dissociation, (ii) internalization rate constants, which describe the internalization rate of each receptor species, and (iii)

dimerization rate constants, which characterize the dimerization and uncoupling of EGFR and HER2 in various states.

In the case of our experiments, we used Fab fragments of anti-HER2 antibodies. Fab binding (k_{on}Fab) and dissociation (k_{off}Fab) were experimentally measured to be $1.4x10^7$ $(M\ min)^{-1}$ and 0.30 min^{-1} (data not shown). As suggested in the literature, Fab binding was assumed to be have no effect on receptor dimerization/uncoupling, EGF binding/dissociation or receptor internalization. EGF binding (k_{on}) and dissociation (k_{off}) for 184A1 human mammary epithelial cells were reported to be $9.7x10^7$ $(M\ min)^{-1}$ and 0.24 $(min)^{-1}$, respectively (Hendriks et al., 2003 (Chapter 2)).

Many of the species-specific internalization rate constants can be estimated from the experimental data. If one assumes that free HER2 and HER2 homodimers internalize at the same rate, their internalization rate constant should be reflected by the case where HER2 expression is much greater than EGFR expression. In the absence of EGF, the internalization rate constant of free HER2 (k_eR2^-) is reflected by the asymptote approached at high HER2 expression levels (0.01 min^{-1}), approximately the rate of membrane turnover (Burke and Wiley, 1999). In the presence of EGF, there is an increase in membrane turnover and the internalization rate of free HER2 (k_eR2^+) is roughly 0.03 min^{-1}. The internalization rate of free EGFR (k_eR1) has been reported to be 0.08 min^{-1} (Hendriks et al., 2003 (Chapter 2)). As with HER2, we assume that unbound EGFR homodimers internalize with the same rate constant as free EGFR. Unbound EGFR/HER2 heterodimers are likely to internalize at a rate between that of HER2

homodimers and EGFR homodimers. We estimate the internalization rate constant of unligated EGFR/HER2 heterodimers (k_eR1R2) to be 0.04 min^{-1}.

The internalization rate of EGF-EGFR complexes, complex homodimers and singly bound EGFR homodimers are assumed to internalize with the same first order rate constant (k_eR1L). This parameter represents the case where no HER2 is present and can be extrapolated to the y-intercept of the graph of EGFR internalization versus HER2 expression level, yielding a value of approximately 0.28 min^{-1}. The internalization rate constant for bound EGFR/HER2 heterodimers (k_eR1R2L) is represented by the asymptote of EGFR internalization with increasing HER2 expression. From the EGFR internalization data, at the highest level of HER2 expression, the internalization rate constant of HER2 heterodimers is estimated to be 0.10 min^{-1}.

All receptor dimer species are estimated to form at the diffusion-limited values, with a coupling rate constant (k_c) of 10^{-3} $(\#/cell\ min)^{-1}$ (Mahama and Linderman, 1994; Shea et al., 1997). The uncoupling rate constants of each dimer species (k_uR1R1, k_uR1R2, and k_uR2R2) were fit to the HER2 internalization data in the absence of EGF. Holding these parameters fixed, the uncoupling rate constants for EGFR complex homodimers and bound heterodimers (k_uLR1R1L and k_uR1R2L) were fit to the either the EGFR internalization data or the HER2 + EGF internalization data. These values are intended as order of magnitude estimates of the various uncoupling rate constants.

3.3.4 Computations

Mathematical equations corresponding to the model described above were coded into MATLAB version 6.5 (Mathworks, Natick, MA) and solved using ODE solver ode23s. Parameters were fit to experimental data using the lsqcurvefit routine from the Optimization Toolbox. Matlab code can be found in Appendix A.1 and A.2.

3.4 Results

Recent work has highlighted the importance of receptor internalization in determining the distribution and induced degradation of EGFR in response to EGF stimulation (Hendriks et al., 2003 (Chapter 2)). HER2 has emerged as a modulator of EGFR internalization presumably through heterodimerization. Here, we explored the importance of heterodimerization in the internalization of both EGFR and HER2 as a function of HER2 expression level using previously published experimental data and a computational model of EGFR and HER2 internalization.

3.4.1 Parameter Determination from Experimental Data

Experimental data demonstrating the effect of increasing HER2 expression on the internalization rate constants of HER2 and EGF is derived from (Hendriks et al., 2003 (Chapter 2)) and shown in Figure 3.2a. In the absence of EGF, HER2 was internalized slowly at a rate comparable to membrane turnover. The addition of EGF accelerated the internalization of HER2. The internalization rate of EGF showed a marked decrease with increasing HER2 expression, while HER2 internalization under similar conditions

showed a mild decline in internalization with increasing HER2 expression. In Figure 3.2b is experimental data (Hendriks et al., 2003 (Chapter 2)) showing the effect of pre-incubation with heterodimerization blocking antibodies (2C4) on the internalization rate constant of EGF. Blocking heterodimerization abrogated any HER2 dependent effect on EGF internalization.

The significance of these results has previously been explored from a global, whole cell perspective. Here, we seek to explore the mechanistic basis for these findings in order to test different models of internalization, determine which receptor species are dominant under different conditions and elucidate which interactions dictate internalization behavior. The distribution of receptors between different signaling states (homodimers vs. heterodimers, for example) should provide insight into the circumstances that contribute to aberrant cell behavior.

3.4.2 Models of Receptor Internalization

The general framework for our internalization models is shown in Figure 3.1. Every binary interaction between EGFR and HER2 with and without EGF addition is included. Individual models differ with regard to certain parameter values, or assumptions regarding species-specific behavior. The first internalization model that we consider is one in which each dimer species is sufficiently stable to be internalized as a single entity, hereafter referred to as the 'coupled-internalization' model. This model is fit to the data by first fitting uncoupling rate constants (k_uR1R1, k_uR1R2, k_uR2R2) to the data in the absence of EGF. Holding those parameters fixed, the remaining uncoupling

rate constants (k_uLR1R1L, k_uR1R2L) are fit to the EGFR data and used to predict the HER2 + EGF internalization data (shown in Figure 3.2a). Nearly identical results are obtained if one fits to the HER2 + EGF data and predicts the EGFR internalization data (data not shown). The parameter values determined are shown in Table 3.1.

We simulated the effect of disrupting heterodimerization on the EGF internalization rate constant by increasing the bound heterodimer uncoupling rate constant (k_uR1R2L), as shown in Figure 3.2b. Model predictions are shown together with experimental data for EGF internalization in the presence of an antibody (2C4) that blocks EGFR/HER2 heterodimerization (Sliwkowski et al., 1994).

An alternative model of internalization might be one in which dimer species are transiently stable so that only individual receptors and complexes are internalized. We simulated this by setting the uncoupling rate constants to sufficiently large values such that no significant degree of dimerization occurs. This model required no fitting of parameters and clearly does not capture the trends seen in the experimental data (Figure 3.3a).

Another possibility is a model proposed by Wang et al, in which they assert that heterodimers do not internalize (Wang et al., 1999). To simulate this model, we have set the internalization rate constant of heterodimers (k_eR1R2L) to zero and fit the same parameters as with the original 'coupled internalization' model. When this model is fit to the EGFR data and used to predict the HER2 data (Figure 3.3b) it predicts the wrong the curvature in the HER2 data at low HER2 expression. While this result still looks

reasonably good, the model fails completely if we do the reciprocal fit, in which we fit the model to the HER2 data first and then predict EGFR data (shown in Figure 3.3c).

Lastly, we present a model in which receptor internalization is indirectly related to HER2 expression level of the form $k_{e,i} = a_i + b_i$(HER2 Level), where subscript i refers to either EGFR or HER2, a_i are the receptor internalization rates in the absence of HER2 and b_i are constants to be fit. Shown in Figure 3.3d are the results from fitting parameters to the HER2 data and predicting EGFR data. Here, the model is able to capture some of the trends in the data, but misses the curvature in the EGFR data. The results are similar for the reciprocal fit.

3.4.3 Experimental Test of the Effect of HER2 Expression on Heterodimerization

We can also use our model to predict quasi steady state distributions of homo- and heterodimers. The time scale for receptor-receptor interactions in the membrane is significantly faster than the time scale for internalization. As such, it can be assumed that the distribution of the various receptor species reaches a quasi steady state prior to internalization. Solving the model at steady state, neglecting internalization and using the dimerization parameters determined from fitting experimental data we have calculated the degree of homo- and heterodimerization as a function of HER2 and EGFR expression levels. Shown in Figure 3.4a is the percent of HER2 that is homodimerized in the absence of EGF. This is strongly dependent on HER2 level and reaches a maximum value of about 90%, with the most pronounced effects occurring between 0 and about 100,000

/cell. In the presence of 1.7 nM EGF, the percent of HER2 that are heterodimerized is shown in Figure 3.4b and the percent of EGFR that are heterodimerized is shown in Figure 3.4c. In both cases there is a strong dependence on HER2 level, and modest dependence on EGFR level. The largest effects are observed over the range of $0 – 2 \times 10^5$ HER2 per cell.

In Figure 3.5 we compare the absolute numbers of homo- and heterodimers as predicted by our model for EGF concentration from 1 to 100 ng/ml. These predictions are made with equal affinities for homo- and heterodimerization, as measured from our parameter determination. As expected, for a given EGFR level, increasing HER2 expression increases the relative amount of heterodimers. Surprisingly, for a given HER2 level, increasing EGFR expression also increases the amount of heterodimers under most conditions. Only when the number of occupied EGFR is equal to or greater than the amount of HER2 does the relative amount of heterodimers decrease with increasing EGFR expression (best seen in the 100 ng/ml case). If one were to compare the absolute number of homo- versus heterodimers as an indirect measure of dimerization affinity the spurious conclusion that heterodimerization is highly favored could easily be made. This apparent preference of EGFR for heterodimerization happens for two reasons: (i) not all EGFR are occupied, especially at lower EGF concentrations so that the number of EGFR interacting with HER2 may actually be significantly less than expected. This is further exacerbated by the fact that EGF-EGFR complexes and homodimers are cleared from the surface more quickly than heterodimers. And, (ii) the equilibrium distribution between EGF-EGFR complexes and homodimers does not completely favor homodimers. Thus,

even if EGFR and HER2 levels are comparable, the dynamics and kinetics of the system will favor the appearance of heterodimers in an absolute sense.

To test the predictions made by our model, we obtained a set of mammary epithelial cells that were not used to estimate the original model parameters. These cells were SV40 immortalized MTSV-1 cells and the derivative Ce2 line, which was engineered to overexpress HER2 (D'Souza et al., 1993). Binding of radolabeled EGF demonstrated that these cells expressed between 3.5-4.5 x 10^5 EGFR each (data not shown). Steady-state binding of radiolabeled anti-HER2 monoclonal 7C2 indicated that MTSV cells express approximately 9 x 10^4 surface HER2 whereas Ce2 cells express approximately 1.7 x 10^6 per cell (Data not shown; also see (Worthylake et al., 1999)). From these relative numbers of EGFR and HER2, we can predict quite distinct degrees of heterodimerization between EGFR and HER2 for the two cell lines (see Figures 3.4b and 3.4c). In the presence of saturating EGF, we expect that few (<25%) EGFR will be found in heterodimers in MTSV cells whereas most should be in heterodimers in Ce2 cells. Conversely, a large fraction of HER2 will be found in heterodimers in MTSV cells, but only a small fraction will be heterodimerized in Ce2 cells. Furthermore, the effect of heterodimerization should be readily observable by its influence on EGFR and HER2 internalization.

To verify the predicted effect of EGFR/HER2 heterodimerization on HER2 internalization, Ce2 cells were incubated in 200 ng/ml of ^{125}I-7C2 or ^{125}I-2C4 antibody for 3 hours and then the amount of internalized antibody was then determined as a function of time following the addition of 100 ng/ml EGF. As shown in Figure 3.6a, the addition

of EGF increases the amount of internalized 7C2 antibody. In contrast, there was no change in the amount of internalized 2C4, verifying that heterodimerization between EGFR and HER2 is necessary to stimulate HER2 internalization.

To measure the internalization of both HER2 and the EGFR, we used radiolabeled monoclonal antibodies against these two receptors. The internalization rate constant (k_e) for HER2 was measured over a ten-minute time period either radiolabeled 7C2 or 2C4 anti-HER2 antibodies in both the presence and absence of EGF. Because mAb 7C2 has no effect on HER2 heterodimerization it should indicate the internalization rate of the entire population of HER2 (Fendly et al., 1990). In contrast, mAb 2C4 blocks HER2 heterodimerization and thus should indicate the internalization rate of non-dimerized HER2.

Shown in Table 3.2 are the internalization rate constants of monoclonal antibodies against HER2 and EGFR in the presence and absence of EGF. We found that in the absence of EGF, the values of k_e were very similar between the different anti-HER2 monoclonals in either cell type. Essentially identical values were obtained when using Fab fragments of 7C2 (data not shown). The anti-EGFR monoclonal 13A9 was also internalized at a similar rate. The observed values (generally between 0.02-0.04 min^{-1}) are similar to previously reported values (Baulida et al., 1996; Worthylake et al., 1999) and are consistent with internalization by constitutive turnover of the plasma membrane (Wiley et al., 1991).

The addition of EGF increased the values of k_e of mAb 7C2 approximately 2-fold in both cell types, but had little if any effect on the heterodimerization-blocking mAb

2C4, again confirming the importance of heterodimerization for EGF-induced internalization of HER2. EGF stimulated the internalization of the anti-EGFR mAb 13A9 approximately 3-4 fold. The internalization rate of the bound 13A9 was very similar to that observed for EGF itself (Table 3.2), indicating that the behavior of the monoclonals accurately reflect that of the receptor population.

The above data demonstrate that EGF stimulates HER2 internalization through heterodimerization, but does not indicate the stoichometries of the internalized EGFR/HER2 heterodimers as a function of HER2 expression. To address this important point, we brought parallel plates of cells to steady state with either radiolabeled 7C2 or 13A9. The fraction of the total HER2 and EGFR population tagged with the antibodies was determined by conducting saturation binding experiments with a parallel set of cells. After the cells reached a steady state distribution of labeled mAbs between the cell surface and intracellular compartment, a saturating amount of EGF was added. The change in intracellular anti-HER2 and anti-EGFR mAbs was then quantified and corrected for their relative fractional occupancies.

As shown in Figure 3.6b, the steady state distribution between the cell surface and the intracellular compartment of antibodies bound to HER2 and EGFR was very similar, with approximately 20-30% being intracellular. Following addition of EGF, however, there was a rapid shift of the bulk of EGFR to an intracellular compartment, accompanied by a relatively minor shift of HER2 to an intracellular compartment (Figure 3.6b, inset). Internalization of both EGFR and HER2 was significantly less in the case of the HER2-overexpressing Ce2 cells. At 15 minutes following EGF addition, approximately 70% of

the EGFR, but only 30% of the HER2 had been internalized in MTSV cells. In the case of Ce2 cells, 55% of the EGFR had been internalized, but only 12% of the HER2. By considering the initial numbers of EGFR and HER2 in the two cells, we calculate that EGF addition stimulated the internalization of 3.2 and 3.7 x 10^5 EGFR in MTSV and Ce2 cells respectively, and stimulated the internalization of 0.2 and 3.1 x 10^5 HER2 in the same cells. Thus we calculate that in MTSV cells, only about 6% (±2% S.D) of the internalized EGFR are internalized as heterodimers, but in Ce2 cells 83% (±33% S.D.) are internalized as heterodimers. Our model predicts 20% and 80% of the EGFR to be in heterodimers for the MTSV and Ce2 cells, respectively. These predictions are slightly different from the experimental calculation, but if we assume that some heterodimers dissociate prior to internalization and consider the experimental error, then the match between predictions and our experimental tests are quite good.

3.4.4 Model Insights

Receptors comprise the primary layer of input to the intracellular signaling machinery of the cell. The generated signals are a function of the distribution of receptor species (complexes vs. heterodimers) as well as receptor location (surface vs. internal). Using our 'coupled-internalization' model of internalization and our derived parameter values, we can gain insight into how varying levels of receptor expression could affect cell signaling. For this analysis, we will only examine short-term signaling in response to 10 ng/ml EGF stimulation. We restrict ourselves to short time scales because our model neglects the effects of receptor recycling. Recycling is very important in determining the

overall system behavior it acts on the time scale of minutes to hours. The early events of ligand binding, receptor dimerization and activation develop very quickly, over a time scale of seconds with internalization acting on the time scale of minutes (Kholodenko et al., 1999; Schoeberl et al., 2002). As such, the short-term responses – on the order of 10 minutes – are sufficient to determine the nature of the initial input to the signaling machinery.

One manner in which HER2 heterodimerization could amplify extracellular signals is by allowing one molecule of EGF to recruit and activate two receptors (one EGFR and one HER2). Consequently, the total number of receptors actively signaling in response to 10 ng/ml EGF should increase with increasing HER2 expression level, as is seen in Figure 3.7a. The distribution of these receptors between homo- and heterodimers is shown in Figure 3.7b. Increasing HER2 expression causes a dramatic increase the number of heterodimers formed, but elicits a relatively small decrease in the amount of homodimers formed.

The fraction of total signaling species that are heterodimerized is shown in Figure 3.7c. Since homodimers and heterodimers are believed to have different signaling abilities and different signaling strengths, this plot demonstrates how the nature of EGF induced signaling may change with increasing HER2 expression. At short time points the EGF binding has not yet reached a steady state so that there is a large excess of HER2 relative to occupied EGFR, even for the parental cell line. At longer timescales the distribution of signal plateaus with a roughly even distribution for the low HER2

expression (30,000 /cell) and a shift in distribution for HER2 expression levels over 100,000 per cell.

Both the number of surface complexes and number of heterodimers reaches a quasi steady state over the short time scale. The fluxes of receptor species, defined as the rate at which a given receptor species is being internalized (flux = [number of species present]×[species internalization rate constant]), parallels this result. Shown in Figure 3.7d is the internalizing flux of heterodimers and the flux of equivalent EGF-EGFR homodimers, defined as (R1L + R1R1L + 2*LR1R1L)/2 to enable the direct comparison with the flux of heterodimers; so chosen because all of these species are postulated to have equivalent internalization behavior. More EGFR homodimers are being internalized than heterodimers at low HER2 levels, but as HER2 levels increase, the flux of EGFR homodimers decreases, matched by a concomitant increase in the flux of heterodimers (Figure 3.7d). This is reflected in our observation that at low levels of HER2 expression, only a small fraction of EGFR are internalized as heterodimers whereas high levels of HER2 expression result in almost all EGFR being internalized as heterodimers. Interestingly, heterodimers do not begin to dominate the internalization flux until a HER2 expression level of over 100,000.

3.5 Discussion

Cell signaling is a complex dynamic process initiated by ligand-receptor binding followed by the recruitment of a cascade of signaling molecules. Signals are transmitted to the nucleus by way of protein modifications and translocations, causing altered gene

and protein expression and ultimately resulting in a cell response. This process is regulated at many levels, including negative feedback in signaling pathways as well as at the level of receptor trafficking. One of the most direct ways to regulate the system output is to regulate the system input. For the EGFR family of receptor tyrosine kinases, the system input is modulated by the formation of receptor homo- and heterodimers, each with potentially different signaling capabilities. This allows signaling to be regulated by controlling the degree of homo- and heterodimerization as well as by controlling receptor distribution between cellular compartments.

To understand how endocytosis and endosomal sorting modulates input into receptor signaling networks, we have compared various models of EGFR and HER2 internalization. With these models we are able to critically assess some of the current hypotheses regarding HER2 internalization and heterodimerization as well as to predict the impact of elevated HER2 expression on intracellular signal generation.

3.5.1 HER2 Internalization

For the most part, studies of HER2 internalization have confined themselves to examining the behavior of HER2 (or EGFR/HER2 chimeras) in isolation. Although there is some disagreement regarding the exact rate of internalization (Drebin et al., 1985; Klapper et al., 1997; Lotti et al., 1992), the generally accepted conclusion is that HER2 is 'internalization impaired' relative to the EGFR (Baulida et al., 1996; Sorkin et al., 1993). Our previous work supports this notion (Hendriks et al., 2003 (Chapter 2)). Because HER2 appears to require dimerization for activation, the internalization behavior of

heterodimers is likely to be of greater interest. Wang et al. have studied the internalization behavior of EGFR-HER2 heterodimers and concluded that they were not endocytosed in response to EGF stimulation (Wang et al., 1999). Our modeling demonstrates that this contention is inconsistent with quantitative internalization data. Instead, heterodimers appear to be internalized at a rate that is lower than EGFR homodimers, but still rapid enough to induce a significant redistribution of receptors.

Our model and experimental data is consistent with the hypothesis that heterodimers are sufficiently stable to traffic as single entities. It appears that heterodimers are internalized at a reduced rate, at about half to one-third of the rate of EGFR complexes. This is consistent with the observation that EGF can induce down-regulation of HER2 in the absence of rapid HER2 internalization. Although heterodimers are internalized relatively slowly, they are still internalized faster than the rate of HER2 loss (Worthylake and Wiley, 1997). Our model was able to recapitulate the complex interplay between the EGFR and HER2 as demonstrated by its ability predict an independent set of data using a constant parameter set, as well as predict the effect of blocking heterodimerization. Lastly, we were able to validate model predictions with experimental measurements of the stoichiometry of EGFR and HER2 internalization. None of the other models that we explored had this ability. Thus, our model of internalization is a reasonable basis for studying the regulatory influence of the trafficking pathway.

3.5.2 HER2 Dimerization

It is commonly understood that HER2 is the 'preferred dimerization partner' of all EGFR family receptors and dimerization takes place with a strict hierarchy (Graus-Porta et al., 1997; Qian et al., 1994; Tzahar et al., 1996). This implies that occupied EGFR, in the presence of all EGFR family members, prefer to heterodimerize with HER2 rather homodimerize with another occupied EGFR or other EGFR family member. We interpret this to mean that following EGF stimulation, the affinity for EGFR-HER2 dimerization should be greater than that EGFR-EGFR dimerization. Our mathematical modeling of receptor dimerization and the effects of elevated expression levels allow us to obtain estimates of these dimerization affinities and thereby critically evaluate this notion.

Our experimentally derived receptor dimerization and uncoupling parameters are the first reported estimates of these values in whole cells with native receptors. EGFR dimerization has previously been monitored in live cells, but in the absence of HER2 (Blakely et al., 2000). Other studies have examined receptor dimerization with solubilized fragments of various ErbB receptors (Ferguson et al., 2000; Tanner and Kyte, 1999). Although we determined the parameters values indirectly, they are consistent with reports that in the absence of EGF, EGFR and HER2 homodimerize with comparable affinities (Mendrola et al., 2002). We also found that the addition of EGF increased both EGFR homo- and heterodimer affinities by 10- to 100- fold relative to empty receptors and found them to be of equal magnitude. Due to the uncertainty in the parameter fitting heterodimerization could be slightly preferred, as suggested in the literature although it appears unlikely (Graus-Porta et al., 1997; Qian et al., 1994; Tzahar et al., 1996). If

EGFR heterodimerization affinity is postulated to be 10 fold greater than that for homodimerization (k_uR1R2L/k_uLR1R1L = 0.1) the model fits the experimental data 24% worse (data not shown). By comparison, if EGFR homodimerization affinity is 10 fold greater than that for heterodimerization (k_uR1R2L/k_uLR1R1L = 10) the model fit differs by less than 2% from the fitted parameters (data not shown). This suggests that the local relative concentration of EGFR and HER2 is the primary determinant of the fraction of homo- versus heterodimers rather than the relative affinities of their interaction. Lastly, these studies do not provide estimates of HER2's dimerization affinity with HER3 or HER4, although it is reasonable to expect that they would be of the same order of magnitude as EGFR/HER2 dimerization.

Our model calculations regarding the extent of whole-cell heterodimerization assumes that all receptors are uniformly distributed on the cell surface. It is clear, however, that locally high concentrations of HER2, such at membrane subdomains (Meier et al., 1997; Ohno et al., 2002), could facilitate the formation of heterodimers. In some tumors, levels of both EGFR and HER2 can vary over several orders of magnitude. Thus, relative expression levels could be the principal factor governing the pattern of homo- and heterodimerization in transformed cells. Unfortunately, most studies investigating the ability of different HER family members to form homo- and heterodimers do not quantify the relative level of receptor expression. This omission obscures the intrinsic propensity of different receptors to form different pairs of homo- versus heterodimers (Lenferink et al., 1998; Pinkas-Kramarski et al., 1998). Our work strongly suggests that relative expression levels are critical determinants in this process.

3.5.3 Signaling Implications

Our predictive model for the distribution of EGFR and HER2 homo- and heterodimers provides a tool for generating testable hypotheses regarding the contribution of this aspect of receptor behavior to intracellular signaling. The model makes obvious predictions that one would expect from increasing HER2 expression; for example, an increase in heterodimerization. However, we can also gain some non-intuitive insight into system dynamics. For example, we found that the dynamics of EGFR–HER2 receptor distribution between the cell surface and endosomal compartment are principally controlled by the level of HER2 expression that, in turn, controls the degree of heterodimerization. Figures 3.4b & 3.4c show that there is a threshold level of HER2 expression (approximately 100,000 /cell) beyond which there is little alteration in receptor behavior and that EGFR expression has only a minor effect on the degree of heterodimerization. This conclusion is supported by the data presented in Figure 3.5 and in Table 3.2 that show similar levels of enhancement of EGF-stimulated HER2 internalization over a 16-fold range of HER2 expression levels. Of course, increasing receptor expression (EGFR and/or HER2) will increase the magnitude of the signals that can be generated. However, this prompts an important question. What is more likely to cause aberrant cell behavior, increased signal strength or a change in the nature of the input signal (i.e., a shift from homo- to heterodimers or a shift from the cell surface to endosomes)? We might anticipate that cells would be more likely affected by qualitative rather than quantitative changes in signal input. These two effects may be difficult to separate from an experimental point of view, but a computational modeling approach

should aid in determining which are the true factors controlling cell behavior and which are the best targets for therapeutic intervention.

3.5.4 Conclusions

The principle findings of this study can be summarized as such: (i) EGFR-HER2 are internalized as single entities, with other models of internalization being inconsistent with the data (Hendriks et al., 2003 (Chapter 2)); (ii) HER2 is not a 'preferred dimerization partner' as previously concluded – rather it has a comparable dimerization affinity as EGFR with the appearance of preferential dimerization arising from relative expression levels and simple mass action kinetics; (iii) There appears to be a threshold level of HER2 (roughly 10^5 for these cells with 2×10^5 EGFR) above which there is little effect on the degree of heterodimerization (see Figure 3.4) but increased HER2 expression may still affect the quantity and nature of signals generated (see Figure 3.7). All of these conclusions underscore the importance of relative EGFR and HER2 expression levels. Consequently, it is not enough to merely examine HER2 level when interpreting downstream signaling data (or looking at a patient population) but the entire complement of interacting receptors should also be determined and taken into consideration.

3.6 Tables

Table 3.1 Internalization Model Parameters

Model Parameter	*Description*	*Value*
binding parameters		
k_{on}	EGF association	9.7×10^{7} (M min)$^{-1}$
k_{off}	EGF dissociation	0.24 min^{-1}
k_{on}Fab	Fab association	1.4×10^{7} (M min)$^{-1}$
k_{off}Fab	Fab dissociation	0.30 min^{-1}
internalization rate constants (estimated from experimental data)		
k_eR1	unoccupied EGFR internalization rate constant	0.08 min^{-1}
k_eR2^{-}	HER2 internalization rate constant, No EGF	0.01 min^{-1}
k_eR2^{+}	HER2 internalization rate constant, + EGF	0.03 min^{-1}
k_eR1R2	EGFR-HER2 unbound heterodimer internalization rate constant	0.04 min^{-1}
k_eR1L	EGF-EGFR complex internalization rate constant	0.28 min^{-1}
k_eR1R2L	EGF-EGFR/HER2 bound heterodimer internalization rate constant	0.10 min^{-1}
dimerization/uncoupling parameters(fit to experimental data)		
k_c[§]	receptor dimerization rate constant	1×10^{-3} (#/cell min)$^{-1}$
k_uR1R1	EGFR/EGFR unbound homodimer uncoupling rate constant	10 min^{-1}
k_uR1R2	EGFR/HER2 unbound heterodimer uncoupling rate constant	10 min^{-1}
k_uR2R2	HER2/HER2 homodimer uncoupling rate constant	1 min^{-1}
k_uR1R2L	EGF-EGFR/HER2 bound heterodimer uncoupling rate constant	0.1 min^{-1}
k_uLR1R1L	EGF-EGFR/EGFR-EGF homodimer uncoupling rate constant	0.1 min^{-1}

[§]set to diffusion-limited value.

Table 3.2 Effect of EGF on internalization rate of EGFR or HER2

Cells were incubated with the indicated radiolabeled probe at 1.3 nM in the presence or absence of 16 nM EGF and the specific internalization rate was measured as described in *Materials and Methods*. Units are min^{-1}. Levels of HER2 in MTSV and Ce2 cells were 0.9 and 17 x 10^5 per cell respectively. EGFR levels were 3.5 and 4.5 x 10^5 per MTSV or Ce2 cell, respectively.

Labeled Probe	***EGF***	***Cell Type***	
		MTSV	**Ce2**
7C2 (HER2)	-	0.035	0.023
	+	0.068	0.049
2C4 (HER2)	-	0.043	0.031
	+	0.049	0.030
13A9 (EGFR)	-	0.028	0.054
	+	0.119	0.132
EGF		0.148	0.112

3.7 Figures

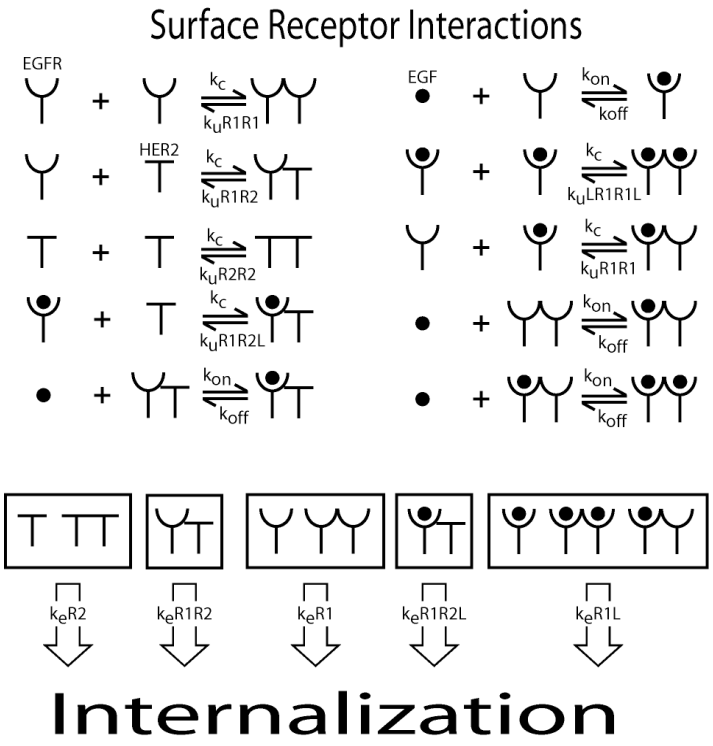

Figure 3.1 Model schematic.

The complete set of binary interactions between EGFR and HER2, with and without EGF. Unoccupied EGFR may homo- or heterodimerize with HER2. HER2 may also homo- or heterodimerize with unoccupied EGFR. EGFR reversibly binds EGF to form complexes that may heterodimerize with HER2 or homodimerize with empty EGFR or other complexes. Each species may be formed in any order and all dimerization and uncoupling events are reversible. Each receptor species is internalized with a species-specific internalization rate constant. Parameters values are either determined from the literature or fit to experimental data as described in *Model Development*.

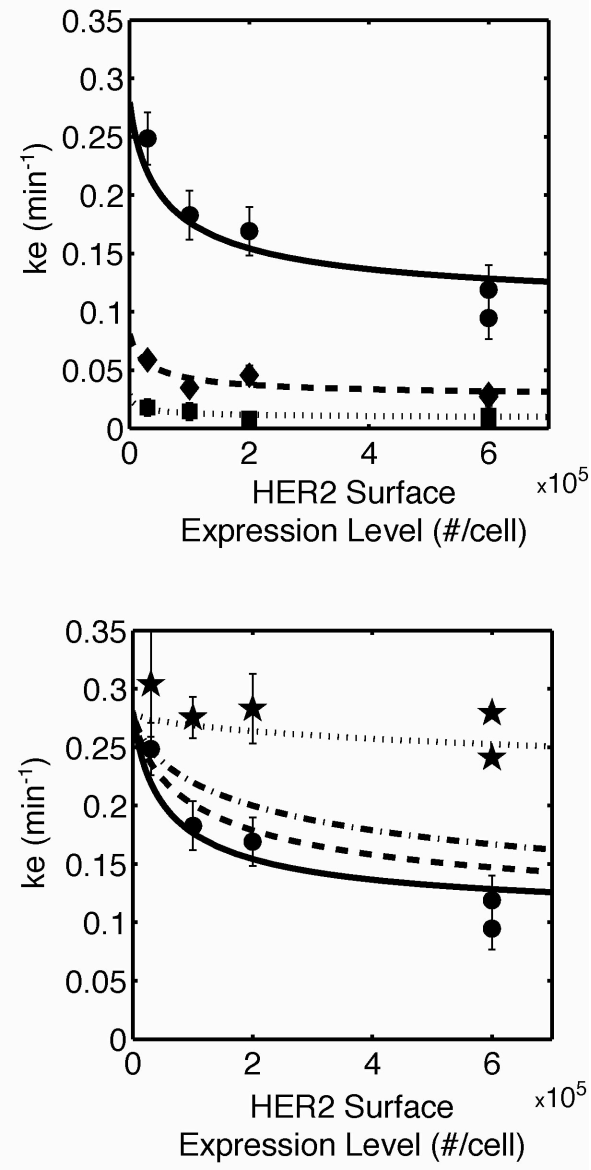

Figure 3.2 Experimental Data and Model Results.

A, experimental internalization data is reprinted from Hendriks, et al., 2003 (Chapter 2). EGF and HER2 internalization rates are plotted as a function of HER2 expression: EGF (circles), HER2 with EGF (diamonds) and HER2 without EGF (squares). The internalization model is fit to the 'HER2 without EGF' data to determine kuR1R1, kuR1R2 and kuR2R2. The remaining parameters, kuR1R2L and kuLR1R1L are fit to the

'EGF' data. The parameters determined from this fitting are used to predict the 'HER2 with EGF' data. The reciprocal fit produces nearly identical results. *B*, experimental internalization data for EGF with and without pre-incubation with heterodimerization blocking antibodies (2C4) is reprinted from Hendriks, et al., 2003a (Chapter 2). Internalization model predictions are shown for increasing values of kuR1R2L from 1x, 5x, 10x, to 100x the base value determined from original parameter fitting (solid, dashed, dash-dotted, and dotted lines, respectively).

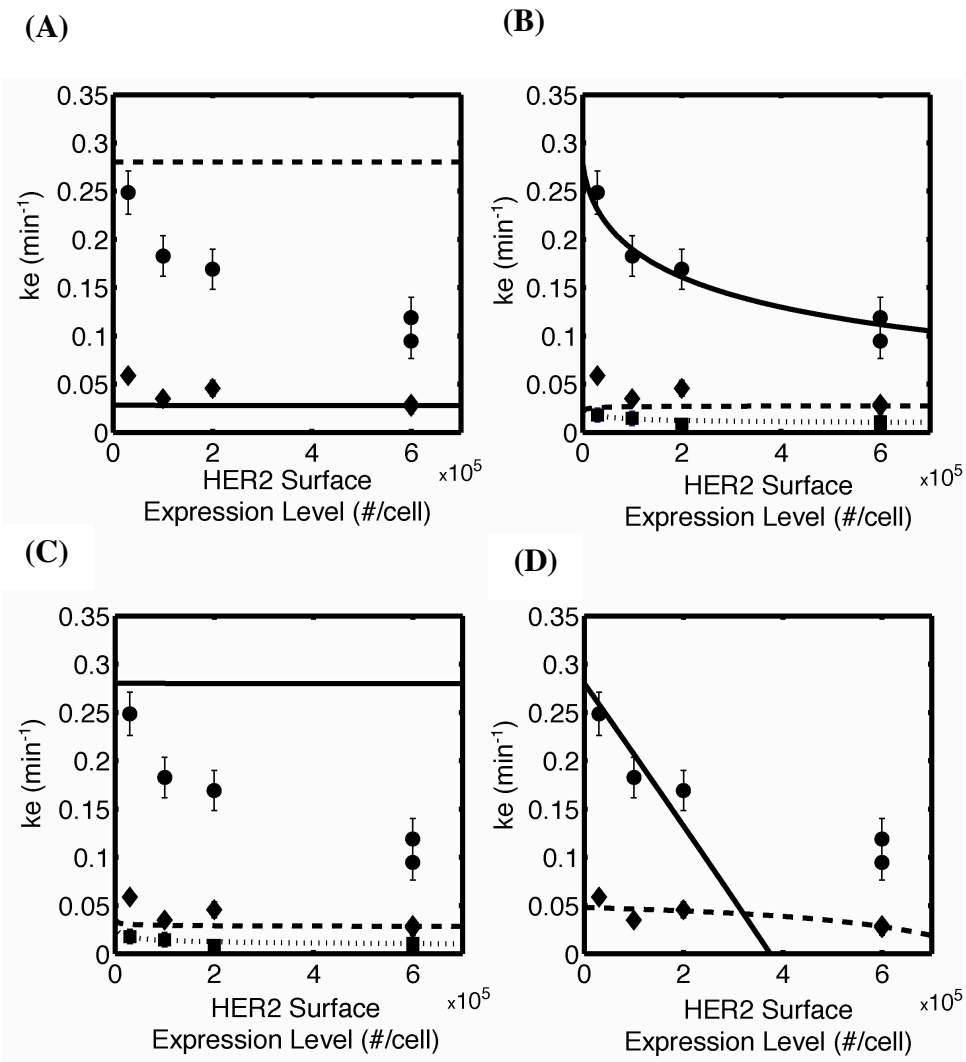

Figure 3.3 Alternative Models of Internalization.

Experimental data and model predictions for alternate models of internalization that have been fit to the data. *A*, internalization model wherein dimers are not sufficiently stable to be internalized as a complex. *B*, internalization model wherein heterodimers do not internalize. Model is fit to EGF internalization data and used to predict HER2 internalization data. *C*, reciprocal fit from *B* – model is fit to HER2 data and used to predict EGF data. *D*, indirect model of internalization wherein the internalization rates of EGFR and HER2 are of the form $k_{e,i} = a_i + b_i$[HER2 Level].

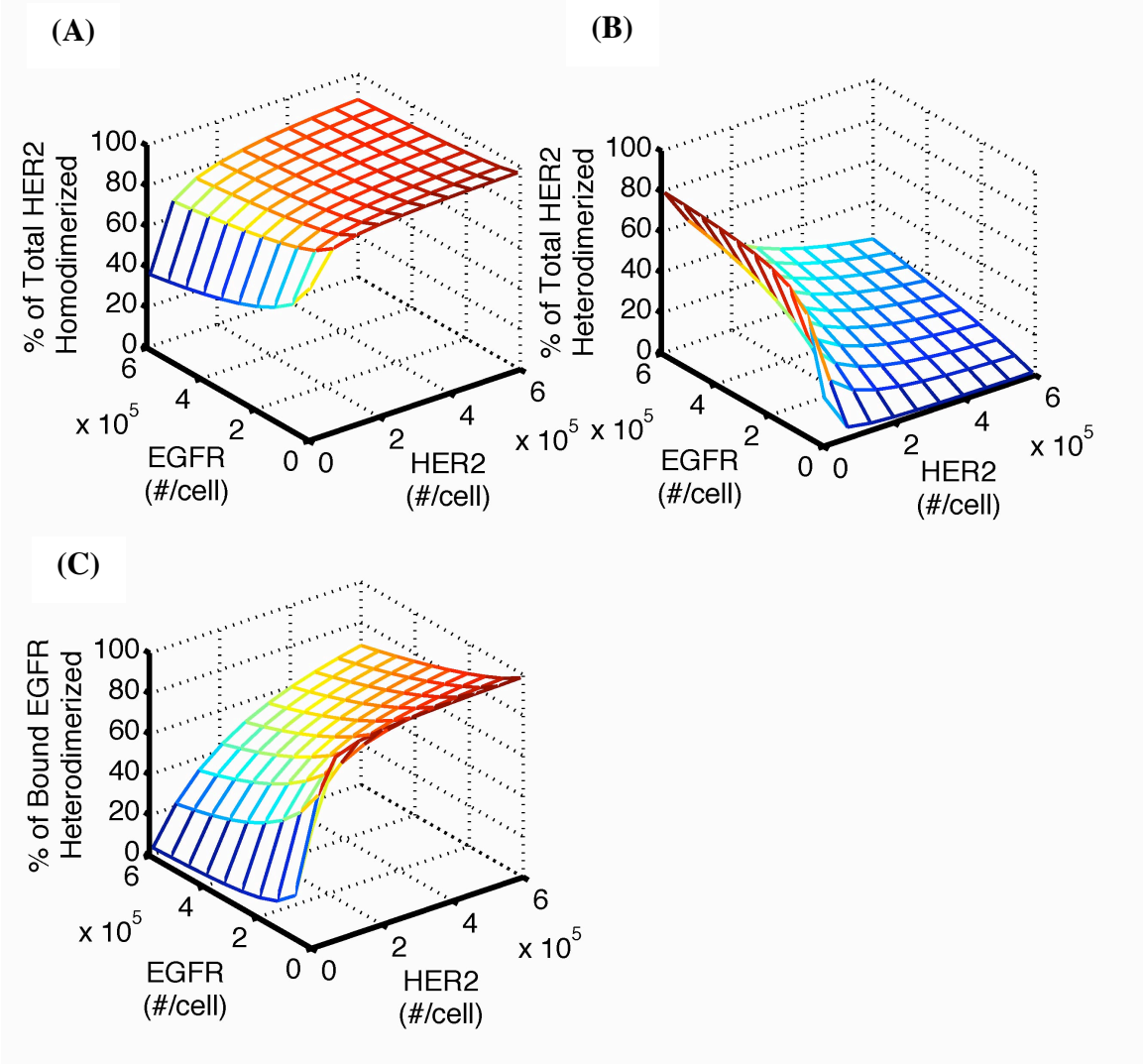

Figure 3.4 EGFR and HER2 Dimerization.

Model predictions of the degree of dimerization for varying levels of EGFR and HER2 expression. *A*, percent of total HER2 homodimerized in the absence of EGF, *B* percent of total HER2 heterodimerized in response to 10 ng/ml EGF stimulation and *C*, percent of bound EGFR heterodimerized in response to 10 ng/ml EGF stimulation.

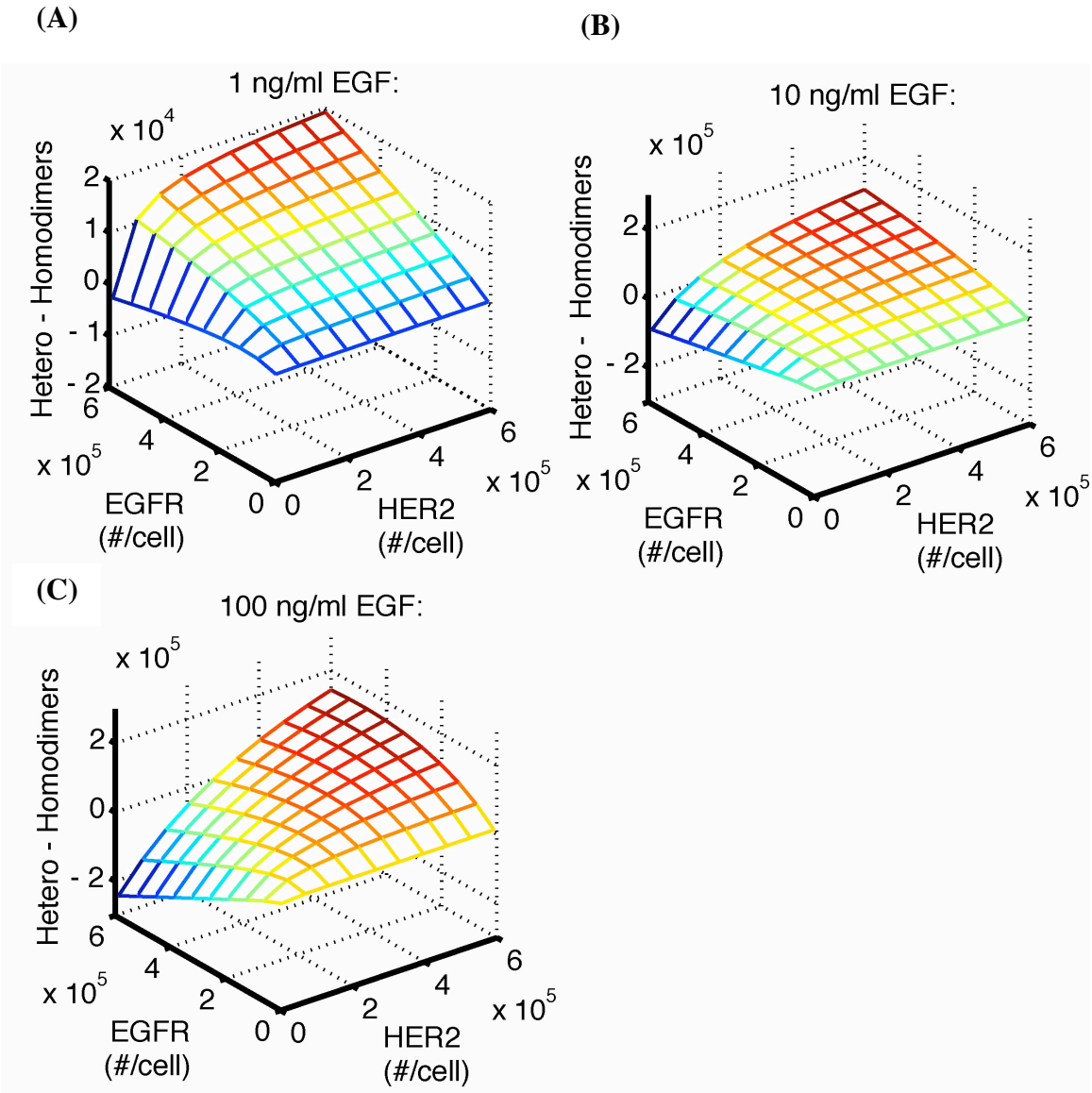

Figure 3.5 Relative Homo- and Heterodimerization.

Model prediction of the relative abundance of homo- and heterodimers (plotted as heterodimers – homodimers) in response to *A*, 1, *B*, 10 and *C*, 100 ng/ml EGF stimulation for varying level of EGFR and HER2 expression.

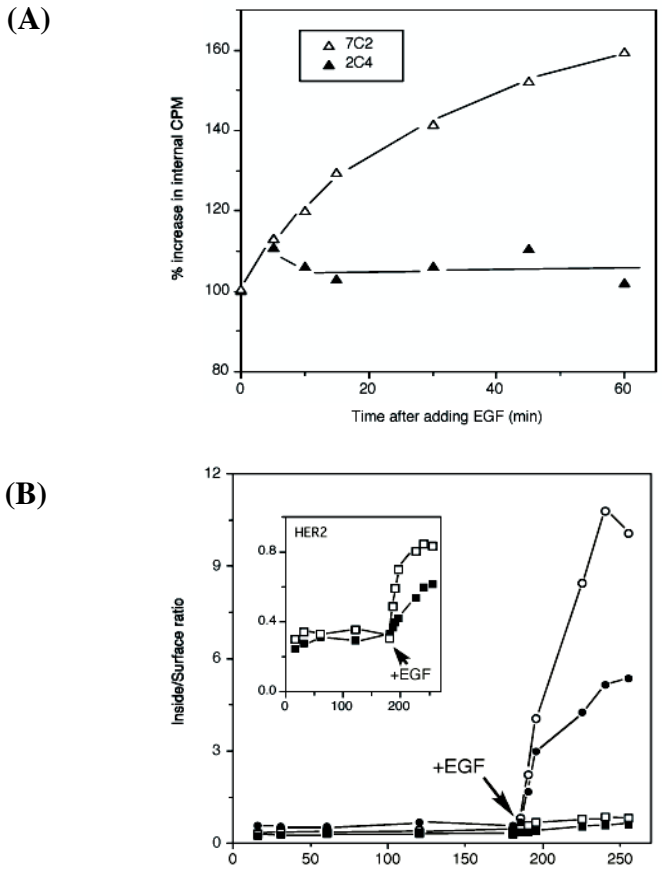

Figure 3.6 Experimental Validation.

A, Ce2 cells were incubated in 200 ng/ml of ^{125}I-7C2 or ^{125}I-2C4 antibody for 3 hours and then the amount of internalized antibody was then determined as a function of time following the addition of 100 ng/ml EGF. The addition of EGF increases the amount of internalized 7C2 antibody, but has no effect on the amount of internalized 2C4, verifying that heterodimerization between EGFR and HER2 is necessary to stimulate HER2 internalization. *B*, distribution between the cell surface and the intracellular compartment of antibodies bound to HER2 (squares) and EGFR (circles) for MTSV (open symbols) and Ce2 (filled symbols) cells before and after 100 ng/ml EGF addition.

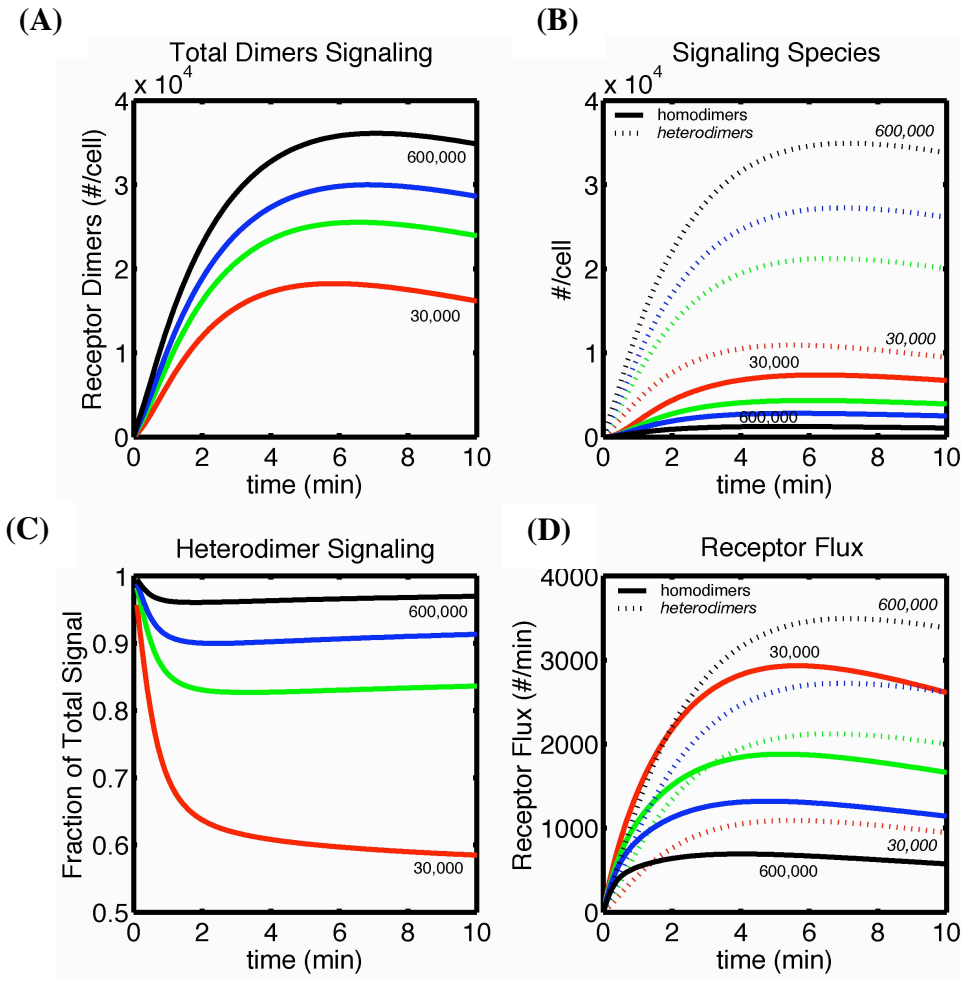

Figure 3.7 Signaling Receptor Dimers.

Model predictions in response to 10 ng/ml EGF stimulation for varying levels of HER2 expression (30,000 (red), 100,000 (green), 200,000 (blue) and 600,000 (black) per cell). *A*, total number of receptor dimers recruited (EEGFR homodimers and EGFR/HER2 heterodimers) *B*, timecourse of homodimers (solid lines) and heterodimers (dotted lines). *C*, timecourse of the fraction of total receptor dimers that are heterodimers. *D*, timecourse of the internalization flux of equivalent homodimers (solid lines) and heterodimers (dotted lines).

3.8 References

Alroy, I. and Yarden, Y. (1997) The ErbB signaling network in embryogenesis and oncogenesis: signal diversification through combinatorial ligand-receptor interactions. *Federation of European Biological Sciences Letters*, **410**, 83-86.

Baulida, J., Kraus, M.H., Alimandi, M., DiFiore, P.P. and Carpenter, G. (1996) All ErbB Receptors Other Than the Epidermal Growth Factor Receptor Are Endocytosis Impaired. *The Journal of Biological Chemistry*, **271**, 5251-5257.

Blakely, B.T., Rossi, F.M.V., Tillostson, B., Palmer, M., Estelles, A. and Blau, H.M. (2000) Epidermal growth factor receptor dimerization monitored in live cells. *Nature Biotechnology*, **18**, 218-222.

Burke, P.M. and Wiley, H.S. (1999) Human Mammary Epithelial Cells Rapidly Exchange Empty EGFR Between Surface and Intracellular Pools. *Journal of Cellular Physiology*, **180**, 448-460.

D'Souza, B., Berdichevsky, F., Kyprianou, N. and Taylor-Papadimitriou, J. (1993) Collagen-induced morphogenesis and expression of the alpha 2-integrin subunit is inhibited in c-erbB2-transfected human mammary epithelial cells. *Oncogene*, **8**, 1797-1806.

Drebin, J.A., Link, V.C., Stern, D.F., Weinberg, R.A. and Greene, M.I. (1985) Down-Modulation of an Oncogene Protein Product and Reversion of the Transformed Phenotype by Monoclonal Antibodies. *Cell*, **41**, 695-706.

Fendly, B.M., Winget, M., Hudziak, R.M., Lipari, M.T., Napier, M.A. and Ullrich, A. (1990) Characterization of Murine Monoclonal Antibodies Reactive to Either the Human Epidermal Growth Factor Receptor or HER2/neu Gene Product. *Cancer Research*, **50**, 1550-1558.

Ferguson, K.M., Darling, P.J., Mohan, M.J., Macatee, T.L. and Lemmon, M.A. (2000) Extracellular domains drive homo- but not hetero-dimerization of erbB receptor. *The European Molecular Biology Organization Journal*, **19**, 4632-4643.

Graus-Porta, D., Beerli, R.R., Daly, J.M. and Hynes, N.E. (1997) ErbB-2, the preferred heterodimerization partner of all ErbB receptors, is a mediator of lateral signaling. *The European Molecular Biology Organization Journal*, **16**, 1647-1655.

Hendriks, B.S., Opresko, L.K., Wiley, H.S. and Lauffenburger, D.A. (2003) Co-Regulation of EGFR/HER2 Levels and Locations: Quantitative Analysis of HER2 Overexpression Effects. *Cancer Research*, **63**, 1130-1137.

Kholodenko, B.N., Demin, O.V., Moehren, G. and Hoek, J.B. (1999) Quantification of Short Tern Signaling by the Epidermal Growth Factor Receptor. *The Journal of Biological Chemistry*, **274**, 30169-30181.

Klapper, L.N., Vaisman, N., Hurwitz, E., Pinkas-Kramarski, R., Yarden, Y. and Sela, M. (1997) A subclass of tumor-inhibitory monoclonal antibodies to ErbB2/HER2 blocks crosstalk with growth factor receptors. *Oncogene*, **14**, 2099-2109.

Lenferink, A.E.G., Pinkas-Kramarski, R., Poll, M.L.M.v.d., Vugt, M.J.H.v., Klapper, L.N., Tzahar, E., Waterman, H., Sela, M., Zoelen, E.J.J.v. and Yarden, Y. (1998) Differential endocytic routing of homo- and hetero-dimeric ErbB tyrosine kinases

confers signaling superiority to receptor heterodimers. *The European Molecular Biology Organization Journal*, **17**, 3385-3397.

Lotti, L.V., DiLazzaro, C., Zompetta, C., Frati, L. and Torrisi, M.R. (1992) Surface Distribution and Internalization of erbB-2 Proteins. *Experimental Cell Research*, **202**, 274-280.

Lund, K.A., Opresko, L.K., Starbuck, C., Walsh, B.J. and Wiley, H.S. (1990) Quantitative Analysis of the Endocytic System Involved in Hormone-induced Receptor Internalization. *The Journal of Biological Chemistry*, **265**, 15713-15723.

Mahama, P.A. and Linderman, J.J. (1994) A Monte Carlo Study of the Dynamics of G-Protein Activation. *Biophysical Journal*, **67**, 1345-1357.

Meier, T., Hauser, D.M., Chiquet, M., Landmann, L., Ruegg, M.A. and Brenner, H.R. (1997) Neural agrin induces ectopic postsynaptic specializations in innervated muscle fibers. *J Neurosci*, **17**, 6534-6544.

Mendrola, J.M., Berger, M.B., King, M.C. and Lemmon, M.A. (2002) The Single Transmembrane domains of ErbB Receptors Self-associate in Cell Membranes. *The Journal of Biological Chemistry*, **277**, 4704-4712.

Ohno, H., Hirabayashi, S., Iizuka, T., Ohnishi, H., Fujita, T. and Hata, Y. (2002) Localization of p0071-interacting proteins, plakophilin-related armadillo-repeat protein-interacting protein (PAPIN) and ERBIN, in epithelial cells. *Oncogene*, **21**, 7042-7049.

Penuel, E., Akita, R.W. and Sliwkowski, M.X. (2002) Identification of a Region Within the ErbB2/HER2 Intracellular Domain That Is Necessary for Ligand-Independent Association. *The Journal of Biological Chemistry*, **277**, 28468-28473.

Pinkas-Kramarski, R., Shelly, M., Guarino, B.C., Wang, L.M., Lyass, L., Alroy, I., Alimandi, M., Kuo, A., Moyer, J.D., Lavi, S., Eisenstein, M., Ratzkin, B.J., Seger, R., Bacus, S.S., Pierce, J.H., Andrews, G.C. and Yarden, Y. (1998) ErbB Tyrosine Kinases and the Two Neuregulin Families Constitute a Ligand-Receptor Network. *Molecular and Cellular Biology*, **18**, 6090-6101.

Qian, X., LeVea, C.M., Freeman, J.K., Dougall, W.C. and Greene, M.I. (1994) Heterodimerization of epidermal growth factor receptor and wild-type or kinase-deficient Neu: A mechansim of interreceptor kinase activation and transphosphorylation.

Schoeberl, B., Eichler-Jonsson, C., Gilles, E.D. and Muller, G. (2002) Computational modeling of the dynamics of the MAP kinase cascade activated by surface and internalized EGF receptors. *Nature Biotechnology*, **20**, 370-375.

Shea, L.D., Omann, G.M. and Linderman, J.J. (1997) Calculation of Diffusion-Limited Kinetics for the Reactions in Collision Coupling and Receptor Cross-Linking. *Biophysical Journal*, **73**, 2949-2959.

Sliwkowski, M.X., Schaefer, G., Akita, R.W., Lofgren, J.A., Fitzpatrick, V.D., Nuijens, A., Fendly, B.M., Cerione, R.A., Vandlen, R.L. and Carraway, K.L., 3rd. (1994) Coexpression of erbB2 and erbB3 proteins reconstitutes a high affinity receptor for heregulin. *J Biol Chem*, **269**, 14661-14665.

Sorkin, A., DiFiore, P.P. and Carpenter, G. (1993) The carboxyl terminus of epidermal growth factor receptor/erbB-2 chimerae is internalization impaired. *Oncogene*, **8**, 3021-3028.

Tanner, K.G. and Kyte, J. (1999) Dimerization of the Extracellular Domain of the Receptor for Epidermal Growth Factor Containing the Membrane-spanning Segment in Response to Treatment with Epidermal Growth Factor. *The Journal of Biological Chemistry*, **274**, 35985-35990.

Tzahar, E., Waterman, H., Chen, X., Levkowitz, G., Karunagaran, D., Lavi, S., Ratzkin, B.J. and Yarden, Y. (1996) A Hierarchical Network of Interreceptor Interactions Determines Signal Transduction by Neu Differentiation Factor/Neuregulin and Epidermal Growth Factor. *Molecular and Cellular Biology*, **16**, 5276-5287.

Wang, Z., Zhang, L., Yeung, T.K. and Chen, X. (1999) Endocytosis Deficiency of Epidermal Growth Factor (EGF) Receptor-ErbB2 Heterodimers in Response to EGF Stimulation. *Molecular Biology of the Cell*, **10**, 1621-1636.

Wiley, H.S. and Cunningham, D.D. (1981) A Steady State Model for Analyzing the Cellular Binding, Internalization and Degradation of Polypeptide Ligands. *Cell*, **25**, 433-440.

Wiley, H.S. and Cunningham, D.D. (1982) The Endocytotic Rate Constant. *The Journal of Biological Chemistry*, **257**, 4222-4229.

Wiley, H.S., Herbst, J.J., Walsh, B.J., Lauffenburger, D.A., Rosenfeld, M.G. and Gill, G.N. (1991) The Role of Tyrosine Kinase Activity in Endocytosis,

Compartmentation, and Down-regulation of the Epidermal Growth Factor Receptor. *The Journal of Biological Chemistry*, **266**, 11083-11094.

Winkler, M.E., O'Connor, L., Winget, M. and Fendly, B. (1989) Epidermal growth factor and transforming growth factor alpha bind differently to the epidermal growth factor receptor. *Biochemistry*, **28**, 6373-6378.

Worthylake, R., Opresko, L.K. and Wiley, H.S. (1999) ErbB-2 Amplification Inhibits Down-regulation and Induces Constitutive Activation of Both ErbB-2 and Epidermal Growth Factor Receptors. *The Journal of Biological Chemistry*, **274**, 8865-8874.

Worthylake, R. and Wiley, H.S. (1997) Structural Aspects of the Epidermal Growth Factor Receptor Required for Transmodulation of erbB-2/neu. *The Journal of Biological Chemistry*, **272**, 8594-8601.

Yu, X., Sharma, K.D., Takahashi, T., Iwamoto, R. and Mekada, E. (2002) Ligand-independent Dimer Formation of Epidermal Growth Factor Receptor (EGFR) Is a Step Separable from Ligand-induced Signaling. *Molecular Biology of the Cell*, **13**, 2547-2557.

3.A Appendix: Internalization Model Equations.

$$\frac{d(R1)}{dt} = -k_c(R1)(R2) + k_u R1R2(R1R2) - 2k_c(R1)(R1) + 2k_u R1R1(R1R1) - k_c(R1)(R2Ab) + k_u R1R2(R1R2Ab) - k_{on}(L)(R1) + k_{off}(R1L) - k_c(R1)(R1L) + k_u R1R1(R1R1L);$$

$$\frac{d(R2)}{dt} = -2k_c(R2)(R2) + 2k_u R2R2(R2R2) - k_c(R1)(R2) + k_u R1R2(R1R2) - k_{on}Fab(R2)(Ab) + k_{off}Fab(R2Ab) - k_c(R2)(R2Ab) + k_u R2R2(R2R2Ab) - k_c(R1L)(R2) + k_u R1R2L(R1R2L);$$

$$\frac{d(R1R1)}{dt} = k_c(R1)(R1) - k_u R1R1(R1R1) - k_{on}(L)(R1R1) + k_{off}(R1R1L);$$

$$\frac{d(R1R2)}{dt} = k_c(R1)(R2) - k_u R1R2(R1R2) - k_{on}Fab(Ab)(R1R2) + k_{off}Fab(R1R2Ab) - k_{on}(L)(R1R2) + k_{off}(R1R2L);$$

$$\frac{d(R2R2)}{dt} = k_c(R2)(R2) - k_u R2R2(R2R2) - k_{on}Fab(Ab)(R2R2) + k_{off}Fab(R2R2Ab);$$

$$\frac{d(R1L)}{dt} = k_{on}(L)(R1) - k_{off}(R1L) - 2k_c(R1L)(R1L) + 2k_u LR1R1L(LR1R1L) - k_c(R1L)(R2) + k_u R1R2L(R1R2L) - k_c(R1L)(R2Ab) + k_u R1R2L(R1R2LAb) - k_c(R1)(R1L) + k_u R1R1(R1R1L) - k_e R1L(R1L);$$

$$\frac{d(R1R2L)}{dt} = k_{on}(L)(R1R2) - k_{off}(R1R2L) + k_c(R1L)(R2) - k_u R1R2L(R1R2L) - k_{on}Fab(Ab)(R1R2L) + k_{off}Fab(R1R2LAb) - k_e R1R2L(R1R2L);$$

$$\frac{d(R1R1L)}{dt} = k_{on}(L)(R1R1) - k_{off}(R1R1L) - k_{on}(L)(R1R1L) + k_{off}(LR1R1L) + k_c(R1)(R1L) - k_u R1R1(R1R1L) - k_e R1L(R1R1L);$$

$$\frac{d(LR1R1L)}{dt} = k_c(R1L)(R1L) - k_u LR1R1L(LR1R1L) + k_{on}(L)(R1R1L) - k_{off}(LR1R1L) - k_e R1L(LR1R1L);$$

$$\frac{d(R2Ab)}{dt} = k_{on}Fab(R2)(Ab) - k_{off}Fab(R2Ab) - 2k_c(R2Ab)(R2Ab) + 2k_u R2R2(AbR2R2Ab) - k_c(R1)(R2Ab) + k_u R1R2(R1R2Ab) - k_c(R1L)(R2Ab) - k_c(R2)(R2Ab) + k_u R2(R2R2Ab) - k_e R2(R2Ab);$$

$$\frac{d(R1R2Ab)}{dt} = k_c(R1)(R2Ab) - k_u R1R2(R1R2Ab) - k_{on}Fab(Ab)(R1R2) + k_{off}Fab(R1R2Ab) - k_{on}(L)(R1R2Ab) + k_{off}(R1R2LAb) - k_e R1R2(R1R2Ab);$$

$$\frac{d(R2R2Ab)}{dt} = k_{on}Fab(Ab)(R2R2) - k_{off}Fab(R2R2Ab) - k_{on}Fab(Ab)(R2R2Ab) + k_{off}Fab(AbR2R2Ab) + k_c(R2)(R2Ab) - k_u R2R2(R2R2Ab) - k_e R2(R2R2Ab);$$

$$\frac{d(AbR2R2Ab)}{dt} = k_{on}Fab(Ab)(R2R2Ab) - k_{off}Fab(AbR2R2Ab) + k_c(R2Ab)(R2Ab) - k_u R2R2(AbR2R2Ab) - k_e R2(AbR2R2Ab);$$

$$\frac{d(R1R2LAb)}{dt} = k_c(R1L)(R2Ab) - k_u R1R2L(R1R2LAb) + k_{on}(L)(R1R2Ab) - k_{off}(R1R2LAb) + k_{on}Fab(Ab)(R1R2L) - k_{off}Fab(R1R2LAb) - k_e R1R2L(R1R2LAb);$$

$$\frac{d(Linside)}{dt} = k_e R1L(R1L) + k_e R1L(R1R1L) + k_e R1R2L(R1R2L) + 2k_e LR1R1L(LR1R1L);$$

$$\frac{d(Abinside)}{dt} = k_e R2(R2Ab) + k_e R2R2(R2R2Ab) + 2k_e R2R2(AbR2R2Ab) + k_e R1R2(R1R2Ab) + k_e R1R2L(R1R2LAb);$$

$$\frac{d(R1inside)}{dt} = k_e R1L(R1L) + 2k_e LR1R1L(LR1R1L) + k_e R1R2L(R1R2L) + 2k_e R1R1L(R1R1L) + k_e R1R2L(R1R2LAb) + k_e R1R1(R1R2Ab);$$

$$\frac{d(R2inside)}{dt} = k_e R1R2L(R1R2L) + k_e R2(R2Ab) + 2k_e R2(AbR2R2Ab) + 2k_e R2(R2R2Ab) + k_e R1R2(R1R2Ab) + k_e R1R2L(R1R2LAb);$$

Chapter 4: HER2-Mediated Effects on EGFR Endosomal Sorting

Overexpression of HER2, a signaling partner for EGFR, has been implicated in numerous experimental and clinical studies as promoting the progression of many types of cancer. One avenue by which HER2 overexpression may dysregulate EGFR-mediated cell responses, such as proliferation and migration, downstream of EGF family ligand binding, is by its modulation on EGFR endocytic trafficking dynamics. EGFR signaling is regulated by down-regulation and compartmental relocalization arising from endocytic internalization and endsomal sorting to degradation versus recycling fates. HER2 overexpression influences both of these processes. At the endosomal sorting stage, increased HER2 levels elicit enhanced EGFR recycling outcomes, but the mechanism by which this transpires is poorly understood. Here, we determine whether alternative mechanisms for HER2-mediated enhancement of EGFR recycling can be distinguished by comparison of corresponding mathematical models to experimental literature data. Indeed, we find that the experimental data are clearly most consistent with a mechanism in which HER2 directly competes with EGFR for a stoichiometrically-limited quantity of endosomal retention components (ERCs), thereby reducing degradation of ERC-coupled EGFR. Model predictions based on this mechanism exhibited qualitative trends highly similar to data on the fraction of EGF/EGFR complexes sorted to recycling fate as a function of the amount of internalized EGF/EGFR complexes. In contrast, model

predictions for alternative mechanisms – blocking of ERC-EGFR coupling, or altering EGF/EGFR dissociation – were inconsistent with the qualitative trends of the experimental data.

4.1 Introduction

Elevated expression of the EGFR and/or HER2 has been implicated in the development of cancer by contributing to aberrant cell behavior including increased motility, increased sensitivity to mitogenic stimuli, anchorage independence and cell transformation (Brandt et al., 1999; Chazin et al., 1992; DiFiore et al., 1987a; DiFiore et al., 1987b; Ignatoski et al., 1999; Spencer et al., 2000). The quantity and intracellular localization of these receptors is able to influence cell behavior by dictating both the strength and quality of signals generated. Thus, understanding the regulatory mechanisms involved in controlling the number of EGFR and/or HER2 is of prime importance in dissecting how elevated receptor expression is able to alter cell signaling that manifests itself in tumorigenesis.

HER2 is an almost ubiquitously expressed EGFR family member that does not bind any ligands and therefore must rely on dimerization with another EGFR family member for complete activation (Graus-Porta et al., 1997; Hynes and Stern, 1994; Karunagaran et al., 1996; Worthylake and Wiley, 1997). Overexpression of HER2 has been demonstrated to inhibit down-regulation of the EGFR and of itself, as well as increase the recycling rate of EGF (Hendriks et al., 2003a (Chapter 2); Worthylake et al., 1999). HER2 expression has been shown to shunt ligand-activated receptors to recycling

to recycling fates suggesting that receptor heterodimer species may have a superior signaling potency as a consequence of their intracellular routing (Lenferink et al., 1998; Waterman et al., 1998). Receptor heterodimerization has been shown to affect the dissociation rate of EGF or heregulin and may also do so inside of endosomal compartments (Karunagaran et al., 1996; Lenferink et al., 1998; Lewis et al., 1996; Wada et al., 1990). While it is apparent that HER2 expression influences the endosomal sorting of EGF and EGFR, the dominant mechanism(s) by which it occurs remain unclear. Theoretical models of endosomal sorting have examined the biophysical requirements for molecular transport out of a central endosomal vesicle into recycling tubules and spawned the development of a mechanistic model (French and Lauffenburger, 1996; Lauffenburger and Linderman, 1993; Linderman and Lauffenburger, 1986). In this model, the endosomal sorting of the EGFR and its ligands were mathematically modeled using a compartmental analysis incorporating endosomal retention components (ERCs) and a representation of endosomal architecture. By detailing the mechanistic and biophysical basis for endosomal sorting, one unified model is able to account for a wide range of experimentally observed sorting results. However, this model does not account for the effects of HER2 on EGF sorting.

The goal of this work is to build upon French and Lauffenburger's ERC model of sorting to understand how different EGFR and HER2 interactions could contribute to qualitative trends in experimental sorting curves. Specifically, we seek to discriminate between three different mechanisms by which HER2 may disrupt the sorting process through the comparison of experimental and modeling outcomes. Our results suggest that

HER2 is able to alter EGF sorting primarily through a competitive mechanism wherein it competes for a limited number of ERCs, rather than by blocking EGF-EGFR interaction with ERCs or by altering the pH sensitivity of EGF.

4.2 Model Development

Our model of endosomal sorting is an extension of the mechanistic sorting model based on ERC sorting model originally proposed by French and Lauffenburger (French and Lauffenburger, 1996). We add HER2 to the model and consider three distinct mechanisms by which HER2 interaction may augment EGF sorting.

The framework of the ERC sorting model is briefly presented here; its development, assumptions and validation are explained in detail elsewhere (French and Lauffenburger, 1996; French and Lauffenburger, 1997). This model (illustrated schematically in Figure 4.1) simulates the quasi-steady state sorting of EGFRs (R1) and ligands (L) as they pass through the endosomal pathway. The cell interior is separated into four compartments: an endosomal vesicular compartment (indicated by subscript v), an endosomal tubular compartment (subscript t), a post-sorting recycling compartment (subscript r) and a post-sorting degradation compartment (subscript d). Ligand may bind to receptors to form complexes and subsequently dissociate at rates k_{on} and k_{off}, respectively. Internalized ligand-receptor complexes (R1L) enter the vesicular compartment of the endosome. Within the vesicular compartment, complexes and unoccupied receptors may diffuse into the tubular compartment with transport rate □

Complexes may interact with ERCs (E), at rate $k_{c,R1E}$ (or at rate $k_{c,R1E,het}$ for the case of heterodimers), in the vesicular compartment to form ternary complexes (R1LE) which have a negligible rate of transport into the tubular compartment. ERCs only bind occupied receptors, their total quantity is assumed to be at steady state and all ERC containing species are restricted to the vesicular compartment of the endosome. Ligands may dissociate from ternary complexes at rate k_{off} leaving binary complexes (R1E) that either rebind ligand at rate k_{on} or uncouple at rate $k_{u,R1E}$ to form free receptors and ERCs. Free ligand may bind unoccupied receptors at rate k_{on} and is assumed to be in equilibrium between the tubular and vesicular lumen, related by partition coefficient, k, accounting for excluded volume due to ligand size. Vesicular receptor and ligand species are targeted for the post-sorting degradation compartment at rate k_{sv}, while tubular receptor and ligand species are targeted for the post-sorting recycling compartment at rate k_{st}. The input into the model is the flux of ligand-receptor complexes (I_{R1L}).

The general changes brought about by HER2 presence are presented here and the details unique to each model follow below (Figure 4.1c). The addition of HER2 to the sorting model adds a few additional species. Free HER2 (R2) is permitted to heterodimerize with occupied EGFR at rate k_c to form occupied heterodimers (R1LR2) and uncouple at rate $k_{u,R1LR2}$. Free HER2 and occupied heterodimers move from the vesicular compartment to the tubular compartment at transport rate g. Ligand may dissociate from heterodimers at rate $k_{off,het}$. Unoccupied heterodimers are assumed to be sufficiently unstable that they instantaneously break apart to yield free EGFR and free HER2. The input to the model consists of the flux of ligand-receptor complexes (I_{R1L}), as

well as the flux of occupied heterodimers (I_{R1LR2}), as cartooned in Figure 4.1d. Elevated HER2 expression drives the formation of heterodimers and shifts the model input from 100% EGF-EGFR complexes to a combination of complexes and heterodimers to 100% heterodimers. The interactions between free HER2 and heterodimers with ERCs are unique to each model, and presented below.

We propose three distinct, although not mutually exclusive, mechanisms by which HER2 may disrupt the normal endosomal sorting of EGF and the EGFR. Each mechanism is considered separately for clarity and ease of interpretation. The complete set of equations encompassing all models is listed in the appendix.

4.2.1 Blockade Model

In this model, we propose that EGF-EGFR complex heterodimerization with HER2 may impair EGFR interaction with ERCs , cartooned in Figure 4.2a. When in the heterodimerized state, complexes are no longer able to bind ERCs ($k_{c,R1E,het}$ is set to zero). As such, HER2 is able to block the selective endosomal retention of EGF-EGFR complexes.

4.2.2 Competition Model

Here, in addition to occupied EGFR, both free HER2 and HER2 that is heterodimerized with EGFRs can bind ERCs. All HER2 containing species bind ERCs at rate $k_{c,R2E}$ or $k_{c,R2E,het}$ to form species R2E or R1LR2E or ER1LR2E, (depending on whether HER2 has heterodimerized and whether the EGF-EGFR complex has an ERC bound or not), and uncouple at rate $k_{u,R2E}$. The model is cartooned in Figure 4.2b.

4.2.3 Affinity Model

In this model, EGF-EGFR complex heterodimerization with HER2 alters the endosomal affinity of EGF for its receptor by altering its rate of dissociation from heterodimers ($k_{off,het}$ is different from k_{off}). The presence of HER2 and heterodimerization does not affect the ability of occupied EGFR to bind ERCs and HER2 does not bind ERCs itself. This model is cartooned in Figure 4.2c.

4.2.4 Model Inputs

The input to the model is a specified flux of ligand-receptor complexes (I_{R1L}) and the flux of ligand-bound heterodimers (I_{R1LR2}) (see Figure 4.1d). These parameters represent the rates of complex and heterodimer internalization, respectively. Although the internalization rate and the number of surface receptors has experimentally been shown to vary with ligand concentration and time, internalization fluxes are held constant for simplicity so that the effects on endosomal sorting may be isolated from effects due to differences in internalization (Wiley et al., 1991).

An increase in HER2 expression level should result in a higher degree of EGF-EGFR/HER2 heterodimerization by simple mass action kinetics. When no HER2 is present, the model input is only I_{R1L} (with I_{R1LR2} set to 0). In the other extreme, when HER2 is in great excess, the model input is only I_{R1LR2} (with I_{R1L} set to 0). The cases in between, where neither $k_{e,R1L}$ nor $k_{e,R1LR2}$ are 0, reflect modest degrees of heterodimerization and directly reflect the receptor expression levels and their affinities for homo- versus hetero-dimerization.

4.2.5 Parameter Determination

While there exists a great deal of cellular data and rate constants in the literature, it is scattered across many cell types. Because of this we have chosen to adopt the physiological reasonable parameters values, based on the ranges used in the original ERC sorting model, shown in Tables 4.1 & 4.2. The uncoupling rate of occupied heterodimers ($k_{u,R1LR2}$) is estimated based on previous work and is set to 0.1 min^{-1} (Hendriks et al., 2003b (Chapter 3)). Parameters with no estimate or those believed to be of particular importance in determining the system output ($k_{u,R1LR2}$, $k_{u,R2E}$, $k_{off,het}$) are varied over wide ranges as shown in *Results*. A complete list of parameter values are shown in Tables 4.1 & 4.2.

4.2.6 Computations

All model equations are simultaneously coded into Matlab, version 6.5 (Mathworks, Natick MA) and solved at steady state. Individual models are examined by setting appropriate parameters to zero and/or varying parameters of interest prior to evaluation. Each simulation is run with a specified flux of ligand-receptor complexes and occupied heterodimers. After 120 min of simulation time, when steady state has been reached, sorting fractions and intracellular ligand concentrations were determined as described in *Results*. By varying the magnitude of the input fluxes of ligand-receptor complexes and occupied heterodimers, holding their ratio constant, sorting curves relating sorting fraction to intracellular ligand concentration were generated. Matlab code can be found in the Appendix A.3.

4.3 Results

4.3.1 Experimental Sorting Outcomes

The motivation for this work comes from the experimental observations of the endosomal sorting of EGF as a function of HER2 expression level originally published in (Hendriks et al., 2003a (Chapter 2)) (reprinted in Figure 4.4a). These results describe steady state sorting outcomes for 184A1 human mammary epithelial cells for varying EGF concentrations as a function of HER2 expression level. Each cell clone shown has a comparable level of EGFR expression (~2×10^5) and HER2 expression levels of 3×10^4, and 6×10^5 for the parental line, and HER2 clone 24H, respectively (Hendriks et al., 2003a (Chapter 2)). In the parental cell line, increasing intracellular EGF resulted in a downward slope in the fraction of EGF recycled. This is consistent with other work demonstrating the selective retention of EGF-EGFR complexes within the endosome (French et al., 1994). Elevated HER2 expression, as seen in clone 24H, demonstrated an increase in the fraction of EGF recycled relative to the parental cell line. The shallow positive relationship between intracellular EGF and the fraction of EGF recycled for clone 24H, suggests that the endosomal cargo is starting to exceed the capacity of the sorting apparatus.

In addition, the role of heterodimerization was examined in steady state sorting experiments following overnight pretreatment with saturating amounts (10 ug/ml) of monoclonal antibody 2C4. 2C4 binds to an extracellular epitope on HER2 and has been shown to block both its transactivation and heterodimerization with the EGFR (Agus et

al., 2002; Baselga, 2002; Fendly et al., 1990; Lewis et al., 1996). As shown in Figure 4.3b (reprinted from (Hendriks et al., 2003a (Chapter 2))), blocking heterodimerization, was sufficient to reverse effect of elevated HER2 expression on sorting fraction. The sorting curve for HER2 clone 24H following 2C4 treatment closely resembled that of the parental cell line. As expected, the addition of 2C4 had no effect on sorting for the parental cell line (Hendriks et al., 2003a (Chapter 2)).

4.3.2 Sorting Fractions

The degree to which internalized ligands are recycled towards the surface versus targeted for endosomal degradation can be described by a sorting fraction. This fraction represents the ratio of ligand molecules that leave the endosomal tubules and enter the recycling compartment to the total amount of ligand molecules that leave the endosomes through either the tubular or vesicular compartment and enter the recycling or degradative compartments, respectively. Ligand molecules may transit through the system either as unbound ligand that is free in the endosomal lumen or as bound ligand that is complexed with EGFR in the form of receptor-ligand complexes or as part of a bound EGF-EGFR/HER2 heterodimer.

When the sorting process is at steady state, the sorting fractions can be defined as as follows:

$$f_x = k_{st}(L_{B,t}+L_{F,t})/(k_{st}(L_{B,t}+L_{F,t})+k_{sv}(L_{B,v}+L_{F,v}))$$

with,

$$L_{F,t} = hkL_vV_vN_A$$

$L_{B,t} = R1L_t + R1LR2_t$

$L_{F,v} = L_v V_v N_A$

$L_{B,v} = R1L_v + R1LE_v + R1LR2_v$, for the blockade model

$= R1L_v + R1LE_v + R1LR2E_v + ER1LR2_v$, for the competition model

$= R1L_v + R1LE_v + R1LR2_v + ER1LR2_v$, affinity model

Where, k_{st} is the tubular sorting rate constant, k_{sv} is the vesicular sorting rate constant, $L_{F,i}$ and $L_{B,i}$ are the free and bound ligand concentration in compartment i, respectively, where compartment i is either the tubular (t) or vesicular (v) compartment of the endosome. V_v is the vesicular volume, N_A is Avogadro's number, $R1L_i$ is the concentration of ligand-receptor complexes (#/cell) in compartment i, $R1LR2_i$ is the concentration of ligand bound heterodimers in compartment i, $R1LE_v$ is the concentration of ternary ligand-receptor-endosomal retention component complexes. $ER1LR2_v$ and $R1LR2E_v$ are bound heterodimers with an ERC bound to the EGFR or HER2, respectively.

The differences in the definitions of the sorting fraction for each model directly reflect each model's construction. Since the differences in each model lie only in the receptor interactions allowed, the expression for free ligand concentration is identical in each case. For each model the bound ligand in the tubular compartment consists of all ligand bound species allowed ($R1L_t$ and $R1LR2_t$). The bound ligand in the vesicular compartment consists of all ligand-bound species allowed by the model including those that contain ERCs.

For comparison with experimental results, sorting fractions are plotted as a function of total intracellular ligand concentration at steady state. Examination of steady state sorting helps to decouple recycling from the effects of internalization. Total intracellular ligand concentration (C_i) is given by:

$$C_i = L_{F,t} + L_{F,v} + L_{F,r} + L_{F,d} + L_{B,t} + L_{B,v} + L_{B,r} + L_{B,d}$$

The intracellular ligand concentration is the sum of the free and bound (subscripts F and B, respectively) ligand in each compartment – the tubular, vesicular, recycling and degradation compartments (subscripts t, v, r, and d, respectively).

4.3.3 ERC Sorting Model Fundamentals

Based on the work of French & Lauffenburger, we have a solid understanding of how different experimental outcomes reflect various molecular-level interactions in the sorting process (French and Lauffenburger, 1996; French and Lauffenburger, 1997). The typical sorting curve can be broken into three regimes (see French & Lauffenburger, 1996), as shown in Figure 4.4. In regime I, at low intracellular EGF, sorting outcomes are the result of fluid phase sorting – the majority of ligands dissociate from their receptors and the recycling fraction reflects the fluid phase partitioning of ligands between the endosomal lumen and recycling tubules. In regime II, at intermediate EGF concentration, occupied receptors are selectively retained by ERCs and targeted for degradation; hence, the downward slope of the sorting curve. Here, endosomal ligand concentration is high

enough to force receptor occupancy, but low enough so that the ERCs are not saturated. In regime III, at high intracellular EGF, the ERCs become saturated and there is a sharp increase in fraction recycled, reflecting the fact that recycling is the default pathway for the EGFR (French et al., 1994). It should be noted that experimental results usually do not contain all three regimes due to limitations in ^{125}I-EGF detection and/or limitations at the level of internalization, including limited internalization capacity and/or EGFR number. Based on the experimental data, it is apparent that the parental cell line falls entirely within regime II, while clone 24H displays the onset of saturation, as seen in the beginning of regime III. The area of interest for our experimental data is outlined in Figure 4.4. All further model results will focus within this region.

4.3.4 Blockade Model

Recent experimental work has demonstrated the differential signaling abilities of heterodimers versus homodimers. Controlled homo- and heterodimerization of EGFR and HER2 has shown that heterodimerization with HER2 impedes the ability of the EGFR to recruit c-Cbl, possibly by failing to phosphorylate a key tyrosine residue on the cytoplasmic domain of the EGFR (Muthuswamy et al., 1999). In this model, we propose that EGF-EGFR complex heterodimerization with HER2 may impair EGFR interaction with ERCs (see Figure 4.2a). Figure 4.5a illustrates how the sorting fraction of EGF is predicted to change for the blockade model as the input ratio is varied from 100% EGF-EGFR complexes to 100% heterodimers.

As the ratio of heterodimers to complexes increases there is an immediate effect on the sorting fraction, particularly at low intracellular ligand concentrations. An input of 100% heterodimers elicits an increase in sorting fraction of up to 0.4 when compared to an input of 100% complexes, at an intracellular ligand concentration of only 10^4 #/cell. In the regime prior to ERC saturation, the entire curve is shifted upward so that the effect of adding HER2 to the system is immediate and is readily observed. In this model, a single molecule of HER2 is able to elicit a direct difference in sorting fraction, particularly at low intracellular EGF concentrations.

The importance of the basic parameters of the endosomal sorting model originally proposed by French & Lauffenburger have already been explored in detail (French and Lauffenburger, 1996; French and Lauffenburger, 1997). As such, we constrain ourselves to examination of the parameters whose response is affected as a consequence of HER2 expression. In particular, the effect of HER2 expression on endosomal sorting can be modulated by changes in the affinity for heterodimerization. As many of the membrane-level receptor interactions are likely to be diffusion limited, we choose to examine changes in heterodimerization affinity by altering the heterodimer uncoupling rate ($k_{u,R1LR2}$) (Shea et al., 1997). As shown in Figure 4.5b, using a model input of 100% heterodimers, a decrease in the heterodimer uncoupling rate increases the efficiency with which a given HER2 expression level is able to enhance EGF sorting towards recycling.

4.3.5 Competition Model

Based on the high degree sequence similarity of the cytoplasmic domains of the EGFR and HER2 it is possible that the presence of HER2 may compete with the EGFR for interaction with ERCs (Earp et al., 1995; Schechter et al., 1985; Ullrich et al., 1984). In this model's construction, both free HER2 and HER2 that is heterodimerized with EGFRs can bind ERCs. Consequently, HER2 competes with the EGFR for a limited quantity of available ERCs (see Figure 4.2b), accelerating the onset of saturation of endosomal sorting.

Figure 4.6a shows the predicted effect of increasing HER2 expression level on the endosomal sorting of EGF-EGFR complexes when HER2 competes for interaction with ERCs. The model input is varied from 100% EGF-EGFR complexes to 50% EGF-EGFR complexes, 50% heterodimers to 100% bound heterodimers. At very low intracellular EGF concentrations ($<10^3$ #/cell) the three curves merge and are indistinguishable (not shown on graph). As intracellular EGF increases, the curves diverge and ultimately converge again (this portion is not shown on the graph) as the sorting machinery becomes saturated. HER2 expression has its greatest impact just prior to ERC saturation at intermediate intracellular EGF concentrations ($\sim 10^4$ #/cell). At this EGF concentration, an input of 100% heterodimers elicits an increase in sorting fraction of about 0.1 over that of an input of 100% complexes. The addition of HER2 accelerates the onset of saturation of the sorting machinery by effectively titrating out the number of ERCs. Consequently, at low EGF concentrations, where the number of ERCs greatly exceeds the number of internal receptors, HER2 is unable to induce any effect on EGF sorting.

In this model, the system interaction is governed by the affinities of HER2 and EGF-EGFR complexes for ERCs. For a model input of 100% bound heterodimers, decreasing the HER2:ERC uncoupling rate resulted in an increase in sorting fraction (Figure 4.6b). Thus, increasing the expression of HER2 has the same effect as decreasing the HER2:ERC uncoupling rate.

4.3.6 Affinity Model

The endosomal sorting of ligands is strongly controlled by their binding properties at endosomal pH. There are many reports of HER2 increasing EGFR affinity for EGF by as much as 6-fold (Karunagaran et al., 1996; Lenferink et al., 1998; Lewis et al., 1996; Wada et al., 1990; Worthylake et al., 1999). Under certain conditions, heightened EGF affinity within the endosome has been shown to enhance ligand recycling (French and Lauffenburger, 1996).

Conversely, Lenferink *et al* demonstrated an increase in EGF dissociation from heterodimers at endosomal pH (Lenferink et al., 1998). The increased dissociation of TGFα at pH 6.0, relative to EGF, results in an increase in recycling (French et al., 1995). Thus, it is conceivable that EGF-EGFR heterodimerization with HER2 may increase EGF recycling by promoting the dissociation of EGF from EGFR.

In this model, EGFR/HER2 heterodimerization acts to alter the dissociation rate of EGF from the EGFR (see Figure 4.2c). Two cases are considered: In the first case we consider the possibility that heterodimerization increases the dissociation rate of EGF, modeled by an increased dissociation rate from 0.5 to 2.5 min^{-1}. Secondly, we consider

the case where heterodimerization enhances EGFR affinity for EGF, modeled by a dissociation rate decreased from 0.5 to 0.1 min^{-1}. HER2 does not interact with ERCs, and heterodimerization does not affect the ability of the EGFR to bind ERCs while EGF is still bound. Similar to the blockade model, altering EGF dissociation results in an immediate effect on EGF sorting such that the entire sorting curve (in the regime prior to saturation) is shifted up in the case where the dissociation rate is increased (Figure 4.7a) and is shifted down in the case where the dissociation rate is decreased (Figure 4.7b). Given the relatively high affinity of human EGF at endosomal pH, we are unable to reproduce the phenomena in which increasing affinity increases recycling (results not shown).

4.4 Discussion

Elevated HER2 expression and its interactions with EGFR family members have been demonstrated to be of great importance in tumor progression (Hynes and Stern, 1994). HER2 amplifies the magnitude of EGFR signaling through the recruitment of additional signaling molecules and also increases the duration of EGFR signaling via the disruption of the normal trafficking and down-regulation of the EGFR (Karunagaran et al., 1996; Worthylake et al., 1999). Impaired EGFR trafficking has been linked to tumor formation in mice and as such, we have chosen to concern ourselves with processes involved in receptor down-regulation, specifically, endosomal sorting (Wells et al., 1990). Recent work has quantitatively demonstrated the importance of endosomal sorting in determining the distribution and down-regulation of EGFR (Hendriks et al., 2003a

(Chapter 2)). Endosomal sorting represents a critical regulatory point in EGFR trafficking by controlling the fraction of receptors and ligands that are targeted for degradation. In this study, we have utilized computational modeling techniques to gain insight into the receptor interactions that govern the qualitative aspects of the observed endosomal sorting outcomes.

From the experimental data, the parental cell line is clearly operating in the regime where EGFR complex interaction with ERCs dominates and mediates EGF degradation. Secondly, over the experimentally accessible range of intracellular EGF concentration we do not see the onset of ERC saturation, as the slope of the sorting curve remains negative. For HER2 clone 24H, however, the shallow positive slope suggests the onset of ERC saturation. Thus, elevated HER2 expression appears to accelerate the onset of endosomal sorting saturation.

In order to account for this result, we have expanded the ERC sorting model to include HER2 and investigated how different HER2 interactions affect the sorting process. Qualitatively, our 3 models give us one of two possible results, with the differences manifesting themselves at low intracellular EGF concentrations. In the blockade and affinity model (in which heterodimerization decreases affinity), recycling is increased at the low intracellular EGF concentrations, where the leftmost portion of the sorting curve is shifted upwards. The increase in recycling with HER2 expression simply reflects the fraction of EGF-EGFR complexes that are in heterodimers and each individual heterodimer directly affects the fraction of EGF recycled. The competition model, by contrast, is a titration effect, where increased presence of HER2 inside the

sorting endosome is unable to alter EGF recycling until its quantity is on the same order of magnitude as the number of ERCs. Consequently, we observe a result where there is no difference at low intracellular EGF concentration for the different levels of HER2 expression. As intracellular EGF increases the curves begin to diverge and elevated HER2 expression expedites the point at which endosomal saturation begins.

While the three models proposed are not mutually exclusive, comparison with experimental results suggests that the competitive mechanism is dominant. Experimental sorting outcomes for varying HER2 expression levels (see in Figure 4.3a) converge at low intracellular EGF, qualitatively similar to the competition model results (see Figure 4.6a). However, it is possible that different mechanisms may dominate in different cell types. Data from Worthylake and Wiley show that increased HER2 expression shifted the entire sorting curve upward (Worthylake et al., 1999). This may be indicative of the blockade or affinity models being dominant, or it is possible that the sorting curves may still converge if experiments were carried out at sufficiently low EGF concentrations.

We remind the reader that the purpose of this work is not to quantitatively fit the data, but rather to understand how various molecular-level interactions are translated into qualitative trends in the experimental data. A number of the model parameters are based upon estimates from other cell types and may not necessarily be optimal choices to reflect our experimental setup. Nonetheless, the qualitative nature of the model results is quite robust, and is insensitive to reasonable parameter variations. Further, the model assumes a constant input flux of receptors and ligands for ease of interpretation. Experimentally, the internalization flux may not be constant since internalization rates have been shown

to be a function of the number of surface complexes and vary with the surface expression levels of HER2 as well (Hendriks et al., 2003a (Chapter 2); Hendriks et al., 2003b (Chatper 3); Wiley et al., 1991). For these reasons, a direct, quantitative comparison of the experimental and modeling results is not appropriate.

Our models contain several simplifications including the fact that EGF-EGFR complex homodimerization is not explicitly included. In the original ERC model the EGF-EGFR complex is the functional unit in terms of interaction within the endosome. Conceptually, this unit could be thought of either as a single EGF-EGFR complex or an EGF-EGFR homodimer with no effect on the sorting results. When HER2 is added to the model it is best to conceptualize the EGF-EGFR representation as a homodimer and the process of heterodimerization with HER2 simply reflects trading an EGF-EGFR complex for a HER2 within the dimer. If one explicitly includes all possible EGFR-HER2 interactions the results are indistinguishable from those presented here (results not shown). These simplifications serve to simplify the computations and do not affect the characteristic qualities of each model – the blockade and affinity models still show immediate influence from HER2 expression, while the competition model requires sufficient HER2 present before any effect is apparent.

If HER2 affects EGF recycling through a competitive mechanism then, at first glance, one would expect heterodimerization to have no effect on the sorting process. As such, the addition of monoclonal antibody 2C4 would be predicted to have no effect on EGF sorting. However, Figure 4.3b shows this is not the case. If one considers the trafficking process as a whole, we find that this is still consistent with HER2 acting via a

competitive mechanism. As a side-effect from blocking heterodimerization, one would predict that 2C4 prevents the EGF-induced internalization of HER2 (Hendriks et al., 2003a (Chapter 2); Hendriks et al., 2003b (Chapter 3)). Thus, addition of 2C4 prevents the internalization of HER2 into the endosomal sorting compartment so that it is unable to compete with EGFR for ERC interaction. Heterodimerization itself is not predicted to have any effect on the sorting process, however, effects at the level of internalization affect the sorting process by dictating the receptor composition within endosomal compartments.

The hypothesis that HER2 is able to alter EGFR sorting through a competitive mechanism suggests that there must be some sequence similarity between the two receptors in the carboxy-terminal domain regions interacting with the sorting apparatus. The precise identity of the endosomal retention component remains unknown at present, but evidence suggests that SNX1 may play such a role (Kurten et al., 1996; Zhong et al., 2002). SNX1 was identified via its interaction with EGFR residues 943-957, and has been shown to localize to endosomal compartments. Its inhibition decreases the rate of ligand-induced EGFR degradation, consistent with the behavior of ERCs in the ERC sorting model (French and Lauffenburger, 1996; Kurten et al., 1996; Zhong et al., 2002). EGFR residues 943-957 are known to interact with SNX1 and share 80% identity with HER2 residues 951-965, strongly suggesting that HER2 may also be able to interact with SNX1.

Another candidate for relevant involvement in the sorting process is c-Cbl. Overexpression of c-Cbl stimulates ligand-induced EGFR degradation (Levkowitz et al.,

1999; Levkowitz et al., 1998). Further, c-Cbl associates only with EGF-EGFR homodimers, but not with EGF-EGFR/HER2 heterodimers, HER2, HER3 or HER4 (Levkowitz et al., 1996; Muthuswamy et al., 1999). A current model has c-Cbl transiently associating with kinase-active EGFR to mediate ubiquitination, with ubiquitin-tagged EGFR then exhibiting increased affinity for the sorting apparatus resulting in enhanced degradation (Wiley and Burke, 2001). The fact that heterodimerization impedes this process is suggestive of a blockade-type mechanism; however, based on our results its role in generating the experimentally-observed sorting outcomes is not obvious.

Our integrative systems approach towards EGFR trafficking has gained us interesting insight into the trafficking process as a whole, especially in the context of a hierarchy of receptor trafficking models (Hendriks et al., 2003a (Chapter 2); Hendriks et al., 2003b (Chapter 3)). The sorting process is tightly regulated and its output (sorting fraction) is heavily dependent on the composition of its input (complexes vs. heterodimers). In the case of the EGFR-HER2 system it appears that the highest level of control is exerted at the surface since this determines the input into the sorting compartment. It is at the surface where the distribution of complexes and heterodimers is determined. Increased formation of heterodimers results in a reduced rate of EGF internalization in addition to an increase in the fraction recycled towards the surface (Hendriks et al., 2003a (Chapter 2); Hendriks et al. 2003b (Chapter 3)). These two processes work in concert to maintain EGFR expression on the surface and presumably maintain signaling through surface-activated signaling pathways, such PLC-□and calpain, both involved in cell migration. Whether or not the distribution of dimer species

reshuffles once inside of internal compartments due to a different receptor composition is unclear. The degree to which these internal species participate in signaling once internalized is also in need of further investigation. Because trafficking is an iterative process, however, we would still expect sorting to play an important role in the dictating long-term behavior following successive rounds of internalization and recycling.

4.5 Tables

Table 4.1 Sorting Parameter Values.

Parameter values used in endosomal sorting model that are common to all models. All values come from the original ERC sorting model (French and Lauffenburger 1996), except as noted.

Parameter	*Description*	*Base Value*
N_{av}	Avogadro's number	6.023×10^{23} #/mol
V_{total}	total endosomal volume	3×10^{-14}
ϕ	ratio of volume in tubular compartments to vesicular compartments	0.67
k_{st}	tubular sorting rate constant	0.53 min^{-1}
k_{sv}	vesicular rate constant	0.06 min^{-1}
σ	partition coefficient accounting for excluded volume in tubules due to ligand size	0.81
η	fraction of internalized ligand non-specifically endocytosed	0
ρ	transport rate constant of receptors out of vesicular compartment into tubular compartment	1 min^{-1}
k_h	degradation rate constant	0.09 min^{-1}
k_x	recycling rate constant	0.15 min^{-1}
k_{on}	EGF binding rate constant	5×10^{7} †
k_{off}	EGF dissociation rate constant from EGFR	0.5 min^{-1} †
k_c	(EGF-EGFR)-HER2 dimerization rate constant	1×10^{-3} $(\#/cell)^{-1} min^{-1}$
$k_{u,R1LR2}$	(EGF-EGFR)-HER2 uncoupling rate constant	0.1 min^{-1} §
$k_{c,R1E}$	(EGF-EGFR)-ERC coupling rate constant	1×10^{-3} $(\#/cell)^{-1} min^{-1}$
$k_{u,R1E}$	EGFR-ERC uncoupling rate constant	0.1 min^{-1}
ERC_{total}	total number of ERCs	10,000 #/cell
I_{R1L}	input flux of EGF-EGFR complexes	varied
I_{R1LR2}	input flux of (EGF-EGFR)-HER2	varied

† Experimentally measured (data not shown).
§ Parameter value from Hendriks et al., 2003b (Chapter 3)

Table 4.2 Model-Specific Parameter Values.

Parameter	*Description*	*Value*		
		Blockade Model	**Competition Model**	**Affinity Model**
k_{off_het}	EGF dissociation rate constant from heterodimers	0.5 min^{-1}	0.5 min^{-1}	0.1 – 2.5 min^{-1}
$k_{c,R1E,het}$	(EGF-EGFR)-ERC coupling rate constant when in a heterodimer	0	$1x10^{-3}$ $(\#/cell)^{-1}min^{-1}$	$1x10^{-3}$ $(\#/cell)^{-1}min^{-1}$
$k_{c,R2E}$	HER2-ERC coupling rate constant	0	$1x10^{-3}$ $(\#/cell)^{-1}min^{-1}$	0
$k_{c,R2E,het}$	HER2-ERC coupling rate constant when in a heterodimer	0	$1x10^{-3}$ $(\#/cell)^{-1}min^{-1}$	$1x10^{-3}$ $(\#/cell)^{-1}min^{-1}$
$k_{u,R2E}$	HER2-ERC uncoupling rate constant	0	0.1 min^{-1}	0

4.6 Figures

(A)

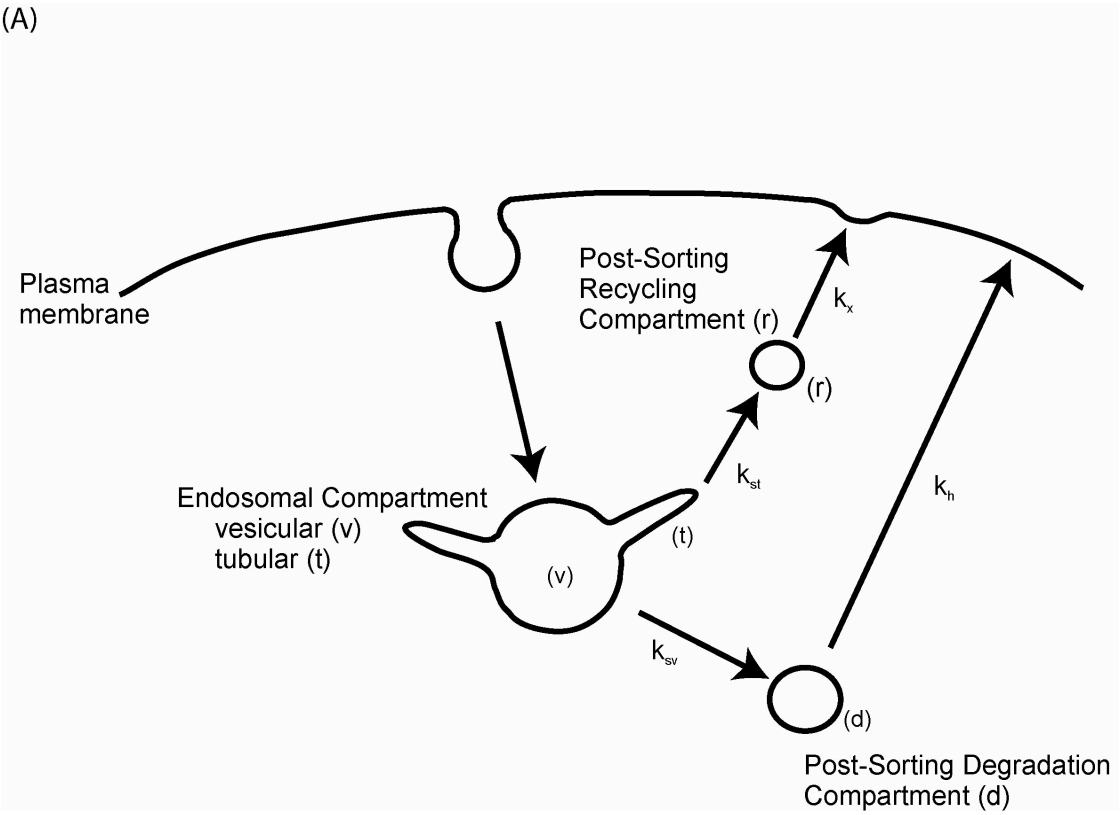
Plasma
membrane
Post-Sorting
Recycling
Compartment (r)
k_x
(r)
k_{st}
k_h
Endosomal Compartment
vesicular (v)
tubular (t)
(t)
(v)
k_{sv}
(d)
Post-Sorting Degradation
Compartment (d)

(B)

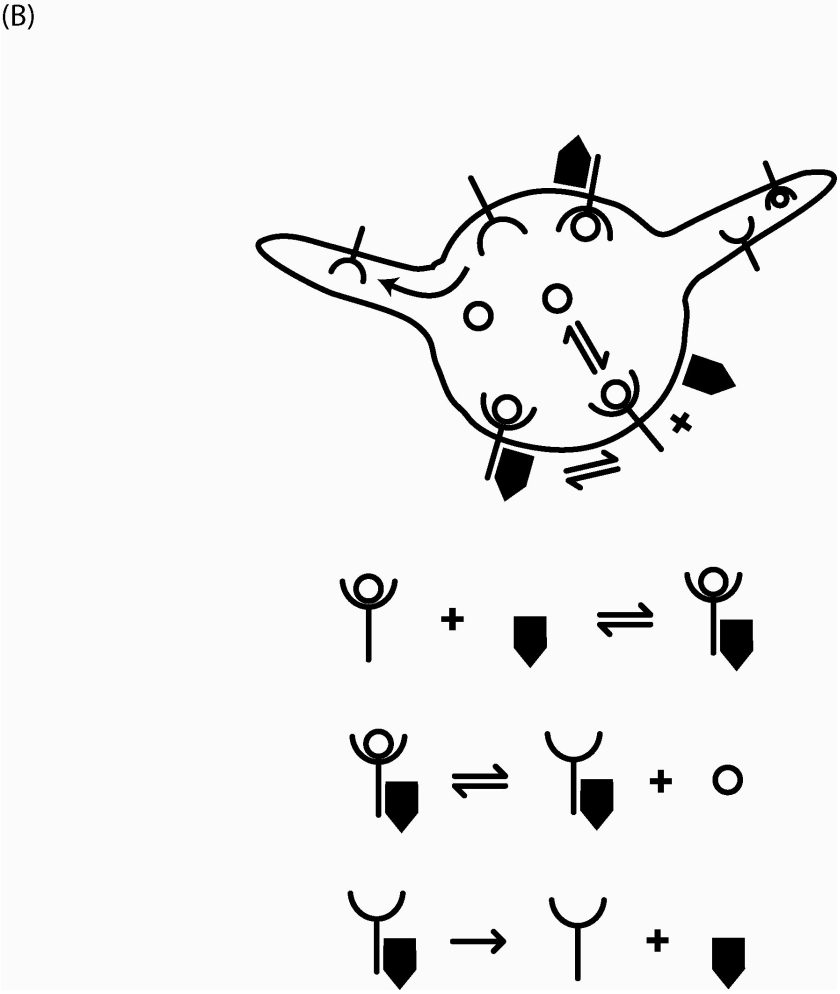

(C)

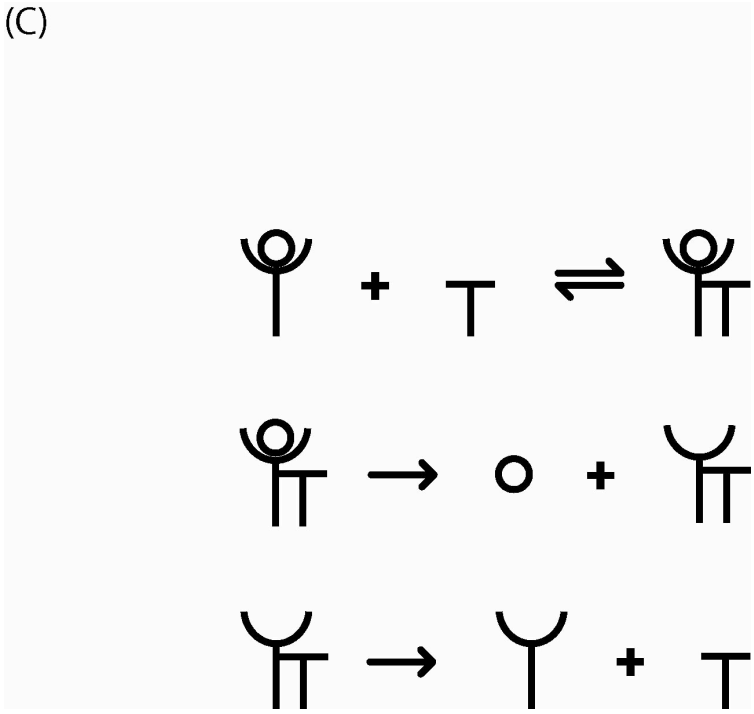

(D)

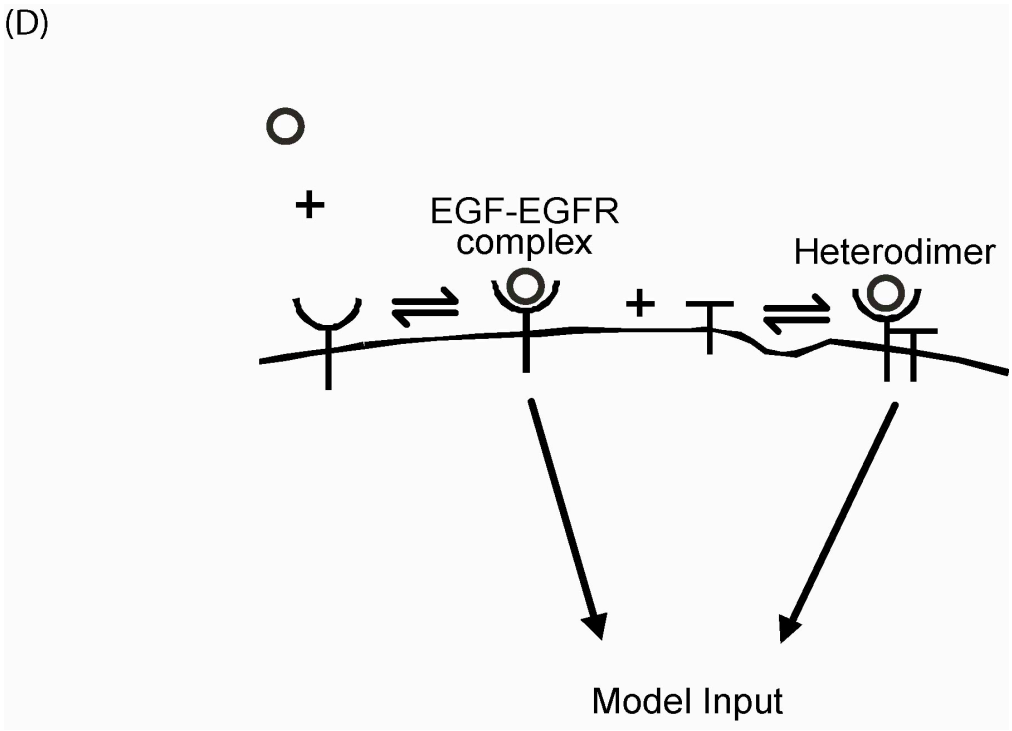

Figure 4.1 ERC Sorting Model.

A, Endosomal Sorting Model, proposed by French and Lauffenburger. The cell is divided into four compartments: endosomal vesicle, endosomal tubule, recycling and degradation compartments. Internalized ligand-receptor complexes enter vesicular compartment where they diffuse into the tubular compartment or are selectively retained in the central vesicle by ERCs. The vesicular compartment of the endosome targets species for degradation while the tubular compartment of the endosome targets species for recycling. *B*, within endosome, occupied EGFR (Y shaped species) are selectively retained in vesicular portion by interaction with ERCs (filled pentagons). Species not bound by ERCs are free to diffuse into tubular compartments for recycling. *C*, additional receptor interactions are added as a result of HER2 (T shaped species) presence. HER2 may dimerize with occupied EGFRs. EGF may dissociate from receptor heterodimers yielding unoccupied heterodimers which instantaneously break apart into unoccupied EGFR and free HER2. *D*, the addition of HER2 to the model drives the formation of heterodimers and shifts the model input from 100% EGF-EGFR complexes to a combination of complexes and heterodimers to 100% heterodimers. This figure is redrawn from French and Lauffenburger, 1996.

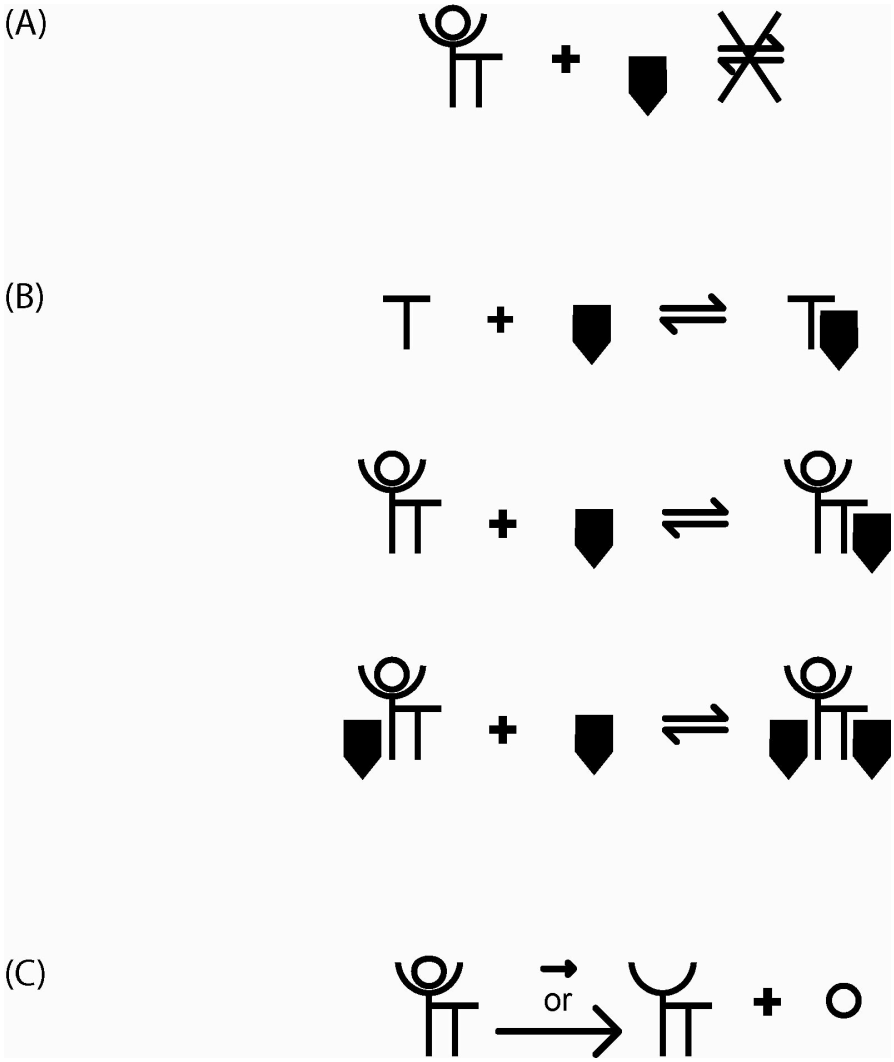

Figure 4.2 Possible HER2 Effects on Sorting.

A, *Blockade model*. Heterodimerization with HER2 prevents EGFR-ERC and (EGF-EGFR)-ERC interaction. *B*, *Competition model*. HER2 competes with EGFR for ERC interaction. Both free and heterodimerized HER2 species may interact with ERCs. *C*, *Affinity model*. EGF-EGFR heterodimerization with HER2 alters the dissociation rate of EGF.

(A)

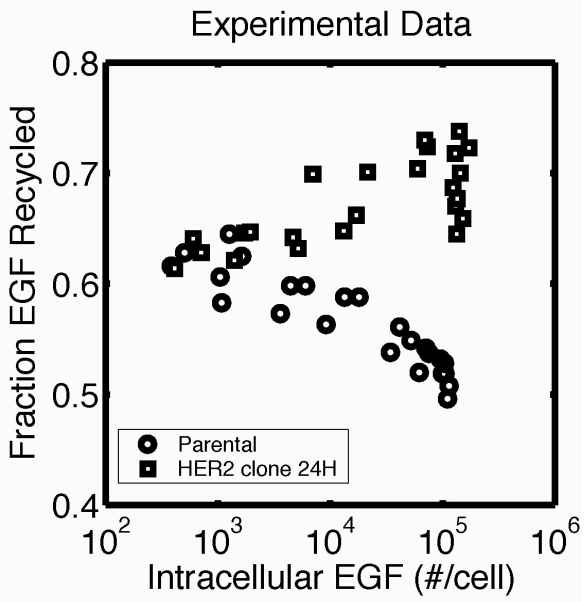

(B)

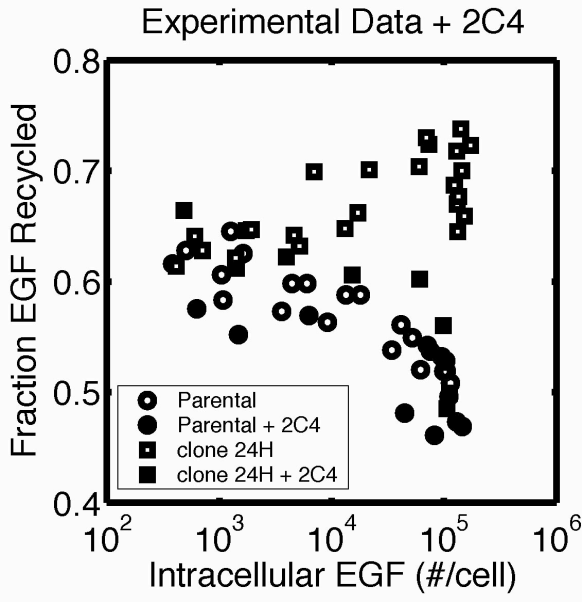

Figure 4.3 Experimental Sorting Data.

A, fraction of EGF recycled as a function of intracellular EGF concentration for cell lines expressing increasing levels of HER2 (reprinted from Hendriks et al., 2003a (Chapter 2)).

Circles and squares represent the parental cell line and HER2 clone 24H, expressing roughly 3×10^4 and 6×10^5 HER2 per cell, respectively. *B*, addition of heterodimerization blocking antibodies (2C4) abrogates HER2 effect on EGF recycling. Steady state sorting assays were conducted with (open symbols) or without (filled symbols) overnight pretreatment of saturating amounts of 2C4 antibody on the parental cell line (circles) and HER2 clone 24H (squares).

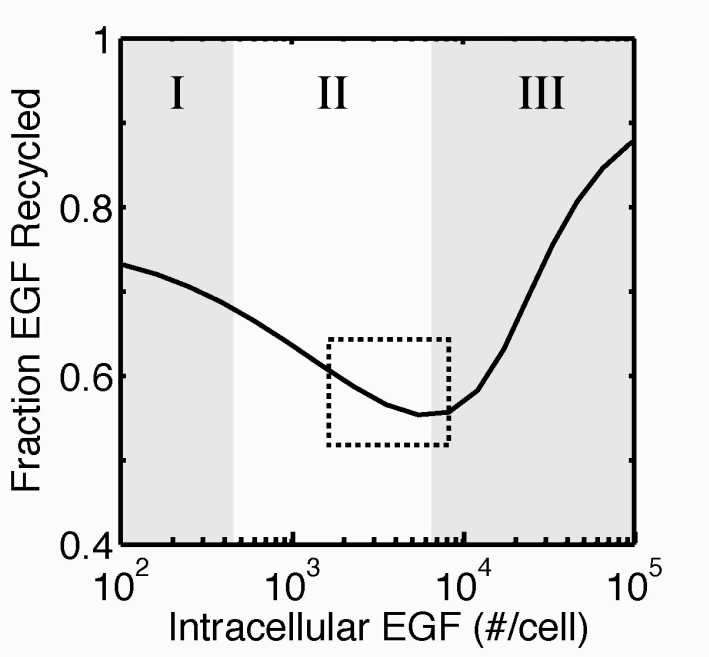

Figure 4.4 Typical Sorting Model Results.

Typical sorting curve from the original ERC sorting model. The curve can be broken into 3 regimes: (I) fluid-phase sorting, (II) EGFR complex interaction with ERCs decreasing the fraction of EGF recycled and (III) saturation of a limited quantity of ERCs. Experimental data shown in Figure 4.3 fall primarily within regime II as indicated by the rectangle.

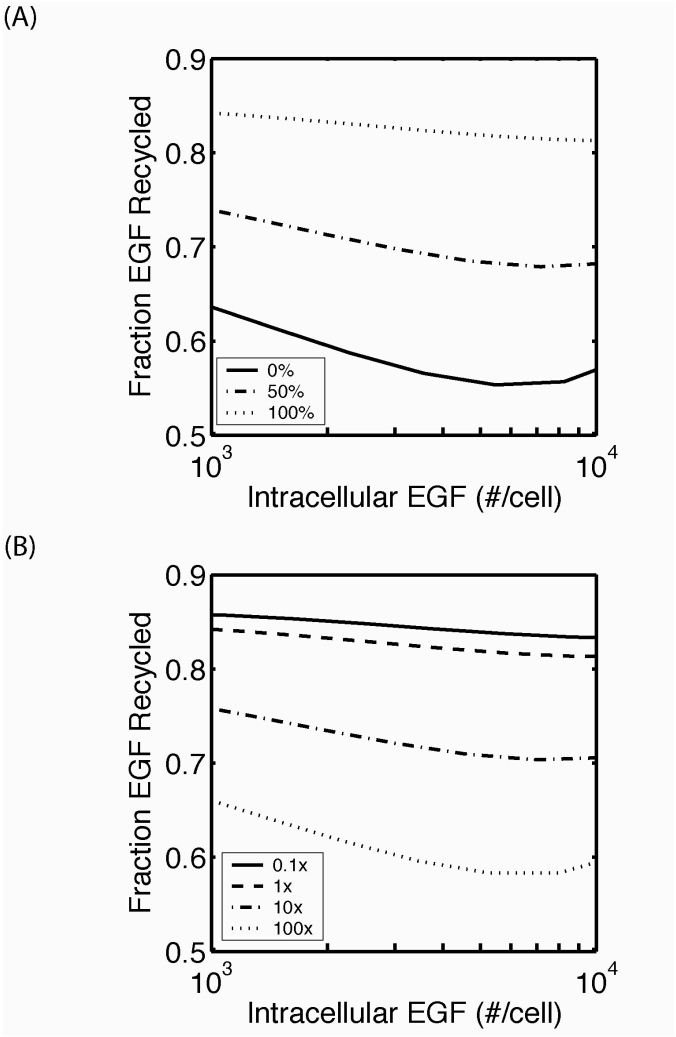

Figure 4.5 Blockade Model Results.

Simulated sorting curves for Blockade Model in which heterodimerization blocks EGFR-ERC interaction. *A*, model input is varied from 100% EGF-EGFR complexes/0% heterodimers (solid line), to 50% EGF-EGFR complexes/50% heterodimers (dashed line), to 0% EGF-EGFR complexes/100% heterodimers (dotted line). *B*, bound heterodimer uncoupling rate constant ($k_{u,R1LR2}$) is varied from 0.1-100x the base value (0.1 min^{-1}), for a model input of 0% EGF-EGFR complexes/100% heterodimers.

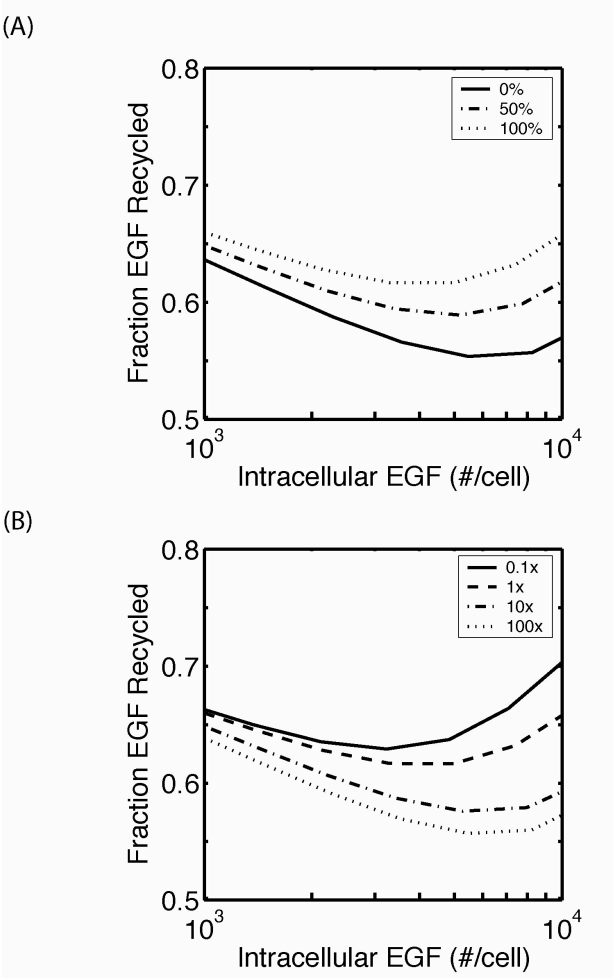

Figure 4.6 Competition Model Results.

Simulated sorting curves for Competition Model in which both free and heterodimerized HER2 competes with EGFR for interaction with ERCs. *A*, model input is varied from 100% EGF-EGFR complexes/0% heterodimers (solid line), to 50% EGF-EGFR complexes/50% heterodimers (dashed line), to 0% EGF-EGFR complexes/100% heterodimers (dotted line). *B*, HER2-ERC uncoupling rate constant ($k_{u,R2E}$) is varied from 0.1-100x the base value (0.1 min^{-1}), for a model input of 0% EGF-EGFR complexes/100% heterodimers.

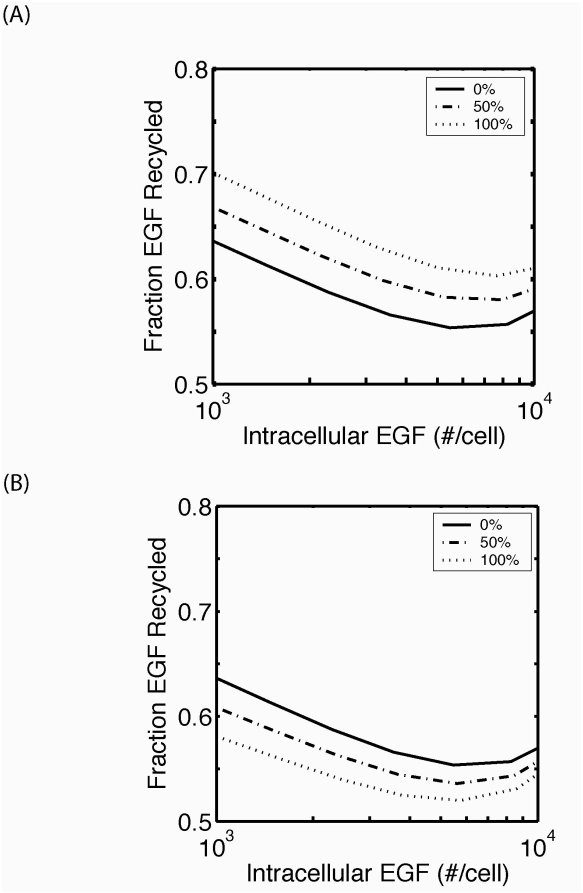

Figure 4.7 Affinity Model Results.

Simulated sorting curves for the *Affinity Model* in which heterodimerization alters the dissociation rate of EGF. *A*, the dissociation rate of EGF from heterodimers ($k_{off,het}$) is increased to 5 min^{-1} model input is varied from 100% EGF-EGFR complexes/0% heterodimers (solid line), to 50% EGF-EGFR complexes/50% heterodimers (dashed line), to 0% EGF-EGFR complexes/100% heterodimers (dotted line). *B*, $k_{off,het}$ is decreased to 0.1 min^{-1}, and model input is varied from 100% EGF-EGFR complexes/0% heterodimers (solid line), to 50% EGF-EGFR complexes/50% heterodimers (dashed line), to 0% EGF-EGFR complexes/100% heterodimers (dotted line).

4.7 References

Agus, D.B., Akita, R.W., Fox, W.D., Lewis, G.D., Higgins, B., Pisacane, P.I., Lofgren, J.A., Tindell, C., Evans, D.P., Maiese, K., Scher, H.I. and Sliwkowski, M.X. (2002) Targeting ligand-activated ErbB2 signaling inhibits breast and prostate tumor growth. *Cancer Cell*, **2**, 127-137.

Baselga, J. (2002) A new anti-ErbB2 strategy in the treatment of cancer: Prevention of ligand-dependent ErbB2 receptor heterodimerization. *Cancer Cell*, **2**, 93-94.

Brandt, B.H., Roetger, A., Dittmar, T., Nikolia, G., Seeling, M., Merschjann, A., Nofer, J.-R., Dehmer-Moller, G., Junker, R., Assmann, G. and Zaenker, K. (1999) c-erbB-2/EGFR as dominant heterodimerization partners determine a motogenic phenotype in human breast cancer cells. *The FASEB Journal*, **13**, 1939-1950.

Chazin, V.R., Kaleko, M., Miller, A.D. and Slamon, D.J. (1992) Transformation mediated by the human HER-2 gene independent of the epidermal growth factor receptor. *Oncogene*, **7**, 1859-1866.

DiFiore, P.P., Pierce, J.H., Fleming, T.P., Hazan, R., Aullrich, A., King, C.R., Schlessinger, J. and Aaronson, S.A. (1987a) Overexpression of the Human EGF Receptor Confers an EGF-Dependent Transformed Phenotype to NIH 3T3 Cells. *Cell*, **51**, 1063-1070.

DiFiore, P.P., Pierce, J.H., Kraus, M.H., Segatto, O., King, C.R. and Aaronson, S.A. (1987b) erbB-2 Is a Potent Oncogene When Overexpressed in NIH/3T3 Cells. *Science*, **237**, 178-182.

Earp, H.S., Dawson, T.L., Li, X. and Yu, H. (1995) Heterodimerization and function interaction between EGF receptor family members: A new signaling paradigm with implications for breast cancer research. *Breast Cancer Research and Treatment*, **35**, 115-132.

Fendly, B.M., Winget, M., Hudziak, R.M., Lipari, M.T., Napier, M.A. and Ullrich, A. (1990) Characterization of Murine Monoclonal Antibodies Reactive to Either the Human Epidermal Growth Factor Receptor or HER2/neu Gene Product. *Cancer Research*, **50**, 1550-1558.

French, A.R. and Lauffenburger, D.A. (1996) Intracellular Receptor/Ligand Sorting Based on Endosomal Retention Components. *Biotechnology and Bioengineering*, **51**, 281-297.

French, A.R. and Lauffenburger, D.A. (1997) Controlling Receptor/Ligand Trafficking: Effects of Cellular and Molecular Porperties on Endosomal Sorting. *Annals of Biomedical Engineering*, **25**, 690-707.

French, A.R., Sudlow, G.P., Wiley, H.S. and Lauffenburger, D.A. (1994) Postendocytic Trafficking of Epidermal Growth Factor-Receptor Complexes Is Mediated through Saturable and Specific Endosomal Interactions. *The Journal of Biological Chemistry*, **269**, 15749-15755.

French, A.R., Tadaki, D.K., Niyogi, S.K. and Lauffenburger, D.A. (1995) Intracellular Trafficking of Epidermal Growth Factor Family Ligands Is Directly Influenced by the pH Sensitivity of the Receptor/Ligand Interaction. *The Journal of Biological Chemistry*, **270**, 4334-4340.

Graus-Porta, D., Beerli, R.R., Daly, J.M. and Hynes, N.E. (1997) ErbB-2, the preferred heterodimerization partner of all ErbB receptors, is a mediator of lateral signaling. *The European Molecular Biology Organization Journal*, **16**, 1647-1655.

Hendriks, B.S., Opresko, L.K., Wiley, H.S. and Lauffenburger, D.A. (2003a) Co-Regulation of EGFR/HER2 Levels and Locations: Quantitative Analysis of HER2 Overexpression Effects. *Cancer Research*, **63**, 1130-1137.

Hendriks, B.S., Opresko, L.K., Wiley, H.S. and Lauffenburger, D.A. (2003b) Quantitative Analysis of HER2-mediated Effects on HER2 and EGFR Enodcytosis: Distribution of Homo- and Hetero-dimers Depends on Relative HER2 Levels. *The Journal of Biological Chemistry*, **278**, 23343-23351.

Hynes, N.E. and Stern, D.F. (1994) The biology of erbB-2/neu/HER-2 and its role in cancer. *Biochimica et Biophysica Acta*, **1198**, 165-184.

Ignatoski, K.M.W., Lapointe, A.J., Radany, E.H. and Ethier, S.P. (1999) erbB-2 Overexpression in Human Mammary Epithelial Cells Confers Growth Factor Independence. *Endocrinology*, **140**, 3615-3622.

Karunagaran, D., Tzahar, E., Beerli, R.R., Chen, X., Graus-Porta, D., Ratzkin, B.J., Seger, R., Hynes, N.E. and Yarden, Y. (1996) ErbB-2 is a common auxiliary subunit of NDF and EGF receptors: implications for breast cancer. *The European Molecular Biology Organization Journal*, **15**, 254-264.

Kurten, R.C., Cadena, D.L. and Gill, G.N. (1996) Enhanced Degradation of EGF Receptors by a Sorting Nexin, SNX1. *Science*, **272**, 1008-1010.

Lauffenburger, D.A. and Linderman, J.J. (1993) *Receptors*. Oxford University Press, Inc., New York.

Lenferink, A.E.G., Pinkas-Kramarski, R., Poll, M.L.M.v.d., Vugt, M.J.H.v., Klapper, L.N., Tzahar, E., Waterman, H., Sela, M., Zoelen, E.J.J.v. and Yarden, Y. (1998) Differential endocytic routing of homo- and hetero-dimeric ErbB tyrosine kinases confers signaling superiority to receptor heterodimers. *The European Molecular Biology Organization Journal*, **17**, 3385-3397.

Levkowitz, G., Klapper, L.N., Tzahar, E., Freywald, A., Sela, M. and Yarden, Y. (1996) Coupling of the c-Cbl protooncogene product to ErbB-1/EGF-receptor but not to other Erbb proteins. *Oncogene*, **12**, 1117-1125.

Levkowitz, G., Waterman, H., Ettenberg, S.A., Katz, M., Tsygankov, A.Y., Alroy, I., Lavi, S., Iwai, K., Reiss, Y., Ciechanover, A., Lipkowitz, S. and Yarden, Y. (1999) Ubiquitin Ligase Activity and Tyrosine Phosphorylation Underlie Suppression of Growth Factor Signaling by c-Cbl/Sli-1. *Molecular Cell*, **4**, 1029-1040.

Levkowitz, G., Waterman, H., Zamir, E., Kam, Z., Oved, S., Langdon, W.Y., Beguinot, L., Geiger, B. and Yarden, Y. (1998) c-Cbl/sli-1 regulates endocytic sorting and ubiquitination of the epidermal growth factor receptor. *Genes & Development*, **12**, 3663-3674.

Lewis, G.D., Lofgren, J.A., McMurtrey, A.E., Nuijens, A., Fendly, B.M., Bauer, K.D. and Sliwkowski, M.X. (1996) Growth Regulation of Human Breast and Ovarin Tumor Cells by Heregulin: Evidence of the Requirement of ErbB2 as a Critical

Component in Mediating Heregulin Responsiveness. *Cancer Research*, **56**, 1457-1465.

Linderman, J.J. and Lauffenburger, D.A. (1986) Analysis of Intracellular Sorting: Calculation of Mean Surface and Bulk Diffusion Times within a Sphere. *Biophysical Journal*, **50**, 295-305.

Muthuswamy, S., Gilman, M. and Brugge, J.S. (1999) Controlled Dimerization of ErbB Receptors Provides Evidence for Differential Signaling by Homo- and Heterodimers. *Molecular and Cellular Biology*, **19**, 6845-6957.

Schechter, A.L., Hung, M.-C., Vaidyanathan, L., Weinberg, R.A., Yang-Feng, T.L., Francke, U., Ullrich, A. and Coussens, L. (1985) The neu Gene: An erbB-homologous Gene Distinct from and Unlinked to the Gene Encoding the EGF Receptor. *Science*, **229**, 976-978.

Shea, L.D., Omann, G.M. and Linderman, J.J. (1997) Calculation of Diffusion-Limited Kinetics for the Reactions in Collision Coupling and Receptor Cross-Linking. *Biophysical Journal*, **73**, 2949-2959.

Spencer, K.S.R., Graus-Porta, D., Leng, J., Hynes, N. and Klemke, R.L. (2000) ErbB2 Is Necesary for Induction of Carcinoma Cell Invasion by ErbB Family Receptor Tyrosine Kinases. *The Journal of Cell Biology*, **148**, 385-397.

Ullrich, A., Coussens, L., Hayflick, J.S., Dull, T.J., Gray, A., Tam, A.W., Lee, J., Yarden, Y., Libermann, T.A., Schlessinger, J., Downward, J., Mayes, E.L.V., Whittle, N., Waterfield, M.D. and Seeburg, P.H. (1984) Human epidermal growth factor

receptor cDNA sequence and aberrant expression of the amplified gene in A431 epidermoid carncinoma cells. *Nature*, **309**, 418-425.

Wada, T., Qian, X. and Greene, M.I. (1990) Intermolecular Association of the p185neu Protein and EGF Receptor Modulates EGF Receptor Function. *Cell*, **61**, 1339-1347.

Waterman, H., Sabanai, I., Geiger, B. and Yarden, Y. (1998) Alternative Intracellular Routing of ErbB Receptors May Determine Signaling Potency. *The Journal of Biological Chemistry*, **273**, 13819-13827.

Wells, A., Welsh, J.B., Lazar, C.S., Wiley, H.S., Gill, G.N. and Rosenfeld, M.G. (1990) Ligand-Induced Transformation by a Noninternalizing Epidermal Growth Factor Receptor. *Science*, **247**, 962-964.

Wiley, H.S. and Burke, P.M. (2001) Regulation of Receptor Tyrosine Kinase Signaling by Endocytic Trafficking. *Traffic*, **2**, 12-18.

Wiley, H.S., Herbst, J.J., Walsh, B.J., Lauffenburger, D.A., Rosenfeld, M.G. and Gill, G.N. (1991) The Role of Tyrosine Kinase Activity in Endocytosis, Compartmentation, and Down-regulation of the Epidermal Growth Factor Receptor. *The Journal of Biological Chemistry*, **266**, 11083-11094.

Worthylake, R., Opresko, L.K. and Wiley, H.S. (1999) ErbB-2 Amplification Inhibits Down-regulation and Induces Constitutive Activation of Both ErbB-2 and Epidermal Growth Factor Receptors. *The Journal of Biological Chemistry*, **274**, 8865-8874.

Worthylake, R. and Wiley, H.S. (1997) Structural Aspects of the Epidermal Growth Factor Receptor Required for Transmodulation of erbB-2/neu. *The Journal of Biological Chemistry*, **272**, 8594-8601.

Zhong, Q., Lazar, C.S., Tronchere, H., Sato, T., Meerloo, T., Yeo, M., Songyang, Z., Emr, S.D. and Gill, G.N. (2002) Endosomal localization and function of sorting nexin 1. *Proceedings of the National Academy of Sciences - USA*, **99**, 6767-6772.

4.A Appendix: Endosomal Sorting Model Equations.

The following equations are used to simulate the various possible effects of HER2 on the steady state endosomal sorting of EGF. The model is solved at steady state for varying inputs of complexes (I_{R1L}) and heterodimers (I_{R1LR2}). Each model (blockade, competition or affinity) is independently simulated by changing the appropriate parameters as described in *Model Development*.

central vesicle:

$d(R1_v)/dt = k_{off,het}*R1LR2E_v - k_{on}*L_v*R1_v + k_{on}*R1L_v + k_{u.R1E}*R1E_v + k_{off,het}*R1LR2_v - (\square+k_{sv})*R1_v$;

$d(R2_v)/dt = - k_c*R1_v*R2_v + k_{u,R1R2}*R1R2_v - k_c*R1L_v*R2_v + k_{u,R1LR2}*R1LR2_v - k_{c,R2E}*R2_v*E_v + k_{u,R2E}*R2E_v - k_c*R1E_v*R2_v + k_{u,R1R2}*ER1R2_v - k_c*R1LE_v*R2_v + k_{u,R1LR2}*ER1LR2_v + k_{off,het}*R1LR2_v + k_{off,het}*ER1LR2_v - (\square+k_{sv})*R2R1_v$;

$d(R1L_v)/dt = I_{R1L} + k_{on}*L_v*R1_v - k_{on}*R1L_v - k_{c,R1E}*R1L_v*E_v + k_{u.R1E}*R1LE_v - k_c*R1L_v*R2_v + k_{u,R1LR2}*R1LR2_v - k_c*R1L_v*R2E_v + k_{u,R1LR2}*R1LR2E_v - (\square+k_{sv})*R1L_v$;

$d(R1LR2_v)/dt = I_{R1LR2} - k_{off,het}*R1LR2_v + k_c*R1L_v*R2_v - k_{u,R1LR2}*R1LR2_v - k_{c,R1E,het}*R1LR2_v*E_v + k_{u.R1E}*ER1LR2_v - k_{c,R2E,het}*R1LR2_v*E_v + k_{u,R2E}*R1LR2E_v - (\square+k_{sv})*R1LR2_v$;

$d(R1LE_v)/dt = - k_{on}*R1LE_v + k_{on}*R1E_v*L_v + k_{c,R1E}*R1L_v*E_v - k_{u.R1E}*R1LE_v - k_c*R1LE_v*R2_v + k_{u,R1LR2}*ER1LR2_v - k_{sv}*R1LE_v$;

$d(L_v)/dt = 1/(N_{av}*(V_v+V_t))*(\square/(1-\square)*(I_{R1L} + I_{R1LR2}) - k_{on}*L_v*R1_v + k_{on}*R1L_v + k_{on}*R1LE_v - k_{on}*R1E_v*L_v + k_{off,het}*R1LR2_v + k_{off,het}*R1LR2E_v + k_{off,het}*ER1LR2_v - k_{sv}*L_v*V_v*N_{av} + 1/\square*(- k_{on}*\square*L_v*R1_t + k_{on}*R1L_t + k_{off,het}*R1LR2_t - k_{st}*\square*L_v*V_t*N_{av})$;

$d(R1E_v)/dt = k_{on}*R1LE_v - k_{on}*R1E_v*L_v - k_{u.R1E}*R1E_v + k_{off,het}*ER1LR2_v - k_{sv}*R1E_v$;

$d(R2E_v)/dt = + k_{c,R2E}*R2_v*E_v - k_{u,R2E}*R2E_v - k_c*R1L_v*R2E_v + k_{u,R1LR2}*R1LR2E_v + k_{off,het}*R1LR2E_v - k_{sv}*R2E_v$;

$d(ER1LR2_v)/dt = k_c*R1LE_v*R2_v - k_{u,R1LR2}*ER1LR2_v + k_{c,R1E,het}*R1LR2_v*E_v - k_{u.R1E}*ER1LR2_v - k_{off,het}*ER1LR2_v - k_{sv}*ER1LR2_v$;

$d(R1LR2E_v)/dt = - k_{off,het}*R1LR2E_v + k_{c,R2E,het}*R1LR2_v*E_v - k_{u,R2E}*R1LR2E_v + k_c*R1L_v*R2E_v - k_{u,R1LR2}*R1LR2E_v - k_{sv}*R1LR2E_v$;

$d(E_v)/dt = - k_{c,R1E}*R1L_v*E_v + k_{u.R1E}*R1LE_v + k_{u.R1E}*R1E_v - k_{c,R2E}*R2_v*E_v + k_{u,R2E}*R2E_v - k_{c,R2E,het}*R1R2_v*E_v + k_{u,R2E}*R1R2E_v + k_{u.R1E}*ER1R2_v - k_{c,R1E,het}*R1LR2_v*E_v + k_{u.R1E}*ER1LR2_v - k_{c,R2E,het}*R1LR2_v*E_v + k_{u,R2E}*R1LR2E_v + k_{sv}*(R1LE_v + R1E_v + R2E_v + ER1R2_v + R1R2E_v + 2*ER1R2E_v + R1LR2E_v + ER1LR2_v)$;

vesicle tubule compartment:

$d(R1_t)/dt = - k_{on}*□*L_v*R1_t + k_{off}*R1L_t + k_{off,het}*R1LR2_t + □*R1_v - k_{st}*R1_t$;

$d(R2_t)/dt = - k_c*R1L_t*R2_t + k_{u,R1LR2}*R1LR2_t + k_{off,het}*R1LR2_t + □*R2_v - k_{st}*R2_t$;

$d(R1L_t)/dt = + k_{on}*□*L_v*R1_t - k_{off}*R1L_t - k_c*R1L_t*R2_t + k_{u,R1LR2}*R1LR2_t + □*R1L_v - k_{st}*R1L_t$;

$d(R1LR2_t)/dt = - k_{off,het}*R1LR2_t + k_c*R1L_t*R2_t - k_{u,R1LR2}*R1LR2_t + □*R1LR2_v - k_{st}*R1LR2_t$;

degradation compartment:

$d(R1_d)/dt = k_{sv}*(R1_v + R1E_v + R1L_v + R1LE_v + R1R2_v + R1LR2_v + ER1R2_v + R1R2E_v + ER1R2E_v + ER1LR2_v + R1LR2E_v) - k_h*R1_d$;

$d(R2_d)/dt = k_{sv}*(R2_v + R1R2_v + R1LR2_v + R2E_v + ER1R2_v + R1R2E_v + ER1R2E_v + ER1LR2_v + R1LR2E_v) - kh*R2_d$;

$d(L_d)/dt = 1/(N_{av}*V_d)*(k_{sv}*L_v*V_v*N_{av} + k_{sv}*(R1L_v + R1LE_v + R1LR2_v + ER1LR2_v + R1LR2E_v) - k_h*L_d*V_d*N_{av})$;

recycling compartment:

$d(R1_r)/dt = k_{st}*(R1_t + R1L_t + R1R2_t + R1LR2_t) - k_x*R1_r$;

$d(R2_r)/dt = k_{st}*(R2_t + R1R2_t + R1LR2_t) - k_x*R2_r$;

$d(L_r)/dt = 1/(N_{av}*V_r)*(k_{st}*L_v*□*V_t*N_{av} + k_{st}*(R1L_t + R1LR2_t) - k_x*L_r*V_r*N_{av})$;

Chapter 5: Deconvolution of HER2-Mediated Signaling and Trafficking Effects on EGFR Signaling

HER2, a member of the human EGFR tyrosine kinase family, functions via heterodimerization simultaneously as an accessory signaling component to EGFR and as a modulator of its trafficking. HER2 overexpression can lead to dysregulation of cell functions including proliferation and migration by altering key signaling pathway activities, a prominent example being amplified and sustained activity of ERK. Because of the intimately coupled nature of trafficking and signaling in HER2/EGFR heterodimers, however, the relative contributions of direct HER2 action (its signaling *per se*) and HER2 indirect action (modulation of EGFR trafficking and its consequent signaling) to cell dysregulation – or even more specifically to ERK signaling alterations – are unclear. In order to deconvolute these direct and indirect actions of HER2 on its particular enhancement of ERK activity, we employ a computational model of EGFR and HER2 trafficking validated by quantitative experiment for human mammary epithelial cells expressing HER2 over a range of levels. We find that, in contrast to previous suggestions in the literature, HER2 and EGFR are essentially equivalent in their intrinsic quantitative ability to activate the ERK pathway. Transient amplification of ERK activity by HER2 arises simply from the 2-to-1 stoichiometry of receptor kinase to ligand in HER2/EGFR heterodimers compared to the 1-to-1 stoichiometry in EGFR/EGFR

homodimers. Sustained ERK activity arises almost exclusively from increased EGFR levels due to the HER2-mediate reduction in EGFR down-regulation.

5.1 Introduction

HER2 is commonly thought of as the problem child of the EGFR family. HER2's affinity for dimerization is on the same order as that of EGFR, although HER2 over expression frequently gives it the appearance of being a preferred dimerization partner relative to other family members (Hendriks et al. 2003b (Chapter 3)). Furthermore, it is generally believed that HER2 has an enhanced signaling capacity relative to other family members, such that HER2 containing heterodimers are particularly potent and efficient transducers of signals to the nucleus (Graus-Porta et al., 1995; Karunagaran et al., 1996; Lenferink et al., 1998; Pinkas-Kramarski et al., 1996; Tzahar et al., 1996). The degree to which this belief is correct in the context of various signaling and trafficking phenomena will be quantitatively examined in this work.

The downstream effect of HER2 overexpression on signaling appears to be two-fold: [a] enhanced cellular sensitivity to growth factor stimulation due to signal amplification via the recruitment of additional signaling molecules (Alroy and Yarden, 1997; Fazioli et al., 1991; Janes et al., 1994; Muthuswamy and Muller, 1995; Ricci et al., 1995); and [b] diminished negative regulatory mechanisms involved in signal attenuation, resulting in prolonged signal duration (Karunagaran et al., 1996; Worthylake et al., 1999).

The overall effect of elevated HER2 expression on EGF signaling can be conceptually divided into two parts: the first is a signaling effect wherein heterodimerization allows the activation of two receptors per one ligand molecule and the second is a trafficking effect, wherein elevated HER2 expression augments the normal trafficking and down-regulation of the EGFR. The signaling effect of HER2 overexpression manifests itself as an increase in signal amplitude whereas the trafficking effect operates at longer timescales resulting in an increase in signal duration. These qualitative characteristics have been seen in ERK, p70/p85^{S6K}, and JNK activation data in response to EGF stimulation (Graus-Porta et al., 1995; Karunagaran et al., 1996). The trafficking and signaling of EGFR and HER2 are intimately linked through their dependence on dimerization and receptor expression levels. Consequently, they cannot easily be separated experimentally and necessitate computational methodologies for their analysis

In this work we quantitatively examine the ERK signaling ability of EGFR and HER2. We have developed a comprehensive mathematical model of EGFR and HER2 trafficking capable of making predictions of various homo- and heterodimers in response to EGF stimulation. By correlating the quantities of activated receptors with experimental ERK signaling data, we are able to tease apart the effects of elevated HER2 expression on EGFR signaling and trafficking and determine the relative signaling abilities of each receptor. We find that EGFR and HER2 do not differ significantly in their intrinsic ERK signaling ability. Furthermore, we are able to successfully predict ERK signaling for a cell line with intermediate HER2 expression as well as predict the EGFR portion of the

ERK signal for a high HER2-expressing cell line as validated with heterodimerization blocking mAb 2C4. Overall, this suggests that effects at the level of trafficking and receptor-receptor interactions are sufficient to explain HER2-mediated differences in ERK signal that are commonly interpreted as 'signal potentiation.'

5.2 Experimental Methods

5.2.1 Reagents/Cell Culture

184A1 human mammary epithelial cells with varying levels of HER2 expression, as described previously, were maintained in DFCI-1 medium supplemented with 12.5 ng/ml EGF (Band and Sager, 1989; Hendriks et al., 2003a (Chapter 2)). Prior to experiments, cells were quiesced overnight in DFCI-1 medium without EGF, bovine pituitary extract, or fetal bovine serum and supplemented with 1 mg/ml bovine serum albumin. Experiments with mAb 2C4 were pre-treated with 10 mg/ml 2C4 for 4 hrs prior to human EGF treatment.

5.2.2 Lysate Preparation

Following appropriate EGF treatment, cells were washed with cold PBS and lysed in cold lysis buffer containing 50 mM Tris, pH 7.5, 150 mM sodium chloride, 50 mM □-glycerophosphate, pH 7.3, 10 mM sodium pyrophosphate, 30 mM sodium fluoride, 1% Triton X-100, 1 mM benzamidine, 2 mM EGTA, 100 □M sodium orthovanadate, 1 mM DTT, 10 □g/ml aprotinin, 10 □g/ml leupeptin, 1 □g/ml pepstatin and 1 mM PMSF. Cells were scraped into lysis buffer, allowed to lyse for 10 minutes, and centrifuged at

16,000□*g* to clear insoluble debris. Protein concentration was adjusted to 1 □g/ml as determined using the micro BCA protein determination kit (Pierce).

5.2.3 ERK Activity Assay

ERK kinase activity was measured using an *in vitro* assay in 96-well format, as described previously (Asthagiri et al., 1999a), with slight modification. Briefly, protein-A coated wells (Pierce) were coated with #06-182 anti-ERK1/2 antibody (Upstate). Following washing, 50 □g of cell lysate were incubated for 3 hrs at 4°C. Wells are washed and re-suspended in kinase assay buffer (20 mM Tris (pH 7.5), 15 mM magnesium chloride, 5 mM □-glycerophosphate (pH 7.3), 1 mM EGTA, 0.2 mM sodium orthovanadate, 0.2 mM DTT, 0.4 □M protein kinase A inhibitor peptide (Upstate Biotech), 4 □M protein kinase C inhibitor peptide (Upstate Biotech), 4 □M calmidazolium (Upstate Biotech)). The *in vitro* reaction is initiated by the addition of 25 □M ATP (1 □Ci[□-^{32}P]dATP] and 40 □g of myelin basic protein. After 1 hr incubation at 37°C with agitation, reactions were quenched with 75 mM phosphoric acid and contents filtered through a 96-well phosphocellulose filter plate (Millipore). Following washing 5x with 75 mM phosphoric acid and 3x with 70% ethanol, ^{32}P on each filter was quantified and corrected for background radioactivity.

5.3 Model Development

5.3.1 Trafficking Model Integration

The complete receptor trafficking model is a composite of the global trafficking model and receptor interaction module presented previously (Hendriks et al., 2003a (Chapter 2); Hendriks et al., 2003b (Chapter 3)). The global trafficking models (equations shown in Appendix 5.1) for EGFR and HER2 are solved at steady state in the absence of EGF stimulation to determine the initial distribution of receptors. Receptor synthesis rates are fit to match reported values of surface EGFR and surface HER2 per cell (Hendriks et al., 2003a (Chapter 2)). Once the initial receptor distributions are determined, the global model equations are solved transiently over a 2 hr timecourse in response to appropriate EGF stimulation. At each timepoint, the total EGF, EGFR and HER2 in each compartment are calculated. These values serve as inputs into a quasi-steady receptor interaction module (equations shown in Appendix 5.A.2), which is used to estimate the quantity of each possible receptor species – including EGF-EGFR homodimers and EGF-EGFR/HER2 heterodimers – in the surface and internal compartments. The receptor interaction module consists of kinetic equations describing every possible binary EGFR-HER2 interaction with and without EGF. Assuming a conservation of mass over the timescale of receptor-receptor interaction – that is, there is no significant gain or loss of receptors or ligand to trafficking – these reactions can be assumed to be at pseudo-steady state, and their solution is readily obtained. All necessary parameter values governing

EGFR and HER2 interactions are found in the literature (Hendriks et al., 2003a (Chapter 2); Hendriks et al., 2003b (Chapter 3)).

5.3.2 Model Implementation

We hypothesize that the total ERK signal generated is the linear combination of the total number signaling receptors multiplied by their respective ERK signaling abilities (see equations (1) & (2), above). The total (surface + inside) number of signaling receptors are determined at each timepoint from the trafficking model for the desired level of HER2 expression. Equations (1) & (2) are written for both the low (parental) and high (clone 24H) HER2 expressing cell lines, with the ERK signal having been experimentally measured (see Figure 5.3). Solving these systems of equations at each timepoint yields the signal generated on a per receptor basis as a function of time. The error bars on these calculations represent the propagation of the standard deviation of ERK signal measurements through the calculations, and do not reflect any error in the trafficking model predictions. The signal generated by only EGFR (or HER2) is generated by determining the number of active EGFR (or HER2) from the trafficking model and multiplying it by the signal generated per EGFR (or HER2) at each timepoint.

5.3.3 Model Validation

For model validation, ERK signal predictions are made for an intermediate level of HER2 expression (2×10^5 /cell) using trafficking model predictions of receptor quantities and the values of α and β calculated from the parental and clone 24H cell lines. Validation of signal parsing is done by comparison of EGFR only signaling with mAb

2C4 experimental data. For clone 24H prediction, adjustment needs to be made for the inaccuracy of the trafficking model in response to 2C4 treatment. From the literature, blocking heterodimerization with mAb 2C4 does not quite return the behavior of clone 24H to that of the parental cell line, most likely due to clonal differences between the two cell lines. Experimental measurements of EGFR down-regulation show that clone 24H following mAb 2C4 pretreatment is off by a factor of 1.34 from mimicking the behavior of the parental cell line (Hendriks et al., 2003a (Chapter 2)). This correction factor is incorporated into model predictions of ERK signal following mAb 2C4 pretreatment by multiplying trafficking model predictions of receptor number by 1.34.

In order to use the trafficking model to make predictions for the 1 ng/ml EGF case, adjustments need to be made to the internalization rates used in the global trafficking model (Hendriks et al., 2003a (Chapter 2)). These internalization rates for EGFR and HER2 are predicted from the internalization model for the parental and clone 24H cell lines (Hendriks et al., 2003b (Chapter 3)). HER2 internalization rates are predicted to be 0.038 and 0.030 min^{-1} and EGF-EGFR complexes internalization rates are predicted to be 0.174 and 0.115 min^{-1} for the parental and clone 24H cell lines, respectively.

To test different signal strengths for HER2 – the EGFR signal strength was set to the average of the calculated values of α and β for each timepiont, in order to smooth out the predicted timecourse. The HER2 signal strength was set to multiples of this average value.

5.3.4 Computations

Model solutions and manipulation are done using MATLAB version 6.5. Matlab code can be found in Appendix A.4.

5.4 Results

In order to separate the signaling and trafficking effects of HER2 on EGFR signaling we first needed to build a quantitative model of receptor location and dimerization as a function of time. Using this model, we could then associate a signal output from each receptor type at each corresponding time. Calculated estimates of the number of actively signaling receptors were compared with experimental signaling measurements to back-calculate the individual signal contributions of EGFR and HER2. This deconvolution of signaling can be considered as three processes: (i) signaling data collection, (ii) trafficking model development, and (iii) model/data correlation analysis.

For our analysis we have examined a downstream signal activated by both EGFR and HER2, namely ERK activity. ERK activity is an important determinant of cell proliferation and thereby a reasonable metric by which to gauge the increased signaling brought about by elevated HER2 expression in the context of tumor progression. For our signaling experiments, we used human mammary epithelial cells with varying levels of HER2 expression that have also been used to develop the trafficking model. Each cell line has roughly 2×10^5 surface EGFR per cell and surface HER2 expression of 3×10^4, 2×10^5 and 6×10^5 per cell for the parental, clone 12 and clone 24H cell lines (Hendriks et al., 2003a (Chapter 2); Hendriks et al., 2003b (Chapter 3)).

We measured ERK activity in response to 100 ng/ml (16nM) EGF stimulation in each cell line with an *in vitro* kinase assay over a 2 hr timecourse (Figure 5.1a and 5.1b). At early timepoints there is an increase in signal amplitude with increasing HER2 expression, corresponding to an increased number of actively signaling receptors. At longer timescales, signal duration increased with increasing HER2 expression, corresponding to the inhibition of receptor down-regulation as a consequence of elevated HER2 expression. Using a lower EGF concentration of 1 ng/ml we found little difference in ERK activity, with clone 24H being marginally higher at longer timepoints (Figure 5.1c).

To probe the role of heterodimerization in ERK activity we repeated the 100 ng/ml EGF experiment following pre-incubation with mAb 2C4, an antibody that has been shown to bind to HER2 and block heterodimeration (Agus et al., 2002; Fendly et al., 1990) (Figure 5.1a and 5.1b). This pharmacological decoupling of HER2 from the EGFR was able to reverse most of the effects of elevated HER2 expression on ERK activity, both in terms of peak levels and prolongation of signaling.

The signaling data was analyzed by correlation with the number of actively signaling receptors, as estimated from the dynamic receptor trafficking model. The full model was derived from the hierarchical combination of previously published models of EGFR and HER2 trafficking (Hendriks et al., 2003a (Chapter 2); Hendriks et al., 2003b (Chapter 3)). The global trafficking models previously published for EGFR and HER2 contain a defined parameter set that have been experimentally validated (Hendriks et al., 2003a (Chapter 2)). These models make *a priori* predictions of empty EGFR, EGF-EGFR

complexes and total HER2 for surface and internal compartments. Their corresponding equations can be solved transiently (as opposed to in the steady state) to give dynamic predictions of these quantities. However, this model does not give any explicit information about the dimerization state of EGFR, or HER2, a required component for the resolution of signaling data.

The timescale for receptor-receptor interactions (<0.1 min) is much faster than the timescale for receptor trafficking (on the order of 10 min). As such, it can be safely assumed that EGFR-HER2 dimerization reaches a quasi-steady state in each compartment prior to a significant change in receptor number attributable to receptor trafficking. Thus, with the knowledge of the total EGF, EGFR and HER2 in each compartment at each timepoint, one can assume a quasi-steady state and determine the distribution of all EGFR-HER2 containing species (Figure 5.2). The kinetic rate constants for these interactions have been estimated in previous work (Hendriks et al., 2003a (Chapter 2); Hendriks et al.2003b (Chapter 3)). Making quasi-steady predictions at each timepoint within an experimentally validated model prevents the propagation of error from any erroneous prediction of dimerization (Hendriks et al., 2003b (Chapter 3)).

Dimerization is the initial event in receptor activation that drives phosphorylation of EGFR complexes as well as HER2. Once phosphorylated, these receptors are able to recruit intracellular signaling molecules, including components of the ERK signaling cascade (Alroy and Yarden, 1997). At the molecular level, the proximal signaling species are EGF-EGFR homodimers and EGF-EGFR/HER2 heterodimers. Using our trafficking model, we can predict the time-dependent profile of the formation of these species as a

function of different levels of EGF stimulation. Shown in Figure 5.3 are predictions of the number of intracellular and surface-localized EGF-EGFR homodimers and EGF-EGFR/HER2 heterodimers for HER2 expression levels corresponding to the parental (3×10^4 HER2/cell) and clone 24H (6×10^5 HER2/cell) cell lines following either 1 and 100 ng/ml EGF stimulation. Similarly, a set of predictions can be made for the total number of actively signaling EGFR and HER2 found in either homo- or heterodimers (Figure 5.4). Note that the active EGFR are distributed between both heterodimers and homodimers whereas EGF-activated HER2 are only found in heterodimers. Signaling due to HER2homodimers will be present in roughly comparable quantities in the presence and absence of EGF stimulation. As such, HER2 homodimer signaling is experimentally observed as part of the background signal and thus can be neglected by our analysis.

To calculate the relative contribution of EGFR and HER2 to overall ERK signaling, we assign the activity coefficients α and β to each ligand-bound EGFR and activated HER2 (i.e. in a heterodimer with an activated EGFR), respectively. The total ERK signal generated is taken to be the sum of the number of signaling species multiplied by their intrinsic ERK signaling ability:

$$(\text{EGFR})\alpha + (\text{HER2})\beta = \text{ERK Signal} \qquad (5.1)$$

Because the ERK pathway can be recruited by receptors both on the surface and within endosomal compartments (Glading et al., 2001; Haugh et al., 1999), the total number (inside + surface) of EGF-EGFR complexes and total number of actively

signaling HER2 are used for this analysis. This equation can be written for both the low (parental) and high (clone 24H) HER2 expressing cells (subscripts P and 24H, respectively) for each timepoint (subscript t):

$$(\text{EGFR complexes}_{P,t})\alpha_{P,t} + (\text{HER2}_{P,t})\beta_{P,t} = \text{ERK Signal}_{P,t} \quad (5.2)$$

$$(\text{EGFR complexes}_{24H,t})\alpha_{24H,t} + (\text{HER2}_{24H,t})\beta_{24H,t} = \text{ERK Signal}_{24H,t} \quad (5.3)$$

These equations are solved for the corresponding α and β in response to either 1 or 100 ng/ml EGF stimulation, based on the experimental ERK data and model predictions of the number EGFR complexes and actively signaling HER2, shown in Figure 5.5a and 5.5b. A similar set of equations can be written in terms of EGF-EGFR homodimers and EGF-EGFR/HER2 heterodimers, each with their own ERK signaling capacity (γ and δ, respectively):

$$(\text{homodimers}_{P,t})\gamma_{P,t} + (\text{heterodimers}_{P,t})\delta_{P,t} = \text{ERK Signal}_{P,t} \quad (5.4)$$

$$(\text{homodimers}_{P,t})\gamma_{24H,t} + (\text{heterodimers}_{24H,t})\delta_{24H,t} = \text{ERK Signal}_{24H,t} \quad (5.5)$$

By utilizing signaling data from two cell lines with different HER2 compositions, we were able to back-calculate the relative signaling abilities of EGFR and HER2. Solutions to this equation are shown in Figure 5.5c and 5.5d. If HER2 has an enhanced ERK signaling ability relative to that of EGFR, as suggested in the literature, then β should be larger than α, and δ should be larger than γ. However, the calculations show

that there is no significant difference in the ERK signal generated by EGFR and HER2 or homodimers and heterodimers for either EGF concentration.

The signal generated per homodimer is twice the signal per EGF-EGFR complex for the 100 ng/ml case (i.e. 5.5c is twice the magnitude of 5.5a). However, for 1 ng/ml EGF stimulation this is not the case at the early timepoints. This result arises from differences in bookkeeping and can be explained as follows. For a given ligand stimulation, the number of actively signaling EGFR in clone 24H will always be greater than or equal to that of the parental cell line. If both of these cell lines produce an equal ERK response, or one where the high HER2 expressing ERK signal is less than that of the low HER2 expressing ERK signal (as seen in Figure 5.1c, 5 min time point) then the signal per HER2 must be close to zero. If one counts homodimers versus heterodimers, then the heterodimers signal will be virtually zero. However, if the heterodimer signal is zero, it implies that the EGFR within heterodimers are not signaling (this implication is not made when counting active EGFR and HER2) and thus, there are fewer number of EGFR that are presumed to be signaling relative to the case where one tallies individual active receptors. Consequently, twice the EGFR signal will be less than the homodimer signal when the cell lines produce equal ERK signals.

Because we can calculate the signal generated per receptor at each interval, it is possible to determine the fraction of the total signal that is generated by the EGFR versus HER2 molecules, shown in Figure 5.6a. As shown in Figure 5.6b, we found that HER2 generates only 10% of the total signal in the parental cell line, while generating 40% of

the total signal in clone 24H. Thus, at an expression level of 6×10^5 per cell, HER2 has 80% of a theoretical maximal effect on ERK signal.

For our analysis, we have related events at the level of receptor interactions and trafficking to the downstream signaling event of ERK activation, leaving out the precise mechanisms of signal transduction. This approach is valid as long as our defined relationships do not change as a function of secondary parameters, such as cell type or receptor expression levels. To explore the validity of this assumption, we have used our trafficking model and calculated values for α and β to predict the ERK signal for a cell type expressing an intermediate level of HER2 (clone 12 – 2×10^5 HER2 per cell). The model prediction and experimental data in response to 100 ng/ml EGF stimulation show excellent agreement (Figure 5.7a) suggesting that our model is robust, at least for mammary epithelial cells.

As a further test of the usefulness of our model, we sought to predict the effect of blocking EGFR-HER2 heterodimerization on ERK activity. Following pretreatment with mAb 2C4 we should only observe signaling through the EGFR, since 2C4 blocks HER2 activation (Agus et al., 2002). We compared the EGFR portion of the original ERK signal (from Figure 5.6a) to the 2C4 data (from Figure 5.3c), making adjustments for some alterations in receptor trafficking observed the presence of 2C4 (Hendriks et al., 2003a (Chapter 2)). As shown in Figure 5.7b,the predicted time profile and magnitude of ERK activity agrees quite well with the experimental data.

Finally, we explicitly tested the sensitivity of our model to different levels of HER2 versus EGFR activity. In Figure 5.8, predictions of the clone 24H ERK signal are

made for three different cases: □=2□□, □=□, and □=0.5□□. Even a modest two fold increase in predicted HER2 versus EGFR activity results in a dramatic overestimation of overall ERK signal levels. We conclude that the EGFR and HER2 are essentially identical in their ability to generate signals through the ERK pathway.

5.5 Discussion

The complex set of EGF, EGFR and HER2 interactions offers great potential for the generation and regulation of cellular signals. Complexity resides at many levels and timescales including, but not limited to, a combinatorial set of inputs through various dimerization possibilities, receptor or dimer-specific trafficking behavior, and possible differences in signaling activities generated by each receptor. In the face of such complexity it is extremely difficult to intuitively estimate the impact of changes in molecular parameters, such as HER2 expression, on cell signaling and cell behavior. The combined application of quantitative experimental and computational techniques allowed us to unravel some of this complexity and gain insight into how elevated HER2 expression affects the dynamics of the system as a whole.

In this work we have adopted an integrative modeling approach enabling us to relate upstream events at the level of ligand binding and receptor interaction to downstream signal activation. This is distinct from previously published models of ERK signaling that incorporate each molecular interaction involved in ERK activation (Asthagiri et al., 1999b; Ferrell, 1996; Heinrich et al., 2002; Kholodenko, 2002; Schoeberl et al., 2002). This is also the first modeling attempt to incorporate the effects of

both trafficking and HER2 expression level effects into the analysis of ERK signaling. By considering different timescales we are able to separate the effect of dimerization and trafficking events. This yielded an extensive trafficking model that provided detailed predictions of receptor dimerization state while remaining constrained by a defined and experimentally validated trafficking model.

From the prediction from the trafficking model, it is clear that EGF concentration plays an important role in determining the relative distribution between homo- and heterodimers (see Figure 5.3c and5.3d). When EGF concentration is low, the number of EGF-EGFR complexes is small. Thus, even cells that express relatively high levels of HER2 cannot form a significant number of heterodimers. Consequently, at low EGF concentrations the parental and clone 24H have little functional difference in their receptor trafficking (see Figure 5.3) and this is borne out in their similar ERK responses (see Figure 5.1). Thus, when ambient ligand concentrations are quite low, elevating HER2 expression above a basal level would have little effect on ligand-dependent ERK signal amplitude. There is likely to be a threshold of HER2 expression that depends on ligand concentration and above which HER2 levels have little effect on heterodimerization and signal generation. Autocrine production of ligand in both normal and pathological conditions could amplify the effect of HER2 overexpression by increasing local ligand concentrations.

Relating receptor dimerization state with ERK activity allows us to construct a model in which the individual molecular steps do not have to be described explicitly. This assumes that receptor kinase activation is the rate-limiting step in ERK activation

(Wiley et al., 2003). Although most of the steps in the ERK cascade appear to be well understood, this relatively high-level approach to linking receptor dynamics to signaling cascades should be especially useful in understanding systems where the details are less well understood or completely undefined. We are implicitly assuming a rapid transfer of information from ligand binding to ERK activation. Other published works (Kholodenko et al., 1999; Schoeberl et al., 2002) support the notion that this transfer is quite fast and on the order of 1 minute.

The signal level generated by both EGFR and HER2 show an initial increase followed by a slow declineClearly, the most potent signals are generated within in the first 5 minutes following ligand addition.The decline in signal per receptor past the 5 minute time probably reflects negative feedback and adaptation (desensitization) within the signaling network (Asthagiri and Lauffenburger, 2001). Since degradation of receptors is accounted for in the trafficking model, any decrease in signal on a per receptor basis represents a loss of activity at the level of the individual receptors. For cells activated by 1 and 100 ng/ml EGF, the signal per receptor had a decay constant of about 50 and 200 min, respectively. Additionally, the 1 ng/ml EGF data, yielded a significantly higher signal per receptor (>10 fold) suggesting that the ERK signaling cascade was saturated at the higher ligand concentration. Nevertheless, EGFR and HER2 signaling through ERK remained equivalent on a per-receptor basis.

The finding that EGFR and HER2 have equal activity in stimulating ERK signaling is consistent with the known high degree of sequence similarity between EGFR and HER2 cytoplasmic domains (Earp et al., 1995) and the experimental findings that

once initiated by different receptors the ERK pathway appear to procede independent of the specific receptor. The nature of the signaling output appears to be determined primarily by the dynamics of the molecular interactions and less by the precise magnitudes of individual interaction parameters. This principle has been especially apparent in the study of EGFR and HER2 trafficking (Hendriks et al., 2003b (Chapter 3); Hendriks et al., 2003c (Chapter 4)).

The excellent agreement between the predicted and actual dynamics of ERK signaling in cells expressing varying numbers of HER2 shows the power inherent in our systematic and quantitative approach to dissecting receptor signaling pathways. The apparent complexity of the EGFR-HER2 system obscures the relatively simple principles that govern it. Namely, EGFR and HER2 are equivalent in stimulating the ERK pathway. The EGFR is internalized faster than HER2, but heterodimers are internalized at an intermediate rate. HER2 interferes with lysosomal targeting of the EGFR. Homodimerization between EGFRs occurs with equal or higher affinity as heterodimerization with HER2 (Hendriks et al., 2003b (Chapter 3)). Each of these properties is quantifiable and contributes to the overall system behavior. We note that several of these observations are in direct opposition to previous reports in the literature, highlighting the difficulties in understanding a complex system in the absence of an adequate model. However, understanding the mechanisms responsible for HER2-enhanced signaling is required for designing more effective treatments for cancers in which HER2 overexpression contributes to disease progression. The modeling approach

we describe here should be particularly valuable in efforts to identify targets for therapeutic interventions.

5.6 Figures

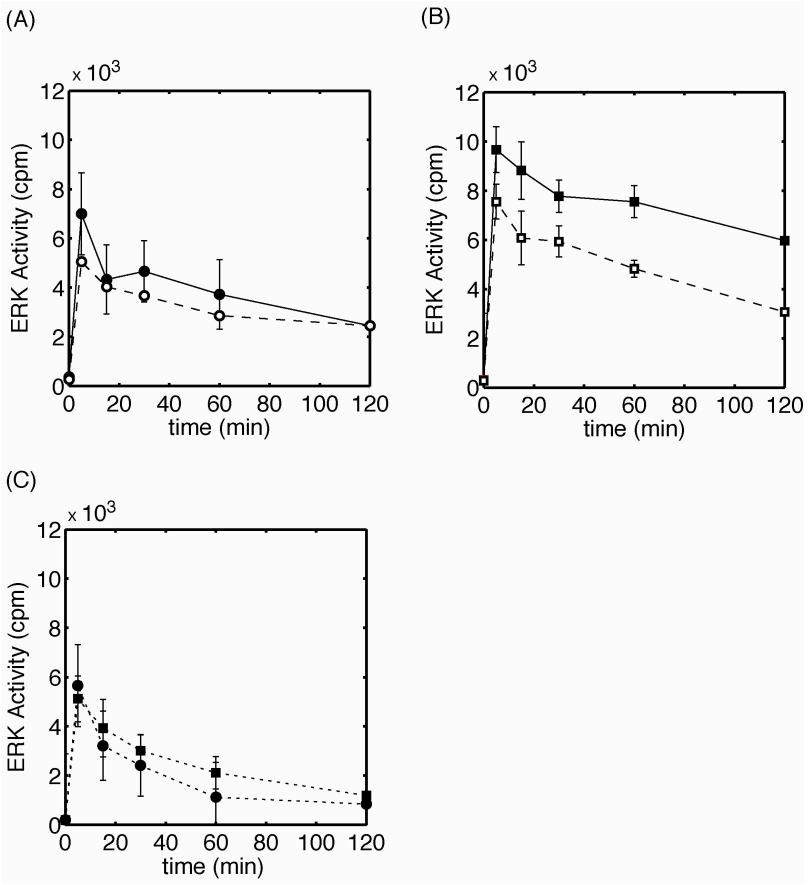

Figure 5.1 ERK Activity Data.

Timecourse of ERK activity in response to sustained EGF stimulation as determined using an *in vitro* kinase assay. *A*, 100 ng/ml EGF stimulation for parental (circles) cell line with (open symbols) and without (filled symbols) pretreatment with heterodimerization blocking mAb 2C4. *B*, 100 ng/ml EGF stimulation for clone 24H (squares) cell line with (open symbols) and without (filled symbols) mAb 2C4. C, ERK activity in response to 1 ng/ml EGF stimulation for parental (circles) and clone 24H (squares) cell lines.

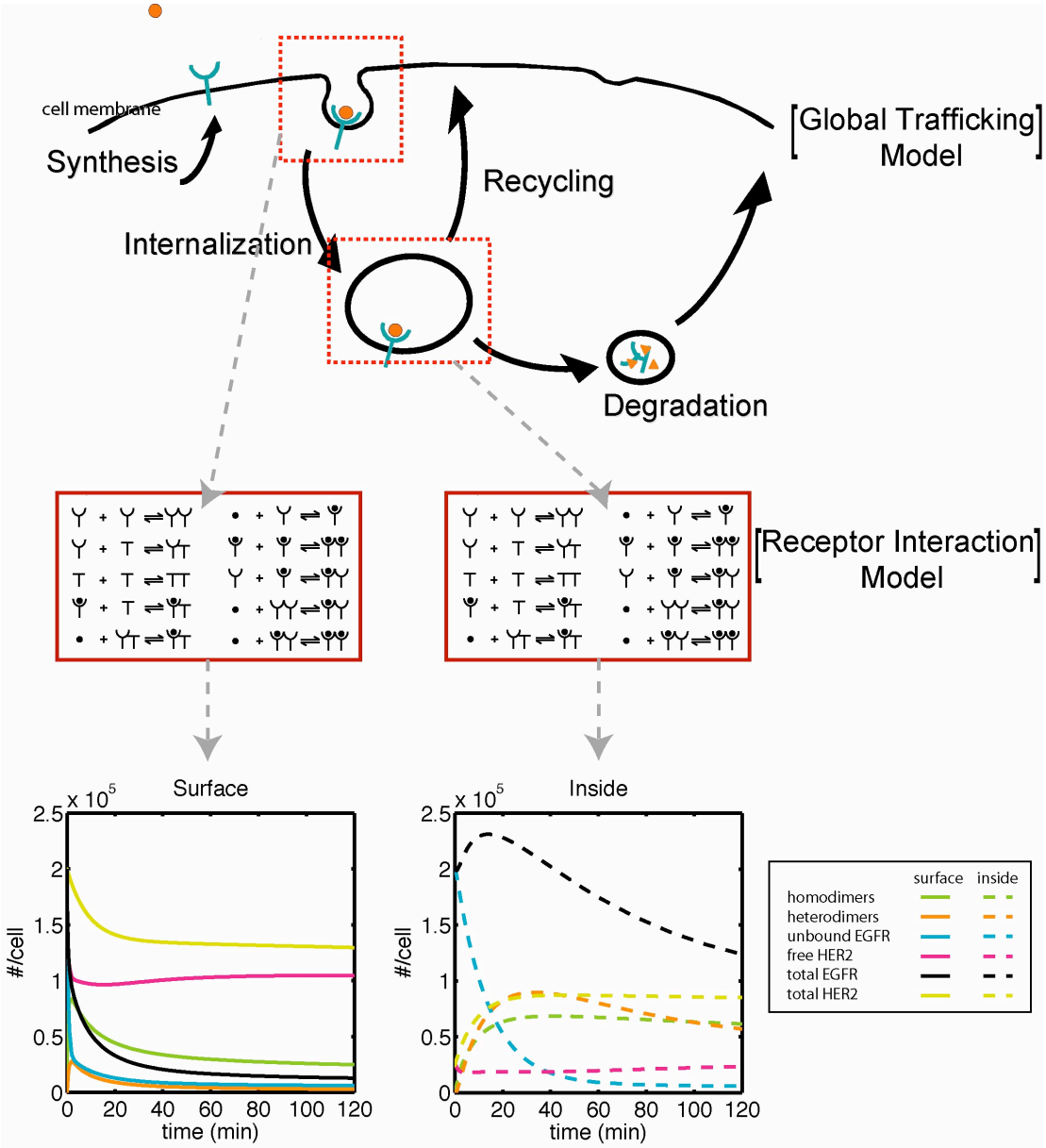

Figure 5.2 Model Integration.

The global trafficking model (upper panel) developed in Hendriks, et al., 2003a (Chapter 2) is solved transiently yielding predictions for surface and intracellular amounts of the total EGFR, unoccupied EGFR and total HER2 in response to EGF stimulation. This model gives no explicit information about dimerization state. At each time point, these

quantities are input into a quasi-steady receptor interaction module (middle panels), developed in Hendriks et al., 2003b (Chapter 3) to determine the entire distribution of each binary receptor species, including the number of homo- and heterodimers (lower panels).

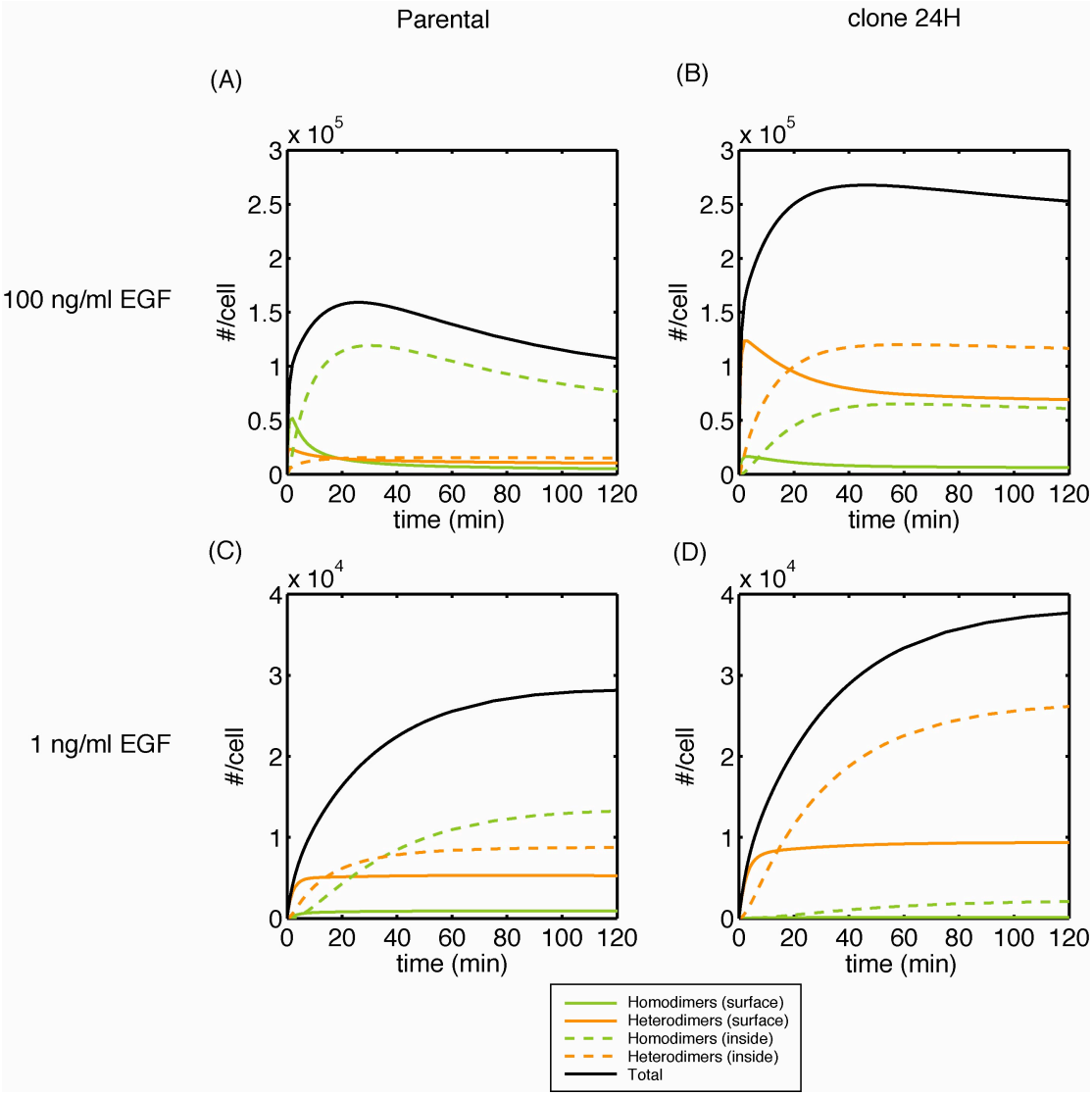

Figure 5.3 Actively Signaling Homo- and Heterodimers.

The complete trafficking model is used to predict the total quantity of EGF-EGFR homodimers and EGF-EGFR/HER2 heterodimers as a function of time for the low and high HER2 case, corresponding to the parental (panels *A* and *C*) and clone 24H (panels *B* and *D*) cell lines, respectively. Predictions are shown for 100 ng/ml EGF stimulation

(panels *A* and *B*) and 1 ng/ml EGF stimulation (panels *C* and *D*). Note the different y-axis scale on *A* and *B* versus *C* and *D*. Surface homodimers, surface heterodimers, intracellular homodimers, intracellular heterodimers and the total number of receptor dimers are marked with solid green, solid orange, dashed green, dashed orange lines and solid black, respectively.

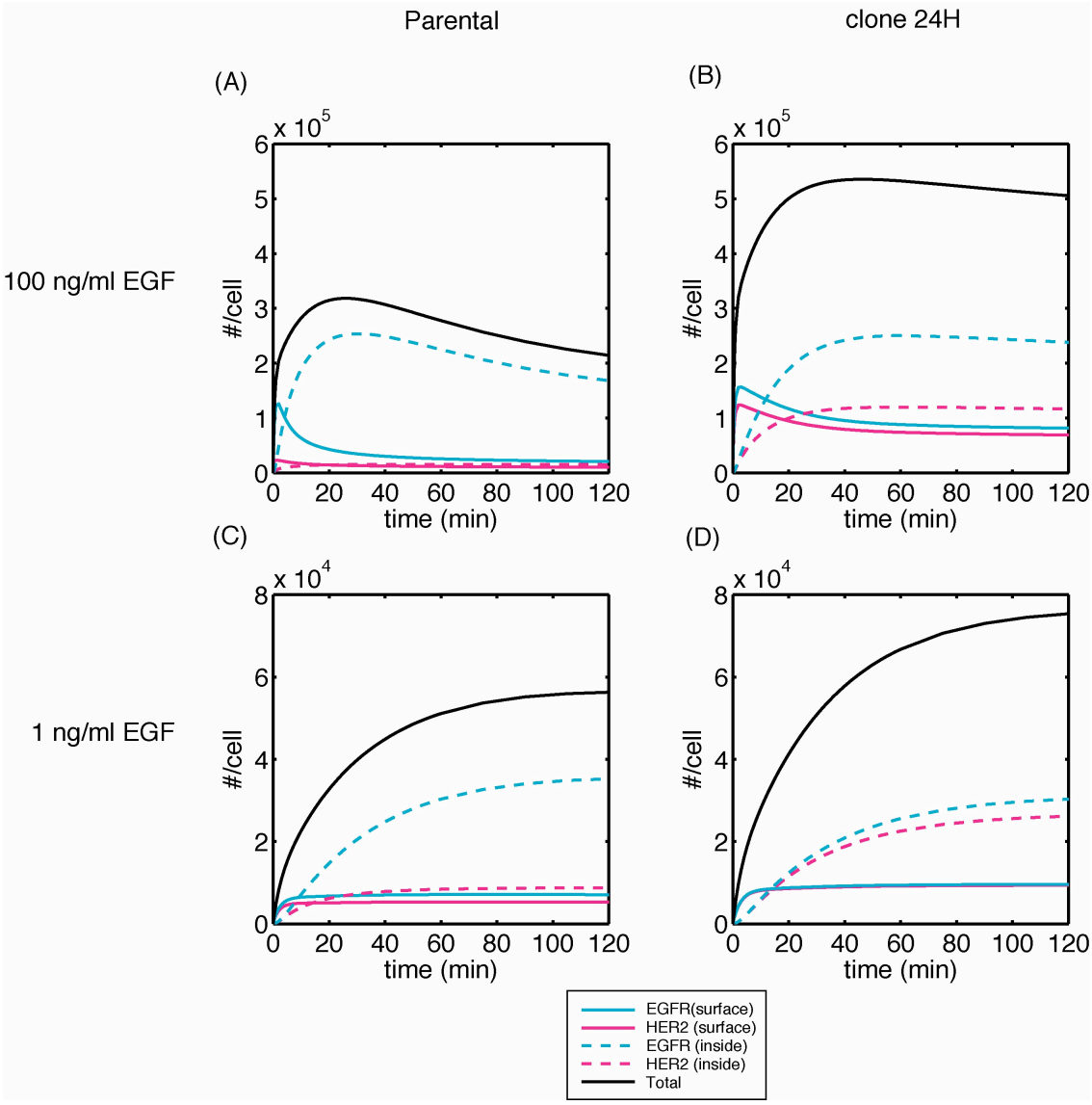

Figure 5.4 Actively Signaling Receptors.

The complete trafficking model is used to predict the total quantity of actively signaling EGFR and HER2 as a function of time for the low and high HER2 case, corresponding to the parental (panels *A* and *C*) and clone 24H (panels *B* and *D*) cell lines, respectively. For one EGF-EGFR homodimer, we assume 2 actively signaling EGFR. For one EGF-EGFR/HER2 heterodimer, we assume 1 actively signaling EGFR and 1 actively signaling

HER2. Predictions are shown for 100 ng/ml EGF stimulation (panels *A* and *B*) and 1 ng/ml EGF stimulation (panels *C* and *D*). Note the different y-axis scale on *A* and *B* versus *C* and *D*. Surface EGFR, surface HER2, intracellular EGFR, intracellular HER2 and the total number of receptors are marked with solid blue, solid magenta, dashed blue, dashed magenta and solid black lines, respectively.

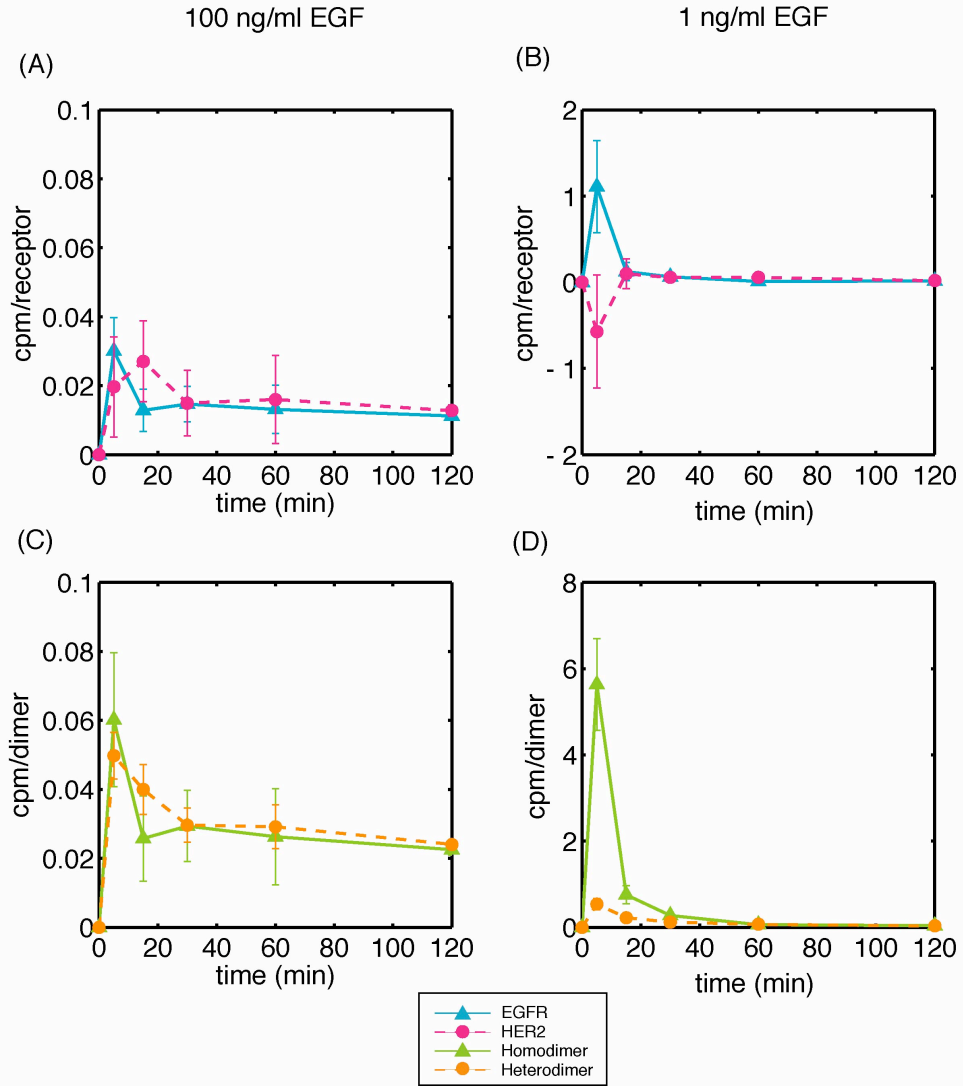

Figure 5.5 Signal per Receptor or Dimer.

Equations (2 and 3) or (3 and 4) are solved to calculate the net ERK signal generated per each EGFR (blue triangles) and HER2 (red circles) molecule as a function of time. *A*, signal per receptor for 100 ng/ml EGF stimulation and *B*, 1 ng/ml EGF. Also shown is the net ERK signal generated per homodimer complex (green triangles) or heterodimer complex (orange circles) in response to *C*, 100 ng/ml EGF and *D*, 1 ng/ml.

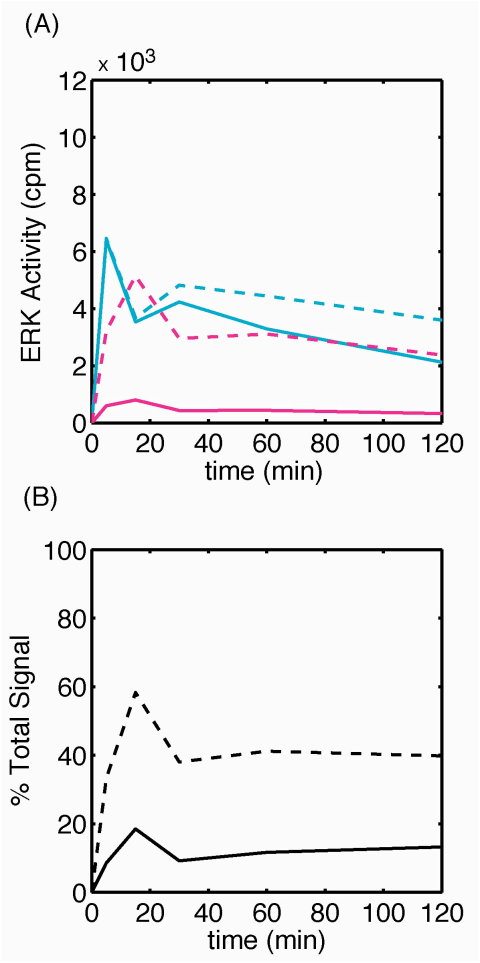

Figure 5.6 Signal Parsing.

A, the model was used to calculate the contribution of each receptor species to overall ERK activity at each timepoint. Shown is the calculated amount the total ERK signal that is generated by EGFR (solid and dashed blue lines for the parental and clone 24H cell lines, respectively) and HER2 (solid and dashed magenta lines, for the parental and clone 24H cell lines, respectively). *B*, the data shown in 6A was used to calculate the percentage of the total signal generated by HER2 (solid and dashed lines correspond to the parental and clone 24H cell lines, respectively).

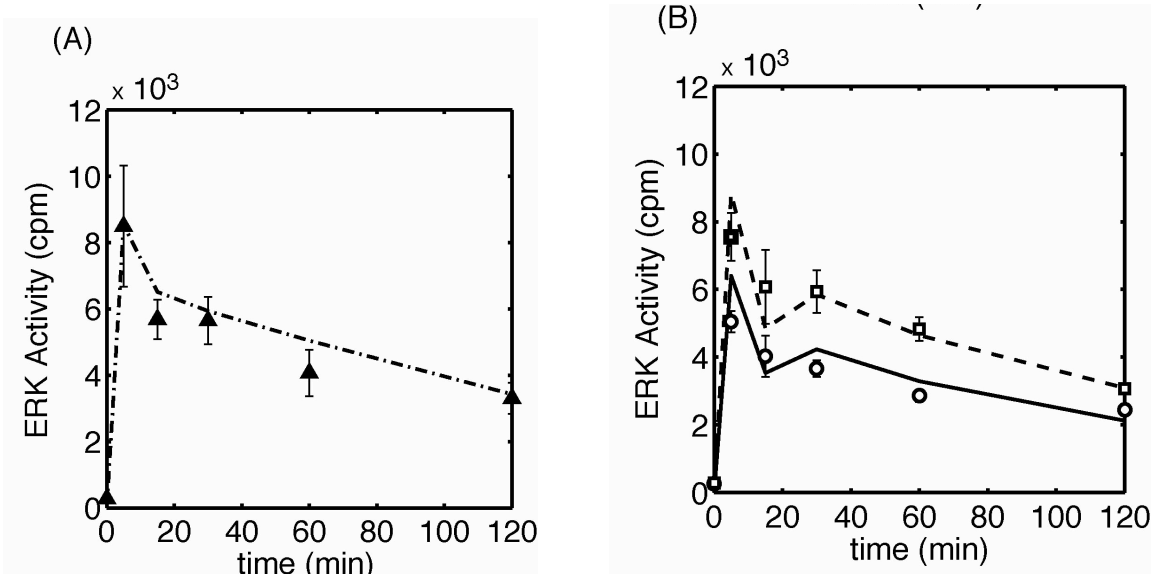

Figure 5.7 Model Validation.

A, the trafficking model and signal generated per receptor are used to predict the ERK signal generated by a cell line with an intermediate HER2 expression level – 2×10^5 surface HER2/cell – corresponding to clone 12. Model prediction (dash-dotted line) is shown in comparison with experimental ERK data (triangles) in response to 100 ng/ml EGF stimulation. *B*, predicted versus experimental results of blocking heterodimerization. Receptor heterodimerization was blocked using mAb 2C4 prior to measuring ERK activity (open circles and squares for the parental and clone 24H cell lines, respectively). These data are shown together with model predictions of ERK signaling through the EGFR exclusively following 100 ng/ml EGF addition (solid and dashed lines for the parental and clone 24H cell lines, respectively).

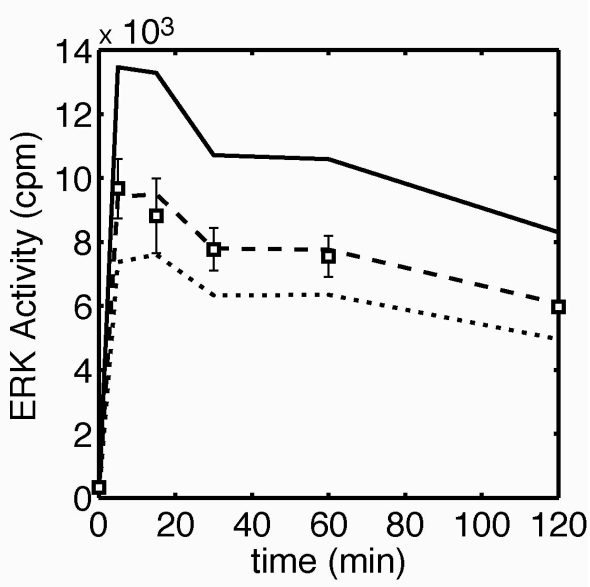

Figure 5.8 Model Test of Hypotheses.

Model predictions of ERK signal are shown for □ = 0.5□□, □ = □ and □ = 2□□ (dotted, dashed and solid lines, respectively) in comparison with experimental ERK activity data for clone 24H (squares) following 100 ng/ml EGF stimulation.

5.7 References

Agus, D.B., Akita, R.W., Fox, W.D., Lewis, G.D., Higgins, B., Pisacane, P.I., Lofgren, J.A., Tindell, C., Evans, D.P., Maiese, K., Scher, H.I. and Sliwkowski, M.X. (2002) Targeting ligand-activated ErbB2 signaling inhibits breast and prostate tumor growth. *Cancer Cell*, **2**, 127-137.

Alroy, I. and Yarden, Y. (1997) The ErbB signaling network in embryogenesis and oncogenesis: signal diversification through combinatorial ligand-receptor interactions. *Federation of European Biological Sciences Letters*, **410**, 83-86.

Asthagiri, A.R., Horwitz, A.F. and Lauffenburger, D.A. (1999a) A rapid and sensitive quantitative kinase activity assay using a convenient 96-well format. *Analytical Biochemistry*, **269**, 342-347.

Asthagiri, A.R. and Lauffenburger, D.A. (2001) A computational study of feedback effects on signal dynamics in a mitogen-activated protein kinase (MAPK) pathway model. *Biotechnology Progress*, **17**, 227-239.

Asthagiri, A.R., Nelson, C.M., Horwitz, A.F. and Lauffenburger, D.A. (1999b) Quantitative Relationship among Integrin-Ligand Binding, Adhesion, and Signaling via Focal Adhesion Kinase and Extracellular Signal-regulated Kinase 2. *The Journal of Biological Chemistry*, **274**, 27119-27127.

Band, V. and Sager, R. (1989) Distinctive traits of normal and tumor-derived human mammary epithelial cells expressed in a medium that supports long-term growth

of both cell types. *Proceedings of the National Academy of Sciences - USA*, **86**, 1249-1253.

Earp, H.S., Dawson, T.L., Li, X. and Yu, H. (1995) Heterodimerization and function interaction between EGF receptor family members: A new signaling paradigm with implications for breast cancer research. *Breast Cancer Research and Treatment*, **35**, 115-132.

Fazioli, F., Kim, U.-H., Rhee, S.G., Molloy, C.J., Segatto, O. and DiFiore, P.P. (1991) The erbB-2 Mitogenic Signaling Pathway: Tyrosine Phosphorylation of Phospholipase C-□and GTPase-Activating Protein Does Not Correlate with erbB-2 Mitogenic Potency. *Molecular and Cellular Biology*, **11**, 2040-2048.

Fendly, B.M., Winget, M., Hudziak, R.M., Lipari, M.T., Napier, M.A. and Ullrich, A. (1990) Characterization of Murine Monoclonal Antibodies Reactive to Either the Human Epidermal Growth Factor Receptor or HER2/neu Gene Product. *Cancer Research*, **50**, 1550-1558.

Ferrell, J.E. (1996) Tripping the switch fantastic: how a protein kinase cascade can convert graded inputs into switch-like outputs. *TIBS*, **21**, 460-466.

Glading, A., Uberall, F., Keyse, S.M., Lauffenburger, D.A. and Wells, A. (2001) Membrane Proximal ERK Signaling Is Required for M-calpain Activation Downstream of Epidermal Growth Factor Receptor Signaling. *The Journal of Biological Chemistry*, **276**, 23341-23348.

Graus-Porta, D., Beerli, R.R. and Hynes, N.E. (1995) Single-Chain Antibody-Mediated Intracellular Retention of ErbB-2 Impairs Neu Differentiation Factor and

Epidermal Growth Factor Signaling. *Molecular and Cellular Biology*, **15**, 1182-1191.

Haugh, J.M., Huang, A.C., Wiley, H.S., Wells, A. and Lauffenburger, D.A. (1999) Internalized Epidermal Growth Factor Receptors Participate in the Activation of p21ras in Fibroblasts. *The Journal of Biological Chemistry*, **274**, 34350-34360.

Heinrich, R., Neel, B.G. and Rapoport, T.A. (2002) Mathematicals Models of Protein Kinase Signal Transduction. *Molecular Cell*, **9**, 957-970.

Hendriks, B.S., Opresko, L.K., Wiley, H.S. and Lauffenburger, D.A. (2003a) Co-Regulation of EGFR/HER2 Levels and Locations: Quantitative Analysis of HER2 Overexpression Effects. *Cancer Research*, **63**, 1130-1137.

Hendriks, B.S., Opresko, L.K., Wiley, H.S. and Lauffenburger, D.A. (2003b) Quantitative Analysis of HER2-mediated Effects on HER2 and EGFR Enodcytosis: Distribution of Homo- and Hetero-dimers Depends on Relative HER2 Levels. *The Journal of Biological Chemistry*, **278**, 23343-23351.

Hendriks, B.S., Wiley, H.S. and Lauffenburger, D.A. (2003c) HER2-Mediated Effects on EGFR Endosomal Sorting: Analysis of Biophysical Mechanisms. *Biophysical Journal*, in press.

Janes, P.W., Daly, R.J., deFazio, A. and Sutherland, R.L. (1994) Activation of the Ras signaling pathway in human breast cancer cells overexpressing erbB-2. *Oncogene*, **9**, 3601-3608.

Karunagaran, D., Tzahar, E., Beerli, R.R., Chen, X., Graus-Porta, D., Ratzkin, B.J., Seger, R., Hynes, N.E. and Yarden, Y. (1996) ErbB-2 is a common auxiliary

subunit of NDF and EGF receptors: implications for breast cancer. *The European Molecular Biology Organization Journal*, **15**, 254-264.

Kholodenko, B.N. (2002) MAP kinase cascade signaling and endocytic trafficking: a marriage of convenience? *Trends in Cell Biology*, **12**, 173-177.

Kholodenko, B.N., Demin, O.V., Moehren, G. and Hoek, J.B. (1999) Quantification of Short Tern Signaling by the Epidermal Growth Factor Receptor. *The Journal of Biological Chemistry*, **274**, 30169-30181.

Lenferink, A.E.G., Pinkas-Kramarski, R., Poll, M.L.M.v.d., Vugt, M.J.H.v., Klapper, L.N., Tzahar, E., Waterman, H., Sela, M., Zoelen, E.J.J.v. and Yarden, Y. (1998) Differential endocytic routing of homo- and hetero-dimeric ErbB tyrosine kinases confers signaling superiority to receptor heterodimers. *The European Molecular Biology Organization Journal*, **17**, 3385-3397.

Muthuswamy, S. and Muller, W.J. (1995) Direct and specific interaction of c-Src with Neu is involved in signaling by the epidermal growth factor receptor. *Oncogene*, **11**, 271-279.

Pinkas-Kramarski, R., Soussan, L., Waterman, H., Levkowitz, G., Alroy, I., Klapper, L., Lavi, S., Seger, R., Ratzkin, B.J., Sela, M. and Yarden, Y. (1996) Diversification of Neu differentiation factor and epidermal growth factor signaling by combinatorial receptor interactions. *The European Molecular Biology Organization Journal*, **15**, 2452-2467.

Ricci, A., Lanfrancone, L., Chiari, R., Belardo, G., Petrica, C., Natali, P. and Pelicci, P. (1995) Analysis of protein-protein interactions involved in the ativation of the Shc/Grb-2 pathway by the ErbB-2 kinase. *Oncogene*, **11**, 1519-1529.

Schoeberl, B., Eichler-Jonsson, C., Gilles, E.D. and Muller, G. (2002) Computational modeling of the dynamics of the MAP kinase cascade activated by surface and internalized EGF receptors. *Nature Biotechnology*, **20**, 370-375.

Tzahar, E., Waterman, H., Chen, X., Levkowitz, G., Karunagaran, D., Lavi, S., Ratzkin, B.J. and Yarden, Y. (1996) A Hierarchical Network of Interreceptor Interactions Determines Signal Transduction by Neu Differentiation Factor/Neuregulin and Epidermal Growth Factor. *Molecular and Cellular Biology*, **16**, 5276-5287.

Wiley, H.S., Shvartsman, S.Y. and Lauffenburger, D.A. (2003) Computational modeling of the EGF-receptor system: a paradigm for systems biology. *Trends in Cell Biology*, **13**, 43-50.

Worthylake, R., Opresko, L.K. and Wiley, H.S. (1999) ErbB-2 Amplification Inhibits Down-regulation and Induces Constitutive Activation of Both ErbB-2 and Epidermal Growth Factor Receptors. *The Journal of Biological Chemistry*, **274**, 8865-8874.

5.A Appendix: Trafficking Model Equations

5.A.1 Global Model Equations.

$$\frac{dRs}{dt} = S_R - k_{on}RsL + k_{off}Cs - k_{er}Rs + k_{xr}f_{xr}Ri$$

$$\frac{dCs}{dt} = k_{on}RsL - k_{off}Cs - k_{ec}Cs + k_{xc}f_{xc}Ci$$

$$\frac{dHs}{dt} = S_H - k_{eh}Hs + k_{xh}f_{xh}Hi$$

$$\frac{dRi}{dt} = k_{er}Rs - k_{xr}f_{xr}Ri - k_{xr}(1 - f_{xr})Ri$$

$$\frac{dCi}{dt} = k_{ec}Cs - k_{xc}f_{xc}Ci - k_{xc}(1 - f_{xc})Ci$$

$$\frac{dHi}{dt} = k_{eh}Hs - k_{xh}f_{xh}Hi - k_{xh}(1 - f_{xh})Hi$$

glossary:
Rs – surface unoccupied EGFR
Cs – surface EGF-EGFR complexes
Hs – surface HER2
Ri – intracellular unoccupied EGFR
Ci – intracellular EGF-EGFR complexes
Hi – intracellular HER2
S_R – synthesis rate of EGFR
S_H – synthesis rate of HER2
k_{on} – EGF association rate
k_{off} – EGF dissociation rate
k_{er} – internalization rate of unoccupied EGFR
k_{ec} – internalization rate of EGF-EGFR complexes
k_{eh} – internalization rate of HER2
k_{xr} – endosomal exit rate of unoccupied EGFR
k_{xc} – endosomal exit rate of EGF-EGFR complexes
k_{xh} – endosomal exit rate of HER2
f_{xr} – recycling fraction of unoccupied EGFR

f_{xc} – recycling fraction of EGF-EGFR complexes
f_{xh} – recycling fraction of HER2

EGF-EGFR complexes include those present in all forms – undimerized, homodimerized and heterodimerized with HER2.

HER2 includes all forms – free, homodimerized and heterodimerized with EGFR or EGF-EGFR complexes.

All parameters, with the exception of the receptor synthesis parameters have been experimentally measured. k_{ec}, $k_{eh=}$, and f_{xc} are empirically determined functions of HER2 expression level.

5.A.2 Receptor Interaction Model Equations.

$$\frac{d(R1)}{dt} = -k_c(R1)(R2) + k_{u\,R1R2}(R1R2) - 2k_c(R1)(R1) + 2k_{u\,R1R1}(R1R1)$$
$$-k_{on}(L)(R1) + k_{off}(R1L) - k_c(R1)(R1L) + k_{u\,R1R1}(R1R1L)$$

$$\frac{d(R2)}{dt} = -2k_c(R2)(R2) + 2k_{u\,R2R2}(R2R2) - k_c(R1)(R2) + k_{u\,R1R2}(R1R2)$$
$$-k_c(R1L)(R2) + k_{u\,R1R2L}(R1R2L)$$

$$\frac{d(R1R1)}{dt} = k_c(R1)(R1) - k_{u\,R1R1}(R1R1) - k_{on}(L)(R1R1) + k_{off}(R1R1L)$$

$$\frac{d(R1R2)}{dt} = k_c(R1)(R2) - k_{u\,R1R2}(R1R2) - k_{on}(L)(R1R2) + k_{off}(R1R2L)$$

$$\frac{d(R2R2)}{dt} = k_c(R2)(R2) - k_{u\,R2R2}(R2R2)$$

$$\frac{d(R1L)}{dt} = k_{on}(L)(R1) - k_{off}(R1L) - 2k_c(R1L)(R1L) + 2k_{u\,LR1R1L}(LR1R1L)$$
$$-k_c(R1L)(R2) + k_{u\,R1R2L}(R1R2L) - k_c(R1)(R1L) + k_{u\,R1R1}(R1R1L)$$

$$\frac{d(R1R2L)}{dt} = k_{on}(L)(R1R2) - k_{off}(R1R2L) + k_c(R1L)(R2) - k_{u\,R1R2L}(R1R2L)$$

$$\frac{d(R1R1L)}{dt} = k_{on}(L)(R1R1) - k_{off}(R1R1L) - k_{on}(L)(R1R1L) + k_{off}(LR1R1L)$$
$$+k_c(R1)(R1L) - k_{u\,R1R1}(R1R1L)$$

$$\frac{d(LR1R1L)}{dt} = k_c(R1L)(R1L) - k_{u\,LR1R1L}(LR1R1L) + k_{on}(L)(R1R1L) - k_{off}(LR1R1L)$$

glossary:
R1 – unoccupied EGFR
R1R1 – homodimerized, unoccupied EGFR
R2 – free HER2
R2R2 – homodimerized HER2
R1R2 – unoccupied EGFR/HER2 heterodimer

R1L – EGF-EGFR complex
R1R1L – singly bound EGFR homodimer
LR1R1L – $(EGF\text{-}EGF)_2$ homodimer
R1R2L – EGF-EGFR/HER2 heterodimer

k_{on} – EGF association rate
k_{off} – EGF dissociation rate
k_c – dimerization rate
$k_{u,R1R1}$ – R1R1 uncoupling rate constant
$k_{u,R2R2}$ – R2R2 uncoupling rate constant
$k_{u,R1R2}$ – R1R2 uncoupling rate constant
$k_{u,LR1R1L}$ – LR1R1L uncoupling rate constant
$k_{u,R1R2L}$ – R1R2L uncoupling rate constant

All parameter values are listed in Hendriks et al., 2003a (Chapter 2).

Appendix: Matlab Code

A.1 Internalization Model

A.1.1 IM_run.

```
function [soln] = IM_run_new(fitparam, HER2Level, parameters)

% InternalizationModel_run.m : this runs odefile: IM_ode
% 03.03.18

flag1 = parameters(1);

% 2 : run with given parameters, + EGF case
% 3 : run with given parameters, No EGF case
% 4 : vary kuR1R2L
% 5 : run Wang model
% 6 : Instantaneous uncoupling model
% 7 : Predict internalization rates for low EGF stimulus

flag2 = parameters(2);
% 0 : predict HER2 internalization rates
% 1 : predict EGFR internalizations rates

keR1R2_IG = 0.04;   % estimate based on data limits: keR2 < keR1R2 <
keR1
keR2_IG = 0.008;    % estimate based on data limits: limit as HER2 ->
infinity (for HER2 No EGF data)
keR2R2_IG = 0.008;  % estimate based on data limits: limit as HER2 ->
infinity
keR1R2L_IG = 0.10;     % estimate based on data limits: limit as HER2 -
> infinity (for EGFR data)
keR2_EGF_IG = 0.028;   % estimate based on data limits: limit as HER2 -
> infinity (for HER2 + EGF data)
inst_uncouple = 10000;


switch flag1

case 2
    % this runs the model with the fitted parameters
    disp('Running model with fitted parameters (+ EGF case)');


    kuR2R2 = parameters(3);    % HER2:HER2 homodimer uncoupling
    kuR1R2 =  parameters(4);   % HER2:EGFR heterodimer uncoupling
    kuR1R1 = parameters(5);    % EGFR:EGFR homodimer uncoupling

    keR1R2 = keR1R2_IG;    % EGFR:HER2 internalization rate constant
    keR2 = keR2_EGF_IG;        % HER2 internalization rate constant
    keR2R2 = keR2R2_IG;    % HER2:HER2 internalization rate constant
```

```
    keR1R2L = keR1R2L_IG;        % EGF-EGFR:HER2 internalization rate
constant

    kuR1R2L = parameters(6);    % EGF-EGFR:HER2 heterodimer uncoupling
    kuLR1R1L = parameters(7);  % EGF-EGFR:EGFR-EGF uncoupling

    kuR1R1L = kuR1R1;        % EGFR:EGFR-EGF uncoupling

    L = 1.6E-9;   % Ligand concentration (M)


 case 3
    disp('Running model with fitted parameters (No EGF case)');


    kuR2R2 = parameters(3);    % HER2:HER2 homodimer uncoupling
    kuR1R2 =  parameters(4);   % HER2:EGFR heterodimer uncoupling
    kuR1R1 = parameters(5);    % EGFR:EGFR homodimer uncoupling

    keR1R2 = keR1R2_IG;    % EGFR:HER2 internalization rate constant
    keR2 = keR2_IG;        % HER2 internalization rate constant
    keR2R2 = keR2R2_IG;    % HER2:HER2 internalization rate constant
    keR1R2L = keR1R2L_IG;        % EGF-EGFR:HER2 internalization rate
constant

    kuR1R2L = 0.1;    % EGF-EGFR:HER2 heterodimer uncoupling  ... it
doesn't matter what this is since L = 0
    kuLR1R1L = 0.1;   % EGF-EGFR:EGFR-EGF uncoupling          ... it
doesn't matter what this is since L = 0

    kuR1R1L = kuR1R1;        % EGFR:EGFR-EGF uncoupling

    L = 0;   % Ligand concentration (M)


case 4
    disp('Running model with varying values for kuR1R2L');

    kuR2R2 = parameters(3);    % HER2:HER2 homodimer uncoupling
    kuR1R2 =  parameters(4);   % HER2:EGFR heterodimer uncoupling
    kuR1R1 = parameters(5);    % EGFR:EGFR homodimer uncoupling

    keR1R2 = keR1R2_IG;    % EGFR:HER2 internalization rate constant
    keR2 = keR2_EGF_IG;        % HER2 internalization rate constant
    keR2R2 = keR2R2_IG;    % HER2:HER2 internalization rate constant
    keR1R2L = keR1R2L_IG;        % EGF-EGFR:HER2 internalization rate
constant

    kuR1R2L = parameters(6);    % EGF-EGFR:HER2 heterodimer uncoupling
    kuLR1R1L = parameters(7);  % EGF-EGFR:EGFR-EGF uncoupling

    kuR1R1L = kuR1R1;        % EGFR:EGFR-EGF uncoupling

    L = 1.6E-9;   % Ligand concentration (M)
```

```
case 5
    % this case is Wang's Model (keR1R2L = 0), and is fit to data
    disp('Wang Model');


    kuR2R2 = parameters(3);    % HER2:HER2 homodimer uncoupling
    kuR1R2 =  parameters(4);   % HER2:EGFR heterodimer uncoupling
    kuR1R1 = parameters(5);    % EGFR:EGFR homodimer uncoupling

    keR1R2 = keR1R2_IG;    % EGFR:HER2 internalization rate constant
    keR2 = keR2_EGF_IG;        % HER2 internalization rate constant
    keR2R2 = keR2R2_IG;    % HER2:HER2 internalization rate constant
    keR1R2L = 0;        % EGF-EGFR:HER2 internalization rate constant

    kuR1R2L = fitparam(1);    % EGF-EGFR:HER2 heterodimer uncoupling
    kuLR1R1L = fitparam(2);  % EGF-EGFR:EGFR-EGF uncoupling

    kuR1R1L = kuR1R1;        % EGFR:EGFR-EGF uncoupling

    L = 1.6E-9;   % Ligand concentration (M)

case 6
    % this case is the Instantaneous Uncoupling model
    disp('Instantaneous Uncoupling Model ...');

    kuR2R2 = inst_uncouple;    % HER2:HER2 homodimer uncoupling
    kuR1R2 =  inst_uncouple;   % HER2:EGFR heterodimer uncoupling
    kuR1R1 = inst_uncouple;    % EGFR:EGFR homodimer uncoupling

    keR1R2 = keR1R2_IG;    % EGFR:HER2 internalization rate constant
    keR2 = keR2_EGF_IG;        % HER2 internalization rate constant
    keR2R2 = keR2R2_IG;    % HER2:HER2 internalization rate constant
    keR1R2L = keR1R2L_IG;        % EGF-EGFR:HER2 internalization rate
constant

    kuR1R2L = inst_uncouple;    % EGF-EGFR:HER2 heterodimer uncoupling
    kuLR1R1L = inst_uncouple;  % EGF-EGFR:EGFR-EGF uncoupling

    kuR1R1L = kuR1R1;        % EGFR:EGFR-EGF uncoupling

    L = 1.6E-9;   % Ligand concentration (M)

case 7
    % this case is used to predict internalization rates for other
ligand
    % concentrations ... in this case, 1 ng/ml EGF
    disp('Predicting Internalization Rates for 1 ng/ml EGF');

    kuR2R2 = parameters(3);    % HER2:HER2 homodimer uncoupling
    kuR1R2 =  parameters(4);   % HER2:EGFR heterodimer uncoupling
    kuR1R1 = parameters(5);    % EGFR:EGFR homodimer uncoupling

    keR1R2 = keR1R2_IG;    % EGFR:HER2 internalization rate constant
```

```
    keR2 = keR2_EGF_IG;        % HER2 internalization rate constant
    keR2R2 = keR2R2_IG;    % HER2:HER2 internalization rate constant
    keR1R2L = keR1R2L_IG;        % EGF-EGFR:HER2 internalization rate
constant

    kuR1R2L = parameters(6);    % EGF-EGFR:HER2 heterodimer uncoupling
    kuLR1R1L = parameters(7);  % EGF-EGFR:EGFR-EGF uncoupling

    kuR1R1L = kuR1R1;        % EGFR:EGFR-EGF uncoupling

    L = 0.16E-9;   % Ligand concentration (M) = 1 ng/ml

end;

% ---------------- Parameter Values ------------------
kf =  9.7E7;      % EGF binding
kr =   0.24;       % EGF dissociation
kfR1R2 = 9.7E7;   % EGF binding to heterodimer
krR1R2 =  0.24;    % EGF dissociation from heterodimer
kfFab =  1.4E7;     % Fab binding
krFab =  0.3;       % Fab dissociation

kc = 1E-3;             % receptor coupling (dimerization)


keR1L = 0.28;               % EGF-EGFR internalization rate constant
keLR1R1L = keR1L;             % EGF-EGFR:EGFR-EGF internalization rate
constant
keR1R1L = keR1L;              % EGFR:EGFR-EGF internalization rate
constant

Ab = 4.0E-9;  % 7C2 Fab concentration (M)

% ---------------- END Parameter Values -----------------

% ------------------ BEGIN CODE -------------------------

EGFRLevel = 2.0E5; % Amount of EGFR on Surface
HER2iterations = size(HER2Level,2);

tmax = 10;
tsteps = 100;
deltat = tmax/(tsteps-1);


% Begin command sequence-----

parameters =
[kf,kr,kfR1R2,krR1R2,kfFab,krFab,kc,kuR2R2,kuR1R2,kuR1R1,kuR1R2L,kuR1R1
L,kuLR1R1L,keR1L,keR1R2L,keLR1R1L,keR1R1L,keR2,keR2R2,keR1R2,L,Ab];

tspan=linspace(0,tmax,tsteps);

soln = [];
```

```
egfrsoln = [];
her2solnnoegf = [];
her2soln = [];

for j=1:HER2iterations
  initcond = [EGFRLevel;HER2Level(j);0;0;0;0;0;0;0;0;0;0;0;0;0;0;0;0];
% initial conditions: R1,r2 R2, etc...
  [t,y]=ode23s('IM_ode', tspan, initcond, [], parameters);
  egfsurface = (y(:,6) + 2*y(:,7) + y(:,8) + y(:,13) + y(:,14));
  egfinside = y(:,15);
  absurface = (y(:,9)+y(:,10)+2*y(:,11)+y(:,12)+y(:,13));
  abinside = y(:,16);

  % figure;
  % plot(tspan,(y(:,19)+y(:,20))); % active free HER2
  % plot(tspan,(y(:,8)+y(:,13)));  % heterodimers

  switch flag2
    case 1
      % CALCULATE EGFR ke from in/sur data:
      [egfintsurdata, egfrke] = intsur(egfsurface, egfinside, deltat);
      egfrsoln = cat(1, egfrsoln, [HER2Level(j),egfrke]);
    case 0
      % CALCULATE HER2 ke from in/sur data:
      [abintsurdata, her2ke] = intsur(absurface, abinside, deltat);
      her2soln = cat(1, her2soln, [HER2Level(j),her2ke]);
  end;
end;

switch flag2
  case 1
    %disp('HER2Level   | EGFR internalization rate:');
    soln = egfrsoln(:,2).';  % solution needs to be transposed to match
dimensions of experimental data matrix
    temp = egfrsoln;
 case 0
    %disp('HER2Level   | HER2 internalization rate:');
    soln = her2soln(:,2).';  % solution needs to be transposed to match
dimensions of experimental data matrix
    temp = her2soln;
end;

temp(:,1) = 1E-6*temp(:,1);
%disp(temp);
t = tspan;
fprintf('.');
return;
```

A.1.2 IM_ode.m

```
function y=IM_ode(t,x,flag,param)
% Internalization model -
% 02.08.26

R1 = x(1);
R2 = x(2);
R1R1 = x(3);
R1R2 = x(4);
R2R2 = x(5);
R1L = x(6);
LR1R1L = x(7);
R1R2L = x(8);
R2A = x(9);
R2R2A = x(10);
AR2R2A = x(11);
R1R2A = x(12);
R1R2LA = x(13);

R1R1L = x(14);

Lint = x(15);
Abint = x(16);
R1int = x(17);
R2int = x(18);


% R2total =
y(:,2)+y(:,4)+2*y(:,5)+y(:,8)+y(:,9)+2*y(:,10)+2*y(:,11)+y(:,12)+y(:,13
)+y(:,18);
% R1total =
y(:,1)+2*y(:,3)+y(:,4)+y(:,6)+2*y(:,7)+y(:,8)+y(:,12)+y(:,13)+2*y(:,14)
+y(:,17);


%--------------- Parameters -------------------------------------
kf = param(1);          % EGF binding
kr = param(2);          % EGF dissociation
kfR1R2 = param(3);      % EGF binding to heterodimer
krR1R2 = param(4);      % EGF dissociation from heterodimer
kfFab = param(5);       % Fab binding
krFab = param(6);       % Fab dissociation

kc = param(7);          % receptor coupling (dimerization)
kuR2R2 = param(8);      % HER2:HER2 homodimer uncoupling
kuR1R2 = param(9);      % HER2:EGFR heterodimer uncoupling
kuR1R1 = param(10);     % EGFR:EGFR homodimer uncoupling

kuR1R2L = param(11);    % EGF-EGFR:HER2 heterodimer uncoupling
kuR1R1L = param(12);    % EGFR:EGFR-EGF uncoupling
kuLR1R1L = param(13);   % EGF-EGFR:EGFR-EGF uncoupling
```

```
keR1L = param(14);      % EGF-EGFR internalization rate constant
keR1R2L = param(15);    % EGF-EGFR:HER2 internalization rate constant
keLR1R1L = param(16);   % EGF-EGFR:EGFR-EGF internalization rate
constant
keR1R1L = param(17);    % EGFR:EGFR-EGF internalization rate constant

keR2A = param(18);      % HER2 internalization rate constant
keR2R2A = param(19);     % HER2:HER2 internalization rate constant
keR1R2A = param(20);    % EGFR:HER2 internalization rate constant

L = param(21);          % Ligand
Ab = param(22);         % Fab

%--------------- END Parameters -------------------------------------


% Only species that get bound by a Fab or EGF get internalized in this
model.
% For all other species, the consitutive internalization must be
balanced by
% synthesis & recycling.

% d(R1)/dt:
y(1,1) = -kc*R1*R2 + kuR1R2*R1R2 - 2*kc*R1*R1 + 2*kuR1R1*R1R1 - kf*L*R1
+ kr*R1L - kc*R1*R1L + kuR1R1L*R1R1L - kc*R1*R2A + kuR1R2*R1R2A;

% d(R2)/dt:
y(2,1) = -2*kc*R2*R2 + 2*kuR2R2*R2R2 - kc*R1*R2 + kuR1R2*R1R2 -
kc*R1L*R2 + kuR1R2L*R1R2L - kfFab*Ab*R2 + krFab*R2A - kc*R2*R2A +
kuR2R2*R2R2A;

% d(R1R1)/dt:
y(3,1) = kc*R1*R1 - kuR1R1*R1R1 - kf*L*R1R1 + kr*R1R1L;

% d(R1R2)/dt:
y(4,1) = kc*R1*R2 - kuR1R2*R1R2 - kfFab*Ab*R1R2 + krFab*R1R2A -
kfR1R2*L*R1R2 + krR1R2*R1R2L;

% d(R2R2)/dt:
y(5,1) = kc*R2*R2 - kuR2R2*R2R2 - kfFab*Ab*R2R2 + krFab*R2R2A;

% d(R1L)/dt:
y(6,1) = kf*L*R1 - kr*R1L - 2*kc*R1L*R1L + 2*kuLR1R1L*LR1R1L -
kc*R1L*R2 + kuR1R2L*R1R2L - kc*R1L*R2A + kuR1R2L*R1R2LA - kc*R1*R1L +
kuR1R1L*R1R1L - keR1L*R1L;

% d(LR1R1L)/dt:
y(7,1) = kc*R1L*R1L - kuLR1R1L*LR1R1L + kf*L*R1R1L - kr*LR1R1L -
keLR1R1L*LR1R1L;

% d(R1R2L)/dt:
```

```
y(8,1) = kfR1R2*L*R1R2 - krR1R2*R1R2L + kc*R1L*R2 - kuR1R2L*R1R2L -
kfFab*Ab*R1R2L + krFab*R1R2LA  - keR1R2L*R1R2L;


% d(R2A)/dt:
y(9,1) = kfFab*Ab*R2 - krFab*R2A - 2*kc*R2A*R2A + 2*kuR2R2*AR2R2A -
kc*R1*R2A + kuR1R2*R1R2A - kc*R1L*R2A - kc*R2*R2A + kuR2R2*R2R2A -
keR2A*R2A;

% d(R2R2A)/dt:
y(10,1) =  kfFab*Ab*R2R2 - krFab*R2R2A - kfFab*Ab*R2R2A + krFab*AR2R2A
+ kc*R2*R2A - kuR2R2*R2R2A - keR2R2A*R2R2A;

% d(AR2R2A)/dt:
y(11,1) = kfFab*Ab*R2R2A - krFab*AR2R2A + kc*R2A*R2A - kuR2R2*AR2R2A -
keR2R2A*AR2R2A;

% d(R1R2A)/dt:
y(12,1) = kc*R1*R2A - kuR1R2*R1R2A + kfFab*Ab*R1R2 - krFab*R1R2A -
kfR1R2*L*R1R2A + krR1R2*R1R2LA - keR1R2A*R1R2A;

% d(R1R2LA)/dt:
y(13,1) = kc*R1L*R2A - kuR1R2L*R1R2LA + kfR1R2*L*R1R2A - krR1R2*R1R2LA
+ kfFab*Ab*R1R2L - krFab*R1R2LA - keR1R2L*R1R2LA;


% d(R1R1L)/dt:
y(14,1) = kf*L*R1R1 - kr*R1R1L - kf*L*R1R1L + kr*LR1R1L + kc*R1*R1L -
kuR1R1L*R1R1L - keR1R1L*R1R1L;




% d(Lint)/dt:
y(15,1) = keR1L*R1L + 2*keLR1R1L*LR1R1L+ keR1R1L*R1R1L + keR1R2L*R1R2L
+ keR1R2L*R1R2LA;

% d(Abint)/dt:
y(16,1) = keR2A*R2A + keR2R2A*R2R2A + 2*keR2R2A*AR2R2A + keR1R2A*R1R2A
+ keR1R2L*R1R2LA;

% d(R1int)/dt:
y(17,1) =  keR1L*R1L + 2*keLR1R1L*LR1R1L + keR1R2L*R1R2L+
2*keR1R1L*R1R1L + keR1R2L*R1R2LA + keR1R2A*R1R2A;

% d(R2int)/dt:
y(18,1) =  keR2A*R2A + 2*keR2R2A*R2R2A + 2*keR2R2A*AR2R2A +
keR1R2A*R1R2A + keR1R2L*R1R2LA + keR1R2L*R1R2L;

return;
```

A.1.3 integral.m

```
function integral = integral(z, intmax, deltat)

% trapezoidal rule integration of discrete, evenly spaced points
(deltat apart)
% integrates from 0 to intmax
% z should be a column vector!

points = floor(intmax/deltat+1);

u = 2*ones(points,1);

u(1) = 1;
u(points) =1;

% disp(u);

w = size(points,1);  % there's got to be a better way to do this...
for i = 1:points
  w(i,1) = z(i,1);
end;

% disp(w);

temp = 0.5*u'*w*(deltat);
% fprintf('\n integral = ')
% disp(temp);
integral = temp;


return;
```

A.1.4 insur.m

```
function [intsur, ke] =  intsur(surface, inside, deltat)

% integrates surface data, returns two columns: [integral(surface),
inside]
% also returns ke

points = 10;
spacing = 0.75;

intsur = [0,0];

%disp(surface);


for i=1:points
  a = integral(surface, spacing*i, deltat);
  b = inside(floor(spacing*i/deltat), 1);
  intsur = cat(1,intsur, [a, b]);
end;

% disp(intsur);

clf;  % clears figure
% plot(intsur(:,1), intsur(:,2));

ke = (intsur(points,2) - intsur(floor(points/2),2))/(intsur(points,1) -
intsur(floor(points/2),1));
% disp(ke);


return;
```

A.1.5 transientplot.m

```
function IM_run_transientplot_v2

% InternalizationModel_run.m : this runs odefile: IM_ode
% 03.04.04

% THIS VERSION ONLY LOOKS AT HOMO VS. HETERODIMERS (except in receptor
% flux)


% Fit Parameters Initial Guesses
init_guess;
% this loads the initial guesses for the parameters:
% kuR2R2_IG kuR1R2_IG kuR1R1_IG keR1R2A_IG keR2A_IG keR2R2A_IG
kuLR1R1L_IG
% kuR1R2L_IG keR1R2L_IG

% this runs the model with the fitted parameters

% this requires that the initial guesses be correct!
kuR2R2 = kuR2R2_IG;
kuR1R2 = kuR1R2_IG;
kuR1R1 = kuR1R1_IG;
kuR1R1L = kuR1R1;
keR1R2A = 0.04;

% this requires that the initial guesses be correct!
kuLR1R1L = kuLR1R1L_IG;   %number from fitting to EGFR data;
kuR1R2L = kuR1R2L_IG; % number from fitting to EGFR data;
keR1R2L = 0.10;
keR2A = 0.028;  % THERE ARE 2 DIFFERENT VALUES FOR THIS ... NO EGF & +
EGF!!! BE CAREFUL TO GET IT RIGHT!!
keR2R2A = 0.028;

L = 1.6E-9; % 10 ng/ml hEGF



% ---------------- Parameter Values -------------------
kf =  9.7E7;      % EGF binding
kr =   0.24;       % EGF dissociation
kfR1R2 = 9.7E7;   % EGF binding to heterodimer
krR1R2 =  0.24;    % EGF dissociation from heterodimer
kfFab =  1.4E7;     % Fab binding
krFab =  0.3;       % Fab dissociation

kc = 1E-3;             % receptor coupling (dimerization)


keR1L = 0.28;               % EGF-EGFR internalization rate constant
```

```
keLR1R1L = keR1L;             % EGF-EGFR:EGFR-EGF internalization rate
constant
keR1R1L = keR1L;              % EGFR:EGFR-EGF internalization rate
constant

Ab = 4.0E-9;  % 7C2 Fab concentration (M)

% ---------------- END Parameter Values ------------------


% ------------------- BEGIN CODE -------------------------

EGFRLevel = 2.0E5; % Amount of EGFR on Surface


tmax = 10;
tsteps = 100;
deltat = tmax/(tsteps-1);


% Begin command sequence-----

parameters =
[kf,kr,kfR1R2,krR1R2,kfFab,krFab,kc,kuR2R2,kuR1R2,kuR1R1,kuR1R2L,kuR1R1
L,kuLR1R1L,keR1L,keR1R2L,keLR1R1L,keR1R1L,keR2A,keR2R2A,keR1R2A,L,Ab];


tspan=linspace(0,tmax,tsteps);

soln = [];
egfrsoln = [];
her2solnnoegf = [];
her2soln = [];

figure;
subplot(2,2,2);
hold on;
set(gca,'Box', 'on');

% HER2 = 30,000
initcond = [EGFRLevel;30000;0;0;0;0;0;0;0;0;0;0;0;0;0;0;0;0;0;0]; % initial
conditions: R1,r2 R2, etc...
[t,y]=ode23s('IM_ode', tspan, initcond, [], parameters);
for i = 1: size(tspan,2)
    fraction_heterodimers_1(i) =
(y(i,8)+y(i,13))/(y(i,8)+y(i,13)+y(i,7));
    total_dimers_1(i) = (y(i,8)+y(i,7)+y(i,13));  % only homo &
heterodimers
    flux_equiv_homodimers_1(i) = (y(i,6)+2*y(i,7)+y(i,14))*keR1L/2; %
Total complexes/2 for comparison with heterodimers
    flux_heterodimers_1(i) = (y(i,8)+y(i,13))*keR1R2L;
end;
plot(tspan,(y(:,7)), 'r-', 'LineWidth', 3);  % homodimers
plot(tspan,(y(:,8)+y(:,13)), 'r:', 'LineWidth', 3);  % heterodimers
```

```
% HER2 = 100,000
initcond = [EGFRLevel;100000;0;0;0;0;0;0;0;0;0;0;0;0;0;0;0;0]; %
initial conditions: R1,r2 R2, etc...
[t,y]=ode23s('IM_ode', tspan, initcond, [], parameters);
for i = 1: size(tspan,2)
    fraction_heterodimers_2(i) =
(y(i,8)+y(i,13))/(y(i,8)+y(i,13)+y(i,7));
    total_dimers_2(i) = (y(i,8)+y(i,7)+y(i,13));  % only homo &
heterodimers
    flux_equiv_homodimers_2(i) = (y(i,6)+2*y(i,7)+y(i,14))*keR1L/2; %
Total complexes/2 for comparison with heterodimers
    flux_heterodimers_2(i) = (y(i,8)+y(i,13))*keR1R2L;
end;
plot(tspan,(y(:,7)), 'g-', 'LineWidth', 3);  % homodimers
plot(tspan,(y(:,8)+y(:,13)), 'g:', 'LineWidth', 3);  % heterodimers

% HER2 = 200,000
initcond = [EGFRLevel;200000;0;0;0;0;0;0;0;0;0;0;0;0;0;0;0;0]; %
initial conditions: R1,r2 R2, etc...
[t,y]=ode23s('IM_ode', tspan, initcond, [], parameters);
for i = 1: size(tspan,2)
    fraction_heterodimers_3(i) =
(y(i,8)+y(i,13))/(y(i,8)+y(i,13)+y(i,7));
    total_dimers_3(i) = (y(i,8)+y(i,7)+y(i,13));  % only homo &
heterodimers
    flux_equiv_homodimers_3(i) = (y(i,6)+2*y(i,7)+y(i,14))*keR1L/2; %
Total complexes/2 for comparison with heterodimers
    flux_heterodimers_3(i) = (y(i,8)+y(i,13))*keR1R2L;
end;
plot(tspan,(y(:,7)), 'b-', 'LineWidth', 3);  % homodimers
plot(tspan,(y(:,8)+y(:,13)), 'b:', 'LineWidth', 3);  % heterodimers

% HER2 = 600,000
initcond = [EGFRLevel;600000;0;0;0;0;0;0;0;0;0;0;0;0;0;0;0;0]; %
initial conditions: R1,r2 R2, etc...
[t,y]=ode23s('IM_ode', tspan, initcond, [], parameters);
for i = 1: size(tspan,2)
    fraction_heterodimers_4(i) =
(y(i,8)+y(i,13))/(y(i,8)+y(i,13)+y(i,7));
    total_dimers_4(i) = (y(i,7)+y(i,8)+y(i,13));  % only homo &
heterodimers
    flux_equiv_homodimers_4(i) = (y(i,6)+2*y(i,7)+y(i,14))*keR1L/2; %
Total complexes/2 for comparison with heterodimers
    flux_heterodimers_4(i) = (y(i,8)+y(i,13))*keR1R2L;
end;
plot(tspan,(y(:,7)), 'k-', 'LineWidth', 3);  % homodimers
plot(tspan,(y(:,8)+y(:,13)), 'k:', 'LineWidth', 3);  % heterodimers

set(gca,'XTick',[0 2 4 6 8 10]);
xlabel('time (min)', 'FontSize', 16);
ylabel('#/cell', 'FontSize', 16);
```

```
title('Signaling Species', 'FontSize', 16);
set(gca, 'LineWidth', 3, 'FontSize', 16);
hold off;

subplot(2,2,3);
hold on;
set(gca,'Box', 'on');
plot(tspan,fraction_heterodimers_1, 'r-', 'LineWidth', 3);
plot(tspan,fraction_heterodimers_2, 'g-', 'LineWidth', 3);
plot(tspan,fraction_heterodimers_3, 'b-', 'LineWidth', 3);
plot(tspan,fraction_heterodimers_4, 'k-', 'LineWidth', 3);
set(gca,'XTick',[0 2 4 6 8 10]);
xlabel('time (min)', 'FontSize', 16);
ylabel('Fraction of Total Signal', 'FontSize', 16);
title('Heterodimer Signaling', 'FontSize', 16);
set(gca, 'LineWidth', 3, 'FontSize', 16);
hold off;

subplot(2,2,1);
hold on;
set(gca,'Box', 'on');
plot(tspan,total_dimers_1, 'r-', 'LineWidth', 3);
plot(tspan,total_dimers_2, 'g-', 'LineWidth', 3);
plot(tspan,total_dimers_3, 'b-', 'LineWidth', 3);
plot(tspan,total_dimers_4, 'k-', 'LineWidth', 3);
set(gca,'XTick',[0 2 4 6 8 10]);
xlabel('time (min)', 'FontSize', 16);
ylabel('Receptor Dimers (#/cell)', 'FontSize', 16);
title('Total Receptor Dimers Signaling', 'FontSize', 16);
set(gca, 'LineWidth', 3, 'FontSize', 16);
hold off;

subplot(2,2,4);
hold on;
set(gca,'Box', 'on');
plot(tspan,flux_equiv_homodimers_1, 'r-', 'LineWidth', 3);
plot(tspan,flux_heterodimers_1, 'r:', 'LineWidth', 3);
plot(tspan,flux_equiv_homodimers_2, 'g-', 'LineWidth', 3);
plot(tspan,flux_heterodimers_2, 'g:', 'LineWidth', 3);
plot(tspan,flux_equiv_homodimers_3, 'b-', 'LineWidth', 3);
plot(tspan,flux_heterodimers_3, 'b:', 'LineWidth', 3);
plot(tspan,flux_equiv_homodimers_4, 'k-', 'LineWidth', 3);
plot(tspan,flux_heterodimers_4, 'k:', 'LineWidth', 3);
set(gca,'XTick',[0 2 4 6 8 10]);
xlabel('time (min)', 'FontSize', 16);
ylabel('Receptor Flux (#/min)', 'FontSize', 16);
title('Receptor Flux', 'FontSize', 16);
set(gca, 'LineWidth', 3, 'FontSize', 16);
hold off;
return;
```

A.1.6 expdata.m

```
% ----------------------- EXPERIMENTAL DATA --------------------
% HER2, No EGF:
xdata_HER2_NoEGF = [30000 100000 200000 600000 600000];
ydata_HER2_NoEGF = [0.0180 0.0147 0.0085 0.0108 0.0077];
yerror_HER2_NoEGF = [0.00555 0.00559 0.00171 0.00457 0.00211];

% HER2, + EGF:
xdata_HER2_EGF = [30000 100000 200000 600000 600000];
ydata_HER2_EGF = [0.0588 0.035 0.0456 0.0292 0.0272];
yerror_HER2_EGF = [0.00171 0.00523 0.00825 0.00289 0.00799];

% EGFR, + EGF:
xdata_EGFR = [30000 100000 200000 600000 600000];
ydata_EGFR = [0.2486 0.1827 0.1691 0.0947 0.1191];
yerror_EGFR = [0.0224 0.0210 0.0207 0.0181 0.0210];

%EGFR, + EGF, + 2C4
xdata_EGFR_2C4 = [30000 100000 200000 600000 600000];
ydata_EGFR_2C4 = [0.3042 0.2755 0.2830 0.241 0.2795];
yerror_EGFR_2C4 = [0.0450 0.0177 0.0297 0.00283 0.00495];
% ----------------------- END EXPERIMENTAL DATA ----------------
```

A.2 Receptor Interaction Model

A.2.1 RIM_run.m

```
%function RIMrun
clear;
disp('Running RImodel');
% these parameters are from the Internalization model parameter fitting
(as
% of 9/23/02)
kc = 1E-3;

keR1L = 0.28;
keR1LR2 = 0.10;
keR2 = 0.028;
keR1R2 = 0.04;


kuR2R2 = 1.075;    % HER2 homodimer uncoupling
kuR1R2 = 16.45;    % HER2:EGFR heterodimer uncoupling
kuR1R1 = 13.51;    % EGFR:EGFR heterodimer uncoupling
kuR1LR2 = 0.1; %0.118;   % HER2:EGFR-EGF uncoupling
kuLR1R1L = 0.1; %0.049;     % EGFR-EGF homodimer uncoupling
%---------------------------------


kon = 9.7E7;       % Ligand-EGFR binding
koff = 0.24;       % Ligand-EGFR dissociation

L = 1.6E-9; %10 ng/ml         %MAKE SURE THIS IS CORRECT FOR YOUR
CONDITION! Ligand concentration

tmax = 20;
tsteps = 50;
deltat = tmax/(tsteps-1);

EGFRmin =   10000;
EGFRmax = 600000;
EGFRstep = 10;

HER2min =   10000;
HER2max = 600000;
HER2step = 10;

HER2Level = linspace(HER2min, HER2max, HER2step);
EGFRLevel = linspace(EGFRmin, EGFRmax, EGFRstep);

%HER2Level = [ 30000 600000];
%EGFRLevel = [200000 200000];

%HER2Level = [0.9e5 17e5];
```

```
%EGFRLevel = [3.5e5 4.5e5]; %(1,1) = MTSV; (2,2) = Ce2

tic;

for j = 1:size(EGFRLevel,2)
  for i = 1:size(HER2Level,2)

    tspan=linspace(0,tmax,tsteps);
    parameters = [kc,kuR2R2,kuR1R2,kuR1R1,kuR1LR2,
kuLR1R1L,kon,koff,L];
    initcond = [EGFRLevel(j);HER2Level(i);0;0;0;0;0;0;0];
    [t,y]=ode23s('RIMode', tspan, initcond, [], parameters);


    Total_Heterodimers(j,i) = y(tsteps,7);
    Total_EquivHomodimers(j,i) =
(2*y(tsteps,9)+y(tsteps,6)+y(tsteps,8))/2;
    Total_Homodimers(j,i) = y(tsteps,9);
    RelativeDimerization(j,i) = Total_Heterodimers(j,i)-
Total_Homodimers(j,i);
    RelativeDimerization_alternate(j,i) = Total_Heterodimers(j,i)-
Total_EquivHomodimers(j,i);

    TotalEGFR = y(:,1)+2*y(:,3)+y(:,4)+y(:,6)+y(:,7)+2*y(:,8)+2*y(:,9);
    TotalBoundEGFR = y(:,6)+y(:,7)+y(:,8)+2*y(:,9);
    TotalHER2 = y(:,2)+y(:,4)+2*y(:,5)+y(:,7);

    if L ~= 0
       frxn_Bound_EGFR_het(j,i) = y(tsteps,7)/TotalBoundEGFR(tsteps);
    end;

    ObservedEGFRIntRate(j,i) =
((y(tsteps,6)+y(tsteps,8)+2*y(tsteps,9))*keR1L +
y(tsteps,7)*keR1LR2)/TotalBoundEGFR(tsteps);
    ObservedHER2IntRate(j,i) = ((y(tsteps,2)+2*y(tsteps,5))*keR2 +
y(tsteps,4)*keR1R2 + y(tsteps,7)*keR1LR2)/TotalHER2(tsteps);

    frxn_Total_EGFR_het(j,i) = y(tsteps,7)/TotalEGFR(tsteps);
    frxn_HER2_het(j,i) = y(tsteps,7)/TotalHER2(tsteps);
    frxn_HER2_hom(j,i) = 2*y(tsteps,5)/TotalHER2(tsteps);

    if TotalBoundEGFR(tsteps) > HER2Level(i)
       frxn_egfr_het(j,i) = y(tsteps,7)/TotalHER2(tsteps);
    else
       frxn_egfr_het(j,i) = y(tsteps,7)/TotalBoundEGFR(tsteps);
    end;

    frxn_egfr_hom = (y(tsteps,9)/(TotalBoundEGFR(tsteps)/2));
    %relative_dimerization(j,i) =
frxn_egfr_het(j,i)/frxn_egfr_hom(j,i);

  end;
end;
```

```
% disp(frxn_Bound_EGFR_het);
if L ~= 0
   figure;
   subplot(2,2,3);
   hold on;
   mesh(HER2Level, EGFRLevel, frxn_Bound_EGFR_het*100, 'LineWidth', 2);
   ylabel('EGFR (#/cell)','FontSize',16);
   xlabel('HER2 (#/cell)','FontSize',16);
   zlabel('% of Bound EGFR Heterodimerized','FontSize',16);
   set(gca, 'XScale', 'linear');
   set(gca, 'YScale', 'linear');
   set(gca,'XLim',[0 600000]);
   set(gca,'YLim',[0 600000]);
   set(gca,'XTick',[0 200000 400000 600000]);
   set(gca,'YTick',[0 200000 400000 600000]);
   set(gca, 'LineWidth', 3, 'FontSize', 16);
    set(findobj('Type','line'),'LineWidth', 3);
   %set(gca, 'YDir', 'reverse');
   view(3);
   grid on;
   hold off;


      subplot(2,2,2);
      hold on;
      mesh(HER2Level, EGFRLevel, frxn_HER2_het*100, 'LineWidth', 2);
    ylabel('EGFR (#/cell)','FontSize',16);
    xlabel('HER2 (#/cell)','FontSize',16);

      zlabel('% of Total HER2 Heterodimerized','FontSize',16);
      set(gca, 'XScale', 'linear');
      set(gca, 'YScale', 'linear');
    set(gca,'XLim',[0 600000]);
    set(gca,'YLim',[0 600000]);
    set(gca,'XTick',[0 200000 400000 600000]);
    set(gca,'YTick',[0 200000 400000 600000]);
    set(gca, 'LineWidth', 3, 'FontSize', 16);
    set(findobj('Type','line'),'LineWidth', 3);
      %set(gca, 'YDir', 'reverse');
      view(3);
      grid on;
   hold off;

   subplot(2,2,4);
      hold on;
      mesh(HER2Level, EGFRLevel, RelativeDimerization, 'LineWidth', 2);
    ylabel('EGFR (#/cell)','FontSize',16);
    xlabel('HER2 (#/cell)','FontSize',16);

      zlabel('Heterodimers-Homodimers','FontSize',16);
      set(gca, 'XScale', 'linear');
      set(gca, 'YScale', 'linear');
    set(gca,'XLim',[0 600000]);
```

```
    set(gca,'YLim',[0 600000]);
    set(gca,'XTick',[0 200000 400000 600000]);
    set(gca,'YTick',[0 200000 400000 600000]);
    set(gca, 'LineWidth', 3, 'FontSize', 16);
    set(findobj('Type','line'),'LineWidth', 3);
      %set(gca, 'YDir', 'reverse');
      view(3);
      grid on;
   hold off;

    subplot(2,2,1);
      hold on;
      mesh(HER2Level, EGFRLevel, RelativeDimerization_alternate,
'LineWidth', 2);
    ylabel('EGFR (#/cell)','FontSize',16);
    xlabel('HER2 (#/cell)','FontSize',16);

      zlabel('Heterodimers-Homodimers','FontSize',16);
      set(gca, 'XScale', 'linear');
      set(gca, 'YScale', 'linear');
    set(gca,'XLim',[0 600000]);
    set(gca,'YLim',[0 600000]);
    set(gca,'XTick',[0 200000 400000 600000]);
    set(gca,'YTick',[0 200000 400000 600000]);
    set(gca, 'LineWidth', 3, 'FontSize', 16);
    set(findobj('Type','line'),'LineWidth', 3);
      %set(gca, 'YDir', 'reverse');
      view(3);
      grid on;
   hold off;

else
   figure;
   subplot(2,2,1);
   hold on;
   mesh(HER2Level, EGFRLevel, frxn_HER2_hom*100, 'LineWidth', 2);
   ylabel('EGFR (#/cell)','FontSize',16);
    xlabel('HER2 (#/cell)','FontSize',16);
      zlabel('% of Total HER2 Homodimerized','FontSize',16);
      set(gca, 'XScale', 'linear');
      set(gca, 'YScale', 'linear');
    set(gca,'XLim',[0 600000]);
    set(gca,'YLim',[0 600000]);
    set(gca,'XTick',[0 200000 400000 600000]);
    set(gca,'YTick',[0 200000 400000 600000]);
    set(gca, 'LineWidth', 3, 'FontSize', 16);
    set(findobj('Type','line'),'LineWidth', 3);
      %set(gca, 'YDir', 'reverse');
      view(3);
      grid on;
   hold off;
end;
% end figure
toc;
```

A.2.2 RIM_ode.m

```
function y=RIMode(t,x,flag,param)
% Receptor Interaction Model odefile
% this is the basic set of receptor interactions that take place on the
cell surface
% last revised 01.02.07

R1 = x(1);
R2 = x(2);
R1R1 = x(3);
R1R2 = x(4);
R2R2 = x(5);
R1L = x(6);
R1LR2 = x(7);
R1R1L = x(8);
LR1R1L = x(9);

kc = param(1);          % HER2 homodimer coupling
kuR2R2 = param(2);      % HER2 homodimer uncoupling
kuR1R2 = param(3);      % HER2:EGFR heterodimer uncoupling
kuR1R1 = param(4);      % EGFR:EGFR heterodimer uncoupling
kuR1LR2 = param(5);     % HER2:EGFR-EGF uncoupling
kuLR1R1L = param(6);    % EGFR-EGF homodimer uncoupling

kon = param(7);         % Ligand-EGFR binding
koff = param(8);        % Ligand-EGFR dissociation

L = param(9);           % Ligand concentration


% d(R1)/dt:
y(1,1) = -kc*R1*R2 + kuR1R2*R1R2 - 2*kc*R1*R1 + 2*kuR1R1*R1R1 -
kon*L*R1 + koff*R1L - kc*R1*R1L + kuR1R1*R1R1L;

% d(R2)/dt:
y(2,1) = -2*kc*R2*R2 + 2*kuR2R2*R2R2 - kc*R1*R2 + kuR1R2*R1R2 -
kc*R1L*R2 + kuR1LR2*R1LR2;

% d(R1R1)/dt:
y(3,1) = kc*R1*R1 - kuR1R1*R1R1 - kon*L*R1R1 + koff*R1R1L;

% d(R1R2)/dt:
y(4,1) = kc*R1*R2 - kuR1R2*R1R2 - kon*L*R1R2 + koff*R1LR2;

% d(R2R2)/dt:
y(5,1) = kc*R2*R2 - kuR2R2*R2R2;

% d(R1L)/dt:
y(6,1) = kon*L*R1 - koff*R1L - 2*kc*R1L*R1L + 2*kuLR1R1L*LR1R1L -
kc*R1L*R2 + kuR1LR2*R1LR2 - kc*R1*R1L + kuR1R1*R1R1L;
```

```
% d(R1LR2)/dt:
y(7,1) = kon*L*R1R2 - koff*R1LR2 + kc*R1L*R2 - kuR1LR2*R1LR2;

% d(R1R1L)/dt:
y(8,1) = kon*L*R1R1 - koff*R1R1L - kon*L*R1R1L + koff*LR1R1L +
kc*R1*R1L - kuR1R1*R1R1L;

% d(LR1R1L)/dt:
y(9,1) = kc*R1L*R1L - kuLR1R1L*LR1R1L + kon*L*R1R1L - koff*LR1R1L;


return;
```

A.3 Recycling Model

A.3.1 SRM_run.m

```
function SRM_run(model_type)
%this runs the simplified recycling model SRM_calc.m and SRM_ode.m
% 02.10.01

kc_het = 1E-3;    % receptor-receptor  coupling (cell min)-1
kc_E1 = 1E-3;     % EGFR-ERC coupling
kc_E1_het = 1E-3; % EGFR-ERC coupling when in heterodimerized state

kc_E2 = 1E-3;     % HER2-ERC coupling
kc_E2_het = 1E-3; % HER2-ERC coupling when in heterodimerized state

kuR1R2 = 16.45;     % EGFR-HER2 (unbound heterodimer) uncoupling (min)-
1 ... 16.45 from IM fit !!NOT USED IN THIS VERSION!!
kuR1LR2 = 0.13;     % bound heterodimer uncoupling (min)-1 ...  0.13
from IM fit
% these values are from Internalization model fitting (as of 10/1/02)

kuR1E = 1E-1;     % EGFR-ERC uncoupling (min)-1
kuR2E = 1E-1;     % HER2 - ERC uncoupling (min)-1

kon = 5E7;        % ligand binding rate at pH 6.0 (M min)-1  ...
koff = 0.5;         % ligand dissociation at pH 6.0 (min)-1  ...
(estimated from data ... hEGF!)
koff_het = 0.5;     % ligand dissociation from heterodimers  ...
(estimated from data ... hEGF!)
kst = 0.53;    % tubular sorting rate constant (min)-1 ... 0.53 from FP
ksv = 0.06;    % vesicular sorting rate constant (min)-1 ... 0.12 from
FP

kx = 0.15;     % recycling rate constant (min)-1 ... 0.15 from French
paper (FP)
kh = 0.09;     % degradation rate constant (min)-1 ... 0.06 from French
paper

gamma = 1;     % receptor transport from vesicles to tubules (min)-1
kappa = 0.81;  % partition coefficient accounting for excluded volume
due to ligand size:
               % ligand in tubule is assumed to be in equilibrium with
ligand in vesicle
xi = 0;        % fraction of internalized ligand nonspecifically
endocytosed

Nav = 6.023E23;  % #/mol
Vr = 0.3E-14;    % recycling volume set equal to tubule volume
(arbitrary)

eta = 0.67;                % eta = Vt/Vv ... 0.43 from FP
```

```
Vtotal = 1E-14;             % Vtotal = Vt + Vv; (total endosomal
volume)
Vt = eta*Vtotal/(1+eta);    %
Vv = Vtotal - Vt;           % vesicle volume

Vd = 0.3E-14;    % degradation volume = tubule volume (arbitrary)



switch model_type
   case 1
      % blockade model:
     plot_title = 'BLOCKADE MODEL';
     kc_E1_het = 0;  % EGFR-ERC coupling when in heterodimerized state
     kc_E2 = 0;      % HER2-ERC coupling
     kc_E2_het = 0;  % HER2-ERC coupling when in heterodimerized state
  case 2
     % competition model:
     plot_title = 'COMPETITION MODEL';
     kc_E1_het = 1E-3;  % EGFR-ERC coupling when in heterodimerized
state
     kc_E2 = 1E-3;      % HER2-ERC coupling
     kc_E2_het = 1E-3;  % HER2-ERC coupling when in heterodimerized
state
     kc_het = 1E-3;
  case 3
     % pH destabilization model:
     plot_title = 'DESTABILIZATION MODEL';
     koff_het = 2.5;   % ligand dissociation from heterodimers
     kc_E2 = 0;        % heterodimerization is allowed but HER2 doesn't
couple with ERCs
     kc_E2_het = 0;
  case 4
     % combined model:
     plot_title = 'COMBINED MODEL';
     kc_E1_het = 0;    % EGFR-ERC coupling when in heterodimerized
state
     kc_E2 = 1E-3;     % HER2-ERC coupling
     kc_E2_het = 0;    % HER2-ERC coupling when in heterodimerized
state
     koff_het = 2.5;   % ligand dissociation from heterodimers
end

disp(plot_title);

rateconsts = [kc_het,kc_E1,kc_E2,kc_E1_het,kc_E2_het,
kuR1R2,kuR1LR2,kuR1E,kuR2E,kon, koff,koff_het,kst,ksv,kx,
kh,gamma,kappa,xi,Vr, Vt,Vv,Vd];
scale = 2;  % scale = 2 for nice plots
% model inputs ------ (these are fluxes that will ultimately determine
the
% steady state relationships)
keR1 = 0;
keR1R2 = 0;
```

```
keR1L = 0.02;    % (min)-1
keR1LR2 = 0;   % (min)-1
keR2 = 0;

inputs = [keR1, keR2, keR1R2, keR1L, keR1LR2];
[model_input1, output1] = SRM_calc(rateconsts,inputs, scale);

keR1L = 0.01;    % (min)-1
keR1LR2 = 0.01;   % (min)-1
keR2 = 0;
inputs = [keR1, keR2, keR1R2, keR1L, keR1LR2];
[model_input2, output2] = SRM_calc(rateconsts,inputs, scale);

keR1L = 0;    % (min)-1
keR1LR2 = 0.02;
keR2 = 0;
inputs = [keR1, keR2, keR1R2, keR1L, keR1LR2];
[model_input3, output3] = SRM_calc(rateconsts,inputs, scale);

figure;
subplot(2,2,1);
hold on;
set(gca,'Box', 'on');
set(gca, 'LineWidth', 3);
xlabel('Intracellular EGF (#/cell)', 'Fontsize', 16);
ylabel('Fraction EGF Recycled', 'Fontsize', 16);
title(plot_title, 'Fontsize', 16);

plot(output1(:,1), output1(:,2), '-k', 'LineWidth', 3);
plot(output2(:,1), output2(:,2), '-.k', 'LineWidth', 3);
plot(output3(:,1), output3(:,2), ':k', 'LineWidth', 3);

legend('0%', '50%', '100%', 1);
set(gca, 'XScale', 'log');
%set(gca,'XTickLabel',{10 100 1000 10000 100000 1000000}, 'FontSize',
14);
set(gca,'YTickLabel',{0 0.2 0.4 0.6 0.8 1.0}, 'FontSize', 16);
axis([100 1000000 0 1]);
set(findobj('Type','line'),'LineWidth', 3);
hold off;

switch model_type
   case 1 % blockade model
      save SRMres_bl model_input1 output1 model_input2 output2
model_input3 output3;

      % this part varies the parameter kuR1LR2 for blockade model
      inputs = [0, 0, 0, 0, 0.02];


      rateconsts(7) = kuR1LR2*0.1;
      [model_input5, output5]= SRM_calc(rateconsts,inputs, scale);
      rateconsts(7) = kuR1LR2*1;
      [model_input6, output6]= SRM_calc(rateconsts,inputs, scale);
```

```
      rateconsts(7) = kuR1LR2*10;
      [model_input7, output7]= SRM_calc(rateconsts,inputs, scale);
      rateconsts(7) = kuR1LR2*100;
      [model_input8, output8]= SRM_calc(rateconsts,inputs, scale);
      rateconsts(7) = kuR1LR2;
      save SRMres_bl_2  model_input5 output5 model_input6 output6
model_input7 output7 model_input8 output8;

   case 2 % competition model
      save SRMres_cp model_input1 output1 model_input2 output2
model_input3 output3;

      % vary HER2-ERC uncoupling for COMPETITION model:
      inputs = [0, 0, 0, 0, 0.02];


      rateconsts(9) = kuR2E*0.1;
      [model_input5, output5]= SRM_calc(rateconsts,inputs, scale);
      rateconsts(9) = kuR2E*1;
      [model_input6, output6]= SRM_calc(rateconsts,inputs, scale);
      rateconsts(9) = kuR2E*10;
      [model_input7, output7]= SRM_calc(rateconsts,inputs, scale);
      rateconsts(9) = kuR2E*100;
      [model_input8, output8]= SRM_calc(rateconsts,inputs, scale);
      rateconsts(9) = kuR2E;
      save SRMres_cp_2 model_input5 output5 model_input6 output6
model_input7 output7 model_input8 output8;

   case 3 %destabilization model
      save SRMres_ds model_input1 output1 model_input2 output2
model_input3 output3;

      inputs = [0, 0, 0, 0, 0.02];

      rateconsts(12) = 0.1;
      [model_input5, output5]= SRM_calc(rateconsts,inputs, scale);
      rateconsts(12) = 0.5;
      [model_input6, output6]= SRM_calc(rateconsts,inputs, scale);

      rateconsts(12) = 10;
      [model_input7, output7]= SRM_calc(rateconsts,inputs, scale);
      rateconsts(12) = 100;
      [model_input8, output8]= SRM_calc(rateconsts,inputs, scale);
      rateconsts(12) = koff_het;
      save SRMres_ds_2 model_input5 output5 model_input6 output6
model_input7 output7 model_input8 output8;



end;


subplot(2,2,3);
hold on;
```

```
set(gca,'Box', 'on');
set(gca, 'LineWidth', 3);
xlabel('Intracellular EGF (#/cell)', 'Fontsize', 16);
ylabel('Fraction EGF Recycled', 'Fontsize', 16);
title(plot_title, 'Fontsize', 16);


plot(output5(:,1), output5(:,2), '-k', 'LineWidth', 3);
plot(output6(:,1), output6(:,2), '--k', 'LineWidth', 3);
plot(output7(:,1), output7(:,2), '-.k', 'LineWidth', 3);
plot(output8(:,1), output8(:,2), ':k', 'LineWidth', 3);

if model_type == 3
    legend('0.1 min-1', '0.5 min-1', '10 min-1', '100 min-1', 1);
else legend('0.1x', '1x', '10x', '100x', 1);
end;

set(gca, 'XScale', 'log');
%set(gca,'XTickLabel',{10 100 1000 10000 100000 1000000}, 'FontSize',
14);
axis([100 1000000 0 1]);
set(findobj('Type','line'),'LineWidth', 3);
set(gca,'YTick',[0  0.2  0.4 0.6 0.8 1.0]);
set(gca,'YTickLabel',{0 0.1 0.2 0.3 0.4 0.5 0.6 0.7 0.8 0.9 1.0},
'FontSize', 16);
hold off;
```

A.3.2 SRM_calc.m

```
function [model_input, sortingfrxn] = SRM_calc(rateconsts, inputs,
scale)

% runs ODEFILE ~/MATLAB/RECYCLING/rebuild.m
% french recycling model + HER2:
% this version does it all!

Nav = 6.023E23;
Vv = rateconsts(22);
Vr = rateconsts(20);
Vd = rateconsts(23);
Vt = rateconsts(21);
kappa = rateconsts(18);
kst = rateconsts(13);
ksv = rateconsts(14);

tmax = 150;
tsteps = 100;
iterationmax = 50;

ERCLevel = 20000; % THIS IS SPECIFIED HERE! 20000 good start

tspan=linspace(0,tmax,tsteps);

% rate constants and model inputs and scale are specified in control.m
parameters = cat(2, rateconsts,inputs);

initcond = [0;0;0;0;0; ERCLevel;0;0;0;0; 0;0;0;0;0; 0;0;0;0;0;
0;0;0;0;0; 0;0];

sortingfrxn = [];
model_input = [];


warning off;

internalligand = 0;
i = 1;

while (internalligand < 3E5) & (i <= iterationmax)

  [t,y] = ode23s('SRM_ode_2', tspan, initcond, [], parameters);
  % SRM_ode has species: ER1LR2E
  % SRM_ode_2 does NOT have species: ER1LR2

  vesicleligand = y(tsteps,2) + y(tsteps,3) + Nav*Vv*y(tsteps,4) +
y(tsteps,9) + y(tsteps,10) + y(tsteps,11) + y(tsteps,12);
  tubuleligand = y(tsteps,19) + kappa*Nav*Vt*y(tsteps,4)+y(tsteps,21);
  otherligand = Nav*Vd*y(tsteps,24) + Nav*Vr*y(tsteps,27);  % free
ligand in degradation & recycling compartments
```

```
  internalligand = vesicleligand + tubuleligand + otherligand;

  frxn = kst*tubuleligand/(kst*tubuleligand + ksv*vesicleligand);
  % is this the frxn we want? ... is sorting first order in ligand or
in receptor species?
  % ... here it's first order in receptor species for no reason in
particular



  sortingfrxn = cat(1,sortingfrxn, [internalligand, frxn]);
  model_input = cat(1,model_input, [parameters(27), parameters(28)]);

  disp(i);
  disp(model_input(i,:));  % latest model input value
  disp(internalligand);
  disp(frxn);

  % total HER2:
  total_HER2 = y(tsteps,7) + y(tsteps,8) + y(tsteps,9) + y(tsteps,10) +
y(tsteps,11) + y(tsteps,12) + y(tsteps,13) + y(tsteps,14) +
y(tsteps,15) + y(tsteps,16) + y(tsteps,18) + y(tsteps,20) +
y(tsteps,21) + y(tsteps,23) + y(tsteps,26);
  fprintf('Total HER2 Inside: %8.2f \n', total_HER2);

  free_vesicle_ligand = Nav*Vv*y(tsteps,4);
  bound_vesicle_ligand = vesicleligand - free_vesicle_ligand;
  fprintf('Free vesicle ligand: %6.2f \n', free_vesicle_ligand);
  fprintf('Bound vesicle ligand: %6.2f \n\n', bound_vesicle_ligand);

  % figure;
  % hold on;
  % plot(tspan, (y(:,2)+y(:,3)+Nav*Vv*y(:,4)+ y(tsteps,9) + y(:,10) +
y(:,11) + y(:,12)), 'Color', 'blue');
  % plot(tspan, (y(:,19) + kappa*Nav*Vt*y(:,4)+y(:,21)), 'Color',
'magenta');
  % plot(tspan, (Nav*Vd*y(:,24)), 'Color', 'red');
  % plot(tspan, (Nav*Vr*y(:,27)), 'Color', 'green');
  % hold off;

  parameters(24) = parameters(24)*1;  % don't increase keR1
  parameters(25) = parameters(25)*1;  %   keR2 ?!??? (* should this be
increased ?!? *)
  parameters(26) = parameters(26)*1;  % don't increase keR1R2
  parameters(27) = parameters(27)*scale;  % increase input: keR1L
  parameters(28) = parameters(28)*scale;  % increase input: keR1LR2
  i = i + 1;
end;
warning on;
```

A.3.2 SRM_ode.m

```
function y = SRM_ode(t, x, flag, param)

% run with SRM_calc.m via SRM_run.m
% based on simple french model + HER2
% this is my recycling model simplified to eliminate species &
parameters


% vesicular species...
R1v = x(1);
R1Lv = x(2);
R1LEv = x(3);

Lv = x(4);
R1Ev = x(5);
Ev = x(6);

R2v = x(7);
R2Ev = x(8);


R1LR2v = x(9);
ER1LR2v = x(10);
R1LR2Ev = x(11);
ER1LR2Ev = x(12);

R1R2v = x(13);   % this species has been eliminated
ER1R2v = x(14);  % this species has been eliminated
R1R2Ev = x(15);  % this species has been eliminated
ER1R2Ev = x(16); % this species has been eliminated




% vesicular tubule species...
R1t = x(17);
R2t = x(18);
R1Lt = x(19);
R1R2t = x(20); % this species has been eliminated
R1LR2t = x(21);


% Lt = kappa*Lv;

% degradation species...
R1d = x(22);
R2d = x(23);
Ld = x(24);

% recycling species...
```

```
R1r = x(25);
R2r = x(26);
Lr = x(27);

%------------parameters----------
kc_het = param(1);
kc_E1 = param(2);
kc_E2 = param(3);

kc_E1_het = param(4);
kc_E2_het = param(5);

kuR1R2 = param(6);
kuR1LR2 = param(7);

kuR1E = param(8);
kuR2E = param(9);

kon = param(10);
koff = param(11);
koff_het = param(12);

kst = param(13);
ksv = param(14);

kx = param(15);
kh = param(16);

gamma = param(17); % should gamma be different for monomers and
dimers??
kappa = param(18);
xi = param(19);

Vr = param(20);
Vt = param(21);
Vv = param(22);
Vd = param(23);

keR1 = param(24);
keR2 = param(25);
keR1R2 = param(26);
keR1L = param(27);
keR1LR2 = param(28);

Nav = 6.023E23;


% vesicular species ...
% d(R1v)/dt:
y(1,1) = keR1 + koff_het*R1LR2Ev + (- kon*Lv*R1v + koff*R1Lv) - (-
kuR1E*R1Ev) + (koff_het*R1LR2v) - (gamma+ksv)*R1v;

% d(R2v)/dt:
```

```
y(7,1) = keR2 + (- kc_het*R1v*R2v + kuR1R2*R1R2v) + (- kc_het*R1Lv*R2v
+ kuR1LR2*R1LR2v) + (- kc_E2*R2v*Ev + kuR2E*R2Ev) - (kc_het*R1Ev*R2v -
kuR1R2*ER1R2v) - (kc_het*R1LEv*R2v - kuR1LR2*ER1LR2v) +
(koff_het*R1LR2v) + koff_het*ER1LR2v - (gamma+ksv)*R2v;

% d(R1R2v)/dt:
y(13,1) = 0;

% d(R1Lv)/dt:
y(2,1) = keR1L - (- kon*Lv*R1v + koff*R1Lv) + (- kc_E1*R1Lv*Ev +
kuR1E*R1LEv) + (- kc_het*R1Lv*R2v + kuR1LR2*R1LR2v) - (kc_het*R1Lv*R2Ev
- kuR1LR2*R1LR2Ev) - (gamma+ksv)*R1Lv;

% d(R1LR2v)/dt:
y(9,1) = keR1LR2 - (koff_het*R1LR2v) - (- kc_het*R1Lv*R2v +
kuR1LR2*R1LR2v) - (kc_E1_het*R1LR2v*Ev - kuR1E*ER1LR2v) -
(kc_E2_het*R1LR2v*Ev - kuR2E*R1LR2Ev) - (gamma+ksv)*R1LR2v;

% d(R1LEv)/dt:
y(3,1) = (- koff*R1LEv + kon*R1Ev*Lv) - (- kc_E1*R1Lv*Ev + kuR1E*R1LEv)
- (kc_het*R1LEv*R2v - kuR1LR2*ER1LR2v) - ksv*R1LEv;

% d(Lv)/dt:
y(4,1) = 1/(Nav*(Vv+Vt))*(xi/(1-xi)*(keR1L + keR1LR2) + (- kon*Lv*R1v +
koff*R1Lv) - (- koff*R1LEv + kon*R1Ev*Lv) + (koff_het*R1LR2v) +
(koff_het*R1LR2Ev) + (koff_het*ER1LR2v) - ksv*Lv*Vv*Nav + 1/kappa*((-
kon*kappa*Lv*R1t + koff*R1Lt) + (koff_het*R1LR2t) -
kst*kappa*Lv*Vt*Nav));


% d(R1Ev)/dt:
y(5,1) = - (- koff*R1LEv + kon*R1Ev*Lv) + (- kuR1E*R1Ev) +
koff_het*ER1LR2v - ksv*R1Ev;

% d(R2Ev)/dt:
y(8,1) =  - (- kc_E2*R2v*Ev + kuR2E*R2Ev) - (kc_het*R1Lv*R2Ev -
kuR1LR2*R1LR2Ev) + koff_het*R1LR2Ev  - ksv*R2Ev;

% d(R1R2Ev)/dt:
y(15,1) = 0;

% d(ER1R2v)/dt:
y(14,1) =  0;

% d(ER1R2Ev)/dt:
y(16,1) =  0;

% d(ER1LR2v)/dt:
y(10,1) = (kc_het*R1LEv*R2v - kuR1LR2*ER1LR2v) + (kc_E1_het*R1LR2v*Ev -
kuR1E*ER1LR2v) + (- koff_het*ER1LR2v)  - ksv*ER1LR2v;

% d(R1LR2Ev)/dt:
y(11,1) =  (- koff_het*R1LR2Ev) + (kc_E2_het*R1LR2v*Ev - kuR2E*R1LR2Ev)
+ (kc_het*R1Lv*R2Ev - kuR1LR2*R1LR2Ev) - ksv*R1LR2Ev;
```

```
% d(ER1LR2Ev)/dt:
y(12,1) =  0;

% d(Ev)/dt:
y(6,1) = (- kc_E1*R1Lv*Ev + kuR1E*R1LEv) - (- kuR1E*R1Ev) + (-
kc_E2*R2v*Ev + kuR2E*R2Ev) - (kc_E2_het*R1R2v*Ev - kuR2E*R1R2Ev)  - (-
kuR1E*ER1R2v) - (kc_E1_het*R1LR2v*Ev - kuR1E*ER1LR2v) -
(kc_E2_het*R1LR2v*Ev - kuR2E*R1LR2Ev) + ksv*(R1LEv + R1Ev + R2Ev +
ER1R2v + R1R2Ev + 2*ER1R2Ev + R1LR2Ev + ER1LR2v);

% vesicle tubule species ...
% need to allow same set of reactions as in vesicle (minus ERC
reactions) because tubule ligand concentration is assumed to be in
equilibrium with vesicle ligand concentration.

% d(R1t)/dt:
y(17,1) = (- kon*kappa*Lv*R1t + koff*R1Lt) + koff_het*R1LR2t +
gamma*R1v - kst*R1t;

% d(R2t)/dt:
y(18,1) = + (- kc_het*R1Lt*R2t + kuR1LR2*R1LR2t) + koff_het*R1LR2t +
gamma*R2v - kst*R2t;

% d(R1R2t)/dt:
y(20,1) =  0;

% d(R1Lt)/dt:
y(19,1) = - (- kon*kappa*Lv*R1t + koff*R1Lt) + (- kc_het*R1Lt*R2t +
kuR1LR2*R1LR2t) + gamma*R1Lv - kst*R1Lt;

% d(R1LR2t)/dt:
y(21,1) = (- koff_het*R1LR2t) - (- kc_het*R1Lt*R2t + kuR1LR2*R1LR2t) +
gamma*R1LR2v - kst*R1LR2t;

% degradation species...
% R1d = total EGFR in degradation compartment
% R2d = total HER2 in degradation compartment
% Ld = total ligand in degradation compartment


% d(R1d)/dt:
y(22,1) = ksv*(R1v + R1Ev + R1Lv + R1LEv + R1R2v + R1LR2v + ER1R2v +
R1R2Ev + ER1R2Ev + ER1LR2v + R1LR2Ev) - kh*R1d;

% d(R2d)/dt:
y(23,1) = ksv*(R2v + R1R2v + R1LR2v + R2Ev + ER1R2v + R1R2Ev + ER1R2Ev
+ ER1LR2v + R1LR2Ev) - kh*R2d;

% d(Ld)/dt:
y(24,1) = 1/(Nav*Vd)*(ksv*Lv*Vv*Nav + ksv*(R1Lv + R1LEv + R1LR2v +
ER1LR2v + R1LR2Ev) - kh*Ld*Vd*Nav);
```

```
% recycling species...
% R1r = total EGFR in recycling compartment
% R2r =
% Lr = total ligand in recycling compartment

% d(R1r)/dt:
y(25,1) = kst*(R1t + R1Lt + R1R2t + R1LR2t) - kx*R1r;

% d(R2r)/dt:
y(26,1) = kst*(R2t + R1R2t + R1LR2t) - kx*R2r;

% d(Lr)/dt:
y(27,1) = 1/(Nav*Vr)*(kst*Lv*kappa*Vt*Nav + kst*(R1Lt + R1LR2t) -
kx*Lr*Vr*Nav);


return;
```

A.3.4 expsortingdata.m

```
% Experimental Sorting Data
% 02.10.03

xdata_P = [504 1266 4453 13461 41478 70989 103708 105136 1052 1633 6035
18080 52556 75403 95360 99208 384 1078 3597 9230 34223 62118 114161
111443];
ydata_P = [0.628 0.645 0.598 0.588 0.561 0.542 0.528 0.519 0.606 0.625
0.598 0.588 0.549 0.537 0.532 0.519 0.616 0.583 0.573 0.563 0.538 0.520
0.508 0.496];


xdata_24H = [710 1732 7006 21583 73648 141396 172421 144166 603 1936
5176 17106 69425 129191 131306 134454 413 1398 4659 13208 60210 123694
151898 133100];
ydata_24H = [0.628 0.646 0.699 0.701 0.724 0.738 0.723 0.700 0.641
0.647 0.632 0.662 0.730 0.718 0.670 0.677 0.614 0.621 0.642 0.648 0.704
0.687 0.659 0.645];

xdata_P_2C4 = [632 1491 6266 44734 82011 145604 130409];
ydata_P_2C4 = [0.575 0.552 0.569 0.481 0.461 0.469 0.473];

xdata_24H_2C4 = [485 1416 3956 15221 60565 99139 112320 105994];
ydata_24H_2C4 = [0.664 0.612 0.622 0.606 0.602 0.560 0.499 0.485];



figure;
subplot(2,2,1);
hold on;
set(gca,'Box', 'on');
xlabel('Intracellular EGF (#/cell)', 'Fontsize', 16);
ylabel('Fraction EGF Recycled', 'Fontsize', 16);
title('Experimental Data', 'Fontsize', 16);

plot(xdata_P, ydata_P, 'ob', 'MarkerSize', 6, 'MarkerFaceColor',
'none');
plot(xdata_24H, ydata_24H, 'sr',  'MarkerSize', 6, 'MarkerFaceColor',
'none');

legend('Parental', 'HER2 clone 24H', 2);
set(gca, 'XScale', 'log');
axis([100 1000000 0.4 0.8]);
%set(gca,'XTickLabel',{10 100 1000 10000 100000 1000000}, 'FontSize',
14);
set(gca,'YTick',[0.4 0.5 0.6 0.7 0.8]);
set(gca,'YTickLabel',{0.4 0.5 0.6 0.7 0.8}, 'FontSize', 16);
set(findobj('Type','line'),'LineWidth', 3);
set(gca, 'LineWidth', 3, 'FontSize', 16);
hold off;
```

```
subplot(2,2,3);
hold on;
set(gca,'Box', 'on');
xlabel('Intracellular EGF (#/cell)', 'Fontsize', 16);
ylabel('Fraction EGF Recycled', 'Fontsize', 16);
title('Experimental Data + 2C4', 'Fontsize', 16);


plot(xdata_P, ydata_P, 'ob', 'LineWidth', 2, 'MarkerSize', 6,
'MarkerFaceColor', 'none');
plot(xdata_P_2C4, ydata_P_2C4, 'ob', 'LineWidth', 2, 'MarkerSize', 6,
'MarkerFaceColor', 'b');
plot(xdata_24H, ydata_24H, 'sr', 'LineWidth', 2, 'MarkerSize', 6,
'MarkerFaceColor', 'none');
plot(xdata_24H_2C4, ydata_24H_2C4, 'sr', 'LineWidth', 2, 'MarkerSize',
6, 'MarkerFaceColor', 'r');

legend('Parental', 'Parental + 2C4', 'HER2 clone 24H','HER2 clone 24H +
2C4', 2);
set(gca, 'XScale', 'log');
axis([100 1000000 0.4 0.8]);
%set(gca,'XTickLabel',{10 100 1000 10000 100000 1000000}, 'FontSize',
14);
set(gca,'YTick',[0.4 0.5 0.6 0.7 0.8]);
set(gca,'YTickLabel',{0.4 0.5 0.6 0.7 0.8}, 'FontSize', 16);
set(findobj('Type','line'),'LineWidth', 3);
set(gca, 'LineWidth', 3, 'FontSize', 16);
hold off;
```

A.4 Signal Deconvolution

A.4.1 SD_run.m

```
% function deconvolution_run
% last modified 03.02.24
clear;
tic;

SD_param_values; % load parameters from file

L_100 = 1.612E-8; % (M) 100 ng/ml
L_1 = 1.612E-10; % (M) 1 ng/ml

HER2internalizationEGF = [keh_P keh_12 keh_24H keh_24H keh_24H keh_P_1
keh_24H_1 keh_P keh_24H keh_P_1 keh_24H_1]; % Here we assume that 2C4
block EGFR-HER2 dimerization in the absence of EGF

ERK_data_no1min; % loads experimental ERK data (without 1 minute
timepoint)



%#################### BEGIN COMPLETE RECEPTOR TRAFFICKING MODEL
####################

parameters_EGFR(1,:)  = [kon,koff,ker,kec_P,       kxr,kxc,fxr,fxc_P,
Sr,0];       % condition 1: parental,        100 ng/ml EGF
parameters_EGFR(2,:)  = [kon,koff,ker,kec_12,      kxr,kxc,fxr,fxc_12,
Sr,0];       % condition 2: clone 12,        100 ng/ml EGF
parameters_EGFR(3,:)  = [kon,koff,ker,kec_24H,     kxr,kxc,fxr,fxc_24H,
Sr,0];       % condition 3: clone 24H,       100 ng/ml EGF
parameters_EGFR(4,:)  = [kon,koff,ker,kec_P,       kxr,kxc,fxr,fxc_P,
Sr,0];       % condition 4: parental + 2C4,  100 ng/ml EGF
parameters_EGFR(5,:)  = [kon,koff,ker,kec_24H_2C4,
kxr,kxc,fxr,fxc_24H_2C4,      Sr,0];       % condition 5: clone 24H +
2C4, 100 ng/ml EGF
parameters_EGFR(6,:)  = [kon,koff,ker,kec_P_1,     kxr,kxc,fxr,fxc_P_1,
Sr,0];       % condition  6: P,     1 ng/ml EGF
parameters_EGFR(7,:)  = [kon,koff,ker,kec_24H_1,
kxr,kxc,fxr,fxc_24H_1,        Sr,0];       % condition  7: 24H,   1
ng/ml EGF
parameters_EGFR(8,:)  = [kon,koff,ker,kec_P,
kxr,kxc,fxr,fxc_P_TGFa,       Sr,0];       % condition  8: P,   100
ng/ml TGFa
parameters_EGFR(9,:)  = [kon,koff,ker,kec_24H,
kxr,kxc,fxr,fxc_24H_TGFa,     Sr,0];       % condition  9: 24H, 100
ng/ml TGFa
```

```
parameters_EGFR(10,:) = [kon,koff,ker,kec_P_1,
kxr,kxc,fxr,fxc_P_TGFa_1,     Sr,0];       % condition  10: P,    1
ng/ml TGFa
parameters_EGFR(11,:) = [kon,koff,ker,kec_24H_1,
kxr,kxc,fxr,fxc_24H_TGFa_1,   Sr,0];       % condition  11: 24H,  1
ng/ml TGFa


parameters_HER2(1,:) =  [keh_P_NoEGF,   kxh, fxh, Sh_P];
parameters_HER2(2,:) =  [keh_12_NoEGF,  kxh, fxh, Sh_12];
parameters_HER2(3,:) =  [keh_24H_NoEGF, kxh, fxh, Sh_24H];
parameters_HER2(4,:) =  [keh_P_NoEGF,   kxh, fxh, Sh_P];
parameters_HER2(5,:) =  [keh_24H_NoEGF, kxh, fxh, Sh_24H];
parameters_HER2(6,:) =  [keh_P_NoEGF,   kxh, fxh, Sh_P];          % P,
1 ng/ml EGF
parameters_HER2(7,:) =  [keh_24H_NoEGF, kxh, fxh, Sh_24H];        %
24H,   1 ng/ml EGF
parameters_HER2(8,:) =  [keh_P_NoEGF,   kxh, fxh, Sh_P];          % P,
100 ng/ml TGFa
parameters_HER2(9,:) =  [keh_24H_NoEGF, kxh, fxh, Sh_24H];        %
24H, 100 ng/ml TGFa
parameters_HER2(10,:) = [keh_P_NoEGF,   kxh, fxh, Sh_P];          % P,
1 ng/ml TGFa
parameters_HER2(11,:) = [keh_24H_NoEGF, kxh, fxh, Sh_24H];        %
24H,   1 ng/ml TGFa


NumberOfConditions = 11; % this specifies the number of conditions to
run through ...


EGFRLevel = 300000; % this is the total EGFR number (roughly the same
for all cells)
HER2Level = 1.11*[30000 200000 600000 30000 600000 30000 600000 30000
600000 30000 600000]; %estimate of the total HER2 level on each cell
for each condition

init_tsteps = 20;
init_tmax = 2000;
init_tspan = linspace(0,init_tmax,init_tsteps);

tmax = 300;
tspan = [linspace(0, 0.5, 20) linspace(0.6, 1, 10) linspace(2,60,59)
linspace(75,300,16)]; %IF YOU CHANGE THIS YOU NEED TO CHANGE INDICES
FOR THE SIGNALING TIMEPOINTS!!
timepoints = [1 34 44 59 89 93]; %corresponds to 0, 5, 15, 30, 60, 120
tsteps = size(tspan,2);

figure;

for i=1:NumberOfConditions
    fprintf('Condition: %1.0f\n', i);
    % this part calculates receptor levels and distribution in the
absence
```

```
    % of EGF as input for the + EGF case...
    pre_initcond_EGFR = [EGFRLevel/2;0;EGFRLevel/2;0];
    pre_initcond_HER2 = [HER2Level(i)*0.9;HER2Level(i)*0.1];

    [t,y]=ode23s('EGFRmodel_ode', init_tspan, pre_initcond_EGFR, [],
parameters_EGFR(i,:));
    [t_HER2, y_HER2] = ode23s('HER2model_ode', init_tspan,
pre_initcond_HER2, [], parameters_HER2(i,:));

    init_Rs = y(:,1);
    init_Cs = y(:,2);
    init_Ri = y(:,3);
    init_Ci = y(:,4);
    init_Hs = y_HER2(:,1);
    init_Hi = y_HER2(:,2);

    initcond_EGFR(:,i) = [init_Rs(init_tsteps); init_Cs(init_tsteps);
init_Ri(init_tsteps); init_Ci(init_tsteps)];
    initcond_HER2(:,i) = [init_Hs(init_tsteps); init_Hi(init_tsteps)];

    fprintf('Initial surface EGFR level: %1.0f\n',
init_Rs(init_tsteps)+init_Cs(init_tsteps));
    fprintf('Initial surface HER2 level: %1.0f\n',
init_Hs(init_tsteps));


    % this part calculates the timecourses of EGFR and HER2 levels and
    % inside surface distributions using the global trafficking model.
    if ((i == 6) || (i == 7) || (i == 10) || (i== 11))
        parameters_EGFR(i,10) = L_1;   % set appropriate ligand
concentration for each condition
    else
        parameters_EGFR(i,10) = L_100;
    end;

    if i == 5
        parameters_EGFR(i,6) = kxc_2C4;
    else
    end;

    parameters_HER2(i,1) = HER2internalizationEGF(i);

    [t,y]=ode23s('EGFRmodel_ode', tspan, initcond_EGFR(:,i), [],
parameters_EGFR(i,:));
    [t_HER2,y_HER2]=ode23s('HER2model_ode', tspan, initcond_HER2(:,i),
[], parameters_HER2(i,:));
    Rs(:,i) = y(:,1);
      Cs(:,i) = y(:,2);
      Ri(:,i) = y(:,3);
      Ci(:,i) = y(:,4);
    Hs(:,i) = y_HER2(:,1);
    Hi(:,i) = y_HER2(:,2);

    RItmax = 20;
```

```
    RItspan = linspace(0,10,10);
    RItsteps = size(RItspan,2);

    fprintf('Running Receptor Interaction Module ...\n\n');
    for j=1:size(tspan,2)
        % this part takes the total receptor predictions from the
global
        % model and uses them as input into the receptor interaction
module
        % to make predictions of the distribution of each receptor
species
        % as a function of time.

        RI_surface_input = [Rs(j,i); Hs(j,i); 0;0;0; Cs(j,i); 0;0;0];
        RI_inside_input =  [Ri(j,i); Hi(j,i); 0;0;0; Ci(j,i); 0;0;0];
        if ((i == 6) || (i == 7) || (i == 10) || (i== 11))
            RI_parameters = [kc kuR2R2 kuR1R2 kuR1R1 kuR1LR2 kuLR1R1L
kon koff L_1];   % set appropriate ligand concentration for each
condition
        else
            RI_parameters = [kc kuR2R2 kuR1R2 kuR1R1 kuR1LR2 kuLR1R1L
kon koff L_100];
        end;
        [RIt,z_surface] = ode23s('RImodel_ode_v2', RItspan,
RI_surface_input, [], RI_parameters);
        [RIt,z_inside] = ode23s('RImodel_ode_v2', RItspan,
RI_inside_input, [], RI_parameters);

        R1s(j,i) = z_surface(RItsteps,1);
        R2s(j,i) = z_surface(RItsteps,2);
        R1R1s(j,i) = z_surface(RItsteps,3);
        R1R2s(j,i) = z_surface(RItsteps,4);
        R2R2s(j,i) = z_surface(RItsteps,5);
        R1Ls(j,i) = z_surface(RItsteps,6);
        R1LR2s(j,i) = z_surface(RItsteps,7);
        R1R1Ls(j,i) = z_surface(RItsteps,8);
        LR1R1Ls(j,i) = z_surface(RItsteps,9);
        SurfaceHeterodimers(j,i) = R1LR2s(j,i);
        SurfaceComplexes(j,i) = R1Ls(j,i) + R1R1Ls(j,i) +
2*LR1R1Ls(j,i);
        SurfaceHomodimers(j,i) = LR1R1Ls(j,i);

        R1i(j,i) = z_inside(RItsteps,1);
        R2i(j,i) = z_inside(RItsteps,2);
        R1R1i(j,i) = z_inside(RItsteps,3);
        R1R2i(j,i) = z_inside(RItsteps,4);
        R2R2i(j,i) = z_inside(RItsteps,5);
        R1Li(j,i) = z_inside(RItsteps,6);
        R1LR2i(j,i) = z_inside(RItsteps,7);
        R1R1Li(j,i) = z_inside(RItsteps,8);
        LR1R1Li(j,i) = z_inside(RItsteps,9);
        InsideHeterodimers(j,i) = R1LR2i(j,i);
        InsideComplexes(j,i) = R1Li(j,i) + R1R1Li(j,i) +
2*LR1R1Li(j,i);
```

```
        InsideHomodimers(j,i) = LR1R1Li(j,i);
    end;


    % this keeps track of surface & total complexes at timepoints:
0,5,15,30,60,120,210,300 min for comparison with ERK signaling data
    for j = 1:size(timepoints,2)
        SurfaceComplexes_ERKtimepts(j,i) =
SurfaceComplexes(timepoints(j),i);
        InsideComplexes_ERKtimepts(j,i) =
InsideComplexes(timepoints(j),i);
        SurfaceHeterodimers_ERKtimepts(j,i) =
SurfaceHeterodimers(timepoints(j),i);
        InsideHeterodimers_ERKtimepts(j,i) =
InsideHeterodimers(timepoints(j),i);
        Homodimers_ERKtimepts(j,i) =
SurfaceHomodimers(timepoints(j),i)+InsideHomodimers(timepoints(j),i);
% these are pure homodimers: LR1R1L


        % These are the actively signaling her2....
        active_HER2_total(j,i) = SurfaceHeterodimers_ERKtimepts(j,i) +
InsideHeterodimers_ERKtimepts(j,i);
        Heterodimers_total(j,i) = SurfaceHeterodimers_ERKtimepts(j,i) +
InsideHeterodimers_ERKtimepts(j,i);

        %************************************
        %THIS IS IMPORTANT!!
        %pick one of these two:
        %(1) Total homodimers = (R1L + R1R1L + 2*LR1R1L)/2
        %Homodimers_total(j,i) = (SurfaceComplexes_ERKtimepts(j,i) +
InsideComplexes_ERKtimepts(j,i))/2;
        %Total_complexes_ERKtimepts(j,i) =
SurfaceComplexes_ERKtimepts(j,i) + InsideComplexes_ERKtimepts(j,i) +
SurfaceHeterodimers_ERKtimepts(j,i) +
InsideHeterodimers_ERKtimepts(j,i);

        %(2) Total homodimers = LR1R1L  ... this implies only LR1R1L
can
        %signal and not R1R1L or R1L; Total complexes signaling =
2*LR1R1L + R1LR2
        Homodimers_total(j,i) = Homodimers_ERKtimepts(j,i);
        Total_complexes_ERKtimepts(j,i) =
2*Homodimers_ERKtimepts(j,i)+Heterodimers_total(j,i);
        %****************************************



    end;


end;
```

```
%#################### END COMPLETE RECEPTOR TRAFFICKING MODEL
#####################



%**************************************************************************
*************
%**************************************************************************
*************
%******************** BEGIN SIGNALING ANALYSIS PORTION OF CODE
**********************
%**************************************************************************
*************
%**************************************************************************
*************



fprintf('Doing Receptor/Signaling Analysis...\n');

% This part predicts the relative signal for expt and model predictions
% between P & 24H assuming an equal signal generated by EGFR & HER2


for k = 1:size(timepoints,2)
    % Do Error for these!!
    % 100 ng/ml EGF:
    RelativeSignal_expt_100E(k) = ERK_24H(k)/ERK_P(k);
    RelativeSignal_expt_100E_stdev(k) =
sqrt((1/ERK_24H(k))^2*(ERK_P_stdev(k))^2+(-
ERK_P(k)/(ERK_24H(k))^2)^2*(ERK_24H_stdev(k))^2);
    RelativeSignal_predicted_100E(k) =
(Homodimers_total(k,3)+Heterodimers_total(k,3))/(Homodimers_total(k,1)+
Heterodimers_total(k,1));

    %   1 ng/ml EGF:
    RelativeSignal_expt_1E(k) = ERK_24H_1(k)/ERK_P_1(k);
    RelativeSignal_expt_1E_stdev(k) =
sqrt((1/ERK_24H_1(k))^2*(ERK_P_1_stdev(k))^2+(-
ERK_P_1(k)/(ERK_24H_1(k))^2)^2*(ERK_24H_1_stdev(k))^2);
    RelativeSignal_predicted_1E(k) =
(Homodimers_total(k,7)+Heterodimers_total(k,7))/(Homodimers_total(k,6)+
Heterodimers_total(k,6));

    % 100 ng/ml TGFa:
    RelativeSignal_expt_100T(k) = ERK_24H_TGF_100(k)/ERK_P_TGF_100(k);
    RelativeSignal_predicted_100T(k) =
(Homodimers_total(k,9)+Heterodimers_total(k,9))/(Homodimers_total(k,8)+
Heterodimers_total(k,8));

    %   1 ng/ml TGFa:
    RelativeSignal_expt_1T(k) = ERK_24H_TGF_1(k)/ERK_P_TGF_1(k);
```

```
    RelativeSignal_predicted_1T(k) =
(Homodimers_total(k,11)+Heterodimers_total(k,11))/(Homodimers_total(k,1
0)+Heterodimers_total(k,10));
end;

% Calculate Signal per active EGFR and signal per active HER2 based on
% parental & clone 24H ERK data and receptor numbers from models

SignalPerEGFR(1) = 0;
SignalPerHER2(1) = 0;
SignalPerHomodimer(1) = 0;
SignalPerHeterodimer(1) = 0;
Signal_24H_2C4_comparison(1) = 0;
SignalPerEGFR_stdev(1) = 0;
SignalPerHER2_stdev(1) = 0;
SignalPerHomodimer_stdev(1) = 0;
SignalPerHeterodimer_stdev(1) = 0;

for i = 2:size(timepoints,2)
    %************************************************
    % WHAT HAPPENS IF WE INCLUDE SIGNALING FROM HER2 HOMODIMERS?? --
THE
    % SIGNAL COMING FROM THESE IS A BACKGROUND SIGNAL THAT IS PRESENT
WITH
    % OR WITHOUT EGF STMULATION - THEREFORE WE HAVE LEFT IT OUT OF THE
    % MODEL...
    %************************************************

    % Calculate signal per EGFR and signal per HER2 for 100 ng/ml EGF
    % this uses NON-Integrated ERK and Non-Integrated receptor number
...
    SignalPerHER2(i) = (ERK_data(i,3) -
Total_complexes_ERKtimepts(i,3)*ERK_data(i,1)/Total_complexes_ERKtimept
s(i,1))/active_HER2_total(i,3)/(1-
Total_complexes_ERKtimepts(i,3)*active_HER2_total(i,1)/active_HER2_tota
l(i,3)/Total_complexes_ERKtimepts(i,1));
    SignalPerEGFR(i) = (ERK_data(i,1)-
active_HER2_total(i,1)*SignalPerHER2(i))/Total_complexes_ERKtimepts(i,1
);



    % this calculates the error for the SignalPerEGFR and SignalPerHER2
    % based solely on ERK data error (and NOT model prediction errors)
    % alpha = Signal Per EGFR
    % beta = Signal Per HER2
    % Sp = Parental ERK Signal
    % Sh = 24H ERk Signal

    dalpha_dSp(i) =
1/Total_complexes_ERKtimepts(i,1)+(active_HER2_total(i,1)/Total_complex
es_ERKtimepts(i,1)*Total_complexes_ERKtimepts(i,3)/Total_complexes_ERKt
imepts(i,1))/(active_HER2_total(i,3)-
```

```
Total_complexes_ERKtimepts(i,3)*active_HER2_total(i,1)/Total_complexes_
ERKtimepts(i,1));
    dalpha_dSh(i) = -
active_HER2_total(i,1)/(Total_complexes_ERKtimepts(i,1)*(active_HER2_to
tal(i,3)-
Total_complexes_ERKtimepts(i,3)*active_HER2_total(i,1)/Total_complexes_
ERKtimepts(i,1)));
    dbeta_dSp(i) = -
Total_complexes_ERKtimepts(i,3)/(Total_complexes_ERKtimepts(i,1)*(activ
e_HER2_total(i,3)-
Total_complexes_ERKtimepts(i,3)*active_HER2_total(i,1)/Total_complexes_
ERKtimepts(i,1)));
    dbeta_dSh(i) = 1/(active_HER2_total(i,3)-
Total_complexes_ERKtimepts(i,3)*active_HER2_total(i,1)/Total_complexes_
ERKtimepts(i,1));


    SignalPerEGFR_stdev(i) =
sqrt((dalpha_dSp(i)*ERK_P_stdev(i))^2+(dalpha_dSh(i)*ERK_24H_stdev(i))^
2);
    SignalPerHER2_stdev(i) =
sqrt((dbeta_dSp(i)*ERK_P_stdev(i))^2+(dbeta_dSh(i)*ERK_24H_stdev(i))^2)
;


    %-----------------------
    % These are the signal generated through each receptor as a
function of
    % time for the various cells & treatments...

    % based on non-integrated signal per cell:
    SignalThruEGFR_P(i) =
SignalPerEGFR(i)*Total_complexes_ERKtimepts(i,1);
    SignalThruEGFR_24H(i) =
SignalPerEGFR(i)*Total_complexes_ERKtimepts(i,3);
    SignalThruEGFR_24H_2C4(i) =
SignalPerEGFR(i)*Total_complexes_ERKtimepts(i,5);
    SignalThruHER2_P(i) = SignalPerHER2(i)*active_HER2_total(i,1);
    SignalThruHER2_24H(i) = SignalPerHER2(i)*active_HER2_total(i,3);
    SignalThruEGFR_12(i) =
SignalPerEGFR(i)*Total_complexes_ERKtimepts(i,2);
    SignalThruHER2_12(i) = SignalPerHER2(i)*active_HER2_total(i,2);
    TotalSignalPrediction_12(i) = SignalThruEGFR_12(i) +
SignalThruHER2_12(i);


    TraffickingContribution(i) = (SignalThruEGFR_24H(i)-
SignalThruEGFR_P(i));
    SignalingContribution(i) = (SignalThruHER2_24H(i) -
SignalThruHER2_P(i));
    PercentTrafficking(i) =
TraffickingContribution(i)/(TraffickingContribution(i)+SignalingContrib
ution(i))*100;
```

```
    PercentTotalSignal_P(i) =
SignalThruHER2_P(i)/(SignalThruHER2_P(i)+SignalThruEGFR_P(i))*100;
    PercentTotalSignal_24H(i) =
SignalThruHER2_24H(i)/(SignalThruHER2_24H(i)+SignalThruEGFR_24H(i))*100
;

    %================================================================
    % This portion calculates the signal per EGFR homodimer and per
    % EGFR-HER2 heterodimer for comparison with per EGFR and per HER2
    % result.

    % this uses NON-Integrated ERK and Non-Integrated receptor number
...
    SignalPerHeterodimer(i) = (ERK_data(i,3) -
Homodimers_total(i,3)/Homodimers_total(i,1)*ERK_data(i,1))/(-
Homodimers_total(i,3)/Homodimers_total(i,1)*Heterodimers_total(i,1)+Het
erodimers_total(i,3));
    SignalPerHomodimer(i) = (ERK_data(i,1)-
Heterodimers_total(i,1)*SignalPerHeterodimer(i))/(Homodimers_total(i,1)
);

    % this calculates the error for the SignalPerEGFR and SignalPerHER2
    % based solely on ERK data error (and NOT model prediction errors)
    % gamma = Signal Per Homodimer
    % delta = Signal Per Heterodimer
    % Sp = Parental ERK Signal
    % Sh = 24H ERk Signal

    dgamma_dSp(i) =
1/Homodimers_total(i,1)+(Heterodimers_total(i,1)/Homodimers_total(i,1)*
Homodimers_total(i,3)/Homodimers_total(i,1))/(Heterodimers_total(i,3)-
Homodimers_total(i,3)*Heterodimers_total(i,1)/Homodimers_total(i,1));
    dgamma_dSh(i) = -
Heterodimers_total(i,1)/(Homodimers_total(i,1)*(Heterodimers_total(i,3)
-Homodimers_total(i,3)*Heterodimers_total(i,1)/Homodimers_total(i,1)));
    ddelta_dSp(i) = -
Homodimers_total(i,3)/(Homodimers_total(i,1)*(Heterodimers_total(i,3)-
Homodimers_total(i,3)*Heterodimers_total(i,1)/Homodimers_total(i,1)));
    ddelta_dSh(i) = 1/(Heterodimers_total(i,3)-
Homodimers_total(i,3)*Heterodimers_total(i,1)/Homodimers_total(i,1));


    SignalPerHomodimer_stdev(i) =
sqrt((dgamma_dSp(i)*ERK_P_stdev(i))^2+(dgamma_dSh(i)*ERK_24H_stdev(i))^
2);
    SignalPerHeterodimer_stdev(i) =
sqrt((ddelta_dSp(i)*ERK_P_stdev(i))^2+(ddelta_dSh(i)*ERK_24H_stdev(i))^
2);
    %================================================================


    %################## BEGIN calculations for 1 ng/ml EGF
####################
```

```
    SignalPerHER2_1(i) = (ERK_data(i,7) -
Total_complexes_ERKtimepts(i,7)*ERK_data(i,6)/Total_complexes_ERKtimept
s(i,6))/active_HER2_total(i,7)/(1-
Total_complexes_ERKtimepts(i,7)*active_HER2_total(i,6)/active_HER2_tota
l(i,7)/Total_complexes_ERKtimepts(i,6));
    SignalPerEGFR_1(i) = (ERK_data(i,6)-
active_HER2_total(i,6)*SignalPerHER2_1(i))/Total_complexes_ERKtimepts(i
,6);
    % this calculates the error for the SignalPerEGFR and SignalPerHER2
    % based solely on ERK data error (and NOT model prediction errors)
    % alpha = Signal Per EGFR
    % beta = Signal Per HER2
    % Sp = Parental ERK Signal
    % Sh = 24H ERk Signal
    dalpha_dSp_1(i) =
1/Total_complexes_ERKtimepts(i,6)+(active_HER2_total(i,6)/Total_complex
es_ERKtimepts(i,6)*Total_complexes_ERKtimepts(i,7)/Total_complexes_ERKt
imepts(i,6))/(active_HER2_total(i,7)-
Total_complexes_ERKtimepts(i,7)*active_HER2_total(i,6)/Total_complexes_
ERKtimepts(i,6));
    dalpha_dSh_1(i) = -
active_HER2_total(i,6)/(Total_complexes_ERKtimepts(i,6)*(active_HER2_to
tal(i,7)-
Total_complexes_ERKtimepts(i,7)*active_HER2_total(i,6)/Total_complexes_
ERKtimepts(i,6)));
    dbeta_dSp_1(i) = -
Total_complexes_ERKtimepts(i,7)/(Total_complexes_ERKtimepts(i,6)*(activ
e_HER2_total(i,7)-
Total_complexes_ERKtimepts(i,7)*active_HER2_total(i,6)/Total_complexes_
ERKtimepts(i,6)));
    dbeta_dSh_1(i) = 1/(active_HER2_total(i,7)-
Total_complexes_ERKtimepts(i,7)*active_HER2_total(i,6)/Total_complexes_
ERKtimepts(i,6));

    SignalPerEGFR_stdev_1(i) =
sqrt((dalpha_dSp_1(i)*ERK_P_1_stdev(i))^2+(dalpha_dSh_1(i)*ERK_24H_1_st
dev(i))^2);
    SignalPerHER2_stdev_1(i) =
sqrt((dbeta_dSp_1(i)*ERK_P_1_stdev(i))^2+(dbeta_dSh_1(i)*ERK_24H_1_stde
v(i))^2);
    %------------
    SignalPerHeterodimer_1(i) = (ERK_data(i,7) -
Homodimers_total(i,7)/Homodimers_total(i,6)*ERK_data(i,6))/(-
Homodimers_total(i,7)/Homodimers_total(i,6)*Heterodimers_total(i,6)+Het
erodimers_total(i,7));
    SignalPerHomodimer_1(i) = (ERK_data(i,6)-
Heterodimers_total(i,6)*SignalPerHeterodimer(i))/(Homodimers_total(i,6)
);
    % this calculates the error for the SignalPerEGFR and SignalPerHER2
    % based solely on ERK data error (and NOT model prediction errors)
    % gamma = Signal Per Homodimer
    % delta = Signal Per Heterodimer
    % Sp = Parental ERK Signal
    % Sh = 24H ERk Signal
```

```
    dgamma_dSp_1(i) =
1/Homodimers_total(i,6)+(Heterodimers_total(i,6)/Homodimers_total(i,6)*
Homodimers_total(i,7)/Homodimers_total(i,6))/(Heterodimers_total(i,7)-
Homodimers_total(i,7)*Heterodimers_total(i,6)/Homodimers_total(i,6));
    dgamma_dSh_1(i) = -
Heterodimers_total(i,6)/(Homodimers_total(i,6)*(Heterodimers_total(i,7)
-Homodimers_total(i,7)*Heterodimers_total(i,6)/Homodimers_total(i,6)));
    ddelta_dSp_1(i) = -
Homodimers_total(i,7)/(Homodimers_total(i,6)*(Heterodimers_total(i,7)-
Homodimers_total(i,7)*Heterodimers_total(i,6)/Homodimers_total(i,6)));
    ddelta_dSh_1(i) = 1/(Heterodimers_total(i,7)-
Homodimers_total(i,7)*Heterodimers_total(i,6)/Homodimers_total(i,6));


    SignalPerHomodimer_stdev_1(i) =
sqrt((dgamma_dSp_1(i)*ERK_P_1_stdev(i))^2+(dgamma_dSh_1(i)*ERK_24H_1_st
dev(i))^2);
    SignalPerHeterodimer_stdev_1(i) =
sqrt((ddelta_dSp_1(i)*ERK_P_1_stdev(i))^2+(ddelta_dSh_1(i)*ERK_24H_1_st
dev(i))^2);
    %################### END calculations for 1 ng/ml EGF
#####################

    %******************** model prediction of dogma beta = 2*alpha vs
beta = 0.5*alpha
    AverageSignal(i) = (SignalPerEGFR(i)+SignalPerHER2(i))*0.5;
    Dogma_2alpha_P(i) =
AverageSignal(i)*Total_complexes_ERKtimepts(i,1)+2*AverageSignal(i)*act
ive_HER2_total(i,1);
    Dogma_2alpha_24H(i) =
AverageSignal(i)*Total_complexes_ERKtimepts(i,3)+2*AverageSignal(i)*act
ive_HER2_total(i,3);
    Dogma_alpha_24H(i) =
AverageSignal(i)*Total_complexes_ERKtimepts(i,3)+1*AverageSignal(i)*act
ive_HER2_total(i,3);
    Dogma_halfalpha_P(i) =
AverageSignal(i)*Total_complexes_ERKtimepts(i,1)+0.5*AverageSignal(i)*a
ctive_HER2_total(i,1);
    Dogma_halfalpha_24H(i) =
AverageSignal(i)*Total_complexes_ERKtimepts(i,3)+0.5*AverageSignal(i)*a
ctive_HER2_total(i,3);



end;



%-------------------------------------------------------------------------
-----------------------------------------------
%-------------------------------------------------------------------------
-----------------------------------------------
```

```
%-------------------------------------------------------------------------
-----------------------------------------
% Figures...
%-------------------------------------------------------------------------
-----------------------------------------
%-------------------------------------------------------------------------
-----------------------------------------
%-------------------------------------------------------------------------
-----------------------------------------

figure; % WE CAN PREDICT A WHOLE BUNCH OF JUNK....
hold on;
i = 2; % clone #12
plot(t, R1LR2s(:,i), 'c'); % surface heterodimers
plot(t, LR1R1Ls(:,i), 'g'); % surface homodimers
plot(t, R1s(:,i)+2*R1R1s(:,i)+R1R2s(:,i), 'b'); % surface unbound EGFR
plot(t, R2s(:,i)+R1R2s(:,i)+2*R2R2s(:,i), 'r'); % surface free HER2
plot(t, R2s(:,i)+R1R2s(:,i)+2*R2R2s(:,i)+R1LR2s(:,i), 'm'); % total
surface HER2
plot(t,
R1s(:,i)+2*R1R1s(:,i)+R1R2s(:,i)+R1Ls(:,i)+2*R1R1Ls(:,i)+2*LR1R1Ls(:,i)
, 'k'); % total surface EGFR

plot(t, R1LR2i(:,i), 'c--'); % inside heterodimers
plot(t, LR1R1Li(:,i), 'g--'); % inside homodimers
plot(t, R1i(:,i)+2*R1R1i(:,i)+R1R2i(:,i), 'b--'); % inside unbound EGFR
plot(t, R2i(:,i)+R1R2i(:,i)+2*R2R2i(:,i), 'r--'); % inside free HER2
plot(t, R2i(:,i)+R1R2i(:,i)+2*R2R2i(:,i)+R1LR2i(:,i), 'm--'); % total
inside HER2
plot(t,
R1i(:,i)+2*R1R1i(:,i)+R1R2i(:,i)+R1Li(:,i)+2*R1R1Li(:,i)+2*LR1R1Li(:,i)
, 'k--'); % total inside EGFR

xlabel('time (min)', 'FontSize', 20);
ylabel('#/cell', 'FontSize', 20);
axis([0 120 0 250000]);
set(gca,'XTick',[0 20 40 60 80 100 120]);
set(gca,'XTick',[0 20 40 60 80 100 120]);
set(gca, 'YScale', 'linear');
set(gca,'Box', 'on');
set(gca, 'LineWidth', 3, 'FontSize', 20);
set(findobj('Type','line'),'LineWidth', 3);
hold off;


figure; % Comparison of EGFR/HER2 to convince Dane we've got it correct
subplot(2,2,1);
hold on;
i = 1; % PARENTAL
plot(t, R1LR2s(:,i), 'r'); % surface HER2 signaling
plot(t, 2*LR1R1Ls(:,i)+R1LR2s(:,i), 'b'); % surface EGFR signaling
plot(t, R1LR2i(:,i), 'r--'); % surface HER2 signaling
plot(t, 2*LR1R1Li(:,i)+R1LR2i(:,i), 'b--'); % surface EGFR signaling
```

```
plot(t,
2*LR1R1Ls(:,i)+R1LR2s(:,i)+2*LR1R1Li(:,i)+R1LR2i(:,i)+R1LR2s(:,i)+R1LR2
i(:,i), 'm'); % total EGFR+HER2 signaling

xlabel('time (min)', 'FontSize', 20);
ylabel('#/cell', 'FontSize', 20);
title('Parental: 100 ng/ml EGF', 'FontSize', 20);
h = legend('HER2 (s)', 'EGFR (s)', 'HER2 (i)', 'EGFR (i)', 'Total', 1);
% set(h, 'FontSize', 16); %change font size of legend
axis([0 120 0 400000]);
set(gca,'XTick',[0 20 40 60 80 100 120]);
set(gca, 'YScale', 'linear');
set(gca,'Box', 'on');
set(gca, 'LineWidth', 3, 'FontSize', 20);
set(findobj('Type','line'),'LineWidth', 3);
hold off;

subplot(2,2,2);
hold on;
i = 3; % CLONE 24H
plot(t, R1LR2s(:,i), 'r'); % surface HER2 signaling
plot(t, 2*LR1R1Ls(:,i)+R1LR2s(:,i), 'b'); % surface EGFR signaling
plot(t, R1LR2i(:,i), 'r--'); % surface HER2 signaling
plot(t, 2*LR1R1Li(:,i)+R1LR2i(:,i), 'b--'); % surface EGFR signaling
plot(t,
2*LR1R1Ls(:,i)+R1LR2s(:,i)+2*LR1R1Li(:,i)+R1LR2i(:,i)+R1LR2s(:,i)+R1LR2
i(:,i), 'm'); % total EGFR+HER2 signaling

xlabel('time (min)', 'FontSize', 20);
ylabel('#/cell', 'FontSize', 20);
title('clone 24H: 100 ng/ml EGF', 'FontSize', 20);
h = legend('HER2 (s)', 'EGFR (s)', 'HER2 (i)', 'EGFR (i)', 'Total', 1);
% set(h, 'FontSize', 16); %change font size of legend
axis([0 120 0 400000]);
set(gca,'XTick',[0 20 40 60 80 100 120]);
set(gca, 'YScale', 'linear');
set(gca,'Box', 'on');
set(gca, 'LineWidth', 3, 'FontSize', 20);
set(findobj('Type','line'),'LineWidth', 3);
hold off;

subplot(2,2,3);
hold on;
i = 6; % PARENTAL
plot(t, R1LR2s(:,i), 'r'); % surface HER2 signaling
plot(t, 2*LR1R1Ls(:,i)+R1LR2s(:,i), 'b'); % surface EGFR signaling
plot(t, R1LR2i(:,i), 'r--'); % surface HER2 signaling
plot(t, 2*LR1R1Li(:,i)+R1LR2i(:,i), 'b--'); % surface EGFR signaling
plot(t,
2*LR1R1Ls(:,i)+R1LR2s(:,i)+2*LR1R1Li(:,i)+R1LR2i(:,i)+R1LR2s(:,i)+R1LR2
i(:,i), 'm'); % total EGFR+HER2 signaling

xlabel('time (min)', 'FontSize', 20);
ylabel('#/cell', 'FontSize', 20);
```

```
title('Parental: 1 ng/ml EGF', 'FontSize', 20);
h = legend('HER2 (s)', 'EGFR (s)', 'HER2 (i)', 'EGFR (i)', 'Total', 1);
% set(h, 'FontSize', 16); %change font size of legend
axis([0 120 0 60000]);
set(gca,'XTick',[0 20 40 60 80 100 120]);
set(gca, 'YScale', 'linear');
set(gca,'Box', 'on');
set(gca, 'LineWidth', 3, 'FontSize', 20);
set(findobj('Type','line'),'LineWidth', 3);
hold off;

subplot(2,2,4);
hold on;
i = 7; % CLONE 24H
plot(t, R1LR2s(:,i), 'r'); % surface HER2 signaling
plot(t, 2*LR1R1Ls(:,i)+R1LR2s(:,i), 'b'); % surface EGFR signaling
plot(t, R1LR2i(:,i), 'r--'); % surface HER2 signaling
plot(t, 2*LR1R1Li(:,i)+R1LR2i(:,i), 'b--'); % surface EGFR signaling
plot(t,
2*LR1R1Ls(:,i)+R1LR2s(:,i)+2*LR1R1Li(:,i)+R1LR2i(:,i)+R1LR2s(:,i)+R1LR2
i(:,i), 'm'); % total EGFR+HER2 signaling

xlabel('time (min)', 'FontSize', 20);
ylabel('#/cell', 'FontSize', 20);
title('clone 24H: 1 ng/ml EGF', 'FontSize', 20);
h = legend('HER2 (s)', 'EGFR (s)', 'HER2 (i)', 'EGFR (i)', 'Total', 1);
% set(h, 'FontSize', 16); %change font size of legend
axis([0 120 0 60000]);
set(gca,'XTick',[0 20 40 60 80 100 120]);
set(gca, 'YScale', 'linear');
set(gca,'Box', 'on');
set(gca, 'LineWidth', 3, 'FontSize', 20);
set(findobj('Type','line'),'LineWidth', 3);
hold off;

figure; % Comparison of homo/heterodimers to convince Dane we've got it
correct
subplot(2,2,1);
hold on;
i = 1; % PARENTAL
plot(t, LR1R1Ls(:,i), 'g'); % surface homodimers
plot(t, R1LR2s(:,i), 'c'); % surface heterodimers
plot(t, LR1R1Li(:,i), 'g--'); % inside homodimers
plot(t, R1LR2i(:,i), 'c--'); % inside heterodimers
plot(t, R1LR2s(:,i)+LR1R1Ls(:,i)+R1LR2i(:,i)+LR1R1Li(:,i), 'k'); %
Total receptors signaling

xlabel('time (min)', 'FontSize', 20);
ylabel('#/cell', 'FontSize', 20);
title('Parental: 100 ng/ml EGF', 'FontSize', 20);
h = legend('Homodimers (s)','Heterodimers (s)', 'Homodimers (i)',
'Heterodimers (i)', 'Total', 1);
axis([0 120 0 400000]);
set(gca,'XTick',[0 20 40 60 80 100 120]);
```

```
%set(h, 'FontSize', 16); %change font size of legend
set(gca, 'YScale', 'linear');
set(gca,'Box', 'on');
set(gca, 'LineWidth', 3, 'FontSize', 20);
set(findobj('Type','line'),'LineWidth', 3);
hold off;

subplot(2,2,2);
hold on;
i = 3; % CLONE 24H
plot(t, LR1R1Ls(:,i), 'g'); % surface homodimers
plot(t, R1LR2s(:,i), 'c'); % surface heterodimers
plot(t, LR1R1Li(:,i), 'g--'); % inside homodimers
plot(t, R1LR2i(:,i), 'c--'); % inside heterodimers
plot(t, R1LR2s(:,i)+LR1R1Ls(:,i)+R1LR2i(:,i)+LR1R1Li(:,i), 'k'); %
Total receptors signaling

xlabel('time (min)', 'FontSize', 20);
ylabel('#/cell', 'FontSize', 20);
title('clone 24H: 100 ng/ml EGF', 'FontSize', 20);
h = legend('Homodimers (s)','Heterodimers (s)', 'Homodimers (i)',
'Heterodimers (i)', 'Total', 1);
% set(h, 'FontSize', 16); %change font size of legend
axis([0 120 0 400000]);
set(gca,'XTick',[0 20 40 60 80 100 120]);
set(gca, 'YScale', 'linear');
set(gca,'Box', 'on');
set(gca, 'LineWidth', 3, 'FontSize', 20);
set(findobj('Type','line'),'LineWidth', 3);
hold off;

subplot(2,2,3);
hold on;
i = 6; % PARENTAL - 1 ng/ml EGF
plot(t, LR1R1Ls(:,i), 'g'); % surface homodimers
plot(t, R1LR2s(:,i), 'c'); % surface heterodimers
plot(t, LR1R1Li(:,i), 'g--'); % inside homodimers
plot(t, R1LR2i(:,i), 'c--'); % inside heterodimers
plot(t, R1LR2s(:,i)+LR1R1Ls(:,i)+R1LR2i(:,i)+LR1R1Li(:,i), 'k'); %
Total receptors signaling

xlabel('time (min)', 'FontSize', 20);
ylabel('#/cell', 'FontSize', 20);
title('Parental: 1 ng/ml EGF', 'FontSize', 20);
h = legend('Homodimers (s)','Heterodimers (s)', 'Homodimers (i)',
'Heterodimers (i)', 'Total', 1);

axis([0 120 0 60000]);
set(gca,'XTick',[0 20 40 60 80 100 120]);
%set(h, 'FontSize', 16); %change font size of legend
set(gca, 'YScale', 'linear');
set(gca,'Box', 'on');
set(gca, 'LineWidth', 3, 'FontSize', 20);
set(findobj('Type','line'),'LineWidth', 3);
```

```
hold off;

subplot(2,2,4);
hold on;
i = 7; % CLONE 24H - 1 gn/ml EGF
plot(t, LR1R1Ls(:,i), 'g'); % surface homodimers
plot(t, R1LR2s(:,i), 'c'); % surface heterodimers
plot(t, LR1R1Li(:,i), 'g--'); % inside homodimers
plot(t, R1LR2i(:,i), 'c--'); % inside heterodimers
plot(t, R1LR2s(:,i)+LR1R1Ls(:,i)+R1LR2i(:,i)+LR1R1Li(:,i), 'k'); %
Total receptors signaling

xlabel('time (min)', 'FontSize', 20);
ylabel('#/cell', 'FontSize', 20);
title('clone 24H: 1 ng/ml EGF', 'FontSize', 20);
h = legend('Homodimers (s)','Heterodimers (s)', 'Homodimers (i)',
'Heterodimers (i)', 'Total', 1);
% set(h, 'FontSize', 16); %change font size of legend
axis([0 120 0 60000]);
set(gca,'XTick',[0 20 40 60 80 100 120]);
set(gca, 'YScale', 'linear');
set(gca,'Box', 'on');
set(gca, 'LineWidth', 3, 'FontSize', 20);
set(findobj('Type','line'),'LineWidth', 3);
hold off;


%----------------------------------------


figure;
subplot(2,2,1);
hold on;
plot(ERK_tspan, SignalThruEGFR_P, 'b');
plot(ERK_tspan, SignalThruEGFR_24H, 'r');
plot(ERK_tspan, SignalThruHER2_P, 'b--');
plot(ERK_tspan, SignalThruHER2_24H, 'r--');

xlabel('time (min)', 'FontSize', 20);
ylabel('ERK Activity (cpm)', 'FontSize', 20);
title('Signal', 'FontSize', 20);
h=legend('EGFR - P', 'EGFR - 24H', 'HER2 - P','HER2 - 24H', 1);
axis([0 120 0 12000]);
set(gca,'XTick',[0 20 40 60 80 100 120]);
set(gca,'YTick',[0 2000 4000 6000 8000 10000 12000]);
%set(h, 'FontSize', 16);
set(gca,'Box', 'on');
set(findobj('Type','line'),'LineWidth', 3);
set(gca, 'LineWidth', 3, 'FontSize', 20);
hold off;

subplot(2,2,3);
hold on;
plot(ERK_tspan, PercentTotalSignal_P, 'b');
```

```
plot(ERK_tspan, PercentTotalSignal_24H, 'r--');

xlabel('time (min)', 'FontSize', 20);
ylabel('% Total Signal', 'FontSize', 20);
title('HER2 Fraction of Total Signal', 'FontSize', 20);
h=legend('P', '24H', 1);
axis([0 120 0 100]);
set(gca,'XTick',[0 20 40 60 80 100 120]);
%set(h, 'FontSize', 16);
set(gca,'Box', 'on');
set(findobj('Type','line'),'LineWidth', 3);
set(gca, 'LineWidth', 3, 'FontSize', 20);
hold off;

subplot(2,2,4);
FudgeFactor = 1.34; % this number is derived from the degree to which
% the global trafficking model is off from experimental prediction of
2C4
% results. (see Cancer Research manuscript)
hold on;
plot(ERK_tspan, SignalThruEGFR_P, 'b');
plot(ERK_tspan, FudgeFactor*SignalThruEGFR_24H_2C4, 'r');
errorbar(ERK_tspan, ERK_P_2C4, ERK_P_2C4_error, 'ob');
errorbar(ERK_tspan, ERK_24H_2C4, ERK_24H_2C4_error, 'sr');

xlabel('time (min)', 'FontSize', 20);
ylabel('ERK Activity (cpm)', 'FontSize', 20);
title('EGFR Signaling: Model vs. 2C4 Data', 'FontSize', 20);
h=legend('model - P', 'model - 24H', 'P + 2C4', '24H + 2C4', 1); % 24H
adjusted for 2C4 trafficking effects
%set(h, 'FontSize', 16);
axis([0 120 0 12000]);
set(gca,'XTick',[0 20 40 60 80 100 120]);
set(gca,'YTick',[0 2000 4000 6000 8000 10000 12000]);
set(gca,'Box', 'on');
set(findobj('Type','line'),'LineWidth', 3);
set(gca, 'LineWidth', 3, 'FontSize', 20);
hold off;

subplot(2,2,2);
hold on;
plot(ERK_tspan, TotalSignalPrediction_12, 'm');
errorbar(ERK_tspan, ERK_12, ERK_12_stdev, 'dm');
%errorbar(ERK_tspan, ERK_P, ERK_P_stdev, 'ob');
%errorbar(ERK_tspan, ERK_24H, ERK_24H_stdev, 'sr');

xlabel('time (min)', 'FontSize', 20);
ylabel('ERK Activity (cpm)', 'FontSize', 20);
title('Model Prediction of clone 12 data', 'FontSize', 20);
h=legend('model prediction', 'data', 1);
%set(h, 'FontSize', 16);
axis([0 120 0 12000]);
set(gca,'XTick',[0 20 40 60 80 100 120]);
set(gca,'YTick',[0 2000 4000 6000 8000 10000 12000]);
```

```
set(gca,'Box', 'on');
set(findobj('Type','line'),'LineWidth', 3);
set(gca, 'LineWidth', 3, 'FontSize', 20);
hold off;

% this plots the signal per receptor complete w/ errorbars
figure;
subplot(2,2,1);
hold on;
errorbar(ERK_tspan, SignalPerEGFR, SignalPerEGFR_stdev, 'b');
errorbar(ERK_tspan, SignalPerHER2, SignalPerHER2_stdev, 'r--');

xlabel('time (min)', 'FontSize', 20);
ylabel('cpm/receptor', 'FontSize', 20);
title('100 ng/ml EGF', 'FontSize', 20);
h=legend('EGFR', 'HER2', 1);
axis([0 120 0 0.10]);
set(gca,'XTick',[0 20 40 60 80 100 120]);
%set(h, 'FontSize', 16);
set(gca,'Box', 'on');
set(findobj('Type','line'),'LineWidth', 3);
set(gca, 'LineWidth', 3, 'FontSize', 20);
hold off;

% this plots the signal per dimer complete w/ errorbars
subplot(2,2,3);
hold on;
errorbar(ERK_tspan, SignalPerHomodimer, SignalPerHomodimer_stdev, 'g');
errorbar(ERK_tspan, SignalPerHeterodimer, SignalPerHeterodimer_stdev,
'c--');

xlabel('time (min)', 'FontSize', 20);
ylabel('cpm/receptor', 'FontSize', 20);
title('100 ng/ml EGF', 'FontSize', 20);
h=legend('Homodimer', 'Heterodimer', 1);
axis([0 120 0 0.1]);
set(gca,'XTick',[0 20 40 60 80 100 120]);
%set(h, 'FontSize', 16);
set(gca,'Box', 'on');
set(findobj('Type','line'),'LineWidth', 3);
set(gca, 'LineWidth', 3, 'FontSize', 20);
hold off;

subplot(2,2,2);
hold on;
errorbar(ERK_tspan, SignalPerEGFR_1, SignalPerEGFR_stdev_1, 'b');
errorbar(ERK_tspan, SignalPerHER2_1, SignalPerHER2_stdev_1, 'r--');

xlabel('time (min)', 'FontSize', 20);
ylabel('cpm/receptor', 'FontSize', 20);
title('1 ng/ml EGF', 'FontSize', 20);
h=legend('EGFR', 'HER2', 1);
%set(h, 'FontSize', 16);
axis([0 120 -2 2]);
```

```
set(gca,'XTick',[0 20 40 60 80 100 120]);
set(gca,'Box', 'on');
set(findobj('Type','line'),'LineWidth', 3);
set(gca, 'LineWidth', 3, 'FontSize', 20);
hold off;

% this plots the signal per dimer complete w/ errorbars
subplot(2,2,4);
hold on;
errorbar(ERK_tspan, SignalPerHomodimer_1, SignalPerHomodimer_stdev_1,
'g');
errorbar(ERK_tspan, SignalPerHeterodimer_1,
SignalPerHeterodimer_stdev_1, 'c--');

xlabel('time (min)', 'FontSize', 20);
ylabel('cpm/receptor', 'FontSize', 20);
title('1 ng/ml EGF', 'FontSize', 20);
h=legend('Homodimer', 'Heterodimer', 1);
%set(h, 'FontSize', 16);
axis([0 120 0 8]);
set(gca,'XTick',[0 20 40 60 80 100 120]);
set(gca,'Box', 'on');
set(findobj('Type','line'),'LineWidth', 3);
set(gca, 'LineWidth', 3, 'FontSize', 20);
hold off;


figure;
hold on;
%plot(ERK_tspan, Dogma_2alpha_P, 'b');
%plot(ERK_tspan, Dogma_halfalpha_P, 'b--');
plot(ERK_tspan, Dogma_2alpha_24H, 'r');
plot(ERK_tspan, Dogma_alpha_24H, 'r--');
plot(ERK_tspan, Dogma_halfalpha_24H, 'r:');
%errorbar(ERK_tspan, ERK_P, ERK_P_stdev, 'ob');
errorbar(ERK_tspan, ERK_24H, ERK_24H_stdev, 'sr');

xlabel('time (min)', 'FontSize', 20);
ylabel('ERK Activity (cpm)', 'FontSize', 20);
title('Dogma: clone 24H', 'FontSize', 20);
h=legend('Beta = 2*Alpha', 'Beta = Alpha', 'Beta = 0.5*Alpha', 'Expt',
1);
%set(h, 'FontSize', 16);
axis([0 120 0 15000]);
set(gca,'XTick',[0 20 40 60 80 100 120]);
set(gca,'YTick',[0 5000 10000 15000]);
set(gca,'Box', 'on');
set(findobj('Type','line'),'LineWidth', 3);
set(gca, 'LineWidth', 3, 'FontSize', 20);
hold off;


figure;
subplot(2,2,1);
```

```
hold on;
errorbar(ERK_tspan, RelativeSignal_expt_100E,
RelativeSignal_expt_100E_stdev, 'b');
plot(ERK_tspan, RelativeSignal_predicted_100E, 'r--');

xlabel('time (min)', 'FontSize', 20);
ylabel('cpm/receptor', 'FontSize', 20);
title('Relative Signal: 100 ng/ml EGF', 'FontSize', 20);
h=legend('experiment', 'model', 1);
axis([0 120 0 3]);
set(gca,'XTick',[0 20 40 60 80 100 120]);
%set(h, 'FontSize', 16);
set(gca,'Box', 'on');
set(findobj('Type','line'),'LineWidth', 3);
set(gca, 'LineWidth', 3, 'FontSize', 20);
hold off;


subplot(2,2,2);
hold on;
errorbar(ERK_tspan, RelativeSignal_expt_1E,
RelativeSignal_expt_100E_stdev, 'b');
plot(ERK_tspan, RelativeSignal_predicted_1E, 'r--');

xlabel('time (min)', 'FontSize', 20);
ylabel('cpm/receptor', 'FontSize', 20);
title('Relative Signal: 1 ng/ml EGF', 'FontSize', 20);
h=legend('experiment', 'model', 1);
axis([0 120 0 3]);
set(gca,'XTick',[0 20 40 60 80 100 120]);
%set(h, 'FontSize', 16);
set(gca,'Box', 'on');
set(findobj('Type','line'),'LineWidth', 3);
set(gca, 'LineWidth', 3, 'FontSize', 20);
hold off;
```

A.4.2 RIM_ode_v2.m

```
function y=RImodel_ode_v2(t,x,flag,param)
% Receptor Interaction Model odefile
% this is the basic set of receptor interactions that take place on the
cell surface
% last revised 02.11.09

R1 = x(1);
R2 = x(2);
R1R1 = x(3);
R1R2 = x(4);
R2R2 = x(5);
R1L = x(6);
R1LR2 = x(7);
R1R1L = x(8);
LR1R1L = x(9);

kc = param(1);          % HER2 homodimer coupling
kuR2R2 = param(2);      % HER2 homodimer uncoupling
kuR1R2 = param(3);      % HER2:EGFR heterodimer uncoupling
kuR1R1 = param(4);      % EGFR:EGFR heterodimer uncoupling
kuR1LR2 = param(5);     % HER2:EGFR-EGF uncoupling
kuLR1R1L = param(6);    % EGFR-EGF homodimer uncoupling

kon = param(7);         % Ligand-EGFR binding
koff = param(8);        % Ligand-EGFR dissociation

L = param(9);           % Ligand concentration


% HERE I HAVED REMOVED LIGAND BINDING & DISSOCIATION SINCE THE INPUT
ALREADY
% CONTAINS THE NUMBER OF COMPLEXES AND AT EARLY TIMEPOINTS BINDING MAY
NOT
% BE AT STEADY STATE

% d(R1)/dt:
y(1,1) = -kc*R1*R2 + kuR1R2*R1R2 - 2*kc*R1*R1 + 2*kuR1R1*R1R1 -
kc*R1*R1L + kuR1R1*R1R1L;

% d(R2)/dt:
y(2,1) = -2*kc*R2*R2 + 2*kuR2R2*R2R2 - kc*R1*R2 + kuR1R2*R1R2 -
kc*R1L*R2 + kuR1LR2*R1LR2;

% d(R1R1)/dt:
y(3,1) = kc*R1*R1 - kuR1R1*R1R1;

% d(R1R2)/dt:
y(4,1) = kc*R1*R2 - kuR1R2*R1R2;

% d(R2R2)/dt:
```

```
y(5,1) = kc*R2*R2 - kuR2R2*R2R2;

% d(R1L)/dt:
y(6,1) =  - 2*kc*R1L*R1L + 2*kuLR1R1L*LR1R1L - kc*R1L*R2 +
kuR1LR2*R1LR2 - kc*R1*R1L + kuR1R1*R1R1L;

% d(R1LR2)/dt:
y(7,1) =  + kc*R1L*R2 - kuR1LR2*R1LR2;

% d(R1R1L)/dt:
y(8,1) =   + kc*R1*R1L - kuR1R1*R1R1L;

% d(LR1R1L)/dt:
y(9,1) = kc*R1L*R1L - kuLR1R1L*LR1R1L;

return;
```

A.4.3 EGFR_ode.m

```
function y = EGFRmodel_ode(t,x,flag,parameter)
% EGFR Model (from co-regulation manuscript) odefile
%
% last revised 02.07.17

Rs = x(1);
Cs = x(2);
Ri = x(3);
Ci = x(4);


kon = parameter(1);    % measured
koff = parameter(2);    % measured

ker = parameter(3);   % measured
kec = parameter(4);   % measured, function of HER2 level
kxr = parameter(5);   % measured
kxc = parameter(6);   % measured

fxr = parameter(7);   % estimated - fraction empty receptors recycled
fxc = parameter(8);  % measured, function of HER2 level


Sr = parameter(9);   % estimated - receptor synthesis

L = parameter(10);

Nav = 6.023E23;


% d(Rs)/dt:
y(1,1) = (- kon*L*Rs + koff*Cs) - ker*Rs + kxr*fxr*Ri + Sr;

% d(Cs)/dt:
y(2,1) = (+ kon*L*Rs - koff*Cs) - kec*Cs + kxc*fxc*Ci;

% d(Ri)/dt:
y(3,1) = + ker*Rs - kxr*fxr*Ri - kxr*(1-fxr)*Ri;

% d(Ci)/dt:
y(4,1) =  + kec*Cs - kxc*fxc*Ci - kxc*(1-fxc)*Ci;


return;
```

A.4.4 HER2_ode.m

```
function y = HER2model_ode(t,x,flag,parameter)
% HER2 Model (from co-regulation manuscript) odefile
%
% last revised 02.11.07

Hs = x(1);
Hi = x(2);


keh = parameter(1);   % measured, function of HER2 level
kxh = parameter(2);   % measured, function of HER2 level
fxh = parameter(3);   % measured


Sh = parameter(4);   % estimated - receptor synthesis




% d(Hs)/dt:
y(1,1) =  - keh*Hs + kxh*fxh*Hi + Sh;

% d(Hi)/dt:
y(2,1) = + keh*Hs - kxh*fxh*Hi - kxh*(1-fxh)*Hi;


return;
```

A.4.5 ERKdata.m

```
% Experimental ERK signaling data: THESE DATA ARE IN CPM

ERK_tspan = [0 5 15 30 60 120];  %time in min
ERK_tsteps = size(ERK_tspan,2);

% These experiments are from 100 ng/ml EGF stimulation:
ERK_P = [355.8386  6998.452 4329.56 4660.223 3723.009 2446.591];
ERK_12 = [276.03  8494.17 5682.10 5643.45 4065.21 3301.56];
ERK_24H = [320.4217  9671.301 8817.633 7774.122 7551.378 5969.263];
ERK_P_2C4 = [266.564  5046.366 4026.053 3661.868 2858.445 2447.186];
ERK_24H_2C4 = [277.51  7552.964 6077.026 5934.073 4827.068 3069.904];


ERK_P_stdev = [169.47  1666.18 1405.70 1242.05 1412.37 111.05];
ERK_P_stderr = [97.84  961.97 811.58 717.10 815.43 111.05];


ERK_12_stdev = [92.34  1828.57 598.85 712.86 701.70 463.59];  % based
on only 1 expt


ERK_24H_stdev = [2690.26  932.17 1164.02 660.19 649.42 140.36];
ERK_24H_stderr = [1902.30  538.19 672.05 381.16 374.94 140.36];


ERK_P_2C4_error = [72.58  320.98 609.87 250.32 182.68 447.77];      %
these are stdev
ERK_24H_2C4_error = [148.00  708.07 1094.38 630.93 347.99 167.59];  %
these are stdev


ERK_stdev = [ERK_P_stdev; ERK_12_stdev; ERK_24H_stdev; ERK_P_2C4_error;
ERK_24H_2C4_error].';

% ----------  END 100 ng/ml EGF



% 1 ng/ml EGF data...

ERK_P_1 = [207.51  5653.02 3212.34 2409.21 1118.09 844.93];
ERK_24H_1 = [190.97  5117.68 3925.54 3012.57 2115.55 1193.55];

ERK_P_1_stdev = [126.41  456.42 270.61 330.85 262.01 383.40];
ERK_24H_1_stdev = [56.31  1151.15 1140.18 565.81 775.36 474.37];
```

```
Placeholder = [0 0 0 0 0 0];


ERK_data_1 = [ERK_P_1; Placeholder; ERK_24H_1].'; % this uses 1 ng/ml
data

ERK_stdev_1 = [ERK_P_1_stdev; Placeholder; ERK_24H_1_stdev].'; % this
uses 1 ng/ml data
% ----------  END 1 ng/ml EGF

% TGFa data:
ERK_P_TGF_100 = [280.42 8678.39 5359.83 5846.83 5564.71 4169.52];
ERK_24H_TGF_100 = [230.40 7111.31 5595.93 4643.45 3650.60 4095.29];

ERK_P_TGF_1 = [362.48 7985.75 3345.61 2678.64 1471.37 241.54];
ERK_24H_TGF_1 = [206.90 4077.70 4066.98 2411.70 1819.61 372.00];

ERK_P_TGF_100_stdev = [84.26 1312.57 537.77 533.18 429.78 80.00];
ERK_24H_TGF_100_stdev = [77.18 1322.92 354.99 438.57 401.34 97.97];

ERK_P_TGF_1_stdev = [138.74 1942.13 264.34 266.96 341.79 154.04];
ERK_24H_TGF_1_stdev = [17.47 526.04 302.87 214.86 521.50 168.03];
% ---------- END TGFa data

ERK_data = [ERK_P; ERK_12; ERK_24H; ERK_P_2C4; ERK_24H_2C4; ERK_P_1;
ERK_24H_1].';

ERK_stdev = [ERK_P_stdev; ERK_12_stdev; ERK_24H_stdev; ERK_P_2C4_error;
ERK_24H_2C4_error; ERK_P_1_stdev; ERK_24H_1_stdev].';
% End ... Experimental Results ------------------------------
```

A.4.6 SD_param_values.m

```
% Model Parameters ============================================
% EGFR  Parameters ------------------
kon = 9.7E7;        % revise these
koff = 0.24;         % revise these

ker = 0.08;   % (min-1)

kec_P = 0.25;         % (min-1)
kec_12 = 0.18;
kec_24H = 0.10;
kec_24H_2C4 = 0.28;

kxr = 0.08;      % DOUBLE CHECK THIS VALUE
kxc = 0.035;     % measured - recycling expts
kxc_2C4 = 0.035;

fxr = 0.85;    % estimated - fraction empty receptors recycled

fxc = 0.5;     % measured - fraction of complexes recycled
fxc_P = 0.50;
fxc_12 = 0.52;
fxc_24H = 0.70;
fxc_24H_2C4 = 0.54; % should double check these numbers

% Parameters for 1 ng/ml EGF (determined from internalization model):
kec_P_1 = 0.174; %0.25;         % (min-1)
kec_24H_1 = 0.115;  %0.10

fxc_P_1 = 0.55;
fxc_24H_1 = 0.68;


Sr = 2400;     % estimated - receptor synthesis (min-1) 3000 ~ 250000
EGFR on surface; 2000 ~ 166000; 2500 ~ 208333

fxc_P_TGFa = 0.65;
fxc_P_TGFa_1 = 0.67;
fxc_24H_TGFa = 0.78;
fxc_24H_TGFa_1 = 0.74;


%------- HER2 Parameters -------------------
keh_P_NoEGF = 0.018; %HER2 internalization rate (No EGF)
keh_12_NoEGF = 0.0085;
keh_24H_NoEGF = 0.0108;

keh_P = 0.0588; %HER2 internalization rate (+ EGF)
keh_12 = 0.0456;
keh_24H = 0.0292;
```

```
% Parameters for 1 ng/ml EGF:

keh_P_1 = 0.0384;
keh_12_1 = 0;
keh_24H_1 = 0.0295;

fxh = 0.98; % HER2 recycling fraction expermental = 0.94; model
suggests 0.98
kxh = 0.07;  % HER2 endosomal exit rate

Sh_P = 12;
Sh_12 = 35;
Sh_24H = 140;

% Receptor Dimerization Parameters for Receptor Interaction Module ----
-
% (from Internalization model fitting)
kc = 1E-3;          % HER2 homodimer coupling
kuR2R2 = 1.075;     % HER2 homodimer uncoupling
kuR1R2 = 16.45;     % HER2:EGFR heterodimer uncoupling
kuR1R1 = 13.51;     % EGFR:EGFR heterodimer uncoupling
kuR1LR2 = 0.13;    % HER2:EGFR-EGF uncoupling
kuLR1R1L = 0.13;   % EGFR-EGF homodimer uncoupling



% End ... Model Parameters ====================================
```